AL/EQ-TR-1996-0039

UNITED STATES AIR FORCE
ARMSTRONG LABORATORY

Groundwater Remediation Field Laboratory - GRFL: Hydrogeology Characterization, Site Characterization and Site Development

R.L. Montgomery, C.J. Bianchi, S.M. Conklin, W.C. Dickerson, J.A. Eddings, S.P. Farrington, J.J. Fuhrmann, J. Madsen, R.M. Morey, T.L. Steinborn, J.D. Shinn, D.L. Sparks, R.E. Walker, L. Zelazny

APPLIED RESEARCH ASSOCIATES, INC.
4300 San Mateo Boulevard, NE, Suite A220
Albuquerque, New Mexico 87110

May 1997

19970711 104

DTIC QUALITY INSPECTED 3

Environnics Directorate
Environmental Risk
Management Division
139 Barnes Drive
Tyndall Air Force Base FL
32403-5323

NOTICES

This report was prepared as an account of work sponsored by an agency of the United States Government. Neither the United States Government nor any agency thereof, nor any employees, nor any of their contractors, subcontractors, or their employees, make any warranty, expressed or implied, or assume any legal liability or responsibility for the accuracy, completeness, or usefulness of any privately owned rights. Reference herein to any specific commercial products, process, or service by trade name, trademark, manufacturer, or otherwise, does not necessarily constitute or imply its endorsement, recommendation, or favoring by the United States Government or any agency, contractor, or subcontractor thereof. The views and opinions of the authors expressed herein do not necessarily state or reflect those of the United States Government or any agency, contractor, or subcontractor thereof.

When Government drawings, specifications, or other data are used for any purpose other than in connection with a definitely Government-related procurement, the United States Government incurs no responsibility or any obligation whatsoever. The fact that the Government may have formulated or in any way supplied the said drawings, specifications, or other data, is not to be regarded by implication, or otherwise in any manner construed, as licensing the holder or any other person or corporation; or as conveying any rights or permission to manufacture, use, or sell any patented invention that may in any way be related thereto.

This technical report has been reviewed by the Public Affairs Office (PA) and is releasable to the National Technical Information Service (NTIS) where it will be available to the general public, including foreign nationals.

This report has been reviewed and is approved for publication.

FOR THE COMMANDER:

ALISON THOMAS
Project Officer

ALLAN M. WEINER, Lt Col, USAF
Chief, Environmental Risk Management Division

1. Report Date (dd-mm-yy) May 1997	2. Report Type Final	3. Dates covered (from... to) 12 Jun 1995 - 28 Jun 1996	
4. Title & subtitle Groundwater Remediation Field Laboratory - GRFL: Hydrogeology Characterization, Site Characterization and Site Development		5a. Contract or Grant # F08635-93-C-0020	
		5b. Program Element #	
6. Author(s) Raymond L. Montgomery, Christopher J. Bianchi, Susanne M. Conklin, Wilhelmina C. Dickerson, James A. Eddings, Stephan P. Farrington, Jeffry J. Fuhrmann, Madsen, Rexford M. Morey, Terry L. Steinborn, James D. Shinn, Donald L. Sparks, Robert E. Walker, and Lucian Zelazny		5c. Project #	
		5d. Task #	
		5e. Work Unit #	
7. Performing Organization Name & Address Applied Research Associates, Inc 4300 San Mateo Blvd NE, Suite A220 Albuquerque NM 87110		8. Performing Organization Report # 5276	
9. Sponsoring/Monitoring Agency Name & Address AL/EQW-OL (Ms Alison Thomas) 139 Barnes Drive, Suite 2 Tyndall AFB FL 32403-5323		10. Monitor Acronym	
		11. Monitor Report # AL/EQ-TR-1996-0039	

13. Supplementary Notes
Contracting Officer's Technical Rep(s): Ms Alison Thomas and Major Mark Smith

14. Abstract
This technical report describes the work performed at the GRFL for site characterization, site preparation, site construction, site monitoring and analysis, and environmental compliance. The objectives of this study were to provide detailed hydrogeological characterization of the proposed experimental controlled-release site at Dover AFB and prepare the GRFL test site for technology demonstrations. The GRFL was established as a national field research and demonstration facility for in situ technologies. DNAPLs will be released under a carefully controlled environment and emerging alternative remediation technologies and processes will be verified under the field laboratory conditions provided by the GRFL. These tests will provide information necessary to design and engineer effective treatment systems for cleanup of DNAPL contaminated soil and groundwater.

15. Subject Terms
Groundwater remediation, Environmental technologies, DNAPLs cleanup, Remediation, Hydrogeology characterization

Security Classification of			19. Limitation of Abstract	20. # of Pages	21. Responsible Person (Name and Telephone #)
16. Report Unclassified	17. Abstract Unclassifed	18. This Page Unclassified	Unlimited	185	Ms Alison Thomas (904)283-6303

i

PREFACE

This report was prepared by Applied Research Associates, Inc., 4300 San Mateo Blvd., NE, Suite A220, Albuquerque, NM 87110, under Contract F08635-93-C-0020, Subtask 14.02.1, for the Armstrong Laboratory, Tyndall AFB, FL 32403-5323.

The report summarizes work done between June 1995 and June 1996. Major Mark Smith and Ms Alison Thomas were the AL/EQW-OL project officers.

The information contained in this volume describes the work performed at the GRFL for site characterization, site preparation, site construction, site monitoring and analysis, and environmental compliance.

EXECUTIVE SUMMARY

In June 1995, Applied Research Associates, Inc. was awarded a contract to conduct hydrogeology characterization investigations at Dover AFB, Delaware and develop the Groundwater Remediation Field Laboratory (GRFL). The project was initiated and completed in approximately twelve months although actual site construction was not started until the environmental assessment received full approval in January 1996. This report describes the development of this unique test facility for demonstration of technologies to treat soil and groundwater contaminated with fuel and solvents, focusing on dense nonaqueous phase liquids (DNAPLs). It is one of the national technology demonstration facilities established under the DoD/National Environmental Technology Test Sites Program (NETTS) funded by the Strategic Environmental Research and Development Program (SERDP). Although the GRFL provides a test site primarily for evaluating transport of DNAPL contamination, it also provides a test site for demonstrating new treatment technologies for fuels and solvents contamination. The purpose of the GRFL test site is to demonstrate emerging concepts, processes and technologies under controlled conditions. These tests will provide information necessary to design and engineer improved treatment systems for cleanup of groundwater and soils contaminated with solvents and fuels.

The first phase of the GRFL development involved detailed characterization of the site hydrogeology to provide data for use in locating the experimental controlled release test cells, to provide baseline hydrogeology and biogeochemical data to researchers, and to comply with regulatory safeguards. The second phase of the project involved insitu testing of the vadose and saturated, installation of monitoring instrumentation and construction of the GRFL facility. The facility provides a data acquisition, management and analysis system to monitor and control experiments and to perform scientific studies and analyses of test results. An on site laboratory is provided with the capability to perform analyses on organic compounds from the GRFL. An initial test cell was constructed of a double wall sheet piling. This project included the following activities:

Hydrogeology Characterization. Site Characterization tasks were performed to provide the site characterization data needed to characterize the Dover site for location of the initial test cell and any future test cells. This work involved applying innovative geotechnical and environmental site characterization technologies for specific project needs.

Using ground penetrating radar (GPR) and cone penetrometer tests (CPT), the subsurface layers were identified and mapped. The site consists of two aquifers, separated by an 8 (26 feet.) to 12 (39 feet.) meter-thick clay layer located 9 (30 feet.) to 13 (43 feet.) meters beneath the surface. The upper unconfined aquifer is composed of a heterogeneous mixture of sand, with occasional lenses of gravel and clay. The water table is approximately 8 (26 feet.) meters below the ground surface. Figure ES-1 shows the detail of the aquitard as mapped from the radar data.
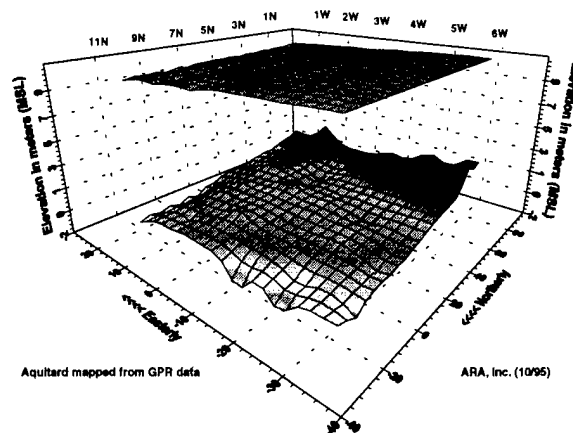
Figure ES-1. Ground Surface and Surface of Aquitard.

A total of 59 cone penetration tests were conducted at the GRFL site. The tip resistances vary from a peak of 4000 psi at the surface, which is representative of a very stiff soil to less than 200 psi at elevation -1 feet, msl, where the aquitard is encountered. The variations in the tip resistance reflect variations in soil strength, which is directly related to soil type. The friction ratio was generally less than 1, indicating sandy soils. At several depths, the friction ratio increases, indicating an increase in the fine grained soil content. From elevation 22.5 to 15 feet, msl, the tip resistance decreased and the friction ratio increased, indicating a fine grained soil. Below elevation 15 feet, msl, this trend reversed indicating a more coarse grained soil. The clay aquitard was readily identified by the rapid decrease in tip resistance and corresponding increase in friction ratio and penetration pore pressures.

Chemical analyses indicate that the soils are slightly to moderately acidic, with pH ranging from 4.9 to 6.4. Organic matter and clay contents are quite low, typical for Coastal Plain soils. The soils are generally sandy. Extractable levels of Ca, Mg, and K were higher than the exchangeable levels of the cations since a stronger extractant was used, and both readily exchangeable (those on planar, external sites of clay minerals and organic matter) and some edge site ions were extracted. The order of extractable ions in the soils is Ca > Mg > K > Fe > P > Mn > Zn > Cu. Both the effective cation exchange capacity (CEC) and the CEC at pH 7.0 (a measure of total negative charge on the soils) were low, reflective of the low quantities of clay (7.9% to 46.9%) and organic matter (0 to 1.7%). Exchangeable acidity was quite low, reflective of the moderately acidic pH of the soils. Soluble salts were very low, as one would expect for acidic soils.

Microbiological analyses indicated that, both heterotrophic and denitrifying bacteria were present at detectable levels in all samples. Bacterial numbers generally decreased with depth, although in some cases counts remained elevated at considerable depths. The autotrophic nitrifying bacteria were only detected in the more shallow samples. The eukaryotic fungi and protozoa were also found to be more prevalent at

shallow depths, although significant populations were detected as deep as 37 feet in some instances.

There was little microbiological evidence that extensive anaerobic metabolism commonly occurs in any of the soil-sediment samples examined. Anaerobiosis can only develop in soils under conditions of reduced O_2 diffusion (generally due to elevated soil moisture) in combination with high rates of microbial metabolism. Denitrifying enzyme activity was low in all samples examined and detectable only in the surface samples.

Analyses performed on the GRFL soil samples revealed a range of mineralogical properties. The highest total sand content (93%) was found between elevations 23 and 29 feet msl with a preponderance of sand in the medium (42%) and fine (28%) fractions. A high total sand fraction (84%) also occurred between elevations 4 and 10 feet msl. Total clay dominated (47%) the soil between elevations -10 and -12 feet msl and was a significant component (36%) between elevations 20 and 22 ft msl at this location. Significant silt (40 to 49%) occurred between elevations -10 and -12 feet msl, and between 20 and 22 feet msl. The soil contained 35% silt at between elevations -7 and -9 feet msl.

These soil/sediment samples contained significant iron oxides and noncrystalline . material. The highest extractable iron oxide occurred in samples taken between elevations -10 to -12 feet msl (7.08%) with intermediate quantities in samples taken between elevations 10 to 18 feet msl (2.12%). The bright red color would support the dominance of hematite although goethite could also be present. Much of this iron oxide occurred as coatings on other particles.

Twenty seven monitoring wells were placed at selected locations at the site for use in sampling the groundwater and to monitor groundwater conditions during GRFL activities. Eleven piezometers were placed in monitoring wells at various locations near the test cell to monitor groundwater levels during demonstrations. Four additional piezometers were located between the inner and outer barriers of the test cell to monitor water levels at the test site during demonstrations.

Site Preparation and Cell Construction. A major goal of this project was to prepare the site and build the GRFL national test site. Work toward this goal included preparing the site, establishing the on-site laboratory, and constructing the test cell.

GRFL Field Operations Facility. A 30 x 50 foot single story building was constructed to serve as the combination field office and laboratory (Figure ES-2). It provides office space for the GRFL on-site staff and is equipped with the appropriate analytical laboratory equipment to support GRFL demonstrations. The GRFL operations facility was equipped with a gas chromatograph (GC) that will be operated under climate controlled conditions in the field laboratory. Other laboratory instrumentation includes a pH/ION Meter, Dissolved Oxygen Probe, portable monitoring/sampling pumps, and other miscellaneous laboratory equipment and supplies.
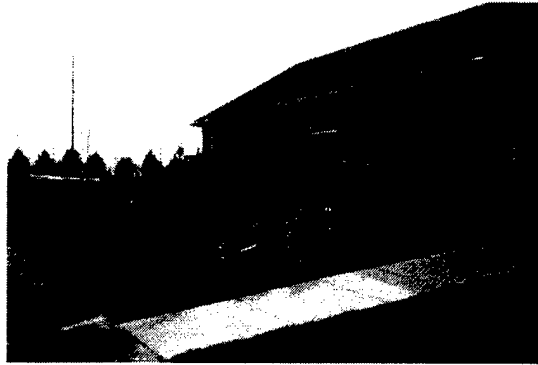

Figure ES-2. Field Operations Facility.

Test Cell Construction. A double walled 16.7 x 33.5 foot test cell was constructed with 45 feet long sheets of W275 Waterloo Barrier™ Sheet Piles (ES-3). The joints were flushed clean and tremie grouted with a specially designed attapulgite grout. Construction techniques were carried out according to the construction practices recommended by the developer of the barrier sheet piles. The materials and construction techniques make the Waterloo sheet piling less prone to leaking than other types of containment walls, thus providing a greater degree of confidence in its performance.

Eight 2-inch extraction/injection wells were installed in the outer ring of the test cell as part of an emergency treatment system. In addition four piezometers were located outside the test cell to monitor ground water quality during demonstrations. This system of wells and monitoring points are part of the three tiered safety plan to protect against any unlikely leakage and contamination of the surrounding area during controlled release demonstrations (Figure ES-4).
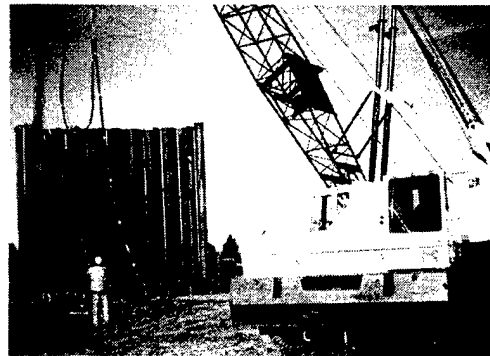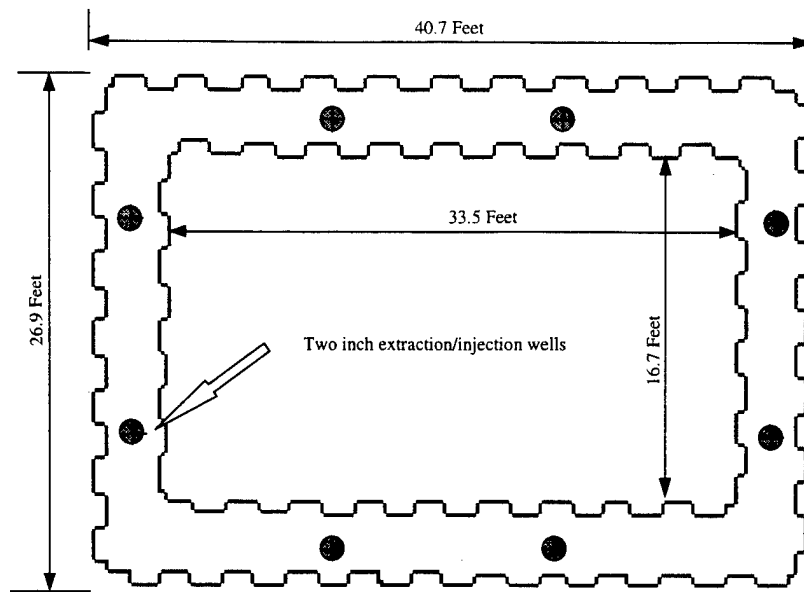

Figure ES-3 Pile Driving

40.7 Feet

33.5 Feet

26.9 Feet

16.7 Feet

Two inch extraction/injection wells

Figure ES-4. Drawing of Test Cell and Locations of Extraction/Injection Wells.

Landscaping. In addition to designing and constructing the GRFL facility to meet the unique requirements of future technology demonstrators, an important feature of the site preparation task was to landscape the site so it would blend in with the Dover AFB facilities. An effective visual screen to the site was provided by planting 275 four to six feet tall White Pine trees in multiple rows on three sides of the site. The trees were staggered in a random pattern to enhance their visual appeal and help them blend the site into the base landscape. In addition, a landscaping scheme around the modular facility was developed by the base landscape architect to blend it into its surroundings and provide a more visually appealing facility for the base

Data Acquisition System. A data acquisition system was developed to meet the requirements for data gathering and management during technology demonstrations at the GRFL.

The data acquisition system will acquire the raw data from the field, place it into a database, provide data security, allow remote data access and experimental control, and provide an analysis and graphics package for the researcher to use in the interpretation and visualization of the data. The software and hardware provide the following capabilities:

- Experimenters can generate color hard copy printouts of results, reports , etc.
- Experimenters can access their data on-site without having to bring special equipment.

- Experimenters can connect their PC to the GRFL network via Ethernet. Customer's PC must have a twisted pair connector (RJ-45) and be configured with TCP/IP software.
- Experimenters have access to their own cell data, as well as some overall site data such as weather information. Experimenters can not access other cell data.
- A mechanism (procedure and/or hardware/software) is available for sensor calibration.
- GRFL personnel have access to all site data, as well as all experimental data.
- Experimenters can control sensor and pump settings within their own test cell only.
- A history log will be kept reflecting the change(s) made to sensor/pump settings, which will minimally retain a time stamp for when the change occurred, the identification of the experimenters making the change, what sensor/pump was changed, and it's new parameter(s).
- GRFL personnel have the ability to control all GRFL site sensors/pumps, including peripherals within test cells.
- Experimenters have the ability to perform uncertainty calculations using on-site software.
- Experimenters have the ability to visualize their data and results from their uncertainty calculations.
- The entire site is characterized and the data are accessible to all personnel through the computer system.
- Experimenters have the ability to add sensors to the system (the software can accommodate new sensors without extensive rework).
- Experimenters have the ability to calibrate sensors. Any such calibration is logged for auditing purposes.
- Original data collected by the computer system will remain in storage without modifications, regardless of calibrations, user initiated changes, etc.
- The experimenter has the ability to modify data values, and such modification are tracked in a log.

Compliance Plans. It is essential that technology demonstrations at the GRFL maintain regulatory compliance at all times during the demonstrations. Compliance measures and plans were developed to ensure that activities carried out at the GRFL are in full compliance with federal, state, local and installation requirements. The compliance measures developed under this study included a waste management plan, safety plan, and emergency pump and treatment system.

Special GRFL Features. The GRFL provides the following special features for future demonstrators and users of the facility:

- Characterized and analyzed site hydrogeology conditions;
- Unique contained release infrastructure for controlled releases and treatment of contaminants in the test cell;
- Computer, technical, laboratory, management and construction/logistics support; and

- Environmental protection features to ensure that environmental protection is maintained during technology demonstration activities.

Significant Findings, Conclusions, and Recommendations.

- Cone penetration tests indicated that the subsurface materials and stratigraphy are generally consistent across the site with a few exceptions. Soils at the GRFL site consist of fine to coarse sands with varying amounts of silt, clay and gravel. A very stiff layer exists at the site at depths below ground surface of about 13 feet to 18 feet. Also present in the aquifer are clay and silt lenses.

- The basic physicochemical properties of the soil are typical of sandy, moderately acidic Atlantic Coastal Plain soils.

- A well defined clay layer, which is about one to two feet thick, was located at a depth of approximately 13 feet. The layer extends south through about half of the site, where it gradually becomes less distinctly clay and transitions to a clayey sand.

- The following values were determined from the pumping tests:

  - vertically averaged horizontal transmissivity of the aquifer ($T_{x,y}$) $= 129 \text{ feet}^2/\text{sec}$
  - specific yield (S_y) $= 0.27$
  - storativity (S) $= 0.0003 \text{ feet}^{-1}$
  - vertically averaged horizontal hydraulic conductivity ($K_{x,y}$) $= 8.5 \text{ feet/day}$

- Extensive measures were taken to minimize any potential impacts to the GRFL environment. Protective measures include two engineered barriers, maintaining an inward hydraulic gradient between the outer and inner barriers, and monitoring wells which can be used as contaminant extraction wells in the unlikely event of a release. An emergency groundwater pump and treatment system was designed and constructed to contain and treat any unexpected leakage of contaminants from the test cells during demonstrations. This system provides protection against contamination of groundwater and soil outside the test cell in the unlikely event of contaminants leakage during the future technology demonstrations.

- The GRFL is a unique resource for the Air Force and DoD. It will provide opportunities to verify treatment technologies for wide technology transfer applications to the user community.

In summary, the GRFL test site is fully operational and ready for technology demonstrations. Demonstration and verification studies conducted at this facility will provide validated data for use in designing improved full-scale remediation treatment systems.

TABLE OF CONTENTS

TABLE OF CONTENTS
(Continued)

TABLE OF CONTENTS
(Continued)

TABLE OF CONTENTS
(Continued)

TABLE OF CONTENTS
(Concluded)

LIST OF FIGURES

LIST OF FIGURES
(Continued)

LIST OF FIGURES
(Continued)

LIST OF FIGURES
(Continued)

LIST OF TABLES

LIST OF TERMS

$T_x T_y$ = Transmissivity in Horizontal Directions x, y

K_r = Hydraulic Conductivity in Horizontal Direction

K_z = Hydraulic Conductivity

S = Storage

S_y = Specific Yield

K = Hydraulic Conductivity

K_h, K_v = Air Permeability in Horizontal and Vertical Directions Respectively

DSC = Differential Scanning Calorimetry

I_x, I_k = Integrated Intensities of an Unknown Mineral Phase and Kaolinite Respectively

SCN = Soil Classification Number

CPT = Cone Penetration Test

Q_{tn} = Normalized Corrected Tip Stress

f_{SN} = Normalized Friction Ration

q_t = Tip Stress

σ_{vo} = Effective Overburden Stress

Bq = Pore Pressure Ratio

f_s = Friction Ration

ψ'	=	Friction Angle
OD	=	Outside Diameter
TDR	=	Time Domain Reflectometry
CSI	=	Cambell Scientific Inc
K_a	=	Dielectric Constant
T_{50}	=	Time During a Pore Pressure Dissipation Test During at 50% of Excess Pore Pressure Has Dissipated
P_n	=	Average of 10 Pore Pressure Measurements
U_o	=	Static Pore Pressure
U_p	=	Peak Pressure Observed During a Pore Pressure Dissipation Test
U_{50}	=	Pore Pressure @ 50% Dissipation
T_{50}	=	Time Factor @ 50% Dissipation
γ_w	=	Unit Weight of Water
C_H	=	Coefficient of Lateral Consolidations
M	=	Constrained Modulus
α	=	Empirical Factor
q_c	=	Measured Tip Resistance
m_v	=	Volumetric Compressibility
D_{10}	=	Sieve Dimension at which 10% of the Elements of the Medium are Smaller than D_{10}

IP	=	Instantaneous Profile Test
Ψ	=	Water Potential
Θ	=	Reduced Water Content
θ	=	Water Content at a Given Water Potential
θ_r	=	Residual Water Content
θ_s	=	Saturated Water Content (Total Porosity)
N	=	van Genuchten parameter
K_{sat}	=	Saturated Hydraulic Conductivity
R_w	=	Radius of Venting Well
k	=	Soil Gas Permeability
μ	=	Viscosity of Air
Q	=	Volumetric Flow Rate from Vent Well
P_{atm}	=	Ambient Air Pressure
R_I	=	Radius of Influence
P_w	=	Pressure Measured at Venting Well
T	=	Temperature
ρ_a	=	Ambient Gas Density
K_h	=	Horizontal Gas Permeability
n	=	Porosity

SECTION I

INTRODUCTION

The cleanup of contamination at Department of Defense (DOD) and Department of Energy (DOE) facilities is a large-scale and technically complex problem. DOD and DOE own and operate thousands of installations, ranging from training bases to industrial production facilities. Some of these facilities have operated for more than a century. Contamination from these operations has resulted in more than 10,000 sites that require some level of environmental cleanup, at a cost currently estimated to exceed $200 billion. Improved cleanup technologies are needed to reduce remediation costs, quicken the pace of cleanup, and to protect human health and the environment.

A.   OBJECTIVES

The objectives of this study were to provide detailed hydrogeological characterization of the proposed experimental controlled-release site at Dover AFB and prepare the GRFL test site for technology demonstrations. The GRFL was established as a national field research and demonstration facility for insitu remediation technologies. DNAPLs will be released under a carefully controlled environment and emerging alternative remediation technologies and processes will be verified under the field laboratory conditions provided by the GRFL. These tests will provide information necessary to design and engineer effective treatment systems for cleanup of DNAPL contaminated soil and groundwater. There is no existing comparable experimental controlled release test-bed facility in existence in the United States today.

B.   BACKGROUND

Dover Air Force Base was selected as the site for the Strategic Environmental Research and Development Program's (SERDP) national Groundwater Remediation Field Laboratory (GRFL). The main objective of the GRFL is to provide a field laboratory for verifying insitu treatment technologies for cleaning up dense non-aqueous-phase liquids (DNAPLs). The GRFL at Dover AFB was selected as a national test site as a part of the National DOD Environmental Technology Test Site Program (NETTS). The NETTS was established to enable efficient, relevant demonstrations of several candidate cleanup technologies. SERDP is a multiagency program funded through DOD and designed to respond to the environmental requirements of the military and those problems that the DOD shares with DOE and EPA. The NETTS complements EPA's Superfund Innovative Technology Evaluation (SITE) and DOE's Integrated Demonstration programs. The SITE program was intended for short-term validation of vendor developed technologies that were aimed at a wide range of Superfund contamination problems. Although demonstrations were performed in the field, operating conditions were often non-optimal; therefore, some of the technologies are candidates for further testing in the NETTS program.

The NETTS test sites will provide well-characterized, hydrogeological conditions to allow long-term field-scale demonstrations, under various climatic cycles. Technologies will be

optimized for treatment of contaminants of representative DOD contamination problems. The NETTS is a test bed for technologies emerging from DOD laboratories. These technologies will be developed under various environmental quality funding sources. The demonstration/validation emphasis will be to provide user and regulatory acceptance of emerging technologies from the DOD laboratory environmental quality programs. In addition, the NETTS site facilities will be available for further demonstration and fine-tuning, of technologies that are emerging from DOE, EPA programs and industry.

C. SCOPE/APPROACH

1. Phase I - Hydrogeology Characterization

Phase I of the project provided detailed characterization of the overall site for use in selecting the best location for the experimental controlled release test cells.

a. Surface Geophysics

Geophysical methods were used for site investigations at the GRFL site. These methods were used during the preliminary site characterization to gather background subsurface information. The results helped in the planning for the final location of the first cell. These methods can also be used during and after the experimental phase of contaminant release. The following methods were used in this study:

- Resistivity
- Ground penetrating radar
- Electromagnetic induction
- Seismic

b. Soil Sampling

Soil borings were made and continuous core samples were taken of the soil strata from the ground surface to the top of the underlying aquitard. Core samples were split and logged in the field. Soil samples were collected and sent to the Air Force Wright Laboratory, University of Delaware and Virginia Polytechnic Institute laboratories for physical, chemical, microbiological, and mineralogical testing.

c. Analysis of Soil/Sediment Physical Properties

The Air Force Wright Laboratory at Tyndall AFB performed tests to determine the physical properties on subsamples collected from the soil cores. Analyses included particle size analyses, bulk density, permeability of clay samples, and specific surface area.

d. Analysis of Soil/Sediment Chemical Properties

The University of Delaware performed analyses of soil chemical properties on soil samples from the soil borings. The chemical analyses included pH, total organic matter, cation exchange capacity (CEC) and total exchangeable bases, major and trace elements.

e. Analysis of Soil/Sediment Microbiology Properties

The University of Delaware performed microbiological analyses on soil samples from the GRFL site. The microbiological analyses provided an evaluation of the microbial communities and the whole soil, as opposed to individual organisms isolated from the soil/sediment samples. The results of this work will provide baseline information for future bioremediation demonstrations in the test cells.

f. Analysis of Soil/Sediment Mineralogical Properties

Virginia Polytechnic Institute performed laboratory analyses on six sub-samples collected from the soil cores to determine the mineralogical properties. Analyses included microscopic analyses, sand particle, x-ray diffraction and thermal analyses of silt and clay size particles.

g. CPT Site Survey

Cone Penetrometer Technology (CPT) was used to survey the site. Analysis of the data collected during the CPT survey included geostatistical analysis and 3-D plots of stratigraphy including, soil type, any drainage channels observed, and any other subsurface features identified. The survey provided ground truth data for the geophysical surveys.

h. Installation of Monitoring Wells

Monitoring wells were placed with the CPT truck. The wells were direct-push 2 inch ID PVC wells. Locations were selected based on the results of the CPT survey.

i. Installation of Permanent Piezometers

Based on the results of the CPT surveys, a piezometer monitoring system was designed and installed to monitor changes in the hydraulic gradient throughout the site. The piezometers were equipped with instrumentation for long-term monitoring. This monitoring package provides a high degree of accuracy and can be remotely monitored.

j. Installation of Permanent Sensors and Probes

Permanent sensors and probes were selected and installed to measure, monitor, record soil moisture, evapotranspiration, infiltration, and meteorological data including

temperature, relative humidity and precipitation. The instrument/interpreter/transmitter design considered: cost, reliability, power supply, case of installation and replacement, transmission distance, and weather protection including lightning susceptibility. Electronic gages were installed for monitoring and collecting weather, and soil moisture data.

2.   Phase II - Hydrogeology Characterization

Phase II of the work was accomplished after evaluation of the data obtained during the Phase I site characterization activities. This work involved specific insitu testing of the vadose zone, aquifer, and the installation of additional sensors and monitoring instrumentation.

a.   Pumping Tests

Pumping tests were designed and conducted within the aquifer at the GRFL site. The results from site characterization data collected during the Phase I work were used to design the pumping test program.

b.   Tracer Tests

Multilevel tracer tests were performed on the unconfined water table aquifer to further characterize and quantify aquifer heterogeneities.

c.   Hydraulic Conductivity in the Vadose Zone

Vadose zone testing was conducted to determine the unsaturated hydraulic conductivity. The vadose zone characterization provided quantitative data about material physical, hydraulic, and pneumatic characteristics that influence the transport and fate of introduced contaminants, along with qualitative information regarding the subsurface geology and lithology.

d.   Air Conductivity in the Vadose Zone

Permeability tests were performed to determine the permeability of the vadose zone.

e.   Data Collection, Management and Analysis Package

The computerized data acquisition, data management and data analysis system was developed to acquire the raw data from the field, place the data into a database, provide data security, allow remote data access and experimental control, and provide an analysis and graphics package for the researcher to use in the interpretation and visualization of the data.

f.   Groundwater Flow Model

A 3-D groundwater flow model was developed and validated for the GRFL site using an appropriate existing model.

g.   Installation of Additional Sensors and Probes

The results of Phase I and Phase II hydrogeology characterization studies were evaluated to determine the need for any additional sensors and probes not specifically identified in the project plan.

3.   Emergency Groundwater Pump and Treatment System

An emergency groundwater pump and treatment system was designed and installed to provide a way to contain and treat contamination in the unlikely event of leakage from the test cell during demonstrations.

4.   Preparation of Site for GRFL

All necessary labor, supplies, transportation and equipment was provided to prepare the GRFL site for the performance of controlled field tests to establish the performance and cost-effectiveness of candidate remediation technologies.

5.   GRFL Operations Facility

The GRFL Operations Facility was equipped with instrumentation which provides the capability to perform analyses on organic compounds from the GRFL field demonstration projects.

6.   Controlled Release Cells

An initial test cell was constructed for conducting field evaluations of treatment technologies under experimental controlled releases of DNAPLs.

7.   Waste Management

A waste management plan was developed to define procedures for minimizing waste production from technology demonstrations at the Groundwater Remediation Field Laboratory (GRFL), and appropriate waste in accordance with Dover AFB requirements as well as municipal, state and Federal regulations.

8.   Site Safety Plan

A safety plan was developed to ensure that health and safety measures are followed during planned demonstrations at the GRFL. All aspects of the work will be conducted

to ensure that the GRFL demonstrations and operations are carried out in a safe manner. The safety plan is intended to act as a supplement and appendix to the existing Dover Air Force Base Health and Safety Plan (HASP).

D.   PROJECT TEAM

Applied Research Associates, Inc. (ARA) established a project team to perform the special requirements of the GRFL project. The team consisted of ARA employees and subcontractors with the skills and expertise required for characterization and development of the GRFL test site. The ARA project manager was Dr. Raymond L. Montgomery.

The ARA team included the following:

ARA Principal Investigators	Tasks Performed
• Rexford M. Morey	Surface Geophysics
• James D. Shinn	Soil Sampling
• Christopher J. Bianchi	CPT Survey
• Christopher J. Bianchi	Installation of Monitoring Wells
• Wilhelmina C. Dickerson	Installation of Permanent Piezometers
• Wilhelmina C. Dickerson	Installation of Permanent Sensors and Probes
• Susanne M. Conklin	Pumping Tests
• Stephen P. Farrington	Tracer Tests
• Christopher J. Bianchi	Hydraulic Conductivity
• James D. Shinn	Air Conductivity
• Robert E. Walker	Data Collection, Management and Analysis Package
• Raymond L. Montgomery	Emergency Groundwater Pump and Treatment System
• James A. Eddings	Preparation of Site for GRFL
• James A. Eddings	GRFL Operations Facility
• James A. Eddings	Controlled-Release Cell
• Raymond L. Montgomery	Waste Management
• Terry L. Steinborn	Site Safety Plan

Major subcontractors for the GRFL project included the following:

Subcontractor	Tasks Performed
• University of Delaware John A. Madsen	GPR Surveys

- University of Delaware   Chemical Properties
  Donald L. Sparks
- University of Delaware   Microbiology Properties
  Jeffry J. Fuhrmann
- Virginia Polytechnic Institute   Mineralogical Properties
  Lucian Zelazny
- Daniel B. Stephens & Assoc., Inc.   Vadose Zone Tests
  Jeff Havlena
- George & Lynch Company   Construct Test Cells
  Vicki Megonigal
- C^3 Environmental   Sheet Pile Sealing
  Minh Le

Each of the subcontractors were selected, because of their special expertise. The team approach used in this study provided the appropriate skills and experience for meeting the various challenges encountered during the development of the GRFL.

SECTION II

SIGNIFICANT FINDINGS

A.   INTRODUCTION

This section of the report presents basic background information on the GRFL site obtained during the site characterization and site development activities. Future demonstrators will need this information to identify appropriate demonstrations for the GRFL and to help in the development of their technology demonstration project plans. A general site layout map is shown in Figure 1.

B.   FINDINGS

1.   Results from Surface Geophysics and CPT Surveys

Each of the surface geophysical methods performed as expected relative to depth of exploration and feature resolution. The GPR surveys were the most informative, providing detailed continuous stratigraphy. Tightly coupling the surface geophysics with the cone penetrometer tests enhanced the interpretation of the subsurface geology, soil stratigraphy, and hydrogeology. As an example, preliminary interpretation of the GPR results was used to locate the initial CPT push points. The CPT soil classification was then used for the final GPR interpretation. GPR results provided a three-dimensional map of the top of the main aquitard, showing that it is continuous. Also, a well-defined clay layer, about one to two feet thick in the northern section of the site, was located and mapped at a depth below ground surface at approximately 13 feet. The layer extends south through about half of the site, where it gradually becomes less distinctly clay and transitions to a clay-rich sand.

The top of the water table was not mapped with surface geophysics because the transition from unsaturated soil to saturated soil is gradual and thick. Surface resistivity, EM-31 and EM-34 results confirmed the general subsurface electrical properties of the site, showing soil conductivity increasing with depth and a major conductivity transition at the aquitard. The seismic sections profiled the top of the aquitard.

Cone penetration tests indicated that the subsurface materials and stratigraphy are generally consistent across the site. Soils at the GRFL site consist of fine to coarse sands with varying amounts of silt, clay and gravel. A very stiff layer exists at the site at depths below ground surface of about 13 feet to 18 feet. Also present in the aquifer are clay and silt lenses. A typical profile (Sounding CPT-14) is presented in Section IV-G. The site has two notable exceptions to the above generalization of the stratigraphy. The first exception is seen in the soundings conducted in the site's northern portion. A well defined clay layer, which is about 1 to 2 feet thick, has been located at a depth of approximately 13 feet. The layer extends south through about half of the site, where it gradually becomes less distinctly clay and transitions to a clay-rich sand.

ARNOLD DRIVE EXTENDED

GRFL OPERATIONS FACILITY

EXISTING PAVED PARKING AREA

EXISTING 100KVA TRANSFORMER

HANDICAP ACCESSIBLE RAMP

4' WIDE SIDEWALK

Trench Locations

NOTE: MONITORING WELL LOCATIONS BASED ON MEAN SEA LEVEL DATUM

Note All Elevations Are Shown In Feet / Mean Sea Level

SCALE IN FEET
25 12.5 0   25   50

EXISTING TREE LINE

EXISTING FENCE LINE

AIR MOBILITY COMMAND
DOVER AIR FORCE BASE   DELAWARE
GROUNDWATER REMEDIATION FIELD LABORATORY
SITE PLAN

DRAWN BY: CAH
DESIGNED BY:
DATE: 27 MAY 96
SHEET: 1 of 3
SCALE: 1" = 50'
PROJECT NO.
DRAWING NO.

Figure 1. Site Plan

9
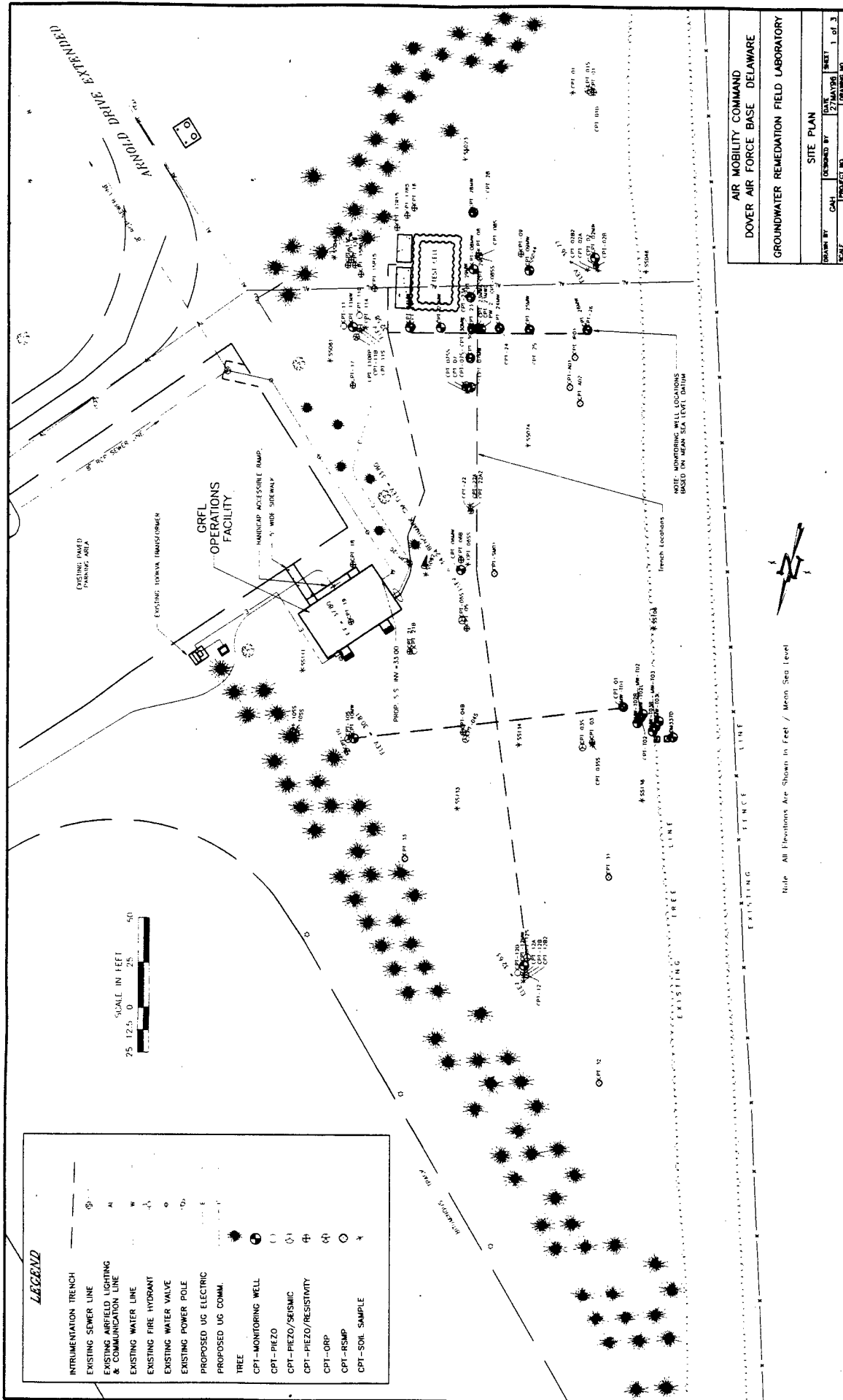
The second exception is that, below the water table, a portion of the CPT pore pressure profile lies on the hydrostatic line, indicating very clean sands. This phenomenon was only observed in CPTs 03, 04B, 10, and T–02, and occurs in a layer which lies immediately above the clay aquitard. We conclude from these observations that a high permeability sand channel may exist along this east–west line and that the channel's permeability is higher than the rest of the aquifer.

A total of 59 cone penetration tests were conducted at the GRFL site. The tip resistances vary from a peak of 4000 psi at the surface, which is representative of a very stiff soil to less than 200 psi at elevation -1 feet (msl), where the aquitard is encountered. The variations in the tip resistance reflect variations in soil strength, which is directly related to soil type. The friction ratio was generally less than 1, indicating sandy soils. At several depths, the friction ratio increases, indicating an increase in the fine-grained soil content. From elevation 22.5 to 15 feet, the tip resistance decreased and the friction ratio increased, indicating a fine-grained soil. Below elevation 15 feet this trend reversed indicating a more coarse grained soil. The clay aquitard was encountered at elevation -1 feet (msl) and was readily identified by the rapid decrease in tip resistance and corresponding increase in friction ratio and penetration pore pressures.

The CPT survey determined that the aquitard is a continuous clay layer about 20 feet thick. No characterization was done beneath the aquitard.

2. Results from Soil/Sediment Chemical Properties Analyses

Chemical analyses indicate that the soils are slightly to moderately acidic, with pH ranging from 4.9 to 6.4. Organic matter (0 to 1.7%) and clay contents (7.9 to 46.9%) are quite low, typical for Coastal Plain soils. The soils are generally sandy. Extractable levels of Ca, Mg, and K were higher than the exchangeable levels of the cations since a stronger extractant was used, and both readily exchangeable (those on planar, external sites of clay minerals and organic matter) and some edge site ions were extracted. The order of extractable ions in the soils is Ca > Mg > K > Fe > P > Mn > Zn > Cu. Both the effective CEC and the CEC at pH 7.0 were reflective of the low quantities of clay and organic matter Exchangeable acidity was quite low, reflective of the moderately acidic pH of the soils. Soluble salts were very low, as one would expect for acidic soils.

3. Results from Soil/Sediment Microbiology Properties Analyses

Microbiological analyses indicated that, both heterotrophic and denitrifying bacteria were present at detectable levels in all samples. Bacterial numbers generally decreased with depth, although in some cases counts remained elevated at considerable depths. The autotrophic nitrifying bacteria were only detected in the more shallow samples. The eukaryotic fungi and protozoa were also found to be more prevalent at shallow depths, although significant populations were detected as deep as 37 feet in some instances.

There was little microbiological evidence that extensive anaerobic metabolism commonly occurs in any of the soil-sediment samples examined. Anaerobiosis can only develop in soils under conditions of reduced O_2 diffusion (generally due to elevated soil moisture) in combination with high rates of microbial metabolism. Denitrifying enzyme activity was low in all samples examined and detectable only in the surface samples.

4.   Results from Soil/Sediment Mineralogical Properties Analyses

Analyses performed on the GRFL soil samples revealed a wide range of mineralogical properties. The highest total sand content (93%) was found between elevations 23 and 29 feet. msl at CPT 12 with a preponderance of sand in the medium (42%) and fine (28%) fractions. A high total sand fraction (84%) also occurred between elevations 4 and 10 ft. msl at CPT 22. Total clay dominated (47%) the soil between elevations -10 and -12 feet msl at CPT 12 and was a significant component (36%) between elevations 20 and 22 feet msl at this location. Significant silt (40 to 49%) occurred between elevations -10 and -12 feet msl, and between 20 and 22 feet. msl at CPT 12. The soil contained 35% silt at between elevations -7 and -9 feet. msl at CPT 10.

These soil/sediment samples contained significant iron oxides and noncrystalline material. The highest extractable iron oxide occurred in samples taken from CPT 12, between elevations -10 to -12 feet. msl (7.08%) with intermediate quantities in samples taken from CPT 11, between elevations 10 to 18 feet. msl (2.12%). The bright red color would support the dominance of hematite although goethite could also be present. Much of this iron oxide occurred as coatings on other particles.

5.   Pumping Tests

Two pumping tests were conducted, with one located near the test cell and the other located at an existing monitoring well. The pumping tests successfully resulted in the following parameter estimations. The vertically averaged horizontal transmissivity of the aquifer ($T_{x,y}$), the specific yield (S_y), the storativity (S) and, the vertically averaged horizontal hydraulic conductivity ($K_{x,y}$) are presented in Table 1.

TABLE 1.   ESTIMATED PARAMETERS FROM AQUIFER TESTS.

Parameter	Estimated Value
$T_{x,y}$	129 ft^2/day (1.39 cm^2/sec)
S_y	0.27
S	0.0003 ft^{-1} (0.00001 cm^{-1})
Kx, y	8.5 ft/day (0.003 cm/sec)

The values reported in Table 1 are average values; significant variation from these values occur in the clay rich and clean sand layers.

In addition to these parameters, the pumping test highlighted how silt in the formation influences well performance. Significant amounts of silt observed during pumping were thought to inhibit the yield a CPT-pushed well could sustain. Advanced well-development techniques using surge blocks combined with pumping significantly increased the well's yield. Installation and development of a drilled well surrounded by a sand pack did not produce a significant increase in the area's well yield. The drilled well and the CPT-pushed well produced the same yield after development. Therefore, more sophisticated development techniques than typically used should be applied at this site due to the presence of large amounts of silt.

The pumping test also revealed the presence of only slight anisotropy. This was deduced from analysis of the drawdown in the surrounding wells during the pumping test.

A low permeability skin was expected near the well screen during the slug testing caused by the method used in well installation. However, analysis of the slug test data indicated no appreciable skin effect for these tests.

Analysis of the drawdown curves from the pumping tests was used to determine the radius of influence and to determine the spacing required between the emergency pumping wells. The radius of influence from the wells was determined to be 30 feet. Emergency pumping wells were placed on the down-gradient sides of the cell and on 30 feet centers or less. The spacing between the wells ensures that the flow fields from nearby well overlap. This assures capture of flow from the cell if any contaminant leaks from the test cell during a demonstration.

6.   Results from Tracer Tests

Although the tracer test did not meet the objective of quantifying dispersion and depth-dependent variability in horizontal hydraulic conductivity at the GRFL, important findings were made. The tracer test effort identified a channel in the vicinity of the tracer test domain which has higher hydraulic conductivity than the rest of the site. This channel is located along the north end of the GRFL area. The top of the aquitard in the vicinity of the channel is lower in elevation than elsewhere on the site and a layer of clean sand making up the channel overlies the aquitard. Understanding the structure and presence of this more conductive channel is important because it impacts flow and transport behavior at the north end of the GRFL site, as evidenced by its influence on the tracer test. For example, the extraction well used in the tracer test showed much higher yield than wells installed at other areas of the site, producing a sustainable flow rate of 3 gpm. Pumping at this rate produced only 1/10th of a foot drawdown in the tracer test wells placed ten feet away. This drawdown is nearly the same as that produced by a 1 gpm flow rate from a well used in the first pumping test, south of the tracer test. A close look at CPT push logs in the vicinity of the tracer test shows the channel to begin at the wells nearest the extraction well. Water is being supplied to the extraction well from clean sand in the channel. The high flow rate from the well did not increase the groundwater flow enough in the tracer test area to qualify as an induced-gradient test.

7.   Results from Hydraulic Conductivity Tests in the Vadose Zone

Hydraulic conductivity estimates of the vadose zone were determined using an Instantaneous Profile (IP) test. The test relied on measurements of soil moisture and soil tension taken at depths of 0, 2, 4, 8, 16, and 20 feet. These data were used to parameterize a closed-form analytical equation (van Genuchten 1980) (Reference 1) which relates hydraulic conductivity to moisture content and soil water potential (pressure head). The soil moisture measurements were made using the TDR (time domain reflectometry) probe designed and fabricated by ARA. All sensors for this test were installed using the CPT system, and the test data were collected, using the GRFL data acquisition system. Complete curves of hydraulic conductivity versus soil water potential and moisture content for each of the five depths listed can be generated from these results.

Results obtained from the infiltration test show that the unsaturated hydraulic conductivity varies as the fine-grained content varies, as expected. While the site of the infiltration test is well characterized, the limited data set (moisture contents at four depths) can not be widely extrapolated to the GRFL site. Soil types, and in particular, the fine- grained soil content at the site can vary widely over short vertical and lateral distances. The current data base are insufficient for developing a correlation to the more extensive CPT data base. Additional testing to develop soil moisture versus hydraulic conductivity should be conducted using laboratory techniques to extend the current database and to provide a data base for correlation to the CPT.

8.   Results from Air Permeability in the Vadose Zone

Air Permeability in the Vadose Zone was determined with two different field tests, as described in Section V-D. One test was conducted with a conventional injection/extraction well and air pressure monitoring points. This test measures the average air permeability over the screen length of the well between the well and the monitoring points at one location on the site. The air conductivity determined from this test was 2.2×10^{-9} ft^2 to 2.1×10^{-6} feet^2. The variation depends upon the analysis method used to estimate the air conductivity.

The other method used a modified ConeSipper® with the CPT system, and measures the air permeability horizontally and vertically at discrete locations on the site. Examination of the CPT-determined air permeability indicates significant variation in the vertical profile at the GRFL site. In layers identified as finer grained soils, the air permeabilities were calculated to be as low as 1.6×10^{-9} feet^2. At some locations in adjacent layers, the air permeability increases rapidly to 1.1×10^{-6} feet^2, which constitutes an increase of 3 orders of magnitude. Changes such as this reflect the influence of the fine-grained content of the soil. The CPT estimated air permeabilities in the vadose zone are more variable than those values estimated from the monitoring well test. This result was expected, as the air permeability testing in conventional monitoring wells will reflect spatially averaged permeability values while the CPT estimated air permeabilities are measured at discrete locations.

9.   Groundwater Flow Model

Two models have been produced. The first represents the natural groundwater flow field with no pumping. This condition was well predicted by the model. The second simulates the pumping test we conducted at the GRFL. For this case, the model overpredicted observed drawdown by 13 percent. A close-up view of the two layers near the pumping well, as well as predictions of groundwater head in the absence of and during pumping, is presented in Section V-F. The parameters that were input to the model are presented in Table 18, in Section V-F.

10.   Data Collection, Management and Analysis Package

The computerized data acquisition, data management and data analysis system was developed to acquire the raw data from the field, place the data into a database, provide data security, allow remote data access and experimental control, and provide an analysis and graphics package for the researcher to use in the interpretation and visualization of the data.

The major focus of the data management task was to provide the necessary software and hardware for the system. Relevant findings are limited to the design of the database scheme. The structure of the database must be planned and reviewed almost continually.

SECTION III

SITE CHARACTERIZATION OVERVIEW

A.   INTRODUCTION

The site characterization effort at the GRFL site focused primarily on the water table aquifer formed by the Columbia formation which overlies the Calvert formation which is an aquitard. Refer to USACE, Dames and Moore, (1995) (Reference 2) for a detailed description of previous work at the Dover Site. The primary objective of the Phase I characterization program was to provide detailed stratigraphy of the Columbia formation, in which the experiments will be conducted, and to provide information on the continuity and thickness of the aquitard. The objective of the Phase II characterization program was to provide information on the hydraulic and transport properties of the GRFL site. Characterization methods used during the Phase I and II efforts included: geophysical methods, cone penetration testing, soil sampling, lab analysis of soil samples, and aquifer tests. A general site characterization map is provided in Figure 2.

In addition to the geologic and hydrogeologic site characterization, a state-of-the-art permanent monitoring control and data storage system was developed and installed at the site. This system monitors and stores weather information, aquifer water levels and temperatures, and soil moisture in the Columbia formation. All of the sensors are logged with a Campbell Scientific CR10, which is linked to an on-site data storage system. Experimenters can add sensors to meet their individual needs and the sensors can be logged by the system as long as they are compatible with the CR10. All of the information is stored in a database at the GRFL site and can be accessed both on site and remotely.

Each of the characterization sub-tasks is detailed in the following subsections.

B.   SITE CHARACTERIZATION OBJECTIVES

The purpose of the site characterization effort was to determine the pertinent geologic and hydrogeologic parameters of the GRFL site. More specifically, the geologic parameters include the site stratigraphy, the soil physical, chemical, microbiological and mineralogical properties and the location of any buried channels or objects. The hydrogeologic parameters include the transmissivity, storage and dispersive characteristics of the aquifer, the hydraulic conductivity and air permeability of the vadose zone, and the natural gradient of the water table. Data from the characterization program were analyzed and used to generate geologic cross-sections of the site. Using geostatistical techniques, three dimensional maps of the site stratigraphy and hydraulic conductivity were generated. These data were then used to develop a three-dimensional hydrogeologic model of the site.

In addition to parameter determination, a monitoring well network was installed to monitor long-term changes in water levels and temperatures. Also, some of the wells

ARNOLD DRIVE EXTENDED

GRFL OPERATIONS FACILITY

HANDICAP ACCESSIBLE RAMP

5' WIDE SIDEWALK

TEST CELL

EXISTING PAVED PARKING AREA

EXISTING 100kVA TRANSFORMER

PROP SS INV =31.00

BENCHMARK

Trench Locations

NOTE: MONITORING WELL LOCATIONS
BASED ON MEAN SEA LEVEL DATUM

EXISTING TREE LINE

EXISTING FENCE LINE

Note All Elevations Are Shown In Feet / Mean Sea Level

LEGEND

INTRUMENTATION TRENCH	
EXISTING SEWER LINE	
EXISTING AIRFIELD LIGHTING & COMMUNICATION LINE	
EXISTING WATER LINE	
EXISTING FIRE HYDRANT	
EXISTING WATER VALVE	
EXISTING POWER POLE	
PROPOSED UG ELECTRIC	
PROPOSED UG COMM.	
TREE	
CPT-MONITORING WELL	
CPT-PIEZO	
CPT-PIEZO/SEISMIC	
CPT-PIEZO/RESISTIVITY	
CPT-ORP	
CPT-RSMP	
CPT-SOIL SAMPLE	
ADJOIN'T SURFACE CONTOUR IN FT/MSL	——15——

SCALE IN FEET
25 12.5 0   25   50

AIR MOBILITY COMMAND

DOVER AIR FORCE BASE DELAWARE

GROUNDWATER REMEDIATION FIELD LABORATORY

SITE CHARACTERIZATION PLAN

DRAWN BY	DESIGNED BY	DATE	SHEET
CAH	CAH	27 MAY 96	3 of 3
SCALE — 50'	PROJECT NO	DRAWING NO	

Figure 2. General Site Characterization Map

16

were designed to serve as extraction wells if contaminant leaked from the test cell. In the event of leakage, these wells would be connected to the emergency pump and treatment system to contain the plume, extract the contaminants, and treat the extracted groundwater. Selected groundwater wells around the cell were further developed to increase well yield and provide the ability to influence the groundwater table. Using the portable Grundfos 2-inch pumps, the selected wells can capture the groundwater flowing directly around the cell.

The information collected during the characterization effort provides a database for future experimenters at the GRFL site. This database is installed on the GRFL field monitor computer (FMC).

C.   SITE DESCRIPTION

The GRFL site covers an area of approximately 3.5 acres, extending 230 feet in the east-west direction and 600 feet in the north-south direction. There is approximately a 6.6 foot change in surface elevation in the east-west direction, as shown in Figures 3 and 4.

The unconfined aquifer in which the experiments were conducted is part of the Columbia formation. Generally this formation consists of fine to course sand with varying amounts of silt, clay and gravel. A very stiff layer exists at depths of about 13 feet to 18 feet and clay and silt lenses are present. A well defined two foot thick clay layer was located in the northern part of the site at a depth of approximately 13 feet, as shown in the cross section shown in Figures 3 and 4. The layer extends south through about half of the site where it gradually "pinches out". The thickness of the Columbia formation varies from 36 to 47 feet across the site from northwest to southeast. The underlying Calvert aquitard is approximately 20 feet thick and consists of a dense gray clay with fine sand laminations. Below the aquitard is the Fredrica formation, a confined aquifer. The water table in the Columbia aquifer is at about 9 feet (msl).

Mineralogy testing of samples from the site indicate a predominance of quartz sand with some K-feldspars. Iron oxide coating of the grains was observed and is a likely source of the cementation observed in the near surface layers. X-ray defraction testing on the clay size components indicates the presents of kaolinite and mica, with several of the tested samples containing montmorillonite and some halloysite. Further details on the mineralogy testing are contained in Section IV-F.

The geophysical testing consisted of four types: ground penetrating radar surveys conducted at several frequencies, surface resistivity surveys, high resolution seismic and low frequency electromagnetic surveys. Data collected during the observation were used to determine the general layering at the site, map the aquitard, and select locations for CPT soundings. Upon completion of the geophysical surveys, CPT was conducted to determine detailed site stratigraphy and to obtain soil samples for geologic logging and laboratory testing. Locations of all CPT soundings, monitoring well locations, and soil sample locations are plotted in Figure 5 through 8. More information is provided in Appendix G. Locations of the aquifer characterization tests (i.e. the pumping, slug, tracer vadose zone hydraulic permeability and air permeability test) are plotted in Figure 9.

Running Track

CPT-12D   A'

34.0   33.0   32.0   31.0

CPT-04S

35.0

GRFL
Building

36.0

CPT-05S

CPT-06B

CPT-22

Parking Lot

Legend

31.0   Minor Contour (ft)

35.0   Major Contour (ft)

CPT Location

Cross-Section Line

CPT-07

CPT-30

CPT-23

CPT-29

Test Cell

CPT-08S

Arnold Drive Ext.

CPT-28

0   50   100

CPT-01D

A

(Feet)
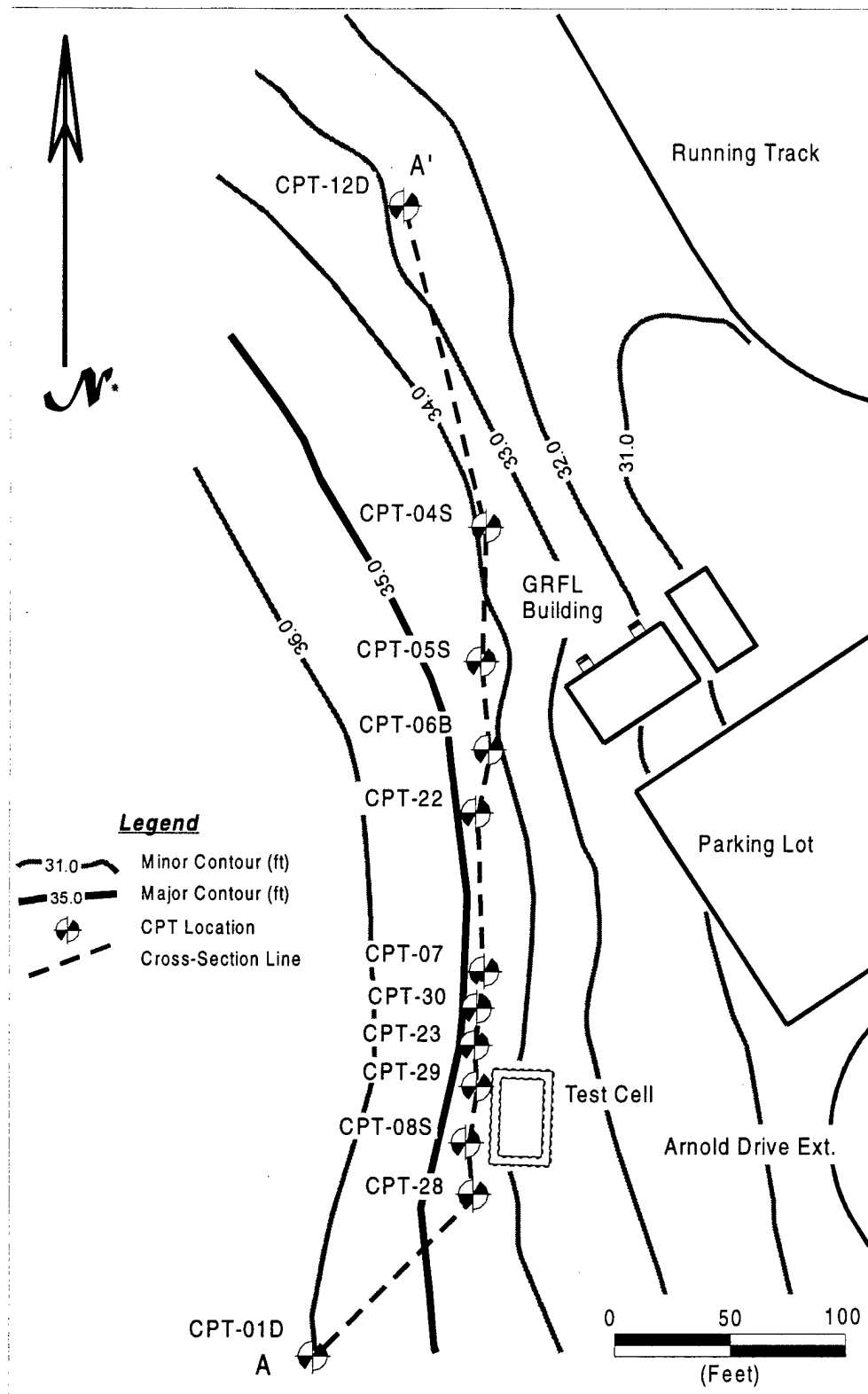
* North based on GRFL coordinate system

**Figure 3. Topography of the GRFL Site Showing the Location of Cross
Section A-A Shown in Figure 4.**

18

Figure 4. Cross-Section A-A ' Showing Elevation of the Ground Surface and the Aquitard.

19
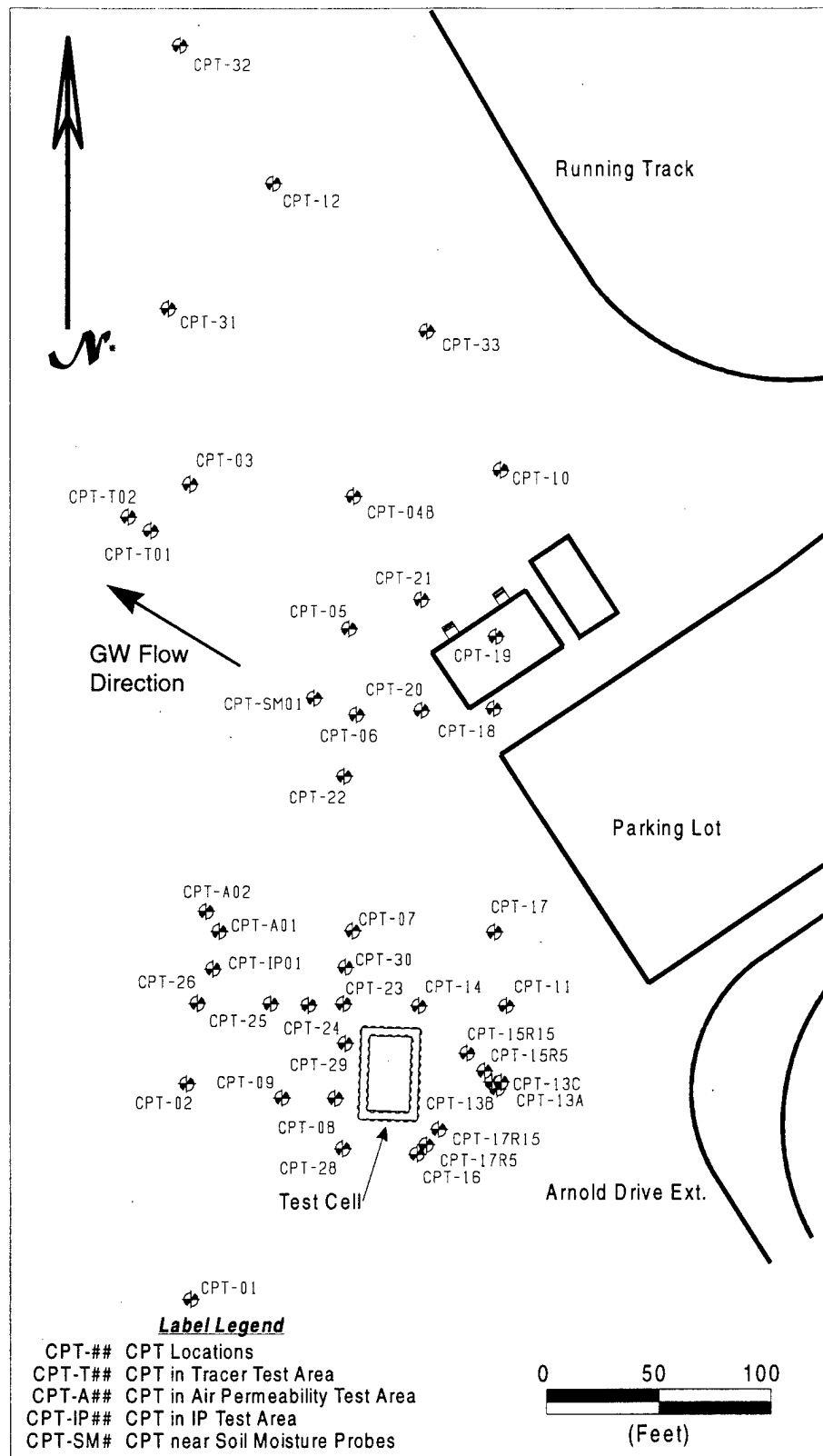
Figure 5. GRFL Site Map Showing the Locations of All the CPT Performed at the Site.
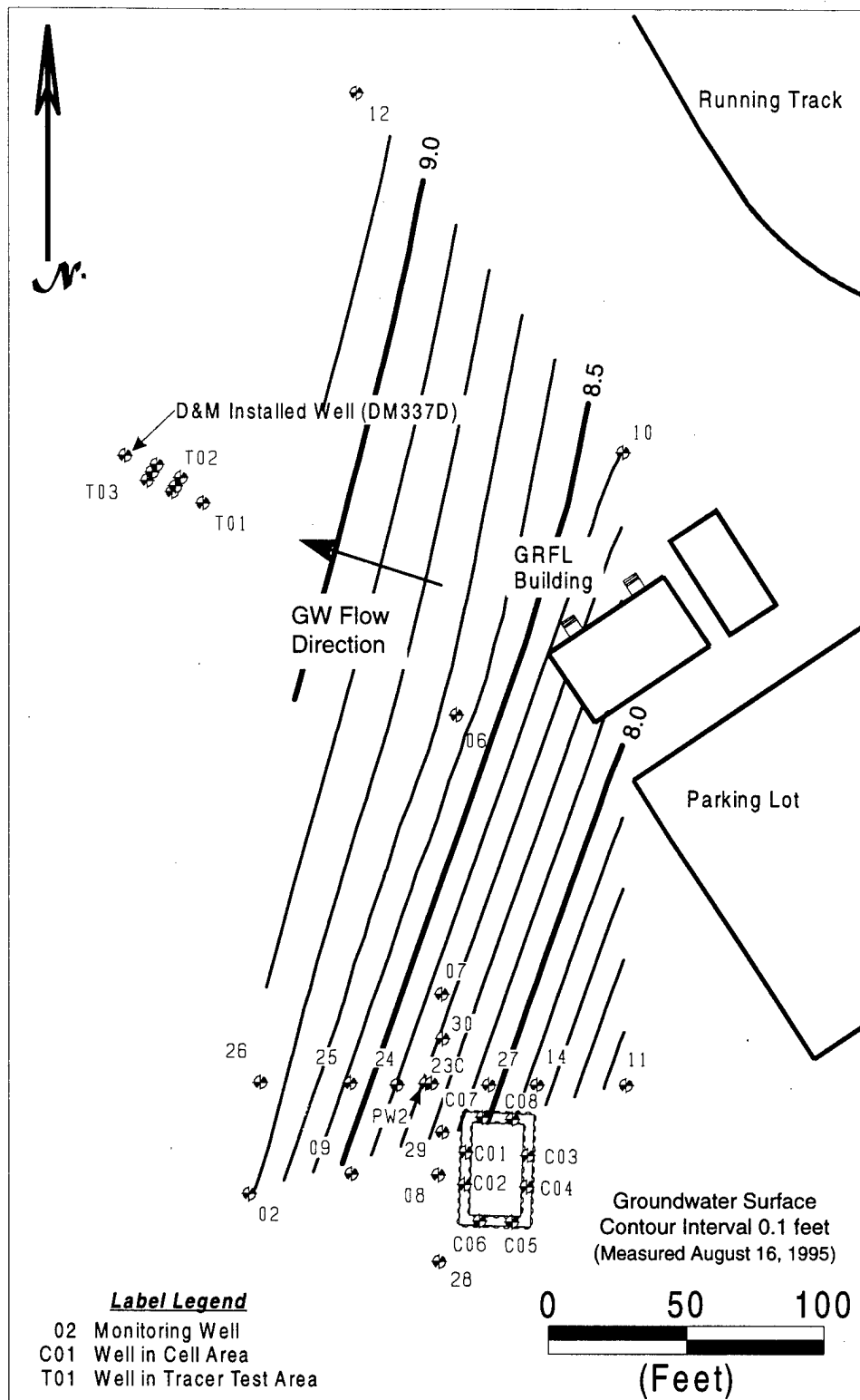
Figure 6.   GRFL Site Map Showing Location of All Monitoring Wells Installed at the Site and the Groundwater Surface Measured August 16, 1995.
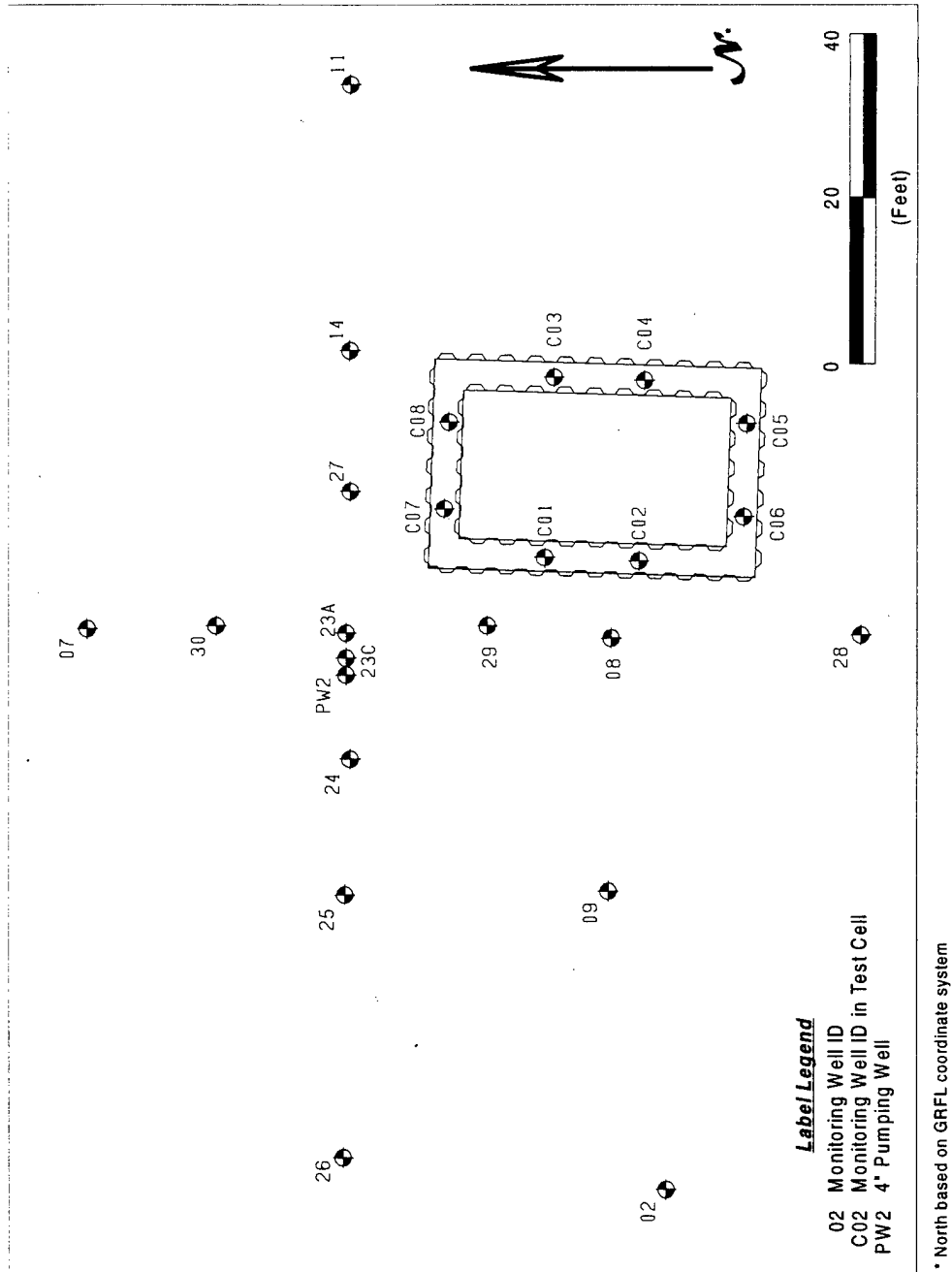
Figure 7. Expanded View of the Locations of the Monitoring Wells Installed in the Cell Area.

Running Track

CPT-12B2
CPT-12B
CPT-12A

SS136

SS133

N*

CPT-03SS   SS134

CPT-10SS

GW Flow
Direction

SS111

SS106

CPT-06SS
SS092

CPT-22A2
CPT-22A

Parking Lot

SS074

CPT-07SS

CPT-23A

SS061

CPT-11B
CPT-11A

CPT-02B
CPT-02B2
CPT-08SS

SS046

CPT-02A   SS044

SS041

Arnold Drive Ext.

SS023

0   50   100

SS023

CPT-01

(Feet)
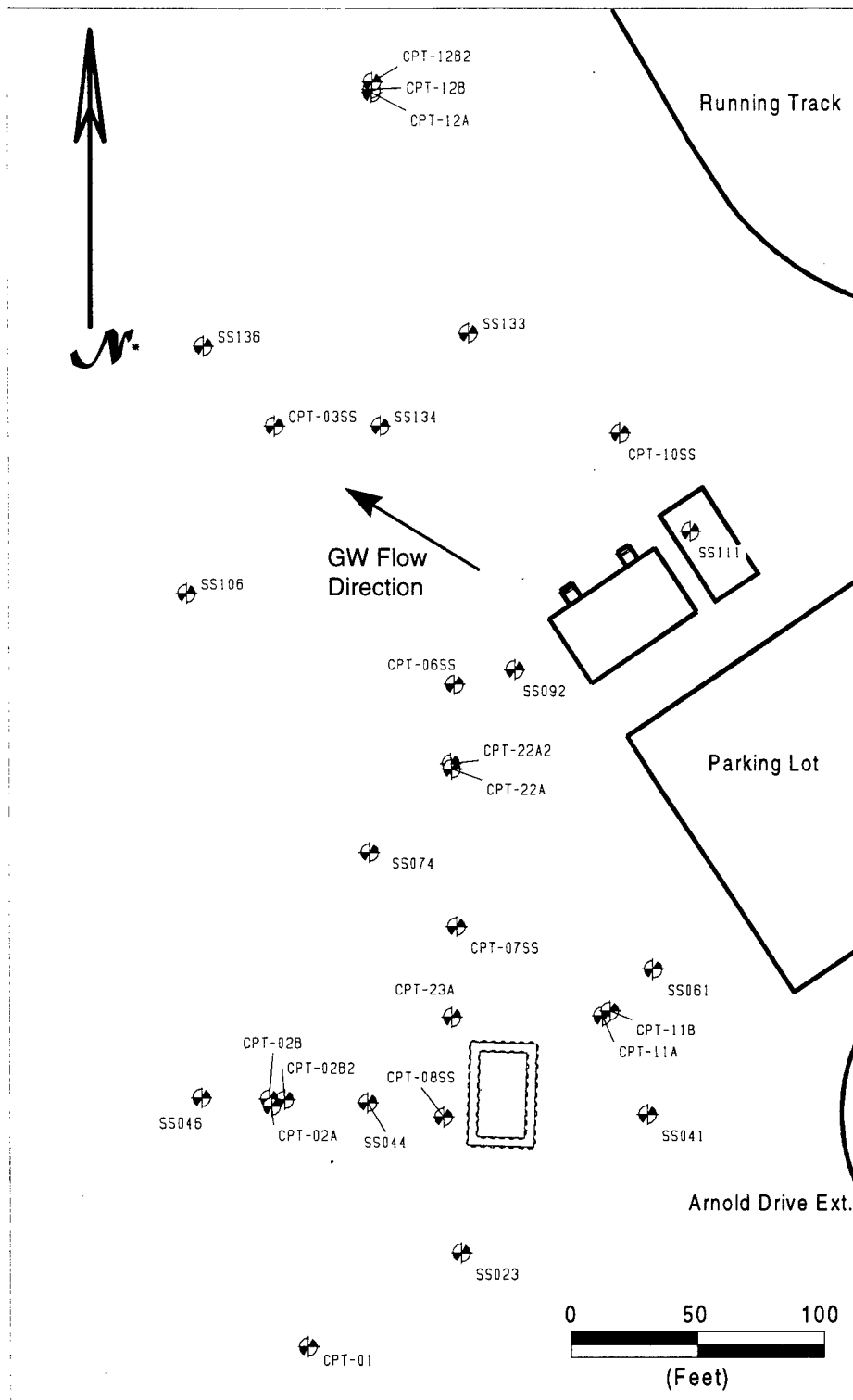
* North based on GRFL coordinate system

**Figure 8.   GRFL Site Map Showing the Locations of All the Soil Sampling
Performed at the GRFL Site.**

23
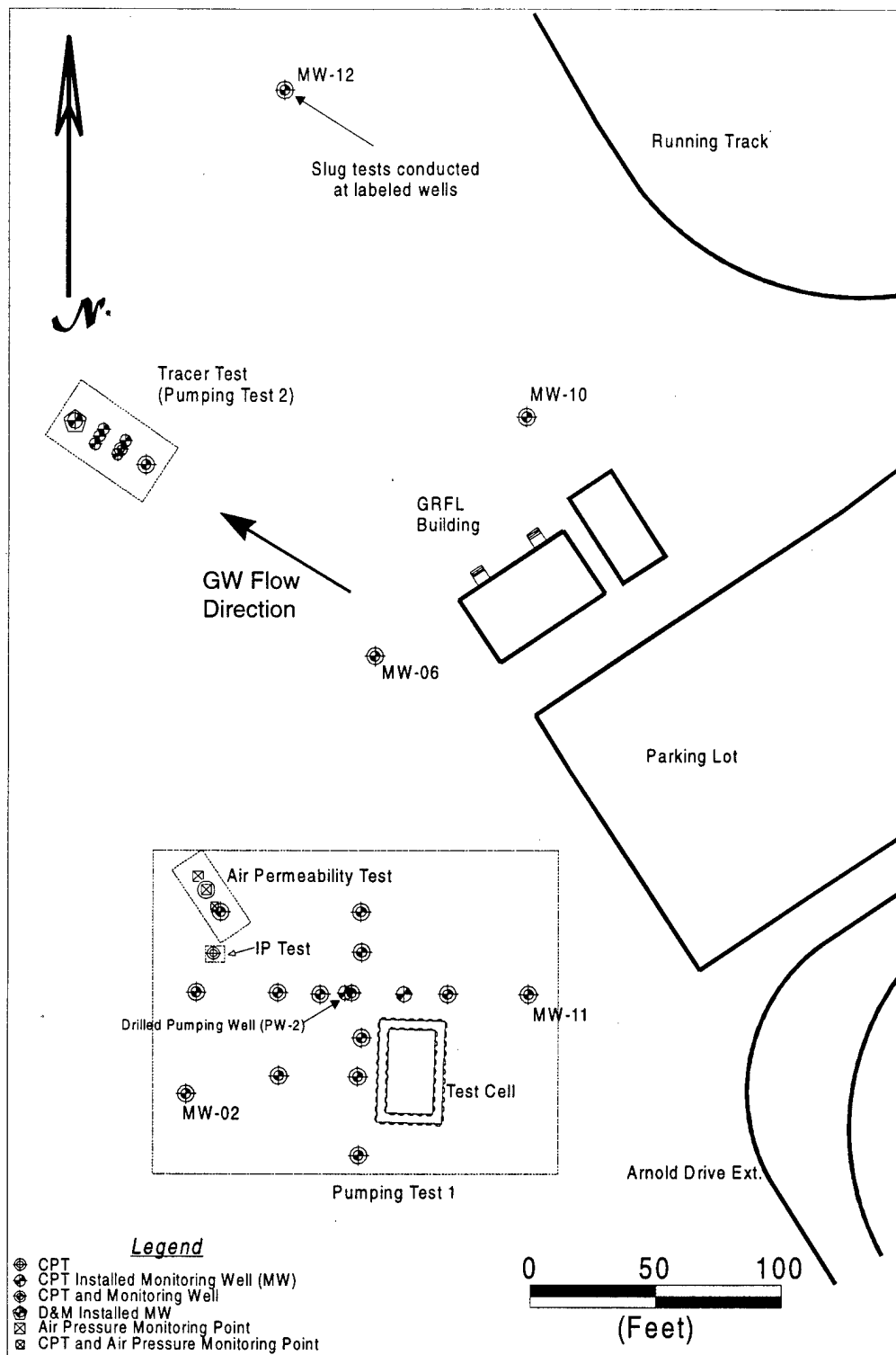
Figure 9. GRFL Site Map Showing the Locations of the Aquifer and Vadose Zone Characterization Tests Performed at the Site.

CPT was also used to install monitoring wells and monitoring instrumentation, such as soil moisture, temperature probes and air pressure monitoring points used in collection of the air permeability data.

Details of testing conducted to determine the site stratigraphy and aquifer characteristics are discussed in more detail in the following section, along with analysis of the results.

SECTION IV

PHASE I - HYDROGEOLOGY CHARACTERIZATION

A.   SURFACE GEOPHYSICS

1.   Objective

The objective of the surface geophysics investigations was to gather subsurface information for use in selecting the initial test cell location and locations for future test cells.

2.   Approach

Surface geophysical surveys were performed during the summer of 1995. A 10 meter by 10 meter (32.8 feet) grid was established with surface markers, along which the geophysical data were recorded. Figure 10 shows the this grid layout at the GRFL site. The x, y, z location of each grid point was surveyed using a laser theodolite. Surface geophysical surveys included:

- High-resolution seismic
- Surface resistivity
- Low frequency electromagnetics
- Ground penetrating radar

At the conclusion of the geophysical surveys, cone penetrometer tests were performed. Preliminary interpretation of the Ground Penetrating Radar (GPR) data was used to locate the initial CPT test points. The CPT investigation was designed to help classify soils in the upper and lower aquifers and estimate the hydraulic properties of the aquifers and the confining clay layer. CPT was also implemented to determine soil resistivity, pore pressure, and to provide support of ground-truth for the geophysical surveys.

High-Resolution Seismic. The seismic survey was carried out by Drs. Katharine Kadinsky-Cade and Steve Cardimona of the Air Force Phillips Laboratory, Hanscom AFB, MA. They used a variety of seismic sources for shallow exploration (hammer, vibrator and shot gun shells). Multiple geophone arrays were used for receiving subsurface reflections. This work was funded by the Phillips Laboratory. They used GRFL as a test site of opportunity, agreeing to exchange seismic results for ground truth data.

Surface Resistivity. Resistivity techniques use electrodes in contact with the ground to measure electrical resistivity. The depth of investigation is a function of the electrode spacing and geometry (larger spacings see deeper but with reduced resolution). By measuring and mapping the changes in electrical resistivity, clay lenses,
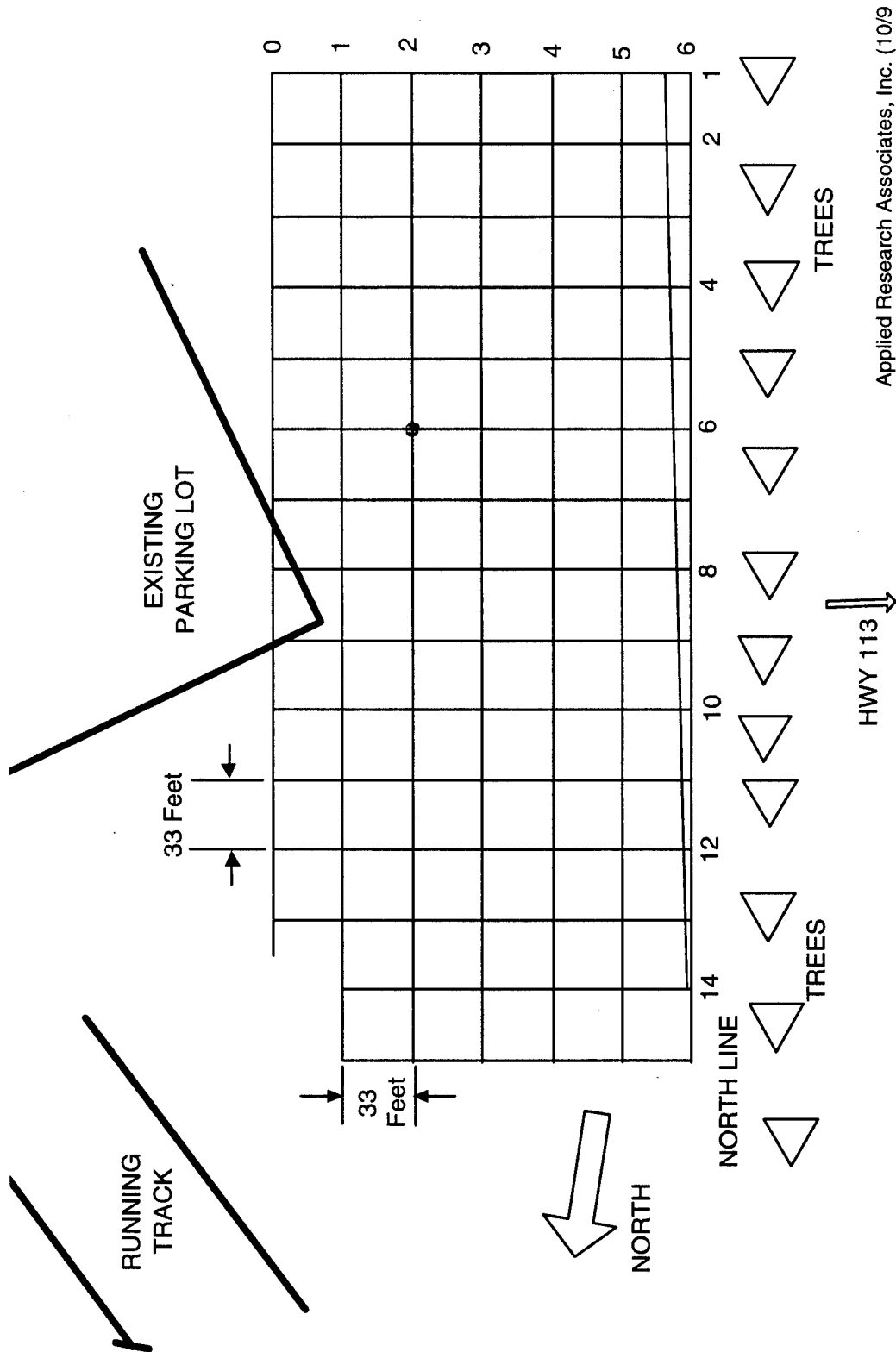
Figure 10.   Geophysics Survey Grid for Groundwater Remediation Field Laboratory , Dover AFB, DE.

Applied Research Associates, Inc. (10/9

clay layers and inhomogeneities in the geology can be located. Kick Geoexploration of Dunstable, MA performed the resistivity survey (see Appendix A).

Low-Frequency Electromagnetics. Geonics EM-31 and EM-34 were used to measure electrical conductivity by inducing currents in the earth and measuring the secondary magnetic field generated by the induced currents. The depth of investigation is a function of the instrument coil spacing and orientation, frequency of measurement, and the electrical conductivity of the ground. The EM-31 operates at a higher frequency than the EM-34; therefore, the depth of investigation is greater for the EM-34. Kick Geoexploration performed the EM-34 survey and Phillips Laboratory performed the EM-31 survey.

Ground-Penetrating Radar. GPR measures changes in the propagation of electromagnetic energy in the ground and is very sensitive to water content and bulk density. Thus, GPR is a sensitive indicator of water content and soil stratification. GPR works well in high electrical resistivity environments such as dry or freshwater-saturated sands and gravels; low resistivity materials such as clays severely limit the depth of penetration and effectiveness of GPR. Also, low radar frequencies penetrate deeper than higher frequencies; however, resolving the depth and thickness of layers is better at higher frequencies.

The University of Delaware made GPR measurements at 25, 50, 100 and 200 MHz using a Sensors & Software, Inc. system. The Colorado School of Mines made GPR measurements at 300 and 500 MHz using a Geophysical Survey and Systems, Inc., (GSSI) system. GPR measurements were made by Hager GeoScience, Inc., Waltham, MA, at 20, 80 and 100 MHz using GSSI equipment. Measurements were made along each of the grid lines, north-south and east-west (see Figure 10).

3.   **Results**

The GPR results were the most definitive in relation to mapping subsurface stratigraphy and water table at the site. Combined with the CPT soil characterization results, subsurface layers were identified and continuously mapped. The site consists of two aquifers, separated by an 30.4-to 45.6-foot-thick clay layer located 34.2 to 49.4 feet beneath the ground surface. The upper unconfined aquifer is composed of a heterogeneous mixture of sand, with occasional lenses of gravel and clay. The water table is approximately 26 feet below ground surface. Figure 11 shows the detail of the aquitard as mapped from the radar data. Figure 12 is a contour map of this clay layer. Figure 11 does not cover the entire site (refer to the aquitard contours shown in Figure 2 for area covered in this figure). The clay layer at the north end of the site prevented the GPR from detecting the aquitard. Additional GPR-interpreted sections are presented in Appendix A. In general, GPR results showed good correlation with CPT logs.
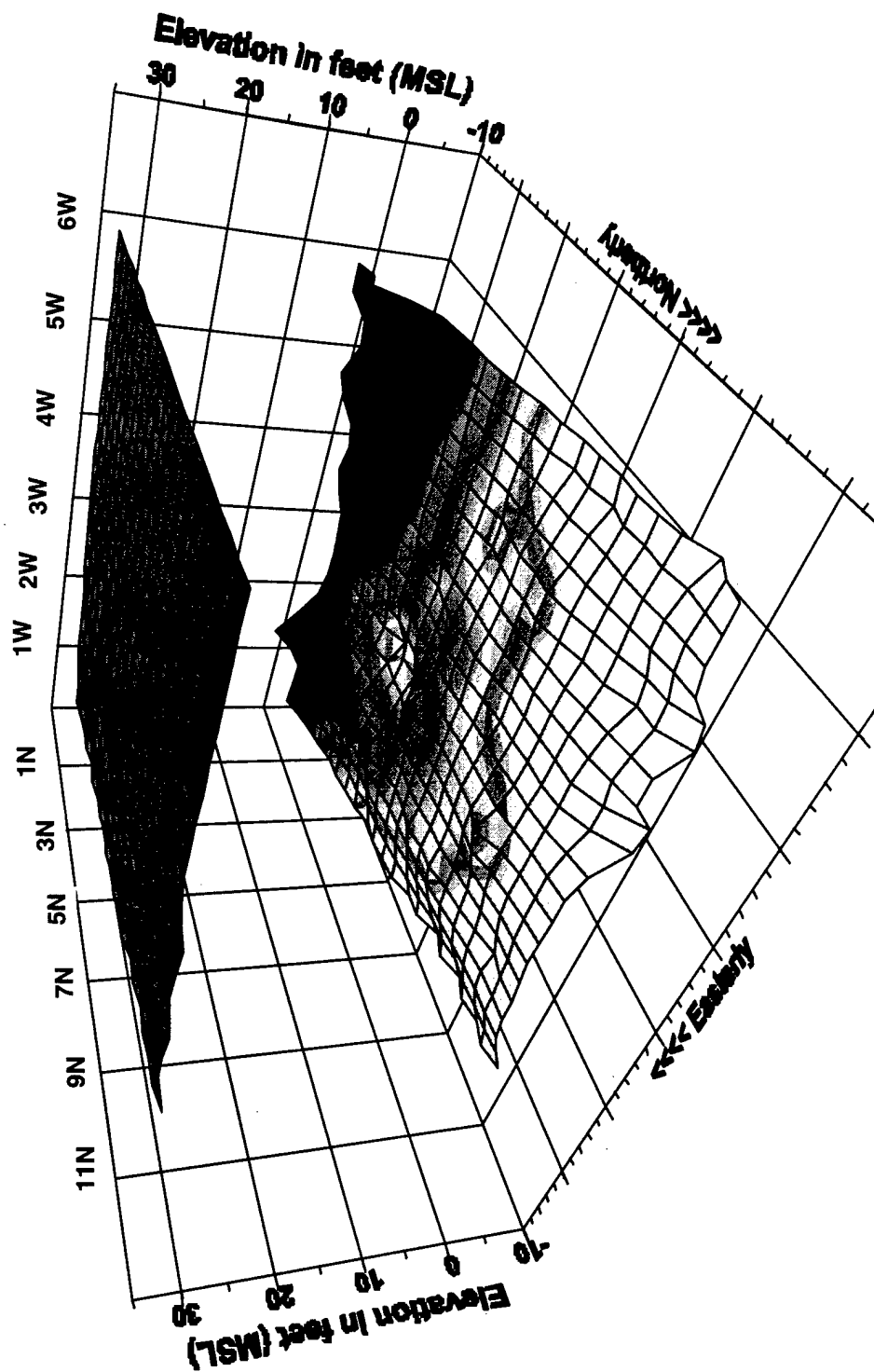
Figure 11. Ground Surface and Surface of Aquitard in Southern Half of Site. Aquitard Mapped from GPR Data.

29
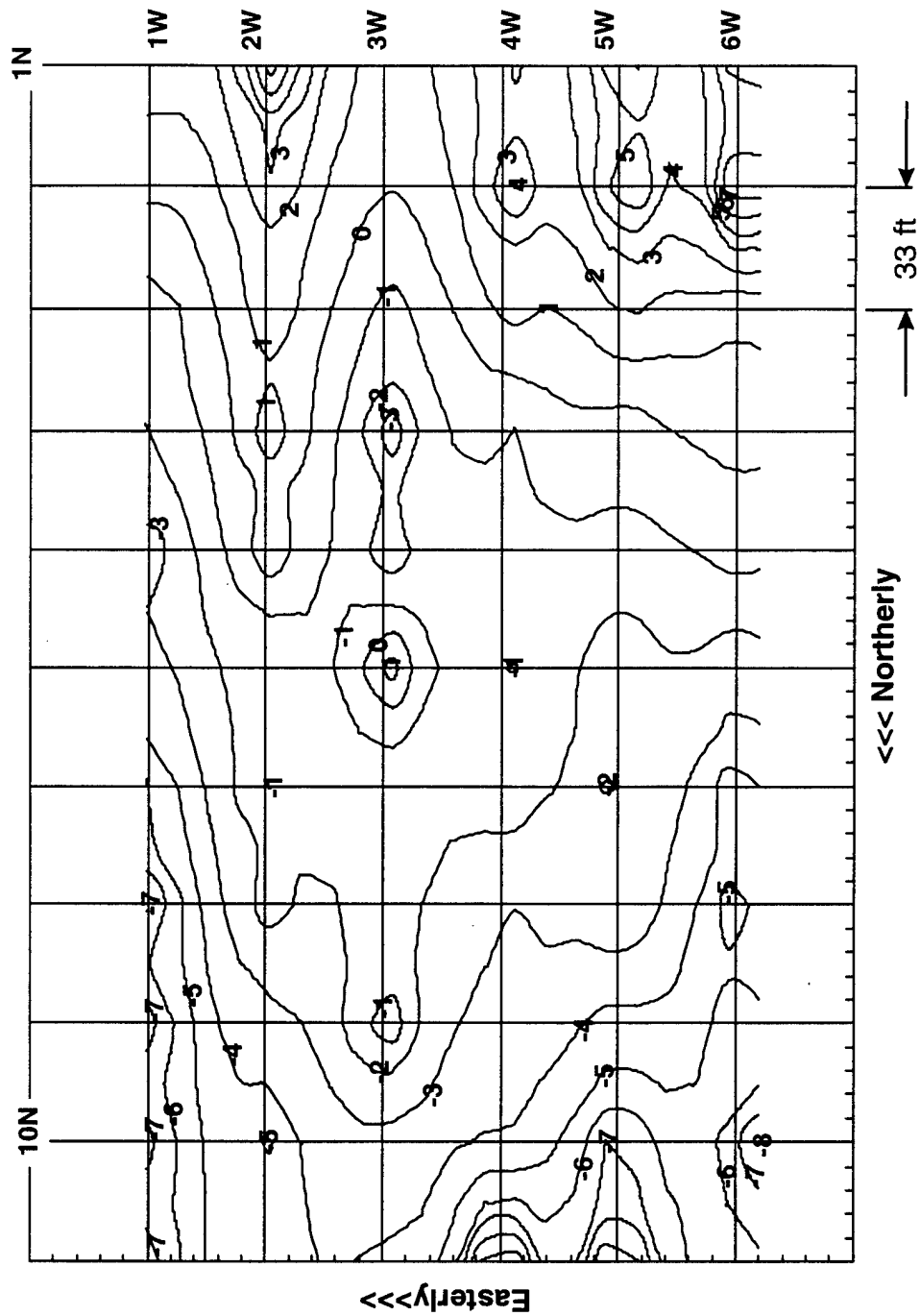
Figure 12.   Aquitard Surface in Southern Half of the Site Mapped from GPR Data (contours feet MSL).

Seismic results correlated with the main features of the radar data, profiling the top of the aquitard. CPT vertical seismic logs were used to calibrate and support the seismic interpretation. In general, the seismic data analysis did not show any results that conflicted with the CPT data or the radar interpretations. Field evaluation of the EM-31 data showed that the readings did not change very much in the top 3 meters (10 feet), the expected depth of penetration.

Results of the surface resistivity and the EM-34 surveys are documented in Appendix A. Five layers were identified from the resistivity soundings:

- Layer 1, about 3 feet thick, is the surficial layer which may contain sand and fill.
- Layer 2, about 20 feet thick, is an unsaturated sandy layer with a pronounced decrease in resistivity from south to north, indicating an increase in clay/silt materials toward the north end.
- Layer 3, about 26 feet deep, is a saturated sediment; materials in Layer 3 are similar to those in Layer 2 and are close to or below the water table.
- Layer 4, clay/silt, corresponds closely with the upper surface of the aquitard indicated in borings and CPT, some sand may be present in this layer.
- Layer 5, about 36 to 46 feet deep, is a low resistivity, clay rich material, extending to considerable depth.

All the field data from the seismic, GPR, and EM-31 surveys are archived on six CD-ROMs for use by other investigators. Copies of these files are provided in Appendix A: Surface Geophysics. Partial support for this research was provided by the Air Force Office of Scientific Research (Phillips Laboratory Task 2302GN). Additional CDs can be obtained from Dr. Steve Cardoimona, USAF Phillips Laboratory, Earth Sciences Division, 29 Randolph Road, Hanscom AFB, MA, 01731-3010, (617) 377-2611.

4.   Discussion

All the surface geophysical data produced the same general results about the site geology. The main difference between each of the methods is the depth of exploration and resolution. GPR, operating at higher frequencies, had higher resolution than the resistivity and EM methods. Tightly coupling the surface geophysics with the cone penetrometer tests enhanced the interpretation of the subsurface geology, soil stratigraphy, and hydrogeology. We performed the preliminary geophysical surveys first, then guided the CPT push locations based on the geophysics results, to achieve a more comprehensive result.

B. SOIL SAMPLING

1. Objective

The objective of this task was to collect soil samples to be sent to laboratories for physical, chemical, microbiological and mineralogical property determination.

2. Approach

Soil samples were collected, using the CPT rig and a MosTap® soil sampler. The MosTap® provides a sample approximately 21 inches long by 1.5 inches in diameter. The soil samples were transferred from the sampler to plastic bags; the bags were labeled with the location, date, time and depth interval of the sample identified. This information was also recorded in the operators daily logs. The bags were stored in a cooler on ice until the end of the day when they were delivered to the on site client representative at the GRFL office. The on-site representative cataloged and distributed the samples to the various laboratories for analysis. Locations of all soil sample collection points are listed in Appendix B.

Several of the laboratory analyses required larger volume samples then could be collected with the MosTap®. These samples were obtained by making multiple CPT sampler pushes conducted in next to each other. The samples were bagged and labeled separately and later combined by the client representative in order to obtain the required sample volume.

In addition to conventional CPT soil sampling, a sonic soil sampling system was procured and installed on the CPT rig. The purpose of the sonic soil sampling device was to obtain continuous long cores. Examination of available sampling technologies indicated that this was the only technology with the potential of meeting the requirement for continuous cores.

The sonic push system was integrated with the CPT push system, and delivered to the GRFL. Testing of the sonic sampler indicated that a very stiff layer at a depth of about 12 to 15 feet could not be penetrated. It was concluded that application of the sonic sampler at the GRFL site was problematic because of the consolidated layer.

3. Results

The samples were obtained using a MosTap® soil sampler, which provides a 21-inch long by 1.5-inch diameter sample. Samples were taken at eight locations. Multiple trips in and out of the hole were made to obtain samples from the surface to 40 feet.

C. ANALYSIS OF SOIL/SEDIMENT PHYSICAL PROPERTIES

Soil samples were analyzed by Wright Laboratory, Tyndall AFB for Armstrong Laboratory for particle size distribution, particle density, and specific surface area. Results of these tests were sent to ARA for use in completing the GRFL site characterization, and are

included here to provide readers with a complete representation of the hydrogeologic environment at the site.

1. Objective

The objective of this investigation was to determine physical properties of soil samples from the GRFL site.

2. Approach

Particle size distribution was completed using wet sieve and hydrometer methods, ASTM standard methods D 422-63, D 854-92, D 2216-92, D 2487-93. A total of 108 samples were analyzed. Samples may be segregated into three groups, sandy sediments from the water table aquifer, clayey sediments from discontinuous clay lenses within the water table aquifer, and clayey sediments from the underlying aquitard.

3. Results

Samples from the water table aquifer generally classify as silty sands, poorly-graded sands, poorly-graded sands with silt, or poorly-graded sands with gravel. Under the Unified Soil Classification System these would be designated as SM (silty sands, sand-silt mixtures) or SP (poorly graded sands, gravelly sands, little or no fines) soils. Soil color, based on the standard Munsell notations for color, typically ranges from yellow (10YR7/8) to brown (10YR5/3), but varies significantly in some samples to white (10YR8/2), gray (10YR5/1), or yellowish red (5YR5/6). Particle density or specific gravity typically ranges from 2.57 to 2.72 g/cm^3.

Samples from the discontinuous clay lenses found to occur within the water table aquifer classify as organic clays. The Unified Soil Classification System designation for these materials is OH (organic clays of medium to high plasticity, organic silts). Soil color is found to be gray (10YR5/1) to dark bluish gray (5PB3/1). Some samples show the presence of carbonized plant material. Particle density is in the range of 2.6 g/cm^3.

Samples from the upper 6 feet of the aquitard classify as elastic silts (MH), fat clays (CH), and sandy fat clays (CH) under the Unified Soil Classification System. Generally the upper 2 feet of this sequence exhibits a oxidized zone with colors ranging from strong brown (7.5YR5/8) to yellow (10YR7/8). Below this oxidized zone the aquitard material is found to be gray (10YR5/1) to very dark gray (7.5YR5/8) in color indicating a reduced geochemical environment.

Results of the particle size distribution analyses may be found on diskette in Appendix C. These data are presented in Excel spreadsheet form. Each file contains the results of analyses of one sample divided over three sheets. The individual sheets have results from coarse sieve, fine sieve, and hydrometer analyses, respectively. Surface area analyses were not

completed during the duration of this study. These analyses will be completed later by the Wright Laboratory.

D.   ANALYSIS OF SOIL CHEMICAL PROPERTIES

The University of Delaware performed analyses of soil chemical properties on soil samples from the soil borings. The chemical analyses included pH, total organic matter, cation exchange capacity (CEC) and total exchangeable bases, major and trace elements. Also soil samples were analyzed for microbiological properties. The appropriate ASTM and SSSA standard methods testing protocols were used in the analyses. Sample identification is provided in Appendix D.

1.   Objective

The objective of this phase of the project was to determine the basic physicochemical properties of the submitted soil samples from Dover Air Force Base, Dover, Delaware.

2.   Approach

The soils were dried and passed through a 2 mm sieve in preparation for physicochemical analysis. The following properties were determined: pH (both water and 0.01 M $CaCl_2$); organic matter content; extractable ions including phosphorus (P), potassium (K), calcium (Ca), magnesium (Mg), manganese (Mn), zinc (Zn), copper (Cu), iron (Fe), and boron (B); exchangeable Ca, Mg, and K; exchangeable acidity; effective cation exchange capacity; cation exchange capacity at pH 7; soluble salts; and particle size analysis. The pH was determined using a 1:1 ratio of soil and water or 0.01 M $CaCl_2$. After equilibration, the pH was determined using a combination H^+/calomel electrode. Organic matter was determined by loss of weight on ignition. All extractable ions except boron, was determined by reacting the soils with the Mehlich 1 extractant ($0.05N$ HCl + $0.025N$ H_2SO_4). For boron, the Mehlich 3 extractant ($0.2N$ CH_3COOH + $0.25N$ NH_4NO_3 + $0.015N$ NH_4F + $0.013N$ HNO_3 + $0.001M$ EDTA), was added to each soil. The slurry was then placed on a shaker for 5 minutes, filtered and analyzed using inductively coupled plasma (ICP) spectrometry. Exchangeable ions were determined by reacting the soils with ammonium acetate ($1N$ NH_4OAc) at the pH of the soil, shaking for 30 minutes, filtering and measured using ICP. Exchangeable acidity was measured by extraction of the soil with $1N$ KCl, filtered, and titrated with $0.01N$ NaOH to a permanent endpoint. Effective CEC was determined by summing the exchangeable bases at the pH of the soil (Ca, Mg, K) and exchangeable acidity (Al). The CEC at pH 7.0 was determined by extraction of the soil with $1N$ ammonium acetate at pH 7.0. The exchangeable bases and acidity were determined as before and summed together to equal CEC at pH 7.0. Soluble salts were determined by measuring electrical conductivity of a 1:2 soil/water extract. Particle size analysis (percentage sand, silt, and clay) were determined by the hydrometer method after dispersion with sodium hexametaphosphate.

3.   Results

The soils are slightly to moderately acidic, with pH ranging from 4.9 to 6.4, except for sample 95034, which is located at CPT-11 at a depth of 38-42 ft., with a pH of 2.9. Organic matter and clay contents were quite low, typical for Coastal Plain soils, except for sample 95032 with a clay content of 46%. The soils are generally quite sandy, except for sample 95032 (silty clay), and samples 95034 and 95035 (loam). Calcium is the predominant exchangeable and extractable cation, with the exception of sample 95034, having a high extractable Fe content. Extractable levels of Ca, Mg, and K were higher than the exchangeable levels of the cations since a stronger extractant was used, and both readily exchangeable (those on planar, external sites of clay minerals and organic matter) and some edge site ions were extracted. The order of extractable ions in the soils was Ca > Mg > K > Fe > P > Mn > Zn > Cu. Both the effective CEC and the CEC at pH 7.0 (a measure of total negative charge on the soils) were low (except for samples 95032 and 95034 where clay contents were considerably higher than for the other soils), reflective of the low quantities of clay (7.9% to 46.9%) and organic matter (0 to 1.7%). Once again, these values are typical of sandy, Atlantic Coastal Plain soils. The CECs at pH 7.0 were higher than the effective CECs since measuring CEC at pH 7.0 inflates the negative charge of soils like these that have variable charge (charge changes with pH, becoming more negative at higher pH). This increased negative charge results from dissociation of surface functional groups (e.g., carboxyl and phenolic groups of organic matter and hydroxyl groups of clay minerals) of variable charge surfaces (e.g., organic matter, and clay minerals such as kaolinite and vermiculite). The effective CEC is a more realistic one since it is determined at the pH of the field soil. Exchangeable acidity was quite low, reflective of the moderately acidic pH of the soils. Soluble salts were very low, as one would expect for acidic soils. Thus, plant growth would not be inhibited. Additional data are provided in Appendix D.

4.   Discussion

The basic physicochemical properties of the soil are typical of sandy, moderately acidic Atlantic Coastal Plain soils. The soils have low contents of clay and organic matter and thus low CECs. Consequently, leaching of metals and organic chemicals could be a problem. However, the small contents of clay and organic matter could still play an important role in contaminant retention.

E.   ANALYSIS OF SOIL MICROBIOLOGY PROPERTIES

The University of Delaware performed analyses of soil and microbiological properties on soil samples from the soil borings. The work was done by a research team lead by Dr. J. Fuhrmann. The microbiological analyses evaluated the microbial communities and the whole soil as opposed to individual organisms isolated from the soil/sediment samples. The results of this work provided base line information for future bioremediation demonstrations in the test cells. Sample identification is provided in Appendix E.

1.   Objective

The objective was to determine taxonomic and physiological characteristics of major microbial populations indigenous to the DAFB soil-sediment samples.

2.   Approach

The analyses were a combination of selected traditional procedures (enumerations, biomass, and enzyme activities) and newer approaches to microbial characterizations (whole-soil substrate utilization and fatty acid methyl ester profiles). Emphasis was placed on attempting to identify practical groupings of the soil-sediment samples, i.e., sample groups that contained indigenous microbial populations that will likely respond similarly to management inputs.

Sample processing. Samples were stored at 4 °C upon arrival and throughout the duration of the analyses. All bags comprising a sample were combined, mixed thoroughly, and passed through a 4-mm sieve; extremely wet samples were partially air-dried prior to sieving. Material remaining on the sieve was dried at 105 °C and weighed. Subsamples of the < 4-mm material were also dried at   105 °C to determine gravimetric moisture content. An additional subsample was completely air-dried, bagged, and stored at room temperature until used in the dehydrogenase activity assay.

Enumerations. For all enumerations, serial 10-fold dilutions of samples were prepared in quarter-strength Ringers solution (Reference 3). The incubation temperature used for all procedures was 25 °C. Numbers of aerobic heterotrophic bacteria and fungi were estimated by plating onto duplicate plates of 1% PTYG agar (Reference 4) and full-strength Martin's rose bengal agar (Reference 5), respectively. Bacterial and fungal colonies were counted 10 and 5 days after plating, respectively. Most probable number (MPN) procedures (Reference 6) were used for the enumeration of protozoa (Reference 7), nitrifying bacteria (Reference 8), and denitrifying bacteria (Reference 9); the corresponding number of replicates used per dilution was 4, 4, and 5. Final observations were taken at 7, 28, and 42 days, respectively.

Biomass. Microbial biomass was determined by the fumigation-extraction technique using a 5-day fumigation period (Reference 9). The analysis was performed in duplicate. Extractable biomass nitrogen was determined by the ninhydrin-reactive nitrogen procedure of Amato and Ladd (Reference 11) as modified for use with K_2SO_4 extractant by Joergensen and Brookes (Reference 12).

The ratio of soil:extractant was reduced from 1:4 to 1:1 to enhance sensitivity of the procedure. Results were expressed as biomass carbon values using the assumptions described by Joergensen and Brookes (Reference 12).

Enzyme Assays. Denitrifying enzyme activity was determined as described in Tiedje (Reference 9). The assay was run in duplicate, and gas samples were taken after 30 and 90 minutes of incubation at 28 °C. Nitrous oxide (N_2O) concentrations in the samples were

measured by gas chromatography using an electron capture detector. Concentrations were corrected using the Bunsen equation as described by Tiedje (Reference 13). Dehydrogenase activity was measured in duplicate on air-dry soil samples as described by Tabatabai (Reference 14).

Substrate Utilization. The ability of the indigenous soil microorganisms to utilize 95 different carbon substrates was determined using GN microplates (Biolog, Inc., Hayward, CA) in a modification of the procedure used by Zak et al. (Reference 15). A standard volume 100 μl of a 10^{-2} dilution of a given soil sample was pipeted in the microplate wells and incubated at 25 °C for 96 hours. Color development in each well was rated visually on a scale of 0 (no color development) to 4 (strong color development).

FAME profiles. Whole-soil fatty acid methyl ester (FAME) analysis was done essentially according to the method of Cavigelli et al. (Reference 15). Moist samples were rapidly air-dried in a hood and duplicate 5-g samples were then analyzed. Final extraction volume was increased from 1.5 to 3.0 mL to improve recovery of the organic phase. Extracted FAMEs were identified and measured by gas chromatography by the MIDI system (Newark, DE) operated using the eukaryote program as supplied by the manufacturer.

Statistical Analyses. Results of the biomass and enzyme assays were analyzed using the GLM procedure of the SAS system (Cary, NC). Mean results for the substrate utilization and FAME profiles were analyzed with the CLUSTER procedure (AVERAGE method), and dendrograms were produced using the TREE procedure.

3.   Results

Bacterial counts results indicated that both heterotrophic and denitrifying bacteria were present at detectable levels in all samples. Bacterial numbers generally decreased with depth, although in some cases counts remained elevated at considerable depths. The autotrophic nitrifying bacteria were only detected in the more shallow samples. The eukaryotic fungi and protozoa were also found to be more prevalent at shallow depths, although significant populations were detected as deep as 37 feet in some instances.

Biomass carbon (a measure of total living biomass) and dehydrogenase activity (a measure of metabolic activity) generally mirrored, and thereby confirmed the enumeration results. Samples that included surface soil horizons generally yielded high values. Values for subsurface horizons were generally lower, especially for the dehydrogenase assay, but exhibited significant variability as was noted for the enumerations.

Denitrifying enzyme activity (an index to a soil's history of anaerobic activity) was generally low and was only detected at significant levels in three surface samples.

Cluster analysis of substrate utilization profiles indicated the presence of three broad functional groupings of samples. Group A (50% of the samples examined) was the most

active in its ability to degrade the organic substrates and included those samples having the greater biomass and numbers of microorganisms. In comparison to Group A, samples in Groups B (23% of samples) and C (27% of samples) were able to metabolize a lower number of substrates. Group B contrasted with Group C in exhibiting relatively high levels of substrate utilization (i.e., strength of color development) rather than differing with respect to its nutritional versatility.

Cluster analysis of FAME profiles also revealed the presence of three sample groups, but these showed only partial agreement with the functional groupings identified using the substrate utilization assay. Additionally, two of the samples were unique and did not correlate with the broader FAME groupings; these two samples apparently segregated due to their near absence of detectable FAME components. Among the three main groups, Group X (27% of samples) produced the broadest range of measurable FAMEs; this group also contained all of the samples which included surface soil horizons. Groups Y and Z yielded progressively lower numbers of detectable FAME components. Examination of signature fatty acids generally confirmed that the surface layers contained greater eukaryotic biomass than did the deeper subsurface materials.

4. Discussion

Based on several of the analyses, it appears that microbial populations present in the more shallow samples were larger and more active than those examined from the deeper soil-sediment layers. The enumerations and particularly the biomass data indicated that microbial populations were larger near the soil surface, presumably due to the addition of plant debris and other carbon inputs. Dehydrogenase activity, an index to metabolic activity, was also greater in the surface samples and this again probably reflected the influence of organic carbon addition. However, microbial numbers and biomass generally decreased less dramatically with depth than did dehydrogenase activity, suggesting that populations in the deeper layers are in a relatively quiescent metabolic state.

The lack of detectable denitrifying enzyme activity in nearly all samples suggests that denitrification occurs only rarely at this site. In addition, the generally high populations of denitrifiers detected indicates that denitrification is limited by low organic carbon levels, lack of reducing conditions, or low nitrate availability rather than by the indigenous microorganisms.

Although microbial populations in the surface layers generally exhibited greater taxonomic breadth and functional diversity than did the remaining samples, this trend for differences with depth was less obvious here than it was for the biomass and dehydrogenase results. This was especially true for the substrate utilization assay in that the most degradatively active grouping (Group A) contained samples collected at depths up to 36 feet. Thus, although all of the surface layer samples were assigned to Group A, many deeper samples also appeared in this group. This indicates that microbial populations in some of the deeper strata possess high functional diversity and degradative potential, despite their apparent relative lack of metabolic activity. Conversely, the results also show that, on average, samples taken from the deeper strata

were more likely to exhibit low functional diversity than were surface samples (e.g., no surface samples were assigned to Groups B or C).

In interpreting all of the diversity results, it is important to realize that the data are necessarily skewed by the detection limits of the analytical technique employed. Taking the substrate utilization assay as an example, the apparent lack of nutritional diversity of the populations from the lower strata does not necessarily mean that the proper degradative organisms are entirely absent. Rather, one can only conclude that the degradative organisms are not sufficiently common to be detected in the aliquot of soil suspension used as inoculum in the assay. Given the proper conditions, these particular populations could increase to a more environmentally significant level.

There was little microbiological evidence that extensive anaerobic metabolism commonly occurs in any of the soil-sediment samples examined. Anaerobiosis can only develop in soils under conditions of reduced O_2 diffusion (generally due to elevated soil moisture) in combination with high rates of microbial metabolism. Denitrifying enzyme activity was low in all samples examined and detectable only in the surface samples. Similarly, signature FAMEs commonly present in anaerobic organisms were, with one exception, detected only in the upper soil layers This suggests that only these upper strata contained sufficient available organic carbon to support the high metabolic rates necessary for the development of anaerobic conditions.

F.   ANALYSIS OF SOIL/SEDIMENT MINERALOGICAL COMPONENTS

1.   Objective

The objective of this analysis was to identify and quantify the inorganic mineralogical components present in samples received from the Dover AFB Project.

2.   Approach

A total of six samples were shipped to the Crop and Soil Environmental Sciences Department at Virginia Tech and received by Dr. Lucian Zelazny on Monday, November 6, 1995. The samples were stored in clear plastic bags and identified by labels marked directly on the sample bags. They were entered into our Virginia Tech laboratory records as Dover samples 1 through 6 as shown in Table 2.

Before analysis, the samples were air-dried and passed through a 2 mm sieve. Mineralogical analysis was divided into four subcatagories: particle size analysis; selective dissolution analysis on the whole soil/sediment fraction (<2 mm) for iron and manganese oxides and noncrystalline soil components; petrographic grain counts on the <40 mesh sand fraction (0.05-0.38 mm); and x-ray and thermal analysis of the clay fraction (<2um).

Particle Size Analysis. Sand, silt, and clay percentages were determined by the pipet method in the Virginia Tech Soil Physics Laboratory. Corrections were made to the raw data for moisture content by oven drying a 10 grams subsample at 110°C for 24 hours and determining percent solids for each sample.

TABLE 2. SAMPLE IDENTIFICATION.

Sample ID	CPT Location	Depth Interval	VT Sample ID
MRN 95114	12	12-14'	Dover 1
MRN 95115	12	4-10'	Dover 2
MRN 95116	12	44-46'	Dover 3
MRN 95117	22	24-30'	Dover 4
MRN 95040	11 A&B	14-22'	Dover 5
MRN 95042	10	37.5-39.5'	Dover 6

Selective Dissolution Analysis. Dithionite-Citrate-Bicarbonate extractable iron oxide was determined by extracting 0.5 g of soil/sediment with 40 mL of 0.3M Na Citrate, 5 mL of 1M $NaHCO_3$, and 1 gram of Na dithionite. The suspension was shaken for 24 hours and centrifuged until a clear supernatant was obtained. The supernatant was subsequently transferred to a 250 mL volumetric flask and diluted with DI water. The dilutions were analyzed for iron by ICP analysis and reported as Fe_2O_3.

Extractable oxides of manganese were determined by the hydroxylamine hydrochloride method. A 0.5 gram sample of soil/sediment was extracted with 20 mL of 0.1M hydroxylamine hydrochloride, which was buffered at pH 3.0 with 0.1M HNO_3. The suspension was shaken for 30 minutes and the clear supernatant was obtained by centrifugation and analyzed for manganese by ICP analysis and reported as MnO_2.

Noncrystalline soil components were determined by selective dissolution with ammonium oxalate. A 250 mg sample of oven dry soil/sediment was added to 50 mL of 0.2N ammonium oxalate at pH 3.0 in a preweighed centrifuge tube and extracted for 2 hours in the dark. The suspensions were centrifuged and the supernatant was removed. The solid residue was washed three times with 25 mL of 1N $(NH_4)_2CO_3$ and once with 25 mL of DI water. The tubes were then dried approximately 24 hours at 110°C and weighed. The percentage of noncrystalline soil components was calculated as follows:

$$\% \text{ noncyrstalline} = \frac{(\text{sample mass before treatment-sample mass after treatment})}{\text{sample mass before treatment}} \times 100$$

Grain Counts. The < 40 mesh sand fractions (0.05-0.38mm) were examined petrographically to quantify mineral suites by the line intersect method. The percent minerals were based on 200 counts per sample.

Mineralogical. Samples for mineralogical analysis were pretreated with Na-dithionite-citrate-bicarbonate (DCB) to remove Fe-oxide coatings. Samples were then adjusted to pH 9.5 with M Na_2CO_3 to effect particle dispersion. Sand was separated by wet sieving; clay and silt fractions were separated by repeated decantation after centrifugation. Oriented mounts for x-ray diffraction (XRD) were prepared by depositing approximately 250 mg of clay (<2um) suspension on an unglazed ceramic tile mounted on a suction apparatus. Diffractograms were obtained from Mg-saturated, glycerol-solvated (Mg-gly) samples with no heat treatment and after 4 hours of heating at 110°C, and also from K-saturated samples with no heat treatment, and after 4 hours heating at 110°, 300°, and 550°C, respectively. A second K-saturated unheated clay sample was treated with formamide to differentiate kaolinite from halloysite by intercalation. Samples were scanned with a Scintag XDS 2000 x-ray diffractometer using CuKα radiation (40 mA, 45 kV) and a step size of 0.075° 2θ with a counting time of 4 seconds per increment.

Differential scanning calorimetry (DSC) was conducted using a DuPont Thermal Analyst 2910. Subsamples of K-saturated clays were heated from 50° to 625°C in an N_2 atmosphere at a rate of 20°C min^{-1}. Kaolinite and gibbsite were quantified by mass-equivalent calibration of endothermic peak areas using poorly crystalline Georgia kaolinite and Reynolds synthetic gibbsite (RH-31F) as standards. Other minerals were quantified by employing soil kaolinite, determined by DSC, as an internal standard using the relationship:

$$I_x/I_k = C(M_x/M_k),$$

where I_x and I_k are the (00l) integrated intensities of an unknown mineral phase and kaolinite, respectively; M_x and M_k are the masses of the unknown mineral and kaolinite respectively; and C is a constant determined empirically as the slope of I_x/I_k vs. M_x/M_k for known binary mixtures of standard reference mineral and kaolinite. Results are presented as percent mineral present in the Fe-removed clay sample.

3.   **Results**

Data from the analyses are shown in Tables 3 through 6.

TABLE 3. PARTICLE SIZE ANALYSIS.

Fraction	VCS	CS	MS	FS	VFS	Total Sand	CSI	MSI	FSI	Total Silt	Total Clay
Sample	-------	-------	-------	-------	-------	%	-------	-------	-------	-------	-------
Dover 1	1.2	2.8	4.6	4.3	1.4	14.3	2.2	33.3	13.8	49.3	36.4
Dover 2	5.2	16.1	42.2	27.7	1.9	93.1	0.0	0.0	0.0	0.0	7.9
Dover 3	1.0	1.3	1.4	2.2	7.1	13.0	14.1	20.4	5.6	40.1	46.9
Dover 4	11.8	30.0	32.6	7.0	2.4	83.8	0.1	2.7	1.6	4.4	11.8
Dover 5	1.2	6.6	32.5	33.2	6.5	80.0	2.2	3.5	2.3	8.0	12.0
Dover 6	14.6	10.3	4.0	4.1	13.5	46.5	10.1	19.9	5.2	35.2	18.3

TABLE 4. SELECTIVE DISSOLUTION ANALYSIS. ELEMENTS CONVERTED TO THEIR OXIDE FORM.

Sample	Fe$_2$O$_3$, ppm	Fe$_2$O$_3$, %	MnO$_2$, ppm	MnO$_2$, %	Noncrystalline, %
Dover 1	4230	0.42	32.00	<0.01	7.6
Dover 2	4650	0.46	10.80	<0.01	6.2
Dover 3	70880	7.08	322.50	<0.03	4.7
Dover 4	10130	1.01	65.70	<0.01	4.0
Dover 5	21270	2.12	3.00	<0.001	11.2
Dover 6	6850	0.68	79.80	<0.01	9.3

TABLE 5. GRAIN COUNT ANALYSIS.

Sample	Qz	KF	Pg	Hm	Hn	Mv	Bi	Ep	Zn	Misc*
Dover 1	56±3.4	18±2.6	2±0.9	-------	-------	1±0.9	5±1.4	Tr**	Tr	18±2.6
Dover 2	78±3.0	10±0.9	10±2.1	1±0.9	1±0.9	------	-------	-------	-------	-------
Dover 3	90±2.1	2±0.9	4±1.5	-------	-------	2±0.9	2±0.9	-------	Tr	-------
Dover 4	56±3.4	34±3.4	5±1.6	2±0.9	------	------	2±0.9	1±0.9	-------	-------
Dover 5	68±3.2	18±2.6	5±1.5	-------	5±1.5	------	3±1.2	1±0.9	-------	-------
Dover 6	79±3.0	17±2.6	2±0.9	-------	-------	------	1±0.9	1±0.9	-------	-------

Qz, quartz; KF, K-feldspar; Pg, plagioclase; Hm, hematite; Hn, hornblende; Mv, muscovite; Bi, biotite; Ep, epidote; Zn, zircon.

*Includes dark brown, semi-opaque, isotropic or slightly anisotropic, highly weathered grains that are covered with Fe-oxide coatings and nodules; some evidence of crosshatched twinning suggest that these grains are K-feldspars in advanced stages of alteration.

**Trace = less than 1%.

TABLE 6. MINERALOGICAL PROPERTIES OF CLAY FRACTION AFTER IRON REMOVAL.

Sample	C	Mont	HIV	Mica	Int %	K	H	Gl	Qz	F
Dover 1	8	7	5	35	-------	35	-------	-------	7	3
Dover 2	-------	5	10	29.3	-------	35	-------	0.7	20	-------
Dover 3	-------	30	-------	15	-------	47	-------	-------	4	4
Dover 4	-------	5	5	10	-------	15	57	-------	6	2
Dover 5	-------	-------	-------	5.6	-------	25	61	0.4	8	-------
Dover 6	-------	50	-------	10	10	25	-------	-------	5	-------

C, chlorite; Mont, montmorillonite; HIV, hydroxy interlayer vermiculite; Int, interstratified; K, kaolinite; H, halloysite; Gl, gibbsite; Qz, quartz; F, feldspar.

4. Discussion

Particle-size analysis indicated an extreme range in these soil/sediment samples. Dover 2 contained the higher total sand (93%) with a preponderance of sand in the medium (42%) and fine (28%) fractions. A high total sand fraction also occurred in Dover 4 (84%) and Dover 5 (80%). Total clay dominated Dover 3 (47%) and was a significant component in Dover 1 (36%). Significant silt occurred in Dover 1 (49%), Dover 3 (40%), and Dover 6 (35%).

These soil/sediment samples contained significant iron oxides and noncrystalline material. The highest extractable iron oxide occurred in Dover 3 (7.08%) with intermediate quantities in Dover 5 (2.12%) and Dover 4 (1.01%). The bright red color would support the dominance of hematite although goethite could also be present. Much of this iron oxide occurred as coatings on other particles.

Noncrystalline components were extracted from the soil/sediment samples by acid ammonium oxalate in the dark. These amorphous components ranged from a high in Dover 5 (11.2%) to a low in Dover 4 (4.0%). A strong reaction with hydrogen peroxide particularly in Dover 1 and 6, suggested a significant quantity of manganese oxides. However, hydroxylamine hydrochloride extractable manganese was extremely low, indicating less than 0.01% manganese oxides present in these soil/sediments. Possibly, the peroxide reaction was oxidizing hydrocarbons.

Grain count analysis of the sand fraction indicated the preponderance of quartz (68 to 90%) in this fraction along with much K-feldspars (2 to 34%). Minor quantities of biotite, muscovite, hematite, hornblende, and epidote were also determined. Dover 1 contained some dark brown, semi-opaque isotropic or slightly anisotropic, highly weathered grains that were iron-oxide coated with some evidence of crosshatched twinning suggesting that these grains are K-feldspars in advanced stages of alteration.

The clay fraction of all these soil/sediment samples contained mica (10 A peak), kaolinite (7 A peak) and quartz (3.34 A peak). Dover 1 was the only sample containing some chlorite (14 A peak after 550°C). Dover 3 and 6 contained a large quantity of montmorillonite (18 A peak for Mg-G at RT). Dover 4 and 5 were low in total clay which was dominated by halloysite (10 A peak at RT which shifted to 7 A at 110°C). Small quantities of gibbsite (0.7% and 0.4%) were determined by DSC analysis in Dover 2 and 5 respectively, which were not detected by X-ray diffraction analysis due to the slight quantity present in these soil/sediment samples. Additional information is provided in Appendix F.

G. CPT SITE SURVEY

1. Objectives

The objectives of the CPT (Cone Penetration Test) survey were to characterize the stratigraphy of the site, develop a detailed three–dimensional representation of the site stratigraphy and provide ground truth measurements for the geophysical survey. As part of determining the site stratigraphy and geology, additional cone sensors were used. These sensors included seismic, soil moisture, soil resistivity and oxidation reduction potential. In addition to determining the site stratigraphy, the CPT system was also used as a platform for conducting air permeability tests, collecting soil samples, installing monitoring wells and installing the TDR soil moisture probes.

2. Approach

The approach to the CPT survey was to conduct cone penetration tests at locations that would both define the stratigraphy and support the geophysical survey. Cone penetration tests were conducted in accordance with ASTM D3441 (1986) using ARA's penetrometer trucks and the GRFL trailer mounted CPT rig. The penetrometer probe has standard dimensions of 1.75–inch diameter, 60° conical tip, and a 1.75–inch diameter by 5.27–inch long friction sleeve. The penetrometer is normally advanced vertically into the soil at a constant rate of 48 inches/minute, although this rate must sometimes be reduced as hard layers are encountered. Inside the probe, two load cells independently measure the vertical resistance against the conical tip and the side friction along the sleeve. Forces are sensed by the load cells and the data are transmitted from the probe via a cable running through the push tubes. The data are recorded and plotted by the computer in the penetrometer truck. The minimum resolution of the data are about one data point every 0.8 inch of cone advance. The depth of penetration is measured using a linear displacement transducer. Upon completion of the test the penetration data are plotted. The digital data are brought to ARA's New England Division in South Royalton, Vermont, for analysis and preparation of report plots. A complete discussion of the approach to cone penetration testing is presented in Appendix G. This appendix describes the methods for conducting and interpreting CPT and the specialized probes used at the site. Also all of the CPT data collected at the GRFL site and the corresponding analysis are included in this appendix.

The design of the CPT survey was to initially conduct widely spaced CPT soundings to meet the needs of the geophysical surveys. The initial CPT survey provided an overall picture of the site and identified primary features, such as the depth to the aquitard, location of the water table and the general nature of the soil type. The initial CPT included standard CPT soil resistivity and downhole seismic tests. After the initial phase, the CPT site survey focused on the south–easterly portion of the site, which was determined to be the most likely location of the test cell from the initial CPT and the GPR survey information. More CPT were conducted in this area, providing a higher level of detail around the location of the test cell. No soundings were conducted at the existing location of the test cell. This was a restriction imposed by the on–site client representative. CPT tests were also conducted at many soil sample

collections locales in order to validate the CPT derived soil class number for this particular site. As new cells are required additional CPT can be performed using the GRFL trailer mounted CPT rig to obtain the necessary details for the particular experiment.

The three–dimensional model of soil stratigraphy was developed by performing a geostatistical analysis of the CPT results to develop a statistical model of the soil class data. Using this model, soil class numbers were estimated for the entire site. This analysis was performed with the UNCERT (Wingle 1995) (Reference 17) software using the variogram, gridding, and visualization tools.

3.   Results

A total of 59 cone penetration tests were conducted at the GRFL site. The locations of these test are presented in Figure 3 and in Appendix G. The results of the CPT site survey include the CPT data report in Appendix G and the results of the statistical modeling. This report includes all of the CPT data plots and discussion of each of the probes used during the CPT site survey.

Typical CPT test results are plotted in Figures 13 and 14 for sounding CPT-14, which is located just north of the first test cell. Plotted in the figures are the CPT tip resistance, · sleeve friction, friction ratio, pore pressure, soil class number, resistivity and hydraulic conductivity.

The tip resistances for Sounding CPT-14 vary from a peak of 4000 psi at the surface, which is representative of a very stiff soil to less than 200 psi at elevation -1 feet msl, where the aquitard is encountered. The variations in the tip resistance reflect variations in soil strength, which is directly related to soil type. The friction ratio is generally less than 1, indicating sandy soils. At several depths, the friction ratio increases, indicating an increase in the fine grained soil content. From elevation 22.5 to 15 feet msl, the tip resistance is decreasing and the friction ratio is increasing, indicating that the soil is becoming finer grained. Below elevation 15 feet msl this trend reverses and the soil profile becomes more coarse grained.

The pore pressure profile from the water table to elevation -1 feet msl is less than zero, indicating a dilative soil. Pore pressure profiles less than the hydrostatic pressure generally indicate that the soils contain a significant fine grained soil content. The low pore pressures below the water table (but above the aquitard) indicate that the hydraulic conductivity of this layer is less than that expected for a clean sand.

The clay aquitard is encountered at MSL -1 feet and is readily identified by the rapid decrease in tip resistance and corresponding increase in friction ratio and penetration pore pressures. This behavior was encountered at all CPT penetrations conducted to the aquitard, making identification of the aquitard very easy. The aquitard was observed in all of the CPT soundings. (A few soundings were terminated at a shallow depth due to difficulties with the test, however, when the test was completed to depth, the clay was observed.)
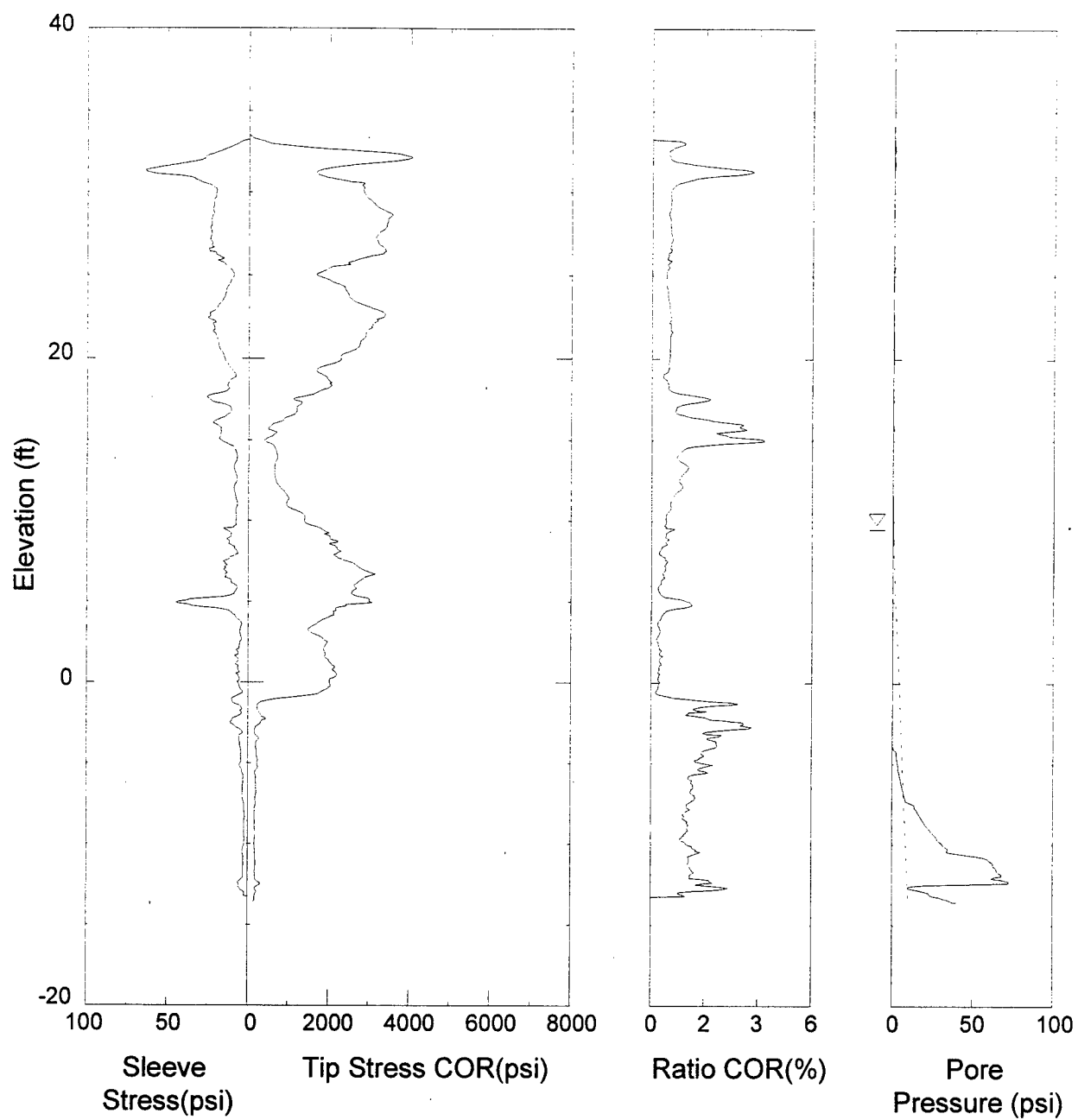
Figure 13.   Typical CPT Profile from the GRFL Site Located at CPT-14 (Page 1).
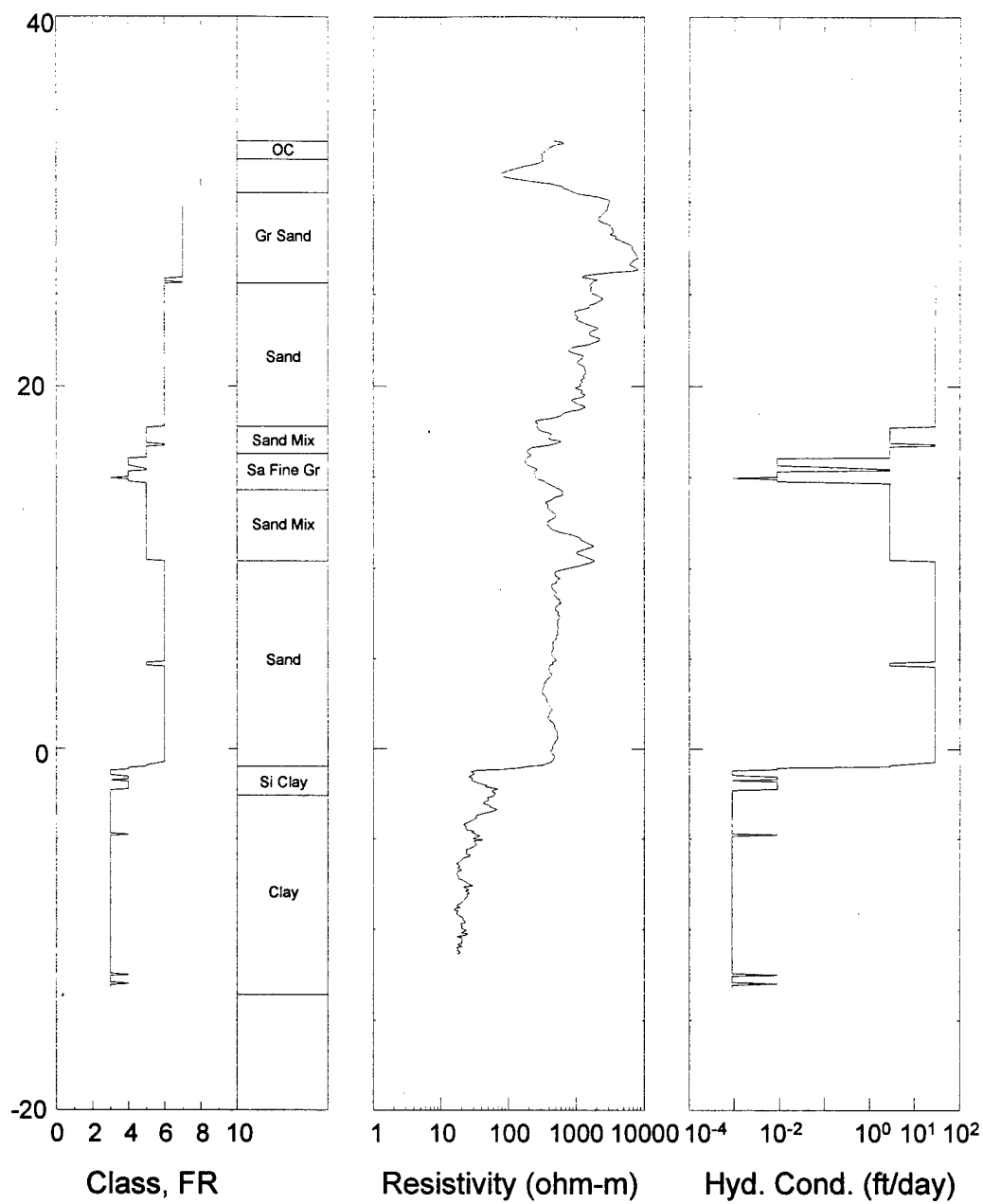
46

Figure 14.   Typical CPT Profile from GRFL Site Located at CPT-14 (page 2).

Cone penetrometer data have been correlated to soil type and classification charts have been developed for predicting soil type (discussed below). Soil classifications derived from the CPT data for Sounding CPT–14 are presented in Figure 14. The Soil Classification Number (SCN) varies from 0 to 10, with the grain size increasing as the SCN increases. A layering profile is presented beside the SCN number with a description of the soil. The soils at this location classify as sands and sand mixes. Only at elevation 15 feet msl is a fine-grained layer observed in this CPT profile, until the aquitard is encountered at elevation -1 feet msl.

Interpretation of CPT data to determine soil layering and properties is greatly enhanced by the SCN and soil layering profiles such as presented in Figure 14. However, analysis should not be limited to just this profile. Significant changes in the physical properties (strength, stratification, etc.) may not show up in the SCN but will be readily apparent in the CPT profile. For example, from elevation 24 feet to 17 feet msl and elevation 11 feet to -1 feet msl, two silty sands with SCN's of 6 are observed. Examination of the tip resistance data shows that the sands are not as uniform as the SCN profile would indicate, but have variation in the tip resistance reflecting minor differences in the fine grained soil content. These differences are subtle.

The resistivity profile in Figure 14 shows a general trend of decreasing resistivity with depth, with layers with lower resistivity at and below -1 feet elevation. The lower resistivity in the aquifer (elevations 19 feet to 12 feet msl) reflects an increase in the fine grained soil content and corresponding increase in water content, which reduces the resistivity. The low resistivity below elevation -1 feet msl is associated with the clay aquitard. The water table was encountered at elevation -9.5 feet msl and the resistivity becomes essentially constant until the aquitard is encountered.

As discussed in the CPT data report in Appendix G, the soil class number is calculated from the normalized corrected tip stress (Q_{tn}) and the normalized friction ratio (f_{SN}). These values are essentially the force on the tip of the cone and the ratio of the tip force to the friction force on the side of the cone. For every data point collected a soil class number is determined from the soil classification chart developed by Robertson (1990) (Reference 18). This chart, shown in Figure 15, is divided into regions representing different soil types. The region on the chart in which the data point falls determines its soil class number and soil type.

At locations where both soil samples were collected and CPT was conducted, the soil class number from the Robertson chart was compared to the soil type determined by physical inspection of the sample. This comparison was used to verify the soil class number from the chart. Soil types were determined by Wright Laboratory before determining grain size distribution of the samples. The grain size data are presented in Appendix B. The Q_{tn} and f_{SN} values from the CPT were averaged over the corresponding soil sample interval and plotted on the Robertson chart. Different symbols were used to represent the soil type as determined by the lab. The resulting chart, shown in Figure 16, verifies the CPT soil class numbers derived from the Robertson chart.

Figure 15.   Soil Classification Chart Developed by Robertson (Robertson, 1990).

49
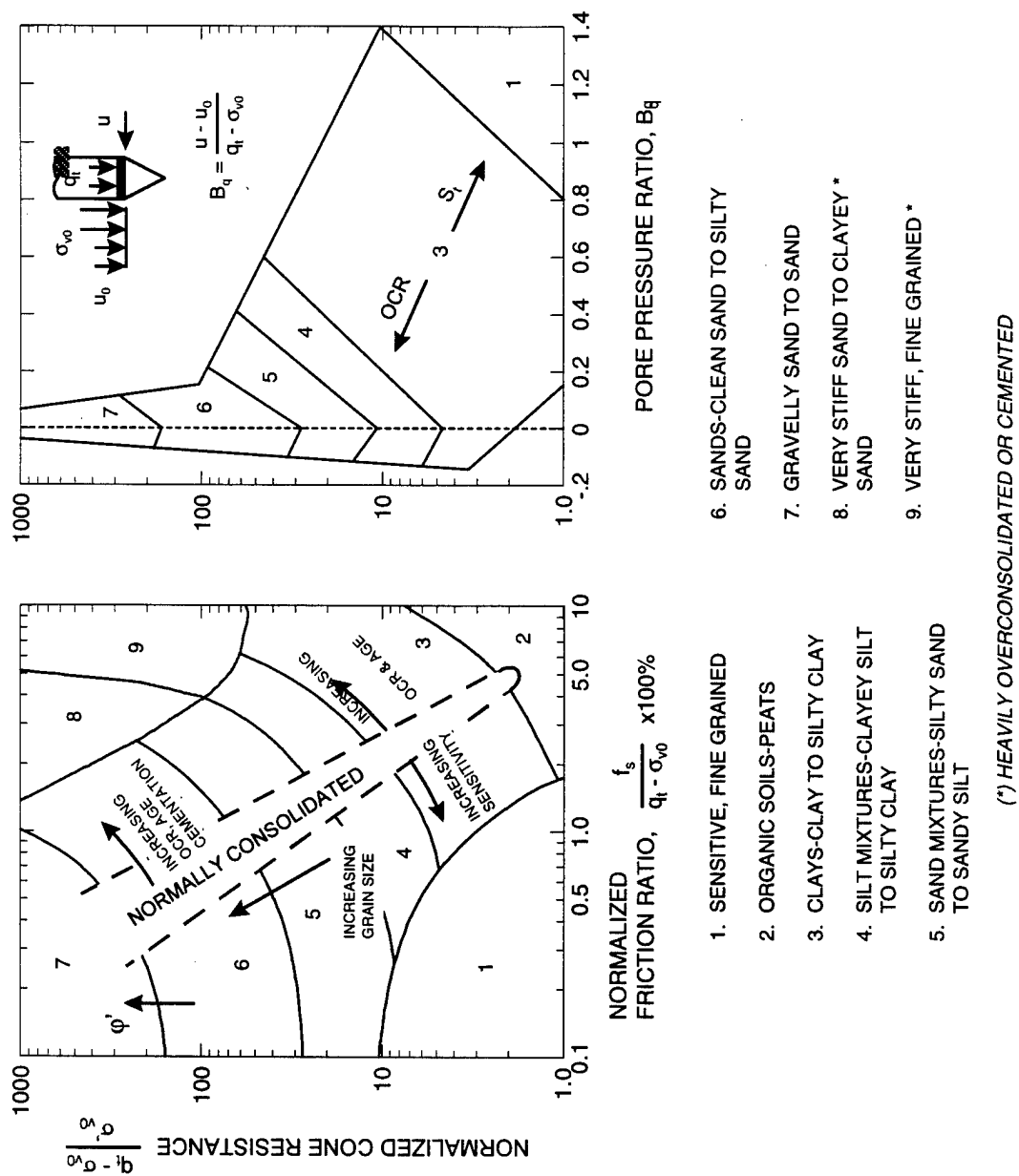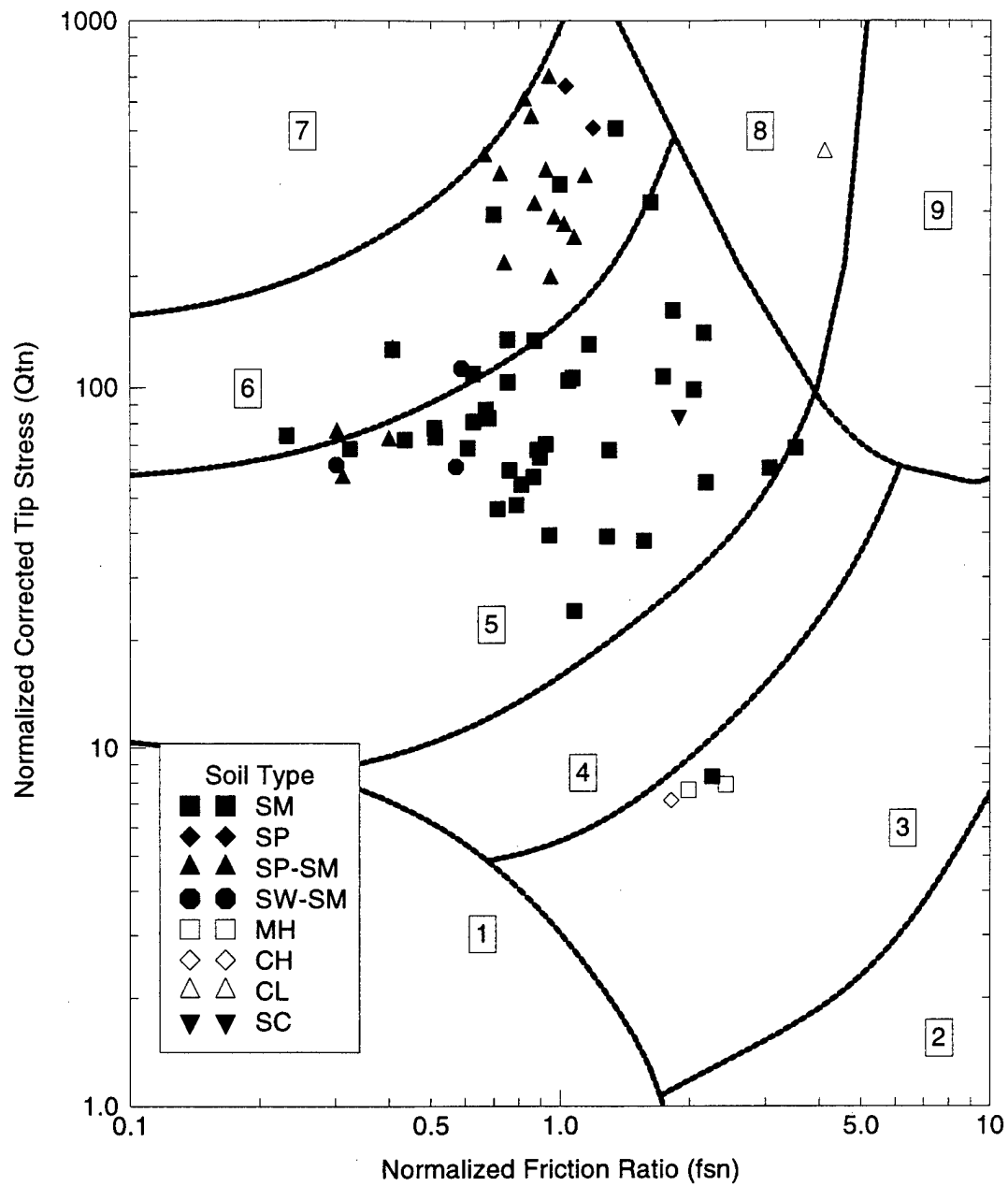
Figure 16. Soil Type Data from Laboratory Analysis Superimposed on the Soil Classification Chart Developed by Robertson and Modified for the GRFL Site Specific Calibration.

50

The soil class numbers are the primary way of determining stratigraphy. Consecutive similar soil class numbers represent a geologic layer. Next to the soil class number profile presented in Figure 14, is shown the corresponding soil type for the particular geologic unit. From this data, geologic cross sections were developed. Figure 17 is a map of the site showing the locations of three cross sections created from the CPT soil class. Also shown on this figure are the CPT that were used as data in each of the cross sections. The cross sections are presented in Figures 18–20. These cross sections show the significant layering and variability in soil type across the site. Also shown in cross section A-A' (Figure 18) is the elevation of the aquitard, which decreases from south to north (lefeet to right in the figure) by approximately 10 feet.

In addition to the cross sections above, a three–dimensional statistical model of the GRFL site was developed from the CPT soil class number. The statistical model is developed from the variogram analysis of the soil class data. A variogram is a measure of the correlation between data points. The sill in the variogram represents the variance in the data and the range represents the distance over which the data are correlated. The range is determined from the variogram curve and is the distance on the X–axis at which the curve reaches the sill and flattens out. By limiting the data to a narrow band in a particular direction many variograms can be calculated for many directions. Each direction is called a search direction. The search direction that results in the variogram with the longest range represents the direction in which the data are most correlated. This direction is known as the longitudinal direction. Once this direction is found, the range for the transverse direction (perpendicular) is determined. The ratio of the two ranges represents the anisotropy in the data. Figures 21 and 22 show the variograms for the longitudinal and transverse directions, respectively. For a more detailed discussion of variograms the reader is referred to Isaaks (1989) (Reference 19).

The ranges for the longitudinal and transverse directions were determined to be 56.1 and 49.0 feet, respectively and the sill is 0.59. The variograms were fit with a Gaussian model. The range, sill, anisotropy and model are input for the kriging calculation that estimates the soil class data at each point in the regular grid across the site. The result of the kriging calculation, shown in Figure 23, is a three–dimensional block model of soil type for the site. The dimensions of this block model are 198 by 552 by 50 feet (width, length, height). The origin, located at coordinates -99,-262,-14 feet, is in the lower left corner of the model.

The location of the aquitard and the location of a clay layer at about 13 feet below ground surface (bgs) are evident in this model. The clay layer is more pronounced in the northern part of the site and pinches out towards the southern part of the site.
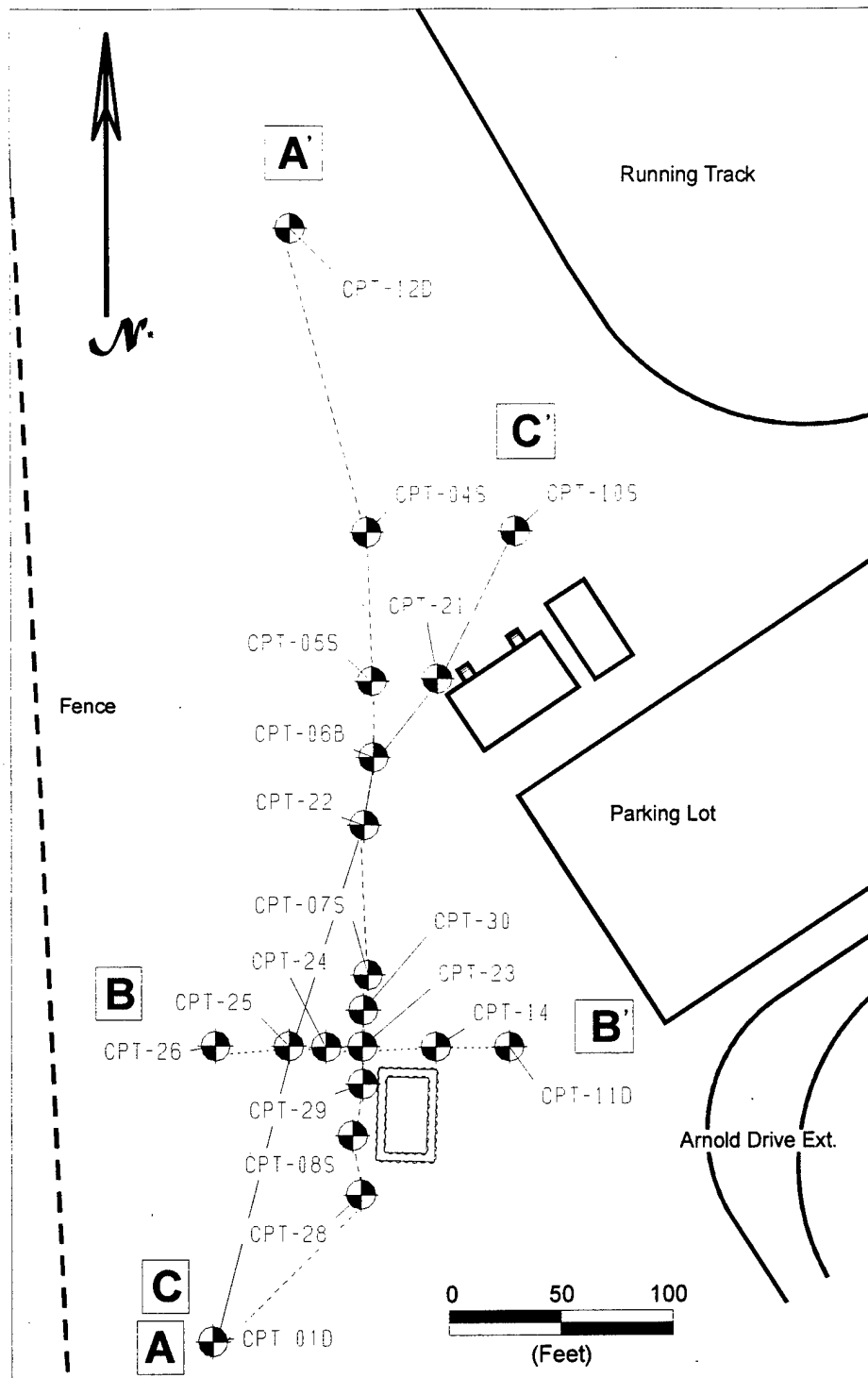
* North based on GRFL coordinate system

Figure 17. **Locations of the Three Cross Sections Superimposed on the GRFL Site Map.**

52
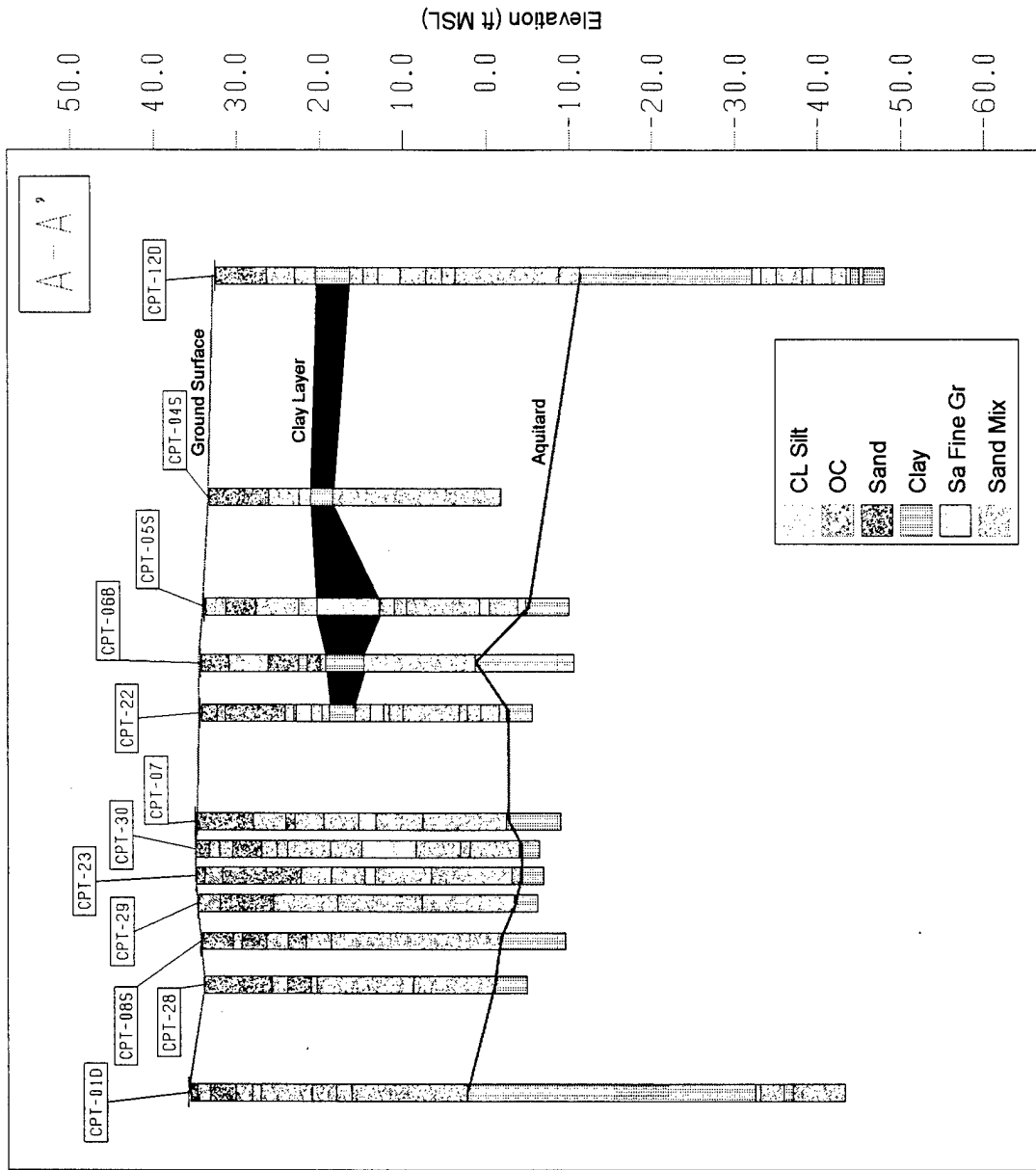
Figure 18. Cross Section A-A', Showing the Delineation of the Aquitard from South to North, Left to Right, Across the Page. The View of the Section is from the East and is Projected onto the Page.
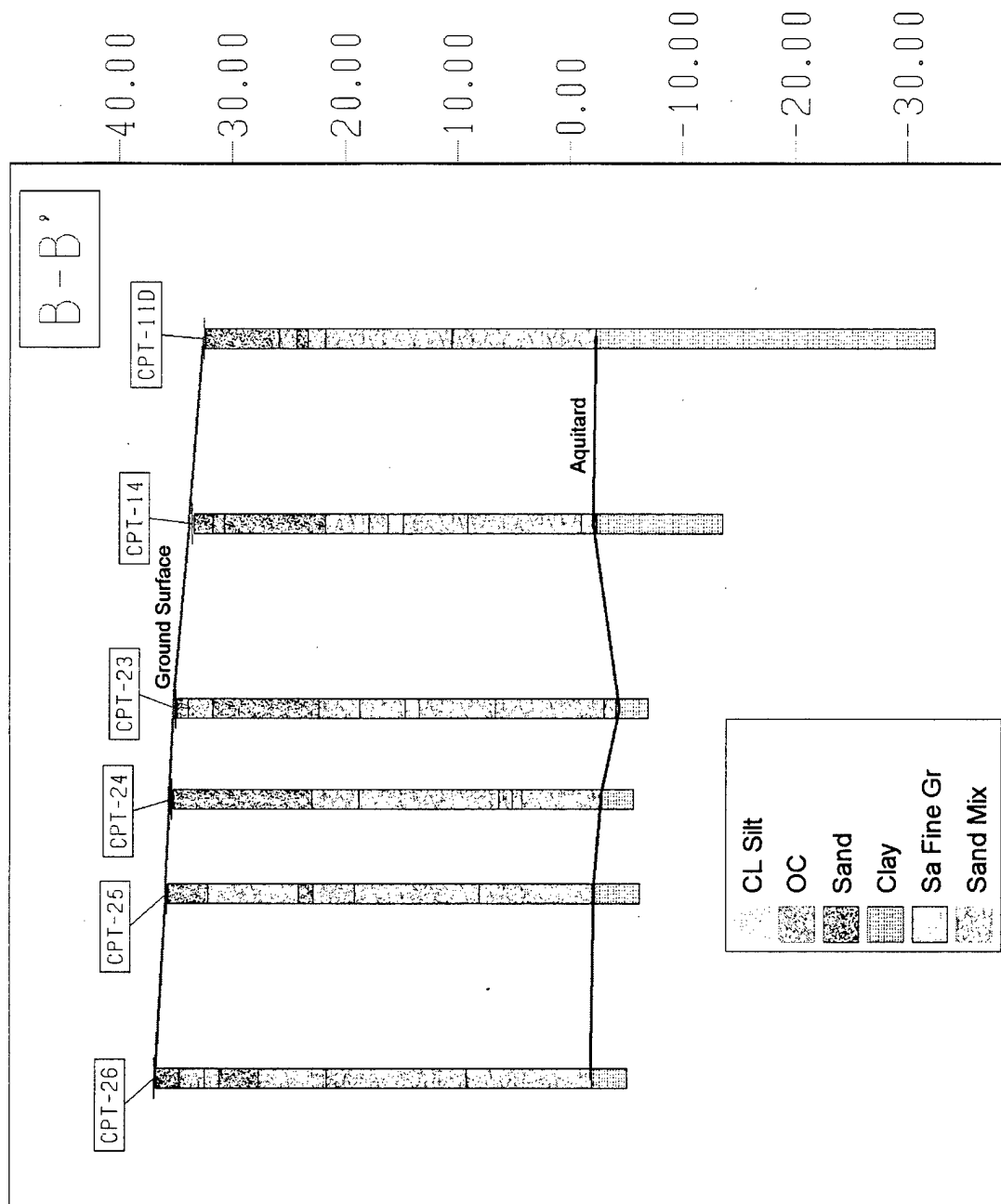
Figure 19. Cross-Section B-B', Showing the Deliniation of the Aquitard from West to East, Left to Right, Across the Page. The View of the Section is from the South and is Projected onto the Page.
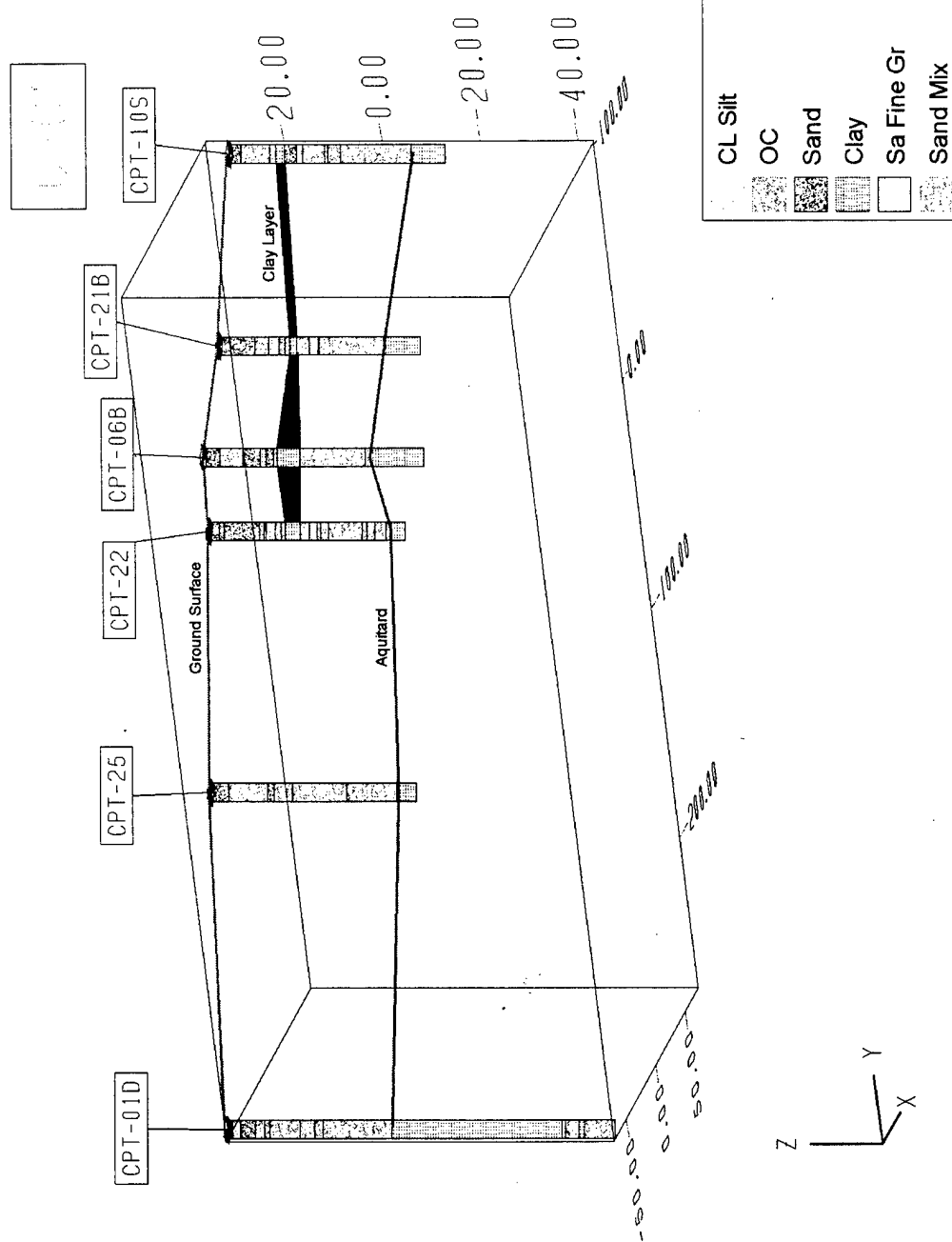
Figure 20. Perspective View of Cross Section C-C', Showing the Perspective View of a Fence Stretching from the South/West to the North/East from Left to Right Across the Page. The Delineation of the Aquitard is also Shown on the Figure.
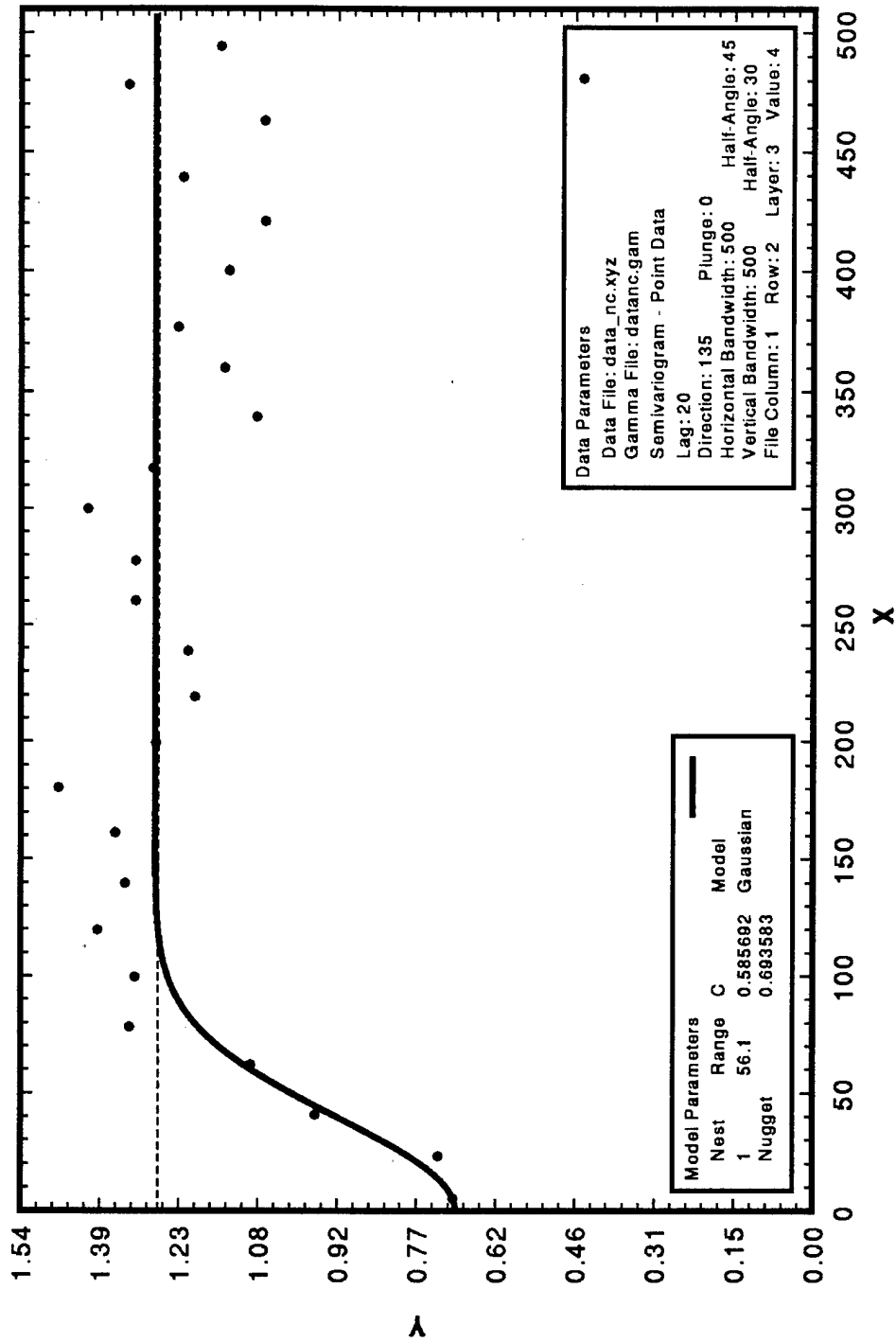
Figure 21. Variogram of the Soil Class Number (SCN) for a Search Direction of 135° (from the North), Which is the Primary Axis of the Data. The Model and Variogram Parameters are Presented in the Figure.
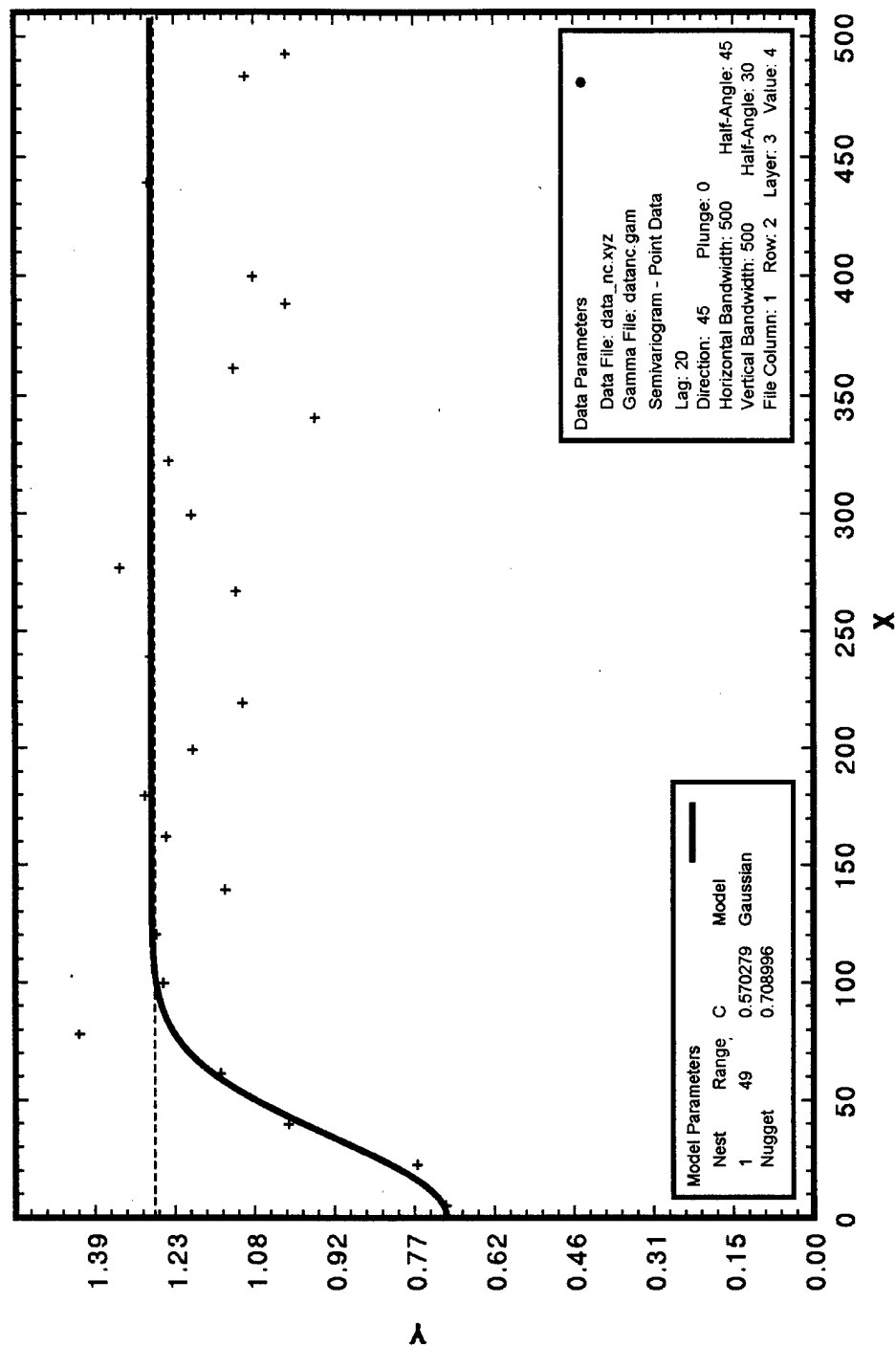
Figure 22. Variogram of the Soil Class Number (SCN) for a Search Direction of 45° (from the North), Which is the Transverse Axis of the Data. The Model and Variogram Parameters are Presented in the Figure.
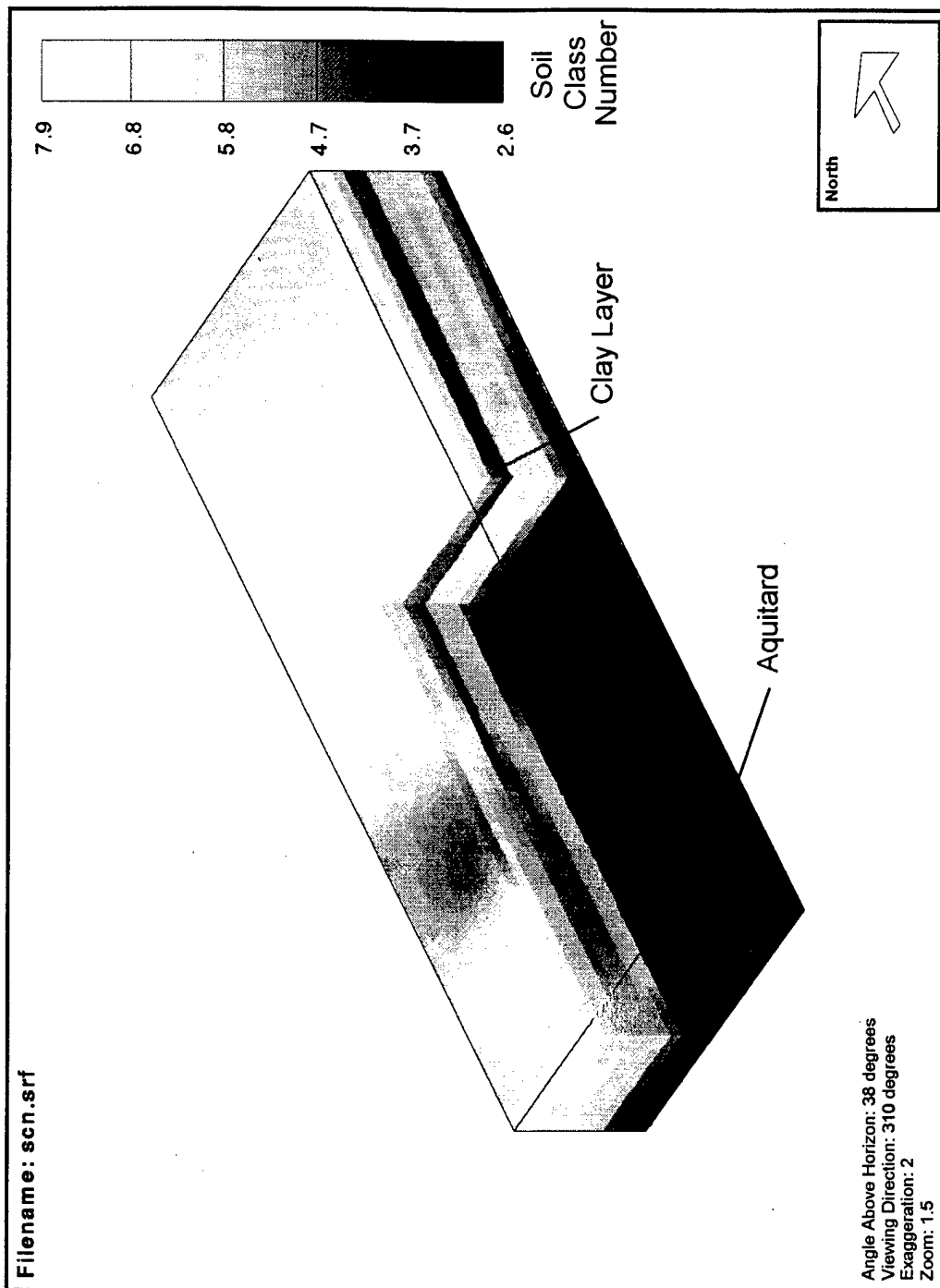
Figure 23. Three Dimensional Block Model of the SCN for the GRFL Site. The Grid is 30 Columns by 90 Rows by 12 Layers. The Dimensions are 198 by 552 by 50 feet (width, length, height) and the Origin is Located at Coordinates -99, -262, -14 feet Relative to the GRFL Assumed Coordinate System. The Model was Calculated Using the Kriging Model in the UNCERT Software and the Statistical Parameters are Presented in Figures 21 & 22.

A particular benefit of a kriging calculation over other interpolation methods, such as inverse distance, is the estimation error value. The estimation error is a value that represents the level of certainty associated with a particular estimated point. An estimation error is calculated for every point estimated in the model. If this number is small relative to the range in the data, then there is a higher degree of certainty associated with the estimated value. A plot of the estimation error is useful to determine where there are uncertainties and where additional data should be collected. The three–dimensional estimation error model corresponding to the SCN model is presented in Figure 24.

This figure clearly shows that there is a higher degree of certainty in the vicinity of the test cell. Another important point to note is the high uncertainties shown near the surface in the north eastern part of the site. This is an anomaly in the model because these grid points are partially in the air above the ground surface. When the model grid is generated by the software, the highest point in the domain is used as the top of the model. In the north eastern part of the site the surface elevation is approximately 6 feet below the highest point in the domain. This is approximately the height of one layer in the model and the estimated values for these grid points are meaningless because they are above the ground surface.

4.   Discussion

Cone penetration tests at other locations on the GRFL site were similar to that at Sounding CPT-14, although layer depths and thicknesses varied. There are two notable exceptions to the generalization of CPT-14 to the entire site. These are highlighted in Figures 25 and 26, showing CPT–03, which was conducted in the northern portion of the site. A clay layer is observed at elevations 31 to 29.5 feet msl. This layer was observed in all of the CPT conducted in the northern section of the site. In the southern end of the site, the soils at this elevation were sands with a significant fine grained content.

The second difference is that below the water table, a portion of the penetration profile lies on the hydrostatic line, indicating very clean sands. This layer lies immediately over the clay aquitard and was only observed on CPTs T–02, 03, 04B and 10, which lie on an east to west line. A conclusion drawn from this observation is that a high hydraulic conductivity sand channel may exist along this east–west line and that the channel has higher permeabilities than the rest of the aquifer.

The aquitard characterization was conducted with three deep penetrations through the aquitard at locations CPT-01D, 11D and 12D. These locations were selected to be on the edges of the site to ensure that they would not be down gradient of the cell and would not cause any cross contamination in the unlikely event of a leak from the cell. For this reason, only three were conducted and they were not located in the center regions of the site. These three CPT, presented in the data report in Appendix G, show the aquitard to be a 20 foot-thick continuous clay layer. In addition to the three-deep CPT, many of the CPT conducted were completed about 5 feet into the aquitard. Of the CPT that were completed to the depth of the aquitard, none indicated any discontinuity in the aquitard. These CPTs indicated that the aquitard was continuous and serves as a barrier between the unconfined and confined
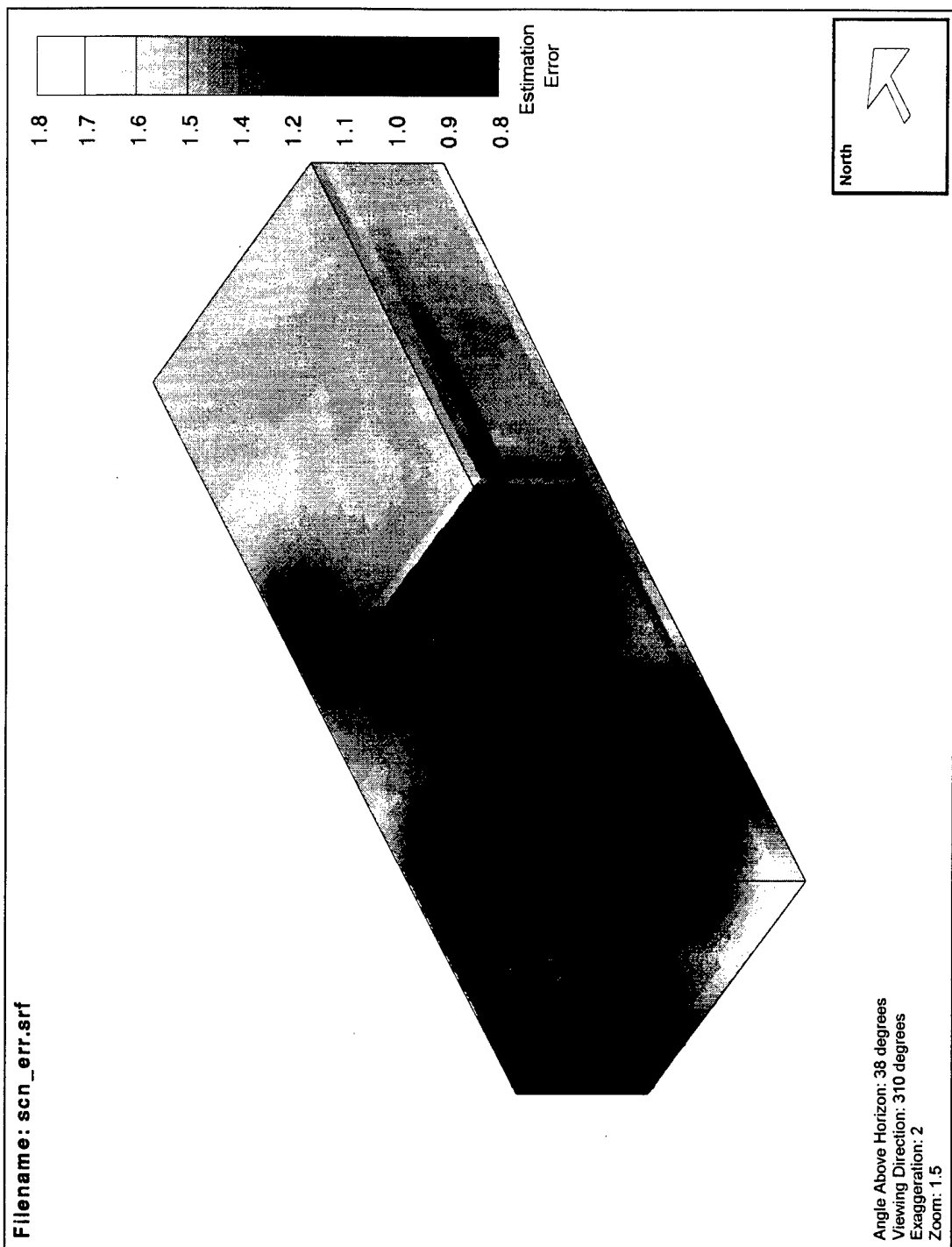
Figure 24. Three Dimension Block Model of the Error of Estimation for the Model Presented in Figure 23.
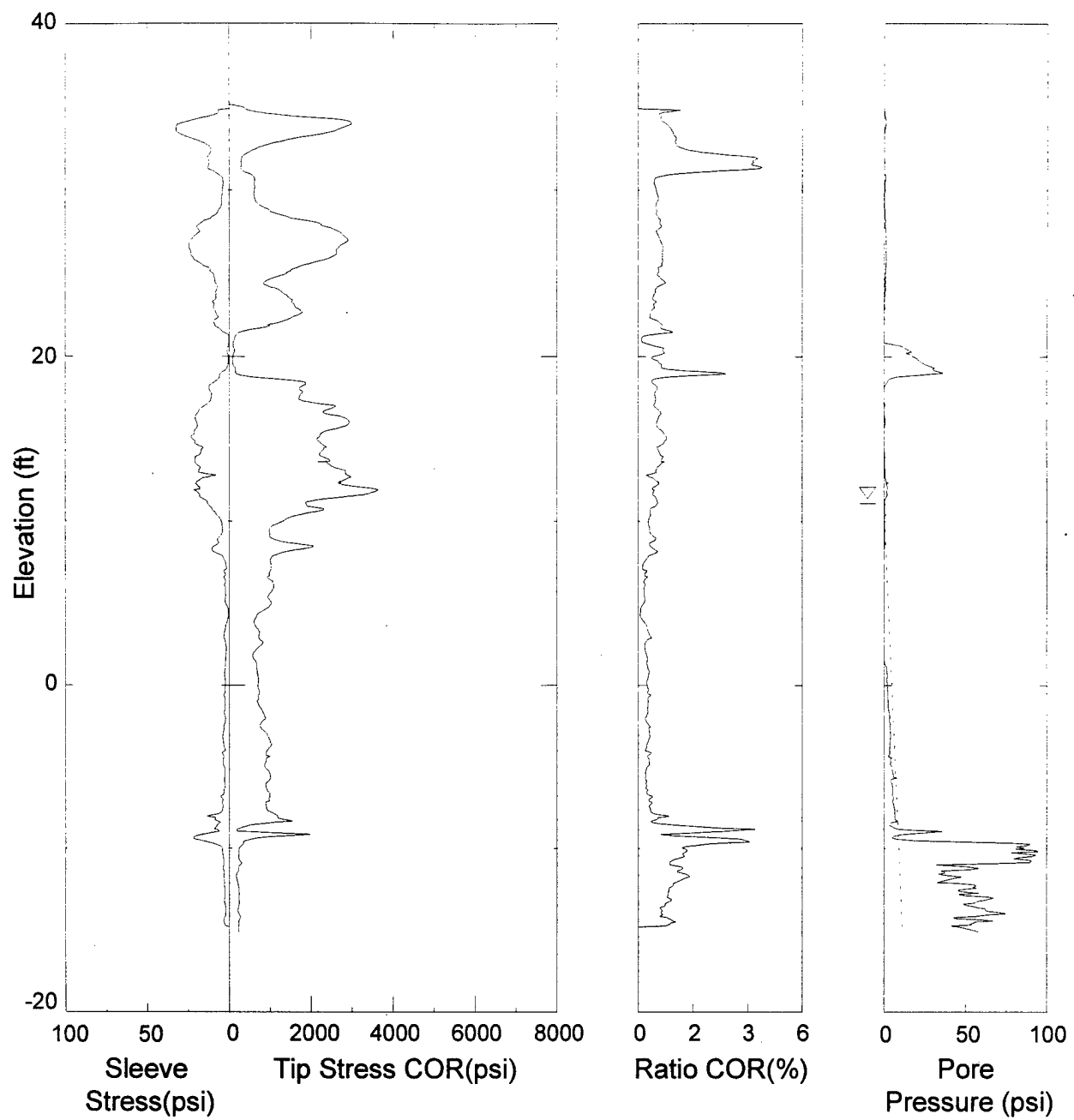
Figure 25. **Typical CPT Profile from the GRFL Site Located at CPT-03 (Page 1).**
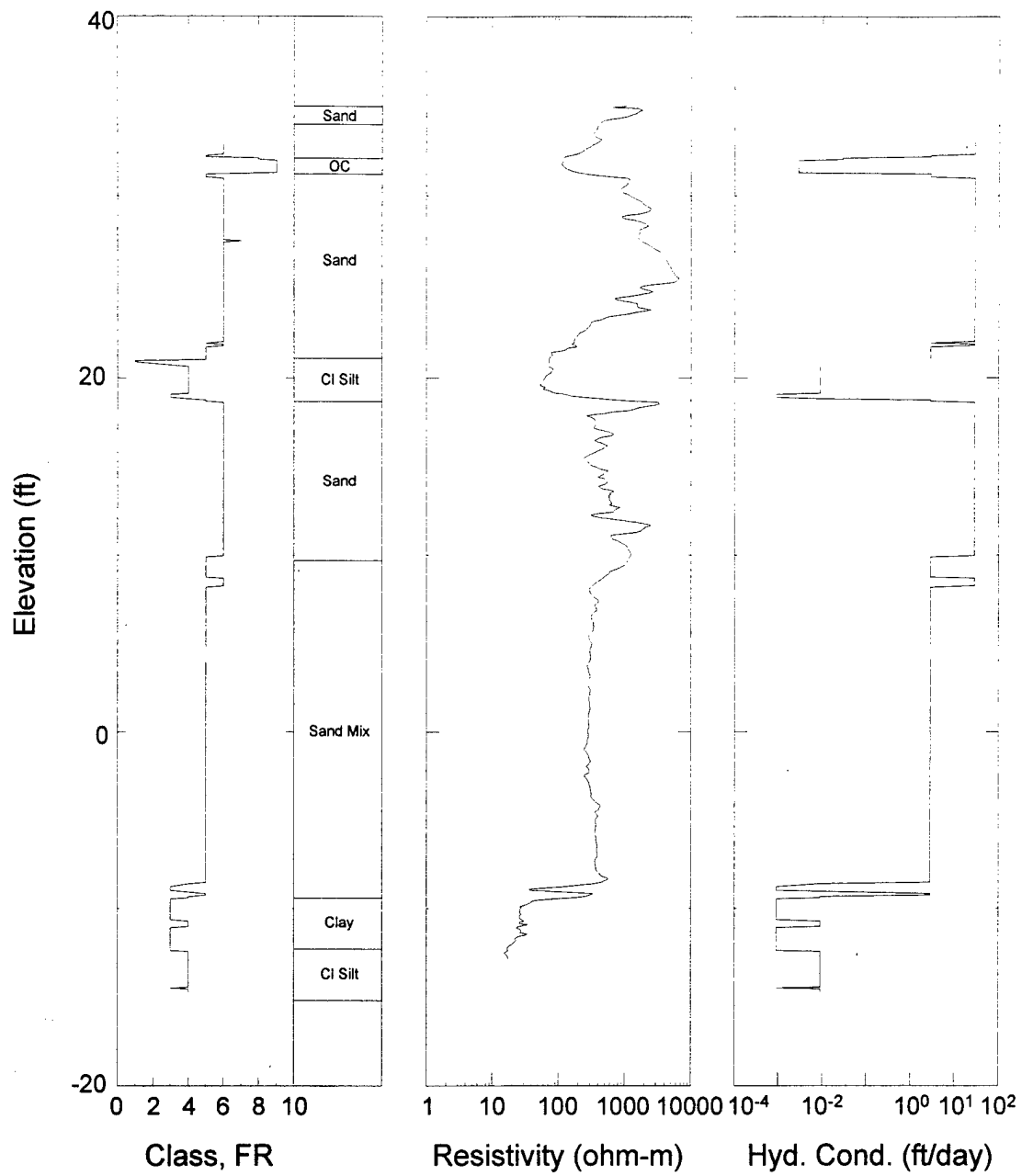
Figure 26.   Typical CPT Profile from GRFL Site Located at CPT-03 (page 2).

H. INSTALLATION OF MONITORING WELLS

1. Objective

The objective of this task was to place monitoring wells at the GRFL site. The wells will be used for groundwater sampling and monitoring the water table depth. An additional objective was to use some of the wells as emergency pumping wells if necessary.

2. Approach

The CPT rig was used to place 2-inch and 1.5-inch ID PVC groundwater monitoring wells at desired locations. Installation with the CPT was selected over conventional drilling techniques because it causes less site disturbance and generates no drilling spoils.

3. Monitoring and Pumping Well Installation

Twenty-seven monitoring wells were placed at the locations shown in Figure 6 The coordinates of the wells are listed Appendix H, which also shows the diameter of the well listed under type of test. Wells were placed as deep as 48 feet using the CPT. The two principal diameters of wells used were 1.5-inch ID PVC wells, which were used solely for monitoring purposes, and 2-inch ID PVC wells, which could be used either for monitoring or pumping.

A schematic of the CPT well placement technique is shown in Figure 27. A steel sacrificial well tip is placed onto a cleaned, slotted PVC section which is then threaded onto a 1-meter section of PVC riser. This composite section is lowered through the head clamping system and the guide tube to the ground surface. The CPT push rods are then lowered down the center for the PVC sections and seated against the steel push point. The head clamp is used to grip the CPT push rods and push the PVC sections into the ground. One-meter sections of PVC riser material and CPT push rods are added sequentially and used to advance the well until the desired depth has been reached. Once the final depth has been reached, the inner CPT push rods are retracted, leaving an installed well.

One difficulty was encountered during the well installation. A high tip resistance layer was encountered at a depth of about 12 feet to 15 feet. Attempts to directly push the wells through this layer resulted in the PVC well material failing due to excessive tensile stresses induce by soil friction against the PVC. A 2.5-inch diameter tip was fabricated and used to advance a dummy hole to the required well depth. The PVC well was then pushed through the dummy hole and soil allowed to collapse and fill the small annulus between the well and soil.

During Installation

1.75" CPT Push Rod

2" SCH 80 PVC

2" SCH 80 Slotted PVC

3.28' (1m)

2.25" Steel Tip
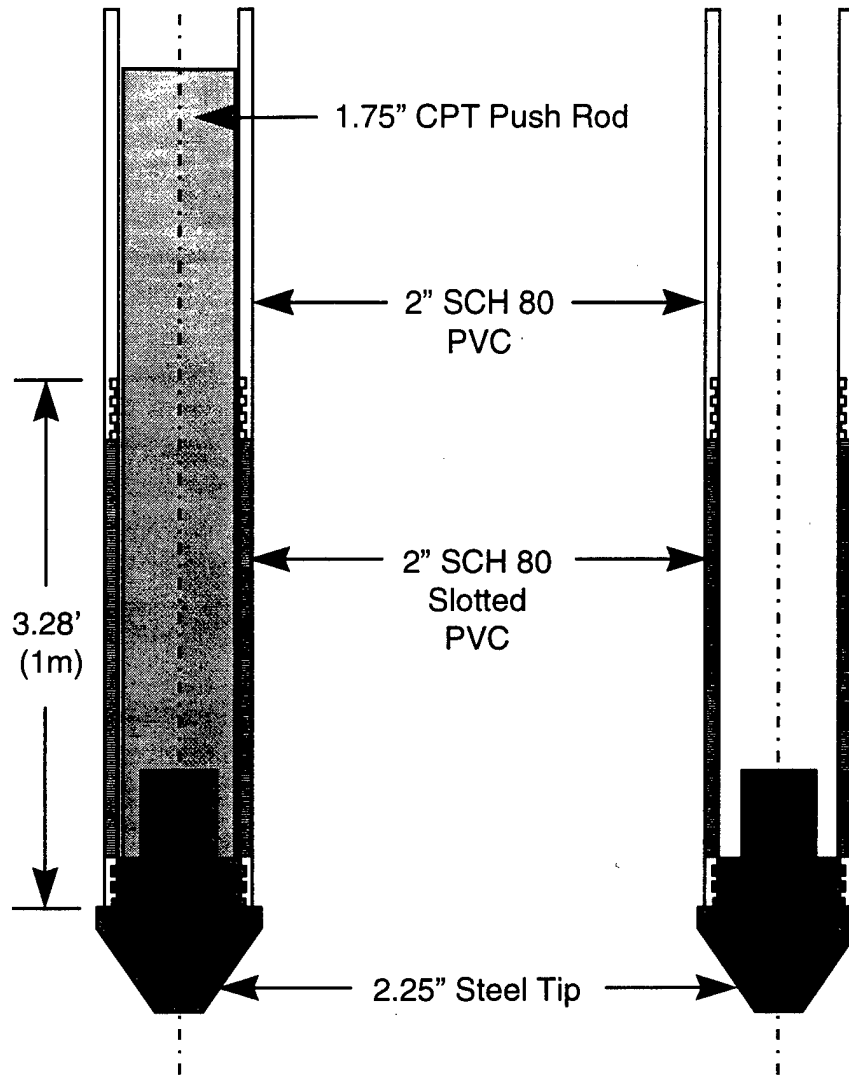
Figure 27.   Schematic of the CPT Well Placement Technique.

64

Direct push wells are generally installed to serve as monitoring points; however, for the GRFL site an additional requirement was that the wells also serve as emergency pumping wells. This requirement resulted in the development of the wells to a greater extent than required for obtaining a water sample. Conventional well development techniques, such as air developing and surging with a surge block, were tried. These techniques were somewhat successful in drawing some of the silt from the surrounding soil into the well. However, after significant time was spent developing the wells, silt would still enter the well when pumped at a high flow rate. A more effective well development technique was needed as silt flow into the well at high flow rates clogged the screens.

A well development system manufactured by AARDVARK was used for further development. This system consists of a dual swap which acts like a surge block and forces water into and out of the media, loosening the fine-grained soil near the well. In addition to the swaps, the AARDVARK system has an air lift system between the swaps which lifts the silt-laden water to the surface as the well is being developed. Using the AARDVARK system, the direct push wells were developed more rapidly and little silt would flow into the wells at high flow rates. It is recommended that any future wells placed at the GRFL site be developed using the AARDVARK system.

4. Monitoring Point Installation

Monitoring points were installed in the cell and consisted of 1/2-inch OD PVC pipe fitted with a slotted sampling section. A schematic of the installation method is shown in Figure 28. In this schematic, the 1.75-inch diameter push rods are used to push a disposable tip down to the desired sampling depth. Attached to the tip is a PVC well screen. This well screen and additional riser sections are protected during the penetration by the CPT push rods. Once the desired depth has been obtained, the push rods are retracted, leaving the PVC well in place. The annulus between the soil and monitoring points is allowed to collapse upon the PVC to create a seal. These monitoring points are developed by purging three well volumes.

During Installation   **After Installation**

1.75" CPT Push Rod

1/2" SCH 40
PVC

3.28'
(1M)

1/2" SCH 40
Slotted
PVC

1.9" Steel Tip
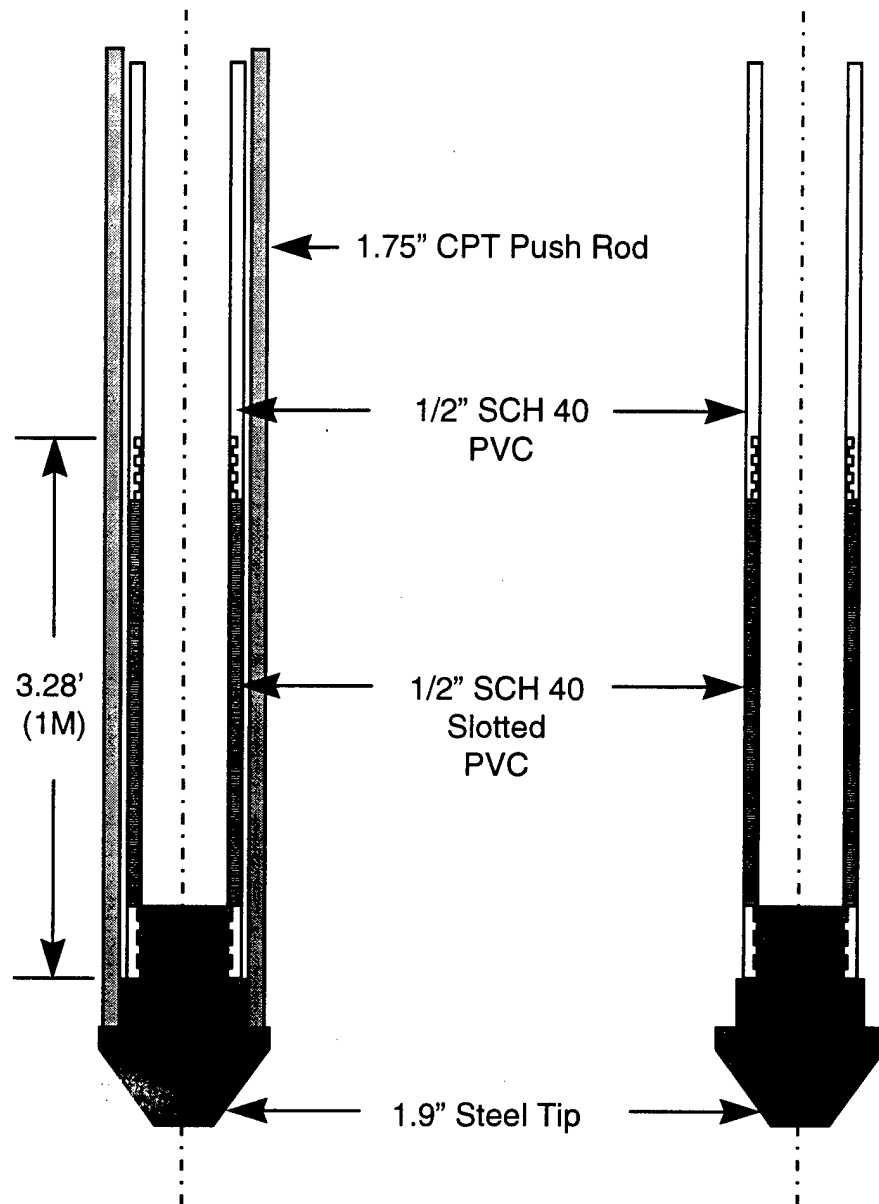
Figure 28.   **Schematic of the CPT Monitoring Point Installation Method.**

I. INSTALLATION OF PERMANENT PIEZOMETERS

1. Objective

The objective of this task was to install a permanent vibrating wire piezometer array to monitor the hydraulic gradient throughout the site. Vibrating wire piezometers were to be installed in monitoring wells throughout the site and surrounding the test cell. The data were monitored using a field data logger and recorded and entered in the database in the laboratory using the FMC computer.

2. System Components

Table 7 lists the equipment required to set up the piezometer array. The vibrating wire piezometers measure fluid pressures. The piezometers operate by using a sensitive diaphragm, coupled with a vibrating wire, that converts fluid pressure to a frequency signal. Electromagnetic coils located close to the wire are used to "pluck" the wire and to convert the vibration to a frequency signal. Changes in pressure on the diaphragm change the tension of the vibrating wire causing the resonant frequency to vary, for each pressure there is a corresponding frequency. This frequency signal is interpreted by the vibrating wire interface to be read by the CR10. Also housed in the piezometer casing is a thermistor to provide a temperature reading of the groundwater. The 4500-2 model is constructed of stainless steel and assembled for long term operation and accuracy. Also, since the signal is a frequency, not a voltage, distance from datalogger is not limited.

TABLE 7. VIBRATING WIRE PIEZOMETER ARRAY EQUIPMENT.

Geokon, Inc.	
16	4500-2, 50 psi vibrating wire piezometers
1	8032/2 16/32 Multiplexer with surge arrester
Campbell Scientific, Inc.	
1	CR10 Datalogger
1	PS12LA Power Supply
1	ENC 16/18 Weatherproof Enclosure
1	AVW1 Single Channel Vibrating Wire Interface
1	PC208E Software
1	MD9 Coaxial Multidrop Interface
1	SC532 9 Pin Peripheral to RS232

The piezometers are multiplexed via the 8032/2 multiplexer and the signal conditioned by the AVW1 interface. The CR10 then reads the signal where it is placed in memory until retrieved by the FMC computer. (See Section V-E, Data Collection, Management, and Analysis Package.) Power is provided to the datalogger from a 12VDC battery that is continuously charged with 110VAC. The battery provides back-up power in the event of loss of power. The FMC computer communicates with the CR10 through the MD9 coaxial interface. A

backbone of coaxial cable connects numerous CR10s (see Section IV-J) to the FMC computer. Each MD9 requires a unique address. The piezometer array MD9's address is 3. Figure 29 shows a block layout of the instrumentation and data-logging equipment for all the permanently installed instrumentation.

3.   System Layout and Installation

The layout for the vibrating wire piezometer array was designed based upon the CPT survey of the site. (See section IV-G) Eleven piezometers were placed in monitoring wells at various locations to provide an overall picture of the area surrounding the test cell. Four additional piezometers were located between the inner and outer barriers around Test Cell 1 to confirm the integrity of the inner barrier. Figure 30 shows the piezometer locations.

The eleven field piezometers were placed in the monitoring wells indicated in Figure 30. The signal wires were encased in underground PVC electrical conduit at a depth of 20 to 24 inches. Conduit was installed from each well to the multiplexer. The four piezometers placed inside the cell are also encased in electrical conduit. This conduit is above ground inside the tent, and buried at a depth of 8 to 10 inches outside the tent. The coaxial connection to the FMC computer in the laboratory is completed through underground conduit also. 110VAC power is also run in a separate underground conduit and provides power to the datalogger. Figure 31 shows the overall conduit layout. Figure 32 shows the instrumentation and data acquisition network for the GRFL.

4.   System Programming and Calibration

The CR10 is programmed (GRFLPIEZ.CSI (.DLD)) to sample each piezometer every 30 seconds and continuously update the data for the FMC computer. Each reading has a calibration factor and offset applied to it. Each piezometer also applies a thermal offset based on the current temperature of the sensor. The eleven piezometers installed outside the cell were placed in the monitoring wells at a depth of 2 feet above the well bottom. The four sensors placed within the cell are 38 feet below the top of the well casing. Table 8 lists the installation and calibration data for each piezometer. The calculated head was used to fine tune the offset value for each piezometer. This takes into account the altitude and barometric pressure. The data are stored in specific numbered input locations. Input locations 1 through 15 hold the current temperature value in degrees C, and input locations 17 through 31 hold the current pressure values in PSI. Refer to Appendix I for more information on the data logging program.
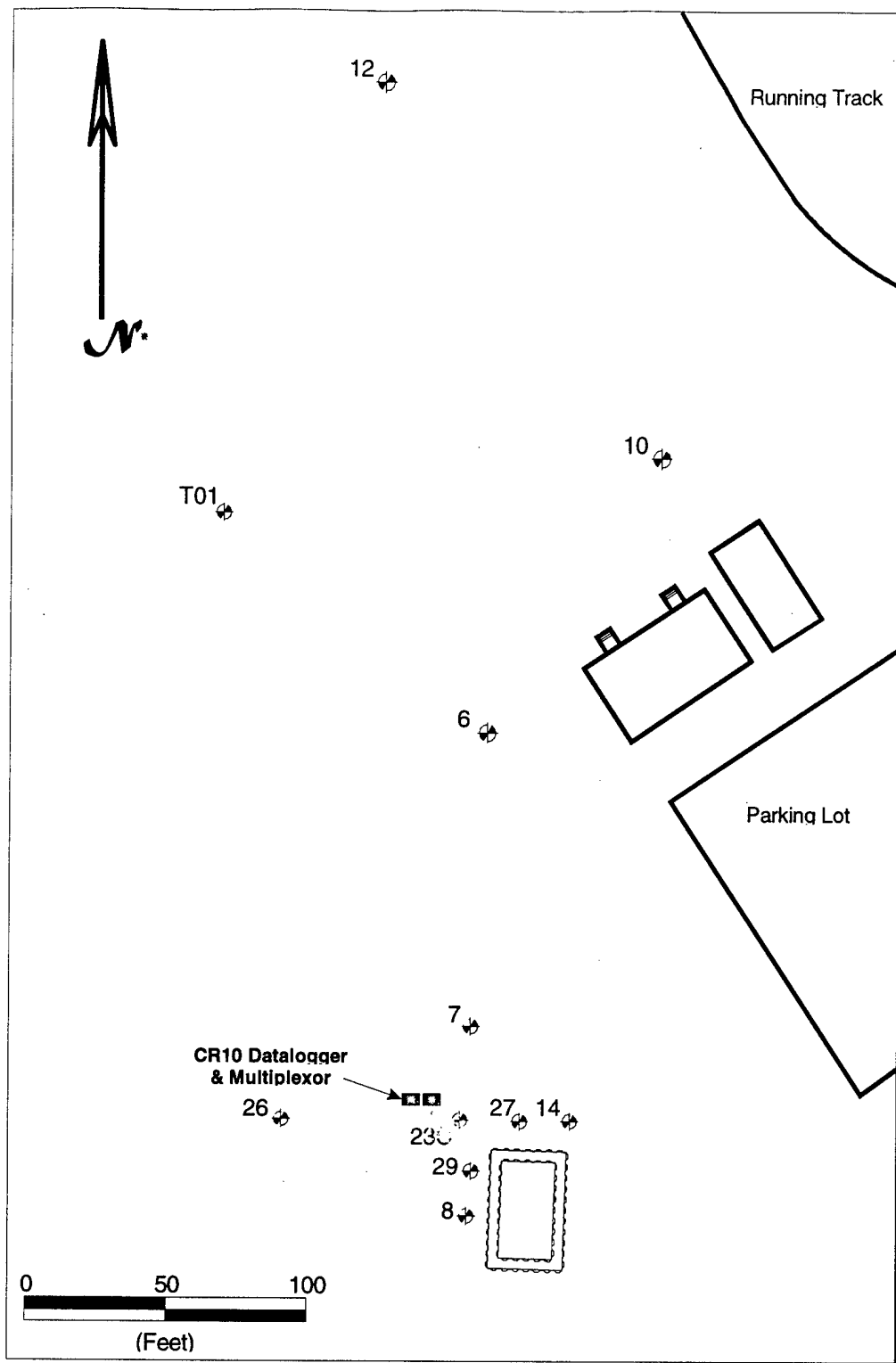
Figure 29.   Overall Instrumentation and Data Logging Block Diagram.

Figure 30.   Piezometer Locations.
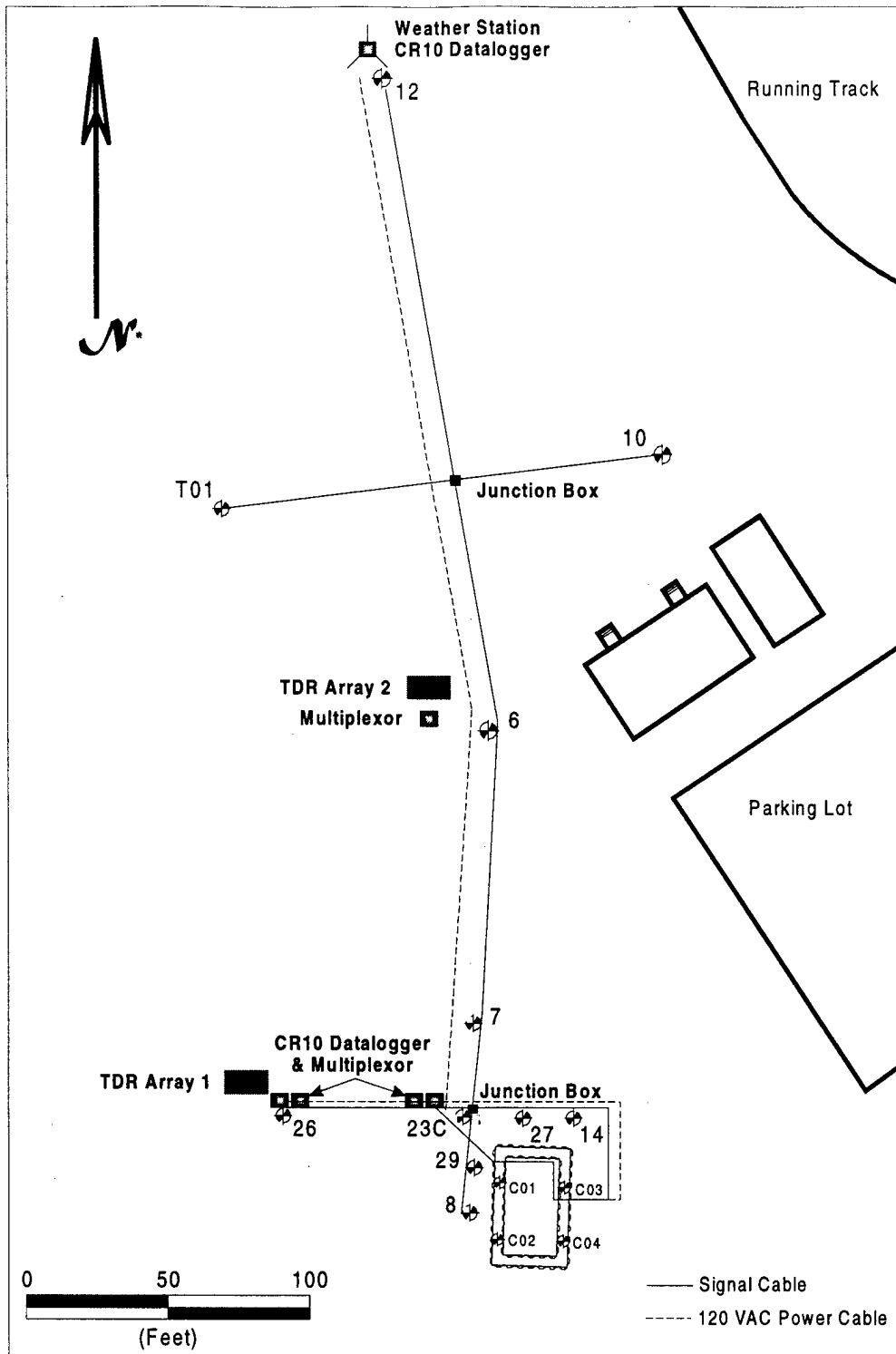
* North based on GRFL coordinate system

Figure 31. Overall System Underground Conduit Layout.
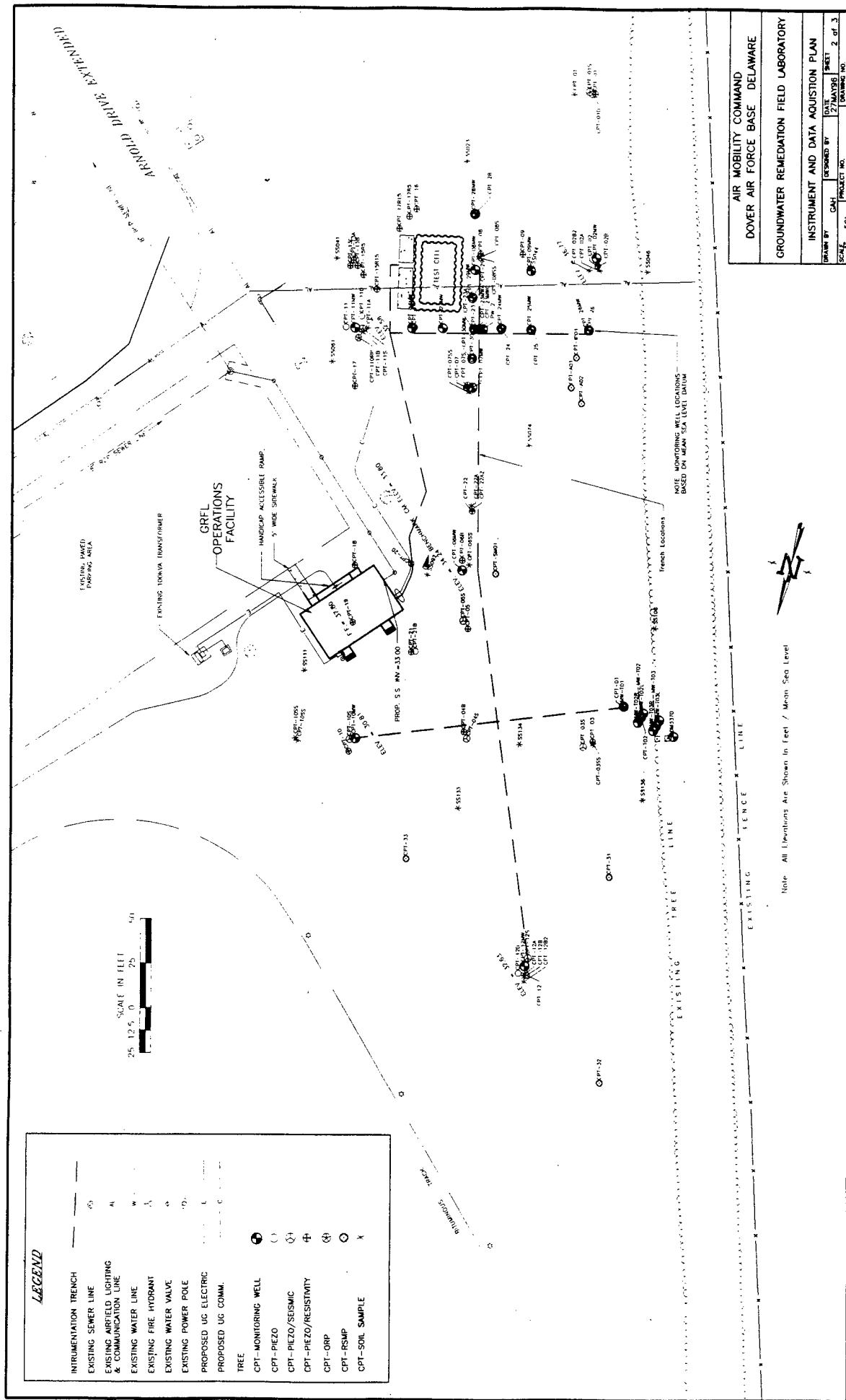
Figure 32. Instrumentation and Data
Acquisition Network

TABLE 8. PIEZOMETER CALIBRATION.

Well ID	Piezometer SN	Piezo Depth	PSI Reading	Depth to Water	Head	Calculated Head
		From top of well casing (feet)	9 May 2:10pm (feet)	9 May 2:10pm (feet)	(feet)	(feet)
a	b	c	d	e	f = c - e	g = (d - baro)*2.31
12	32198	41	22.85	22.48	18.52	18.47
10	32199	32	20.42	19.12	12.88	12.85
T01	32200	40	20.96	25.81	14.19	14.10
6	32201	34	19.67	22.84	11.16	11.12
7	32202	36	20.48	22.96	13.04	12.99
23	32203	29	17.45	23.00	6.00	5.99
27	32204	36	20.97	21.81	14.19	14.12
14	32205	32	19.67	20.85	11.15	11.12
26	32206	34	18.38	25.84	8.16	8.14
29	32207	36	20.58	22.72	13.28	13.22
8	32208	33	19.41	22.43	10.57	10.52
Cell - 1	32209	38	25.30	13.78	24.22	24.13
Cell - 2	32210	38	25.34	13.67	24.33	24.22
Cell - 3	32211	38	25.18	14.06	23.94	23.85
Cell - 4	32212	38	24.60	15.36	22.64	22.51
Barometric Pressure (2:10pm) = 14.856 psi						

J. INSTALLATION OF PERMANENT SENSORS AND PROBES

1. Objective

The objective of this task was to select and install permanent sensors and probes to measure and record soil moisture and meteorological data. The sensors were monitored at field dataloggers and recorded and entered in the database in the laboratory using the FMC computer.

2. System Components

A complete weather station was installed at the north end of the site to monitor meteorological conditions at the site. Table 9 lists the equipment and sensors used. A 10 foot tower was erected to mount the sensors, datalogger, and transmission equipment. Figure 29 is a block diagram of the weather station system.

TABLE 9. WEATHER STATION EQUIPMENT.

Campbell Scientific, Inc.

CR10 data logger w/ OS10-0.1PROM
ENC 16/18 Enclosure
PS12LA Power Supply
MD9 Coaxial Multidrop Interface
HMP35C Temp/RH probe
41002 Radiation shield 12-plate
385-L20 Heated precipitation gage
380MB Leveling Base
03001 Anemometer and Vane
CS105 600-1060mbar Barometric Pressure Sensor
LI200X Si Pyranometer (outdoor use)
LI2003S Leveling Base
O15 Sensor Mount
CM6 6feet Tower w/ grounding kit
019ALU Al crossarm sensor mount

Time Domain Reflectometry (TDR) is a method for measuring volumetric soil moisture by measuring the time of flight of an energy pulse through a probe surrounded by the soil in question. Current TDR probes are designed for installation near the ground surface and could not be used at the GRFL site. ARA developed a robust TDR probe which could be installed with a CPT to the required depths. The probe, shown in Figure 33 consists of a 4 around 1 electrode design. The developed probe is fully discussed in Appendix J. The probe was interfaced with the Campbell Scientific Data Acquisition System.

74
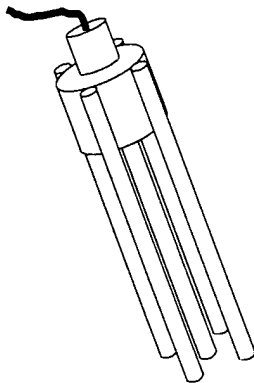
Figure 33. The ARA Developed TDR Probe Capable of Surviving a CPT Push

Two arrays of six TDR probes were installed at the site. A soil temperature probe was co-located with each TDR probe. To accommodate 12 probes, two multiplexers were needed, as well as data logging and transmission equipment. Table 10 lists the equipment needed to install the TDR arrays and Figure 29 includes a block diagram of the TDR datalogging setup.

TABLE 10. TDR ARRAY EQUIPMENT.

Campbell Scientific, Inc.

1	CR10 datalogger with OS10 0.1 PROM
1	PS12LA Power Supply
1	ENC TDR Enclosure
1	MD9 Coaxial Multidrop Interface
1	1502B Tektronix Cable Tester
1	SDM1502 Communication Interface
1	PS1502B Power Control Module
2	SDMX50 8:1 TDR Multiplexer
2	CS600 TDR Probes
12	ARA TDR Probes

3. **System Layout and Programming**

The weather station is located at the north end of the site away from tall trees and buildings which may effect the sensors. It measures air temperature (degrees C), relative humidity (percent), precipitation (inches), wind speed (mph), wind direction (degrees, 0 being north), barometric pressure (PSI), and solar radiation (w/m^2). The precipitation sensor is heated and allows the measurement of snow as well as rain. It totals the precipitation over a 24 hour period and resets to zero at midnight. The CR10 is programmed (WEATHTS.CSI (.DLD)) to

update the data every 5 seconds and store the values in input Locations 1 through 7 in the order stated above. The MD9 address for the weather station is 5.

The soil moisture measuring system consists of two TDR probe arrays located at separate points on the site. A separate multiplexer is used for each array and is installed next to each array (See Figure 29). Each array was to originally consist of six TDR and temperature probes installed at depths ranging from 2 feet to 20 feet. Installation was accomplished using the CPT rig. During the installation of the probes a very dense layer was encountered at about 15 feet. This layer would not stay open after the "dummy" push and prevented installation at the 20-foot depth. Table 11 shows the depths at which each probe was installed. A blank indicates the probe was not installed or failed to produce a signal. The CR10 is programmed (GRFLTDR.CSI (.DLD)) to take a reading every 5 minutes and hold the data in input Locations 1 through 12, Array 1 being the first 6 locations, Array 2 being the second 6 locations. The MD9 address for the TDR array is 4.

TABLE 11. TDR INSTALLATION DEPTHS.

ARRAY 1			ARRAY 2		
PROBE	INPUT LOCATION	DEPTH	PROBE	INPUT LOCATION	DEPTH
TDR 1	1	2.5 feet	TDR 7	8	4 feet
TDR 2	2	4.5 feet	TDR 8	9	8 feet
TDR 3		–	TDR 9	7	2 feet
CSI	3	7.5 feet	TDR 10	12	20 feet
TDR 4		–	TDR 11	10	12 feet
TDR 5	4	12 feet	TDR 12	11	16 feet
TDR 6	5	15.5 feet			

SECTION V

PHASE II - HYDROGEOLOGY CHARACTERIZATION

Data obtained during the Phase I site characterization activities were evaluated and used to support the Phase II activities. The Phase II work involved specific in situ testing of the vadose zone, aquifer, and the installation of additional sensors and monitoring instrumentation. These investigations focused on the entire GRFL site and provided characterization data for selecting the first test cell location. These data will be used for selecting locations for future test cell at the GRFL.

A.   PUMPING TESTS

1.   Objective

The objective of this task was to determine the saturated hydraulic conductivity (K) of the aquifer at the GRFL site. Understanding the spatial variability of K is critical to predicting the regional groundwater flow, the effect of test cells on the groundwater flow, and for designing experiments to be conducted at the GRFL site. Pumping and slug tests are normally used to determine K; however, due to the expense of these tests, generally only a few are conducted as part of a characterization program. Since relatively few field data points are generally available, understanding the spatial variability of K is often uncertain.

The primary objective of efforts under this task was to develop a correlation between the limited field permeability tests and the more extensive CPT database. The correlation was then used to estimate K at other locations using CPT and to access uncertainties using geostatistical methods. To extend the field test database, laboratory grain size data were also used to estimate K.

2.   Approach

A combination of slug and pumping tests was conducted to characterize the saturated portion of the aquifer. Slug tests were conducted at five locations with six tests at each location. The slug test data were used to provide initial estimates of the aquifer properties in order to aid in the design of the more costly pumping test. The format of the slug test was to induce a pressure head change in a monitoring well and collect the pressure data as it dissipated with time. At the GRFL, the slug was a solid rod of known volume. The slug test was conducted by measuring the changes in pressure over time in the well once the slug was introduced, and also when it was withdrawn from the well.

Pumping tests were conducted at two locations. The general format of the pumping test was to pump the aquifer over time, which yielded a cone of depression around the pumping well. The drawdown was then observed with respect to the pumping schedule. Analysis of the drawdown over time in the surrounding wells yielded an estimate of the transmissivity of the saturated aquifer. The drawdowns at a radial distance from the well were

compared to estimated drawdowns at the same radial distance for a known value of transmissivity and storage coefficient. Changing the estimated curves until they match the collected data yielded estimates of transmissivity (T) and storativity (S). The hydraulic conductivity is a function of transmissivity and the saturated thickness.

3.   Slug Tests Results

Tests were conducted at the five locations shown in Figure 9 and in the pumping test well MW-23C. Typical data from a slug test are plotted in Figure 34. Analysis of the data consisted of matching types curves to the field results. A number of slug test models can be used to generate type curves. For this analysis effort, the Kansas Geological Survey model (KGS) was used. The KGS, particularly James Butler and Carl McElwee (1995) (Reference 20), have done extensive work in the development, testing, and analysis of slug test methodologies and the use of slug tests for determining estimates of in situ hydraulic conductivity. Their model incorporates anisotropy, storativity, transmissivity, and skin effects. When analyzing slug tests, there is concern whether the permeability of soils near the well has been altered due to the installation of the monitoring well. This is known as the skin effect. If the installation has compressed the material near the well screen, the permeability near the well will be lower than the surrounding material, as the skin limits pressure dissipation. A high permeability skin can produce vertical flow, resulting in calculated K values much higher than the actual K. (See Butler et al., 1994 (Reference 21) for a complete discussion on the skin effect). Since the wells used at the GRFL were pushed into the formation using a CPT rig, it was hypothesized that a compressed soil layer near the well would act like a low conductivity skin.

The slug test data were analyzed using the KGS model with and without possible low-permeability skins. In all cases, the curves which best fit the data were created without a skin effect, as can be seen in Figure 35. Each type curve was well matched when it was assumed that there was no skin effect. A sensitivity study was conducted which showed that slight variations from the best estimate of hydraulic conductivity produced large deviations of the curve from the data points. The tentative conclusion was that the CPT pushed wells showed no evidence of a low conductivity skin at the GRFL site.

Estimates of K from the slug tests are listed in Table 12, along with the pumping tests results. The slug test results and KGS type curve matches to the slug test data are plotted in Appendix K. The slug test indicates K values in a range of 2.2 feet/day to 8.8 feet/day. These values are in accordance with estimates for silty sand from Freeze and Cherry (1979) (Reference 22) and were used in designing the pumping test and in correlating CPT results.
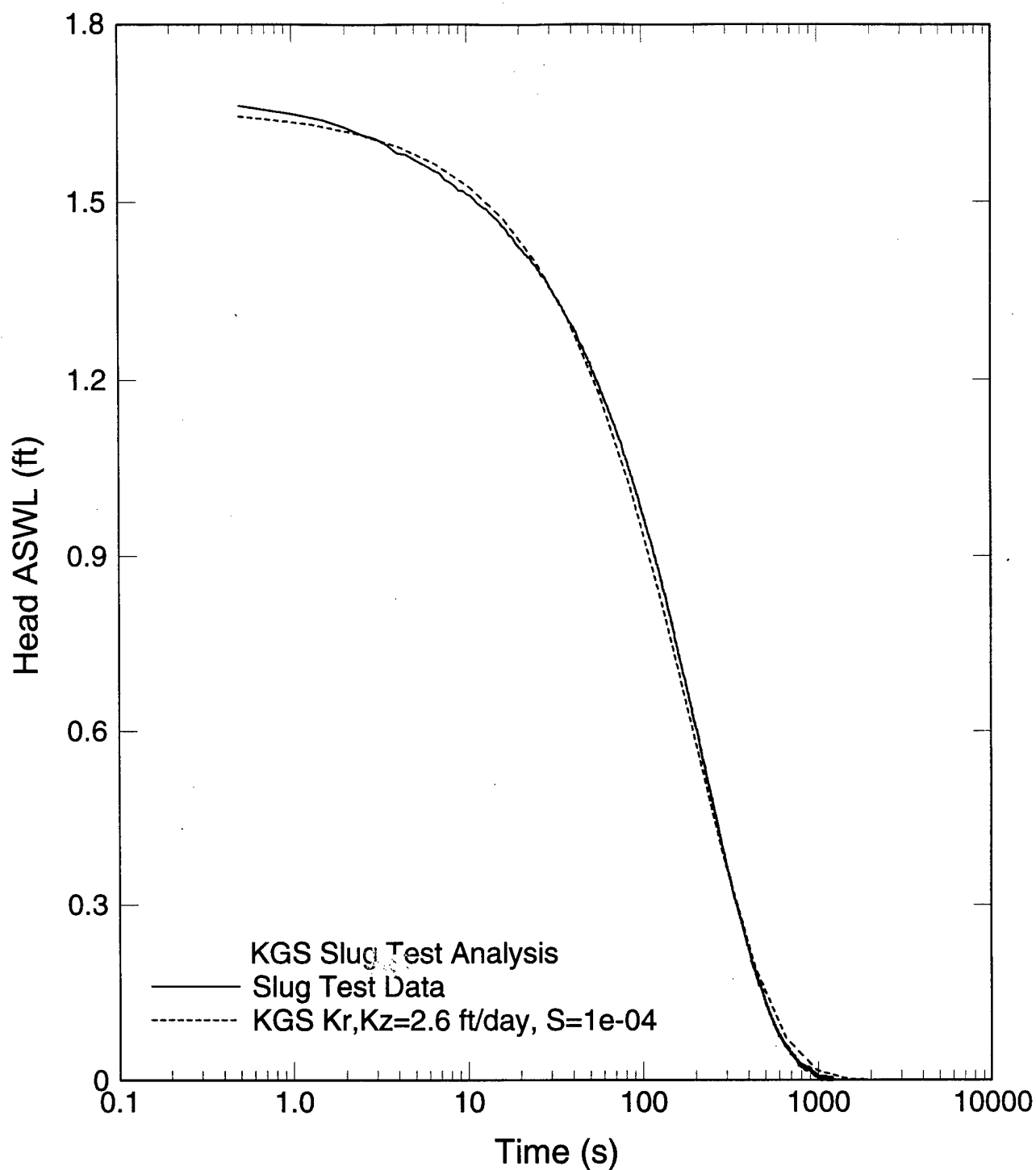
Figure 34. Typical Slug Test Results Showing Data and Match of Type Curve to Data. Note the Good Fit to the Beginning and End of the Slug Test, Which Is Only Obtained for a Relatively Narrow Range of K Values.
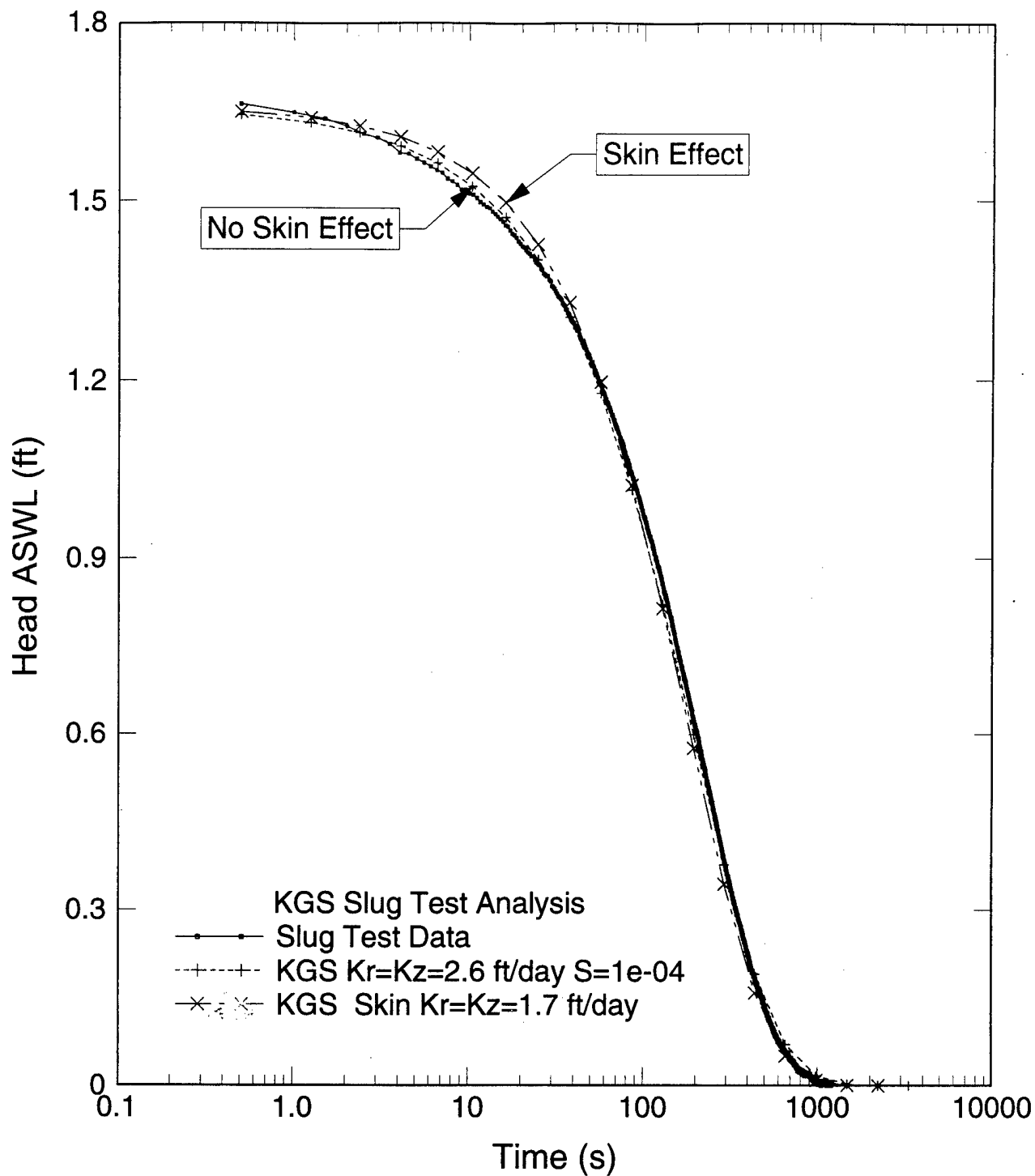
Figure 35. Comparison of Slug Test Data to KGS Model Calculations Conducted
With and Without Low Permeability Skin Effect. Calculation
Without the Skin Effect Is a Better Match to the Slug Test Data.

4.   Pumping Test Results

The pumping test consisted of installing a 2-inch pumping well with 2-inch monitoring wells located at radial distances from the pumping well . A schematic of the pumping tests is shown in Figures 36 – 37. The monitoring wells consisted of schedule 80 PVC pipe installed to the confining layer with 6.6 feet of 10 slot screen beginning at the confining layer. All monitoring wells were direct pushed into the aquifer to the aquitard using a CPT rig. In the area of the first pumping test, the water table depth is approximately 27 feet below the ground surface with the confining layer located at approximately 40 feet below the ground surface. The saturated thickness of the Columbia aquifer is 13 feet. At the second pumping test location, the aquitard was deeper (45-50 feet) resulting in a saturated thickness of 18 to 20 feet.

Initially a 2 inch pumping well was direct push installed with the CPT rig at the first pumping test location. This well yielded slightly less than one gallon per minute (gpm) of flow during the preliminary tests which less than the desired rate for the tracer test.

In an attempt to increase the flow rate, a conventional 4 inch PVC pumping well was installed using a 6-inch auger. The 4 inch well was installed to the confining layer with a 1-foot sump and an 8 foot 20 slot screen with a sand pack around the screen. The annular space above the sand pack was sealed with Bentonite.

The drilled well also exhibited a yield flow rate of 1 gpm which was the same as that of the CPT installed well. Several conclusions were made from comparisons of the wells.

- The CPT installed well performed as well as the drill rig installed well;
- At the GRFL site, a significant in-flow of silt is observed in the wells and vigorous well development, (such as provided by the Aardvark system), is necessary; and
- The drilled well provided sufficient flow for a pumping test.

The first pumping test was conducted using the drilled well. The pumping phase of the test was completed within 14 hours. Once pumping was stopped, the well recovery phase was monitored. During the well recovery phase, a storm occurred and separation of the rain infiltration from the recovery phase was difficult. Therefore this portion of the test was not used in the pumping test analysis.

Continuous monitoring of the nearby wells was accomplished using vibrating wire piezometers, a multiplexer and a programmable CR10 data logger. The CR10 was programmed to log absolute pressure measured at each monitoring point once a minute. One of the piezometers was used to monitor atmospheric pressure continuously over the course of the test which was used to convert the absolute pressure measurements to changes in hydraulic head.
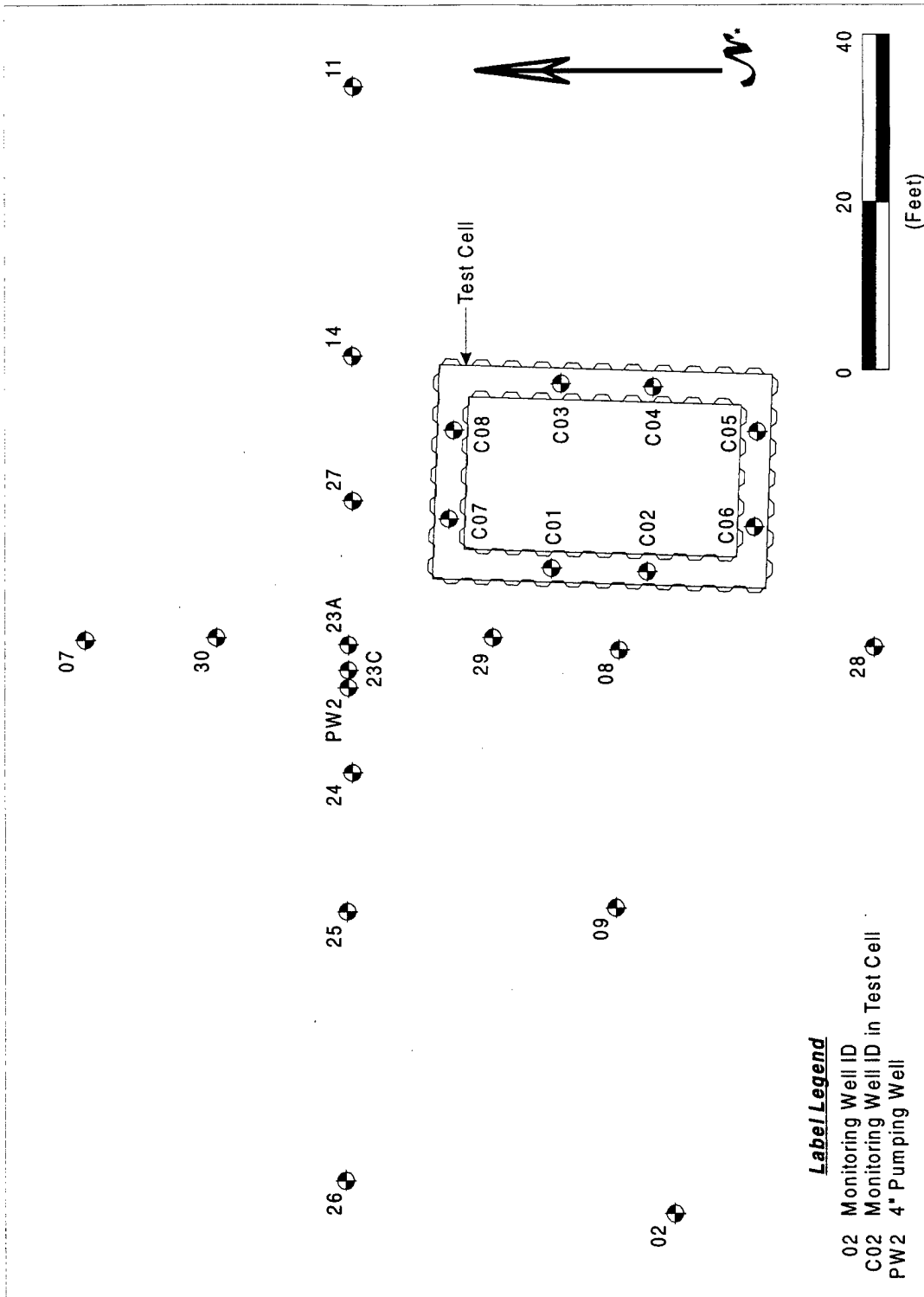
Figure 36. Map Showing Layout of Pumping Test Number 1 Monitoring Wells. Test Cell, Shown for Reference, Was Constructed After the Pumping Test Was Completed.

Label Legend
02   Monitoring Well ID
C02 Monitoring Well ID in Test Cell
PW2 4" Pumping Well
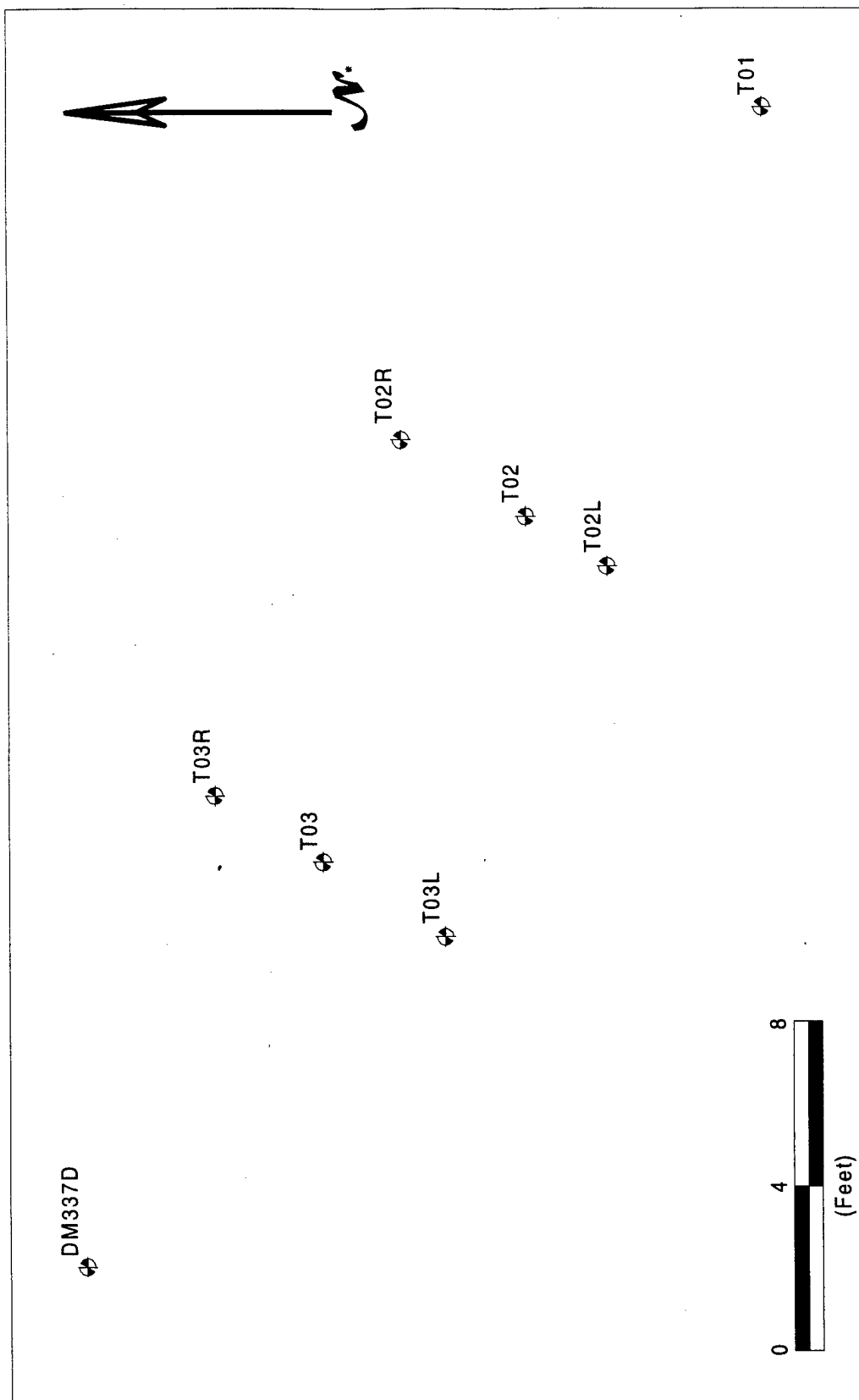
* North based on GRFL coordinate system

Figure 37.   Map Showing Layout of Second Pumping Test Monitoring Wells.

* North based on GRFL coordinate system

The flow rate of 1 gpm was steadily maintained during the first 6 hours of the test, after which for the same level of head in the well the flow dropped to less than 1 gpm. Over the course of the test, the flow rate never dropped below 7 percent of the original flow rate; therefore, a constant flow rate was assumed for the analysis. As will be discussed in the section on the tracer testing, it was decided that the hydraulic head and hydraulic conductivity in the vicinity of the first pumping tests were too low to conduct the planned induced gradient tracer test. An area with higher heads was located to the north of the first pumping test and appeared to be better suited for the tracer test. A 2-inch well had been previously installed by Dames & Moore (Reference 2) and a preliminary yield test was conducted. The test demonstrated that a 3 gpm flow rate could be maintained, which was adequate for the tracer tests. A second pumping test was conducted at this location with the monitoring well locations shown in Figure 37. This test was conducted at a pumping rate of 3.18 gpm for 16 hours. Data from both pumping tests were analyzed using the methods presented below. Typical pumping test data are presented in Figure 38. Data obtained from all of the pumping tests are presented in Appendix K.

Three analytical methods were used to estimate aquifer parameters. The first method was developed by Boulton (1963) (Reference 23) for an unconfined aquifer in which the water table decline due to pumping is a small portion of the initial saturated thickness. This method best fits the conditions observed at GRFL. Two additional analytical methods were used. The first was a two-dimensional steady-state solution, the Dupuis solution (deMarsily, 1986) (Reference 24) for radial flow to a well in an unconfined formation. The second was the transient Jacob analysis for radial flow to a well in a confined aquifer. For a complete discussion and the formulation of the models see Boulton (1963), Jacob (1952) (Reference 25), and deMarsily (1986). Assumptions employed to analyze time-drawdown curves from an unconfined aquifer include (1) the aquifer is bounded above by a water table at atmospheric pressure and below by a horizontal impermeable bed, (2) the transmissivity of the aquifer is constant in time and space, (3) the pumping well is fully penetrating, and (4) the observation wells are also fully penetrating.

Aquifer parameters estimated from the three different methods are shown in Table 12. A range of values are given for each analysis because multiple wells were used for both the pumping test and the slug tests. Further discussion of the results is presented below.
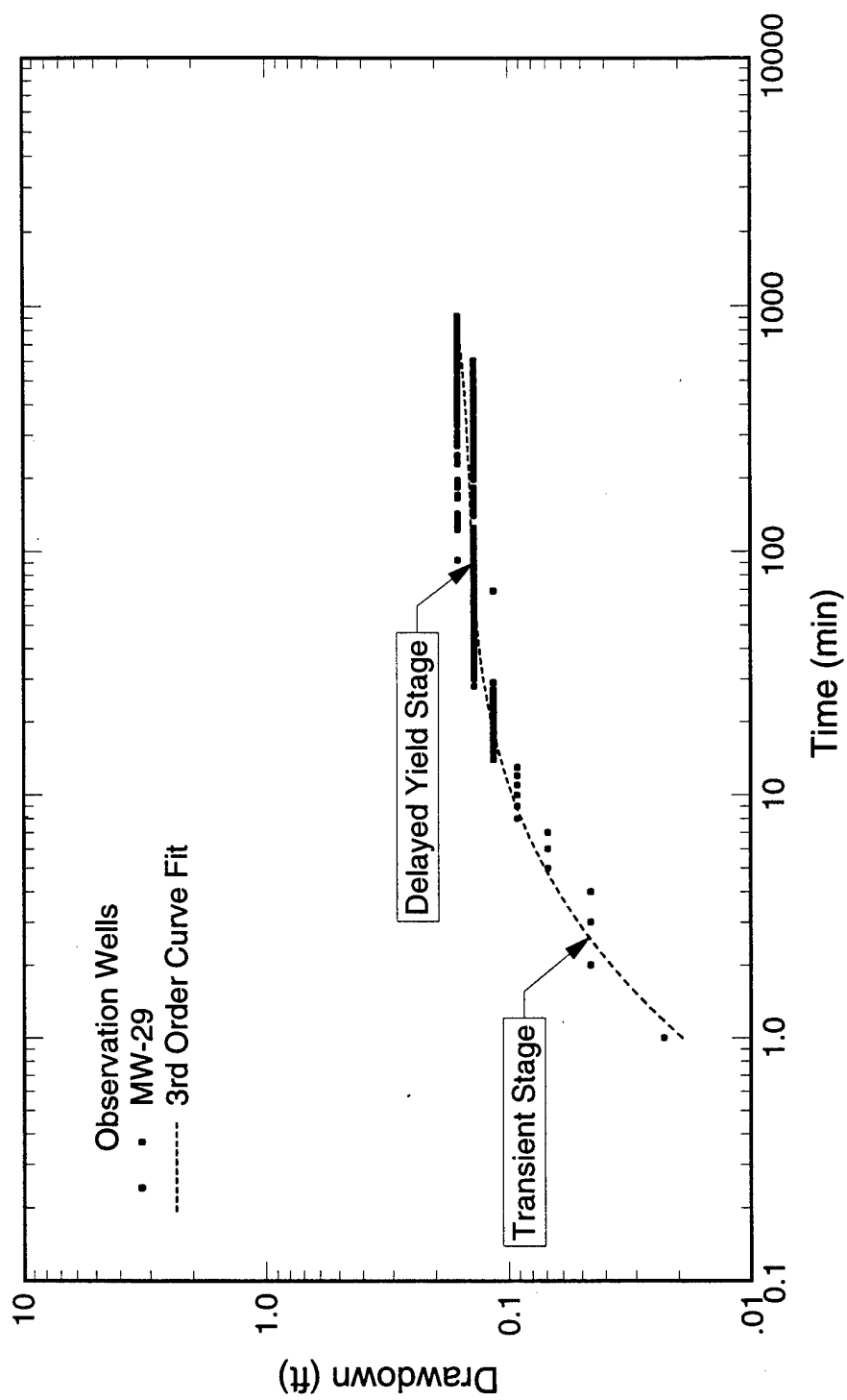
Figure 38. Typical Pumping Test Data Showing the Initial Transient and Delayed Yield Stages of the Test.

TABLE 12. SUMMARY OF TRANSMISSIVITY, HYDRAULIC CONDUCTIVITY AND STORAGE VALUES.

Estimates for the GRFL, Lower half of the Columbia Aquifer

Test Method	Analysis Method	Type	Tx, Ty (ft²/day)	K_r^* ft/day	K_z^* ft/day	S (1/ft)	Sy
Pumping Test #1	Boulton	Transient early and late time unconfined	100.45 to 374.83	7.94 to 28.35	1.02 to 2.04	6.56×10^{-5} to 6.56×10^{-4}	0.22 to 0.36
	Jacob	Transient early time confined	354.36 to 530.15	28.35 to 45.52	N/A	N/A	N/A
	Dupuis	Steady-state unconfined	22.32 to 56.74	1.76 to 4.54	N/A	N/A	N/A
Pumping Test #2	Boulton	Transient early and late time unconfined	306.93 to 558.06	18.43 to 34.02	0.45 to 1.08	N/A	0.28
	Dupuis	Steady-state unconfined	0.6 to 0.9	3.40 to 5.10	N/A	N/A	N/A
Slug Test	Kansas Geological	Unconfined well-skin transient	N/A	2.15 to 8.78	0.99 to 2.55	9.48×10^{-4} to 0.19	N/A

* K_r radial direction; K_z vertical direction

While the slug test results are generally lower than the pumping test results, the difference is less than an order of magnitude. These differences are attributed to factors such as: (1) slug tests are point estimates, whereas pumping tests estimate the average K between the pumping and observation wells; (2) slug tests were conducted at a number of locations; and (3) differences in analysis methods.

The specific yield estimates from the Boulton analysis of an average of 0.29 are high when compared to typical values. Specific yield, which is a measure of drainable porosity in an unconfined aquifer, is typically reported to be 0.28, 0.08 and 0.44 respectively for sand, silt and peat (Domenico & Schwartz 1990) (Reference 26).

Generally, the more coarse the material the more specific yield approaches the total porosity of the material (Reference 24). Since the lower half of the Columbia formation at the GRFL contains coarse sands and gravel, as well as silts, an average specific yield of 0.29 is not unreasonable.

The steady-state and early-time transient analyses, produced estimates of hydraulic conductivity lower and higher then the Boulton method by at least 50%. The steady-state solution for the unconfined case is limited to one estimate of transmissivity in the radial direction and relies on accurate measurements of the radius of influence, constant flow rate, and measurement of the pressure head directly outside the bore hole. In general, K is more sensitive to the head measurement than to the other parameters. Nevertheless, the steady-state solution is close to the other estimates for hydraulic conductivity. The early time drawdown method, or Jacob analysis, is commonly used for analyzing drawdown data in confined aquifers only; it can only be used for the early time where the unconfined aquifer acts like a confined aquifer. After the initial storage is depleted the unconfined aquifer no longer behaves like a confined aquifer and Jacob's assumptions are no longer valid.

The best estimate of hydraulic conductivity from the first pumping test is the Boulton method estimate of 14 feet/day (5×10^{-03} cm/sec) in the radial direction and 0.85 feet/day (3×10^{-04} cm/sec) in the vertical. The specific yield is estimated to be 0.29 and the storage to be 3×10^{-4} 1/feet. (1×10^{-05} 1/cm). The transmissivity is estimated in the radial direction to be 2.5×10^4 feet/day(1.9 cm^2/sec).

A second pumping test was conducted using the Dames and Moore deep well (DM337D) as the pumping well and the tracer test observation wells as monitoring wells. This pumping test revealed slightly higher hydraulic conductivity than at other areas of the GRFL. The range of conductivity reported in the Table 12 reflects a trend of increasing hydraulic conductivity as one moves from Location T-01. Measured K values at wells T-01, T-02L, T-02, and T-02R tended to be lower than at wells T-03R, T-03, and T-03L, which are closer to the Dames and Moore well. Although the range itself is less than an order of magnitude, the pumping test indicates higher conductivity in this area than in the area of the first pumping test (see Appendix K for the time-drawdown curves). Also notable is that the Dames & Moore well is only screened in the bottom 10 feet of the aquifer, not over the entire depth. Thus it does not conform to the assumption of a fully penetrating pumping well. This condition implies that the analysis may underestimate the hydraulic conductivity of the screened section.

Examination of the CPT pushes in the location reveal that the penetration pore pressures in the lower portion of the aquifer lie on the hydrostatic line, indicating a clean sand. In the upper portion of the saturated thickness of the aquifer, the CPT pore pressures were lower than hydrostatic, indicating a silty sand dilation which would have a lower conductivity than the deeper clean sands. There appears to be a clean sand lying in a buried channel near the Dames and Moore (Reference 2) well. This conclusion is drawn from the pumping test results and examination of the penetration pore pressure data and the deeper depth to the aquitard observed in CPT sounding T-02 as compared to CPT sounding T-01.

5. Results of Correlation of CPT to Hydraulic Conductivity

Analysis of the CPT data to determine hydraulic conductivity was conducted using two approaches. For the aquitard, which has a low hydraulic conductivity, pore water

pressures in excess of the static water pressure will be generated as the CPT penetrates the soil. These excess pressures will decay, once the CPT tip has passed, and the decay rate is related to the hydraulic conductivity. For normally consolidated soils, theoretical relationships between the rate of excess pore pressure decay and hydraulic conductivity are widely used to estimate the radial conductivity (K_r). This was the approach used to determine the hydraulic conductivity of the Calvert formation clay aquitard. To confirm the CPT dissipation results, laboratory permeameter test on Shelby tube samples were conducted.

For soils with relatively high hydraulic conductivities, such as sands and clayey sands, few CPT field test methods are available for direct determination of the hydraulic conductivity; and none of the field methods are applicable to the vadose zone. As the water table was significantly deeper than expected and many of the test cells will be flooded to raise the water table, a method to estimate the hydraulic conductivity from the CPT data was required. The approach taken was to determine an empirical correlation between the CPT data and available field hydraulic conductivity tests (i.e. the slug and pumping tests). Empirical relations between grain size distribution data and hydraulic conductivities were used to extend the limited slug and pumping test data and increase the database which could be correlated to the CPT results.

K in Calvert Formation Aquitard

At selected depths in the aquitard the penetrometer was stopped and the dissipation of excess pore pressure was observed. All of the dissipation tests were usually run until at least 50 percent of the excess pore pressure had dissipated. This length of time, t_{50}, was then used to determine the lateral coefficient of consolidation and permeability in the given soil layer..

A dissipation test in the aquitard clay soil is shown in Figure 39. Total pore pressure is presented on a semi-log plot versus time. The value of P_n in Figure 39 is the average of the last ten pore pressure measurements. If the dissipation test is sufficiently long, P_n will be equal to the static pore pressure. This value can also be determined from the water table elevation at some sites. Knowing the static pore pressure (u_o), as well as the peak pressure observed during the test (u_p), the pore pressure at 50 percent of dissipation (u_{50}) can be determined. As indicated in Figure 39, t_{50} can then be read directly from the dissipation profile.
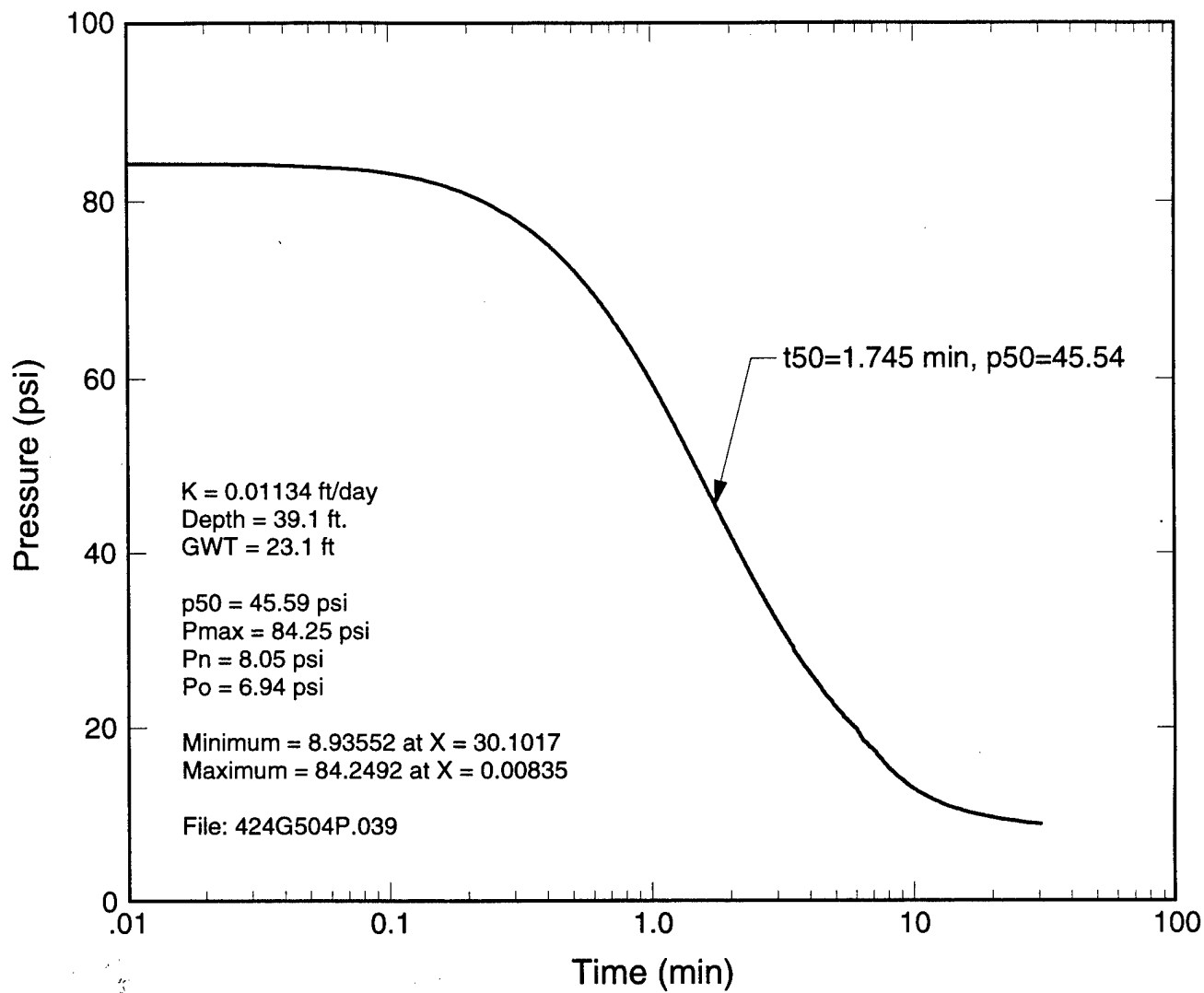
Figure 39. Example of a CPT Dissipation Test Conducted in the Clay Aquitard.

An estimate of K_r was made using the techniques developed by Baligh and Levadoux, (1980) (Reference 27). The method uses the coefficient of consolidation which is calculated as

$$C_H = \frac{T_{50}R^2}{t_{50}}$$ Eq. 1

where: T_{50} = theoretical time factor at 50% dissipation = 5.5 for ARA's cone

R = radius of cone in centimeters

t_{50} = measured time at 50% dissipation in seconds

from which the K_r is calculated as:

$$K_r = \frac{C_N \gamma_w}{M}$$ Eq. 2

where: C_H = coefficient of lateral consolidations

γ_w = unit of weight of water

M = constrained modulus

The constrained modulus is calculated as:

$$M = \alpha q_c = \frac{1}{m_v}$$ Eq. 3

where: α = empirical factor = 4 for the GRFL site

q_c = measured tip resistance, not corrected for pore pressure effects

m_v = volumetric compressibility.

Dissipation data were obtained at five locations in the aquitard and one location at the interface between the aquitard and underlying soils. Table 13 is a summary of the hydraulic conductivities calculated from the dissipation data and laboratory test results.

The average K_r value was calculated by taking the inverse log of the average of the log (K_r). The CPT hydraulic conductivity in the aquitard is 8.4 x 10^{-3} feet/day, which is slightly higher that the laboratory determined value of 4 x 10^{-3} feet/day. The CPT is primarily measuring the horizontal conductivity, while the laboratory test is measuring the vertical conductivity which is general less than the horizontal.

As discussed above, analysis of the CPT data was conducted to determine a relationship between the CPT data and K. The pumping and slug test data and grain size distribution data were used in the correlation effort. Correlations between the K and grain diameter assume that as grain diameter decreases K also decreases. Theoretical relationships such as that developed by Taylor (1948) (Reference 28) have confirmed the relation of K to the square of the grain diameter. Since Taylor's work, other formulations have been developed such as the Kozeny-Carman equation. Hazen proposed a simplified relationship between K and grain size as:

$$K = 2.84 \times 10^5 \, D_{10}{}^2 \qquad \qquad \text{Eq. 4}$$

where D_{10} =   Diameter of 10 percent passing
        K   =   ft/day

Work by Lane et al (1946) (Reference 29) indicated that the coefficient in Equation 4 varies as a function of soil type as show in Table 14.

TABLE 13. SUMMARY OF AQUITARD HYDRAULIC CONDUCTIVITY TESTS

CPT DISSIPATION ANALYSIS RESULTS			
CPT No.	**Depth (feet)**	**K (ft/day)**	**Soil Type**
CPT 01	41.5	5.7×10^{-3}	Silty Clay
CPT 01	45.5	9.3×10^{-3}	Silty Clay
CPT 11 D	39.1	1.1×10^{-2}	Silty Clay
CPT 11 D	50.2	4×10^{-3}	Silty Clay
CPT 12 D	51.1	2.2×10^{-3}	Silty Clay
CPT 12 D	60.1	4.2×10^{-2}	Silty Clay
Average		8.4×10^{-3}	
Assumed Alpha Value = 4			
LAB Hydraulic Conductivity Results			
	Depth (feet)	**K_z (ft/day)**	
	39.8 - 40	3.7×10^{-3}	
	41.7 - 42.0	4.5×10^{-3}	

TABLE 14. CORRELATION HYDRAULIC CONDUCTIVITY TEST DATA TO D_{10} AS A FUNCTION OF SOIL TYPE.

Soil	Particle Size, D_{10}(cm)	Hydraulic Conductivity (μ/sec)	k/D_{10}^2 (1/sec cm)
Coarse Gravel	0.082	1100	16
Sandy Gravel	0.020	160	40
Fine Gravel	0.030	71	8
Silty Gravel	0.006	4.6	11
Coarse sand	0.011	1.1	1
Medium sand	0.002	0.29	7
Fine sand	0.003	0.096	1
Silt	0.0006	0.15	42
		Average =	16

Because the soils at GRFL encompass the range of coefficients in Table 14, the average coefficient of 16 was used:

$$K = 16\, D_{10}^2 \qquad\qquad \text{Eq. 5}$$

A correlation of the CPT data to the K data was developed based on the CPT Soil Classification Number (SCN), which relates CPT tip and sleeve resistance to soil type, as is shown in Figure 15. As can be seen in Figure 15, the SCN number increases as the coarse grained content increases. Increases in the grain size of a soil correlate to an increase in hydraulic conductivity; several researches have developed methods to predict K, based on grain size (see Masch and Denny, 1966 (Reference 30), Bear 1972 (Reference 31) and Todd 1959 (Reference 32)). Freeze and Cherry (1979) (Reference 22) have summarized the variation in K as a function of soil type as shown in Figure 40. This figure demonstrates a similar variation in grain size, that is as the grain size becomes fine, K decreases. As can be seen, hydraulic conductivity varies by 13 orders of magnitude, and Freeze and Cherry suggest that an order of magnitude knowledge of hydraulic conductivity is very useful.

Hydraulic conductivity can be related to the CPT soil classification number as:

$$K = 10^{(scn-8.5)} \quad \text{for } 4.0 < SCN \le 7.5 \qquad\qquad \text{Eq. 6a}$$

$$K = 10^{(scn-9.5)} \quad \text{for } SCN \le 4.0 \qquad\qquad \text{Eq. 6b}$$

for unconsolidated soils (and SCN of less than or equal to 7.5). The hydraulic conductivity of consolidated clayey sands and clays is assumed to be the same as that of unconsolidated clayey sands and clays and can be estimated for very stiff silty sands (7.5< SCN < 8.5) as:
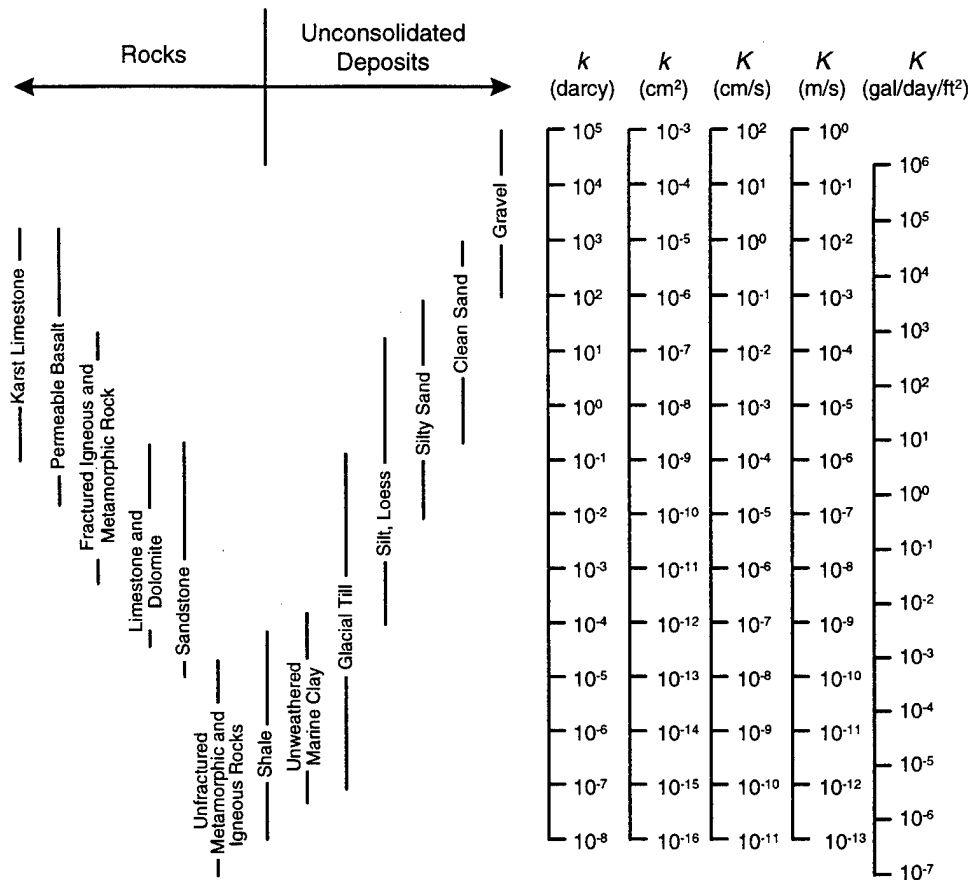
Figure 40. Freeze's Chart Relating Soil Type to Hydraulic Conductivity (Freeze, R. 1979).

$$K = 10^{-5} \qquad\qquad \text{Eq. 7}$$

and for very stiff silts and clays (SCN>8.5) as:

$$K = 10^{-6} \qquad\qquad \text{Eq. 8}$$

A comparison of estimates of K based on Equation 6, the pumping test, and K values determined from grain size data is plotted in Figure 41 (refer to additional comparisons in Appendix K).
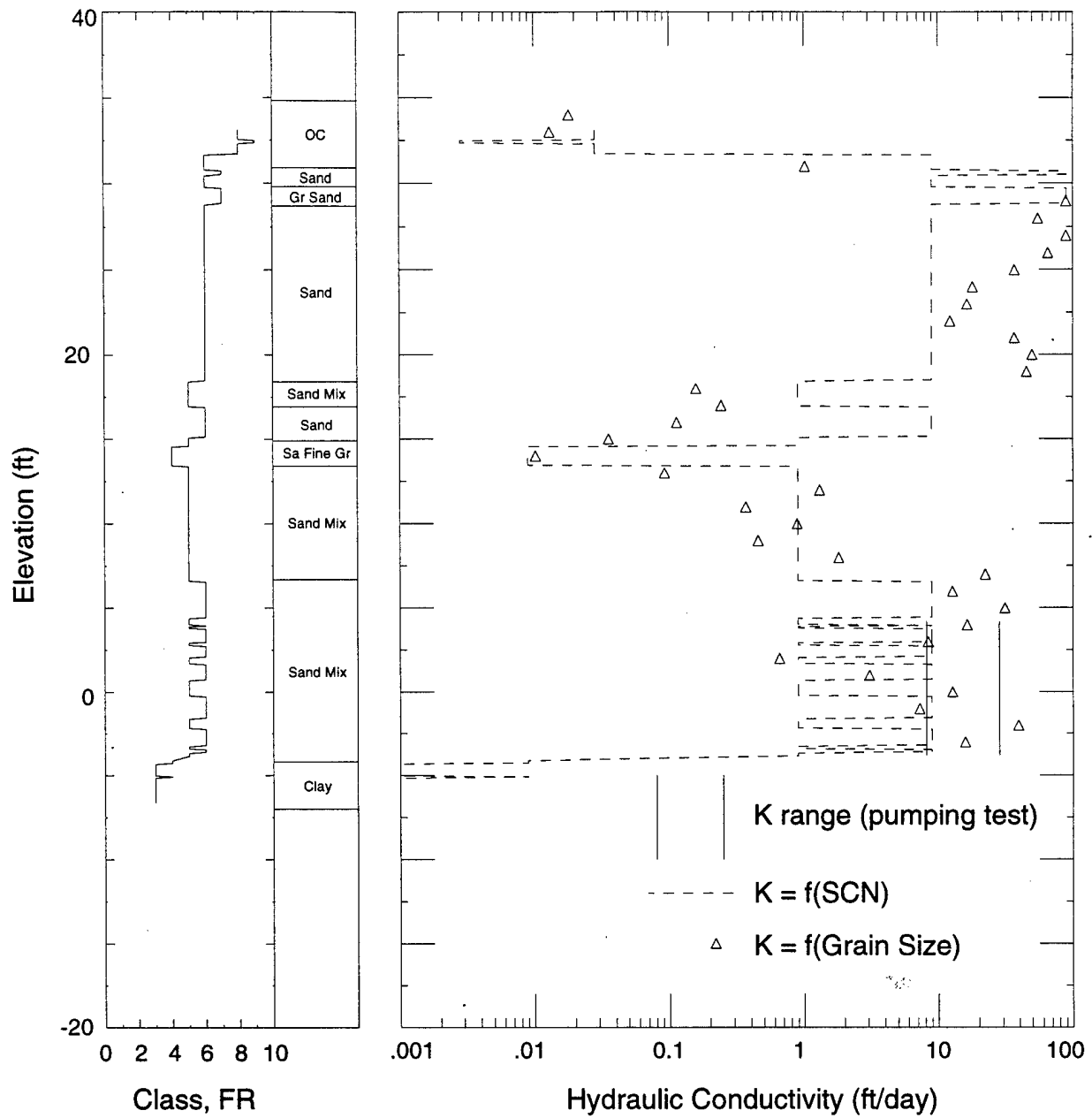
Figure 41.   Comparison of K Estimated from Soil Class Number (SCN) to Available Data.

In general, the CPT derived K estimates and grain size estimates of K are in good agreement. The CPT empirical equation does estimate a somewhat higher permeability in some of the finer grained soils such as between depths of 17 feet and 20 feet in Figure 41. However, K values derived from the grain size analysis are based upon an empirical correlation, and have an associated degree of uncertainty of at least a factor of 6 (based on Hazen's empirical factor of 100 and Lambs average factor of 16). Given the high degree of uncertainty in the K derived from grain size data and the good agreement to the pumping and slug test data, no modification to the simple equation presented above was warranted. Note that the slug and pumping test data were conducted at about the same depth in the formation and do not vary significantly. Additional K data, from field tests or laboratory tests in different soil types, would be desirable to further evaluate the correlation between CPT SCN and K.

6.   Discussion

Equations 6 through 8 provide an order-of-magnitude estimate of the hydraulic conductivity based on soil type. Examination of Figure 41 shows that soil hydraulic conductivity can vary by two orders of magnitude over short vertical distances (as between elevations of 12 to 14 feet). Hydraulic conductivity values over this depth interval varied from 1×10^{-2} to 1.0 feet/day (3.5×10^{-6} cm/s to 4×10^{-4} cm/s). This variation occurred in thin zones, and was not predicted from the grain size data. The grain size data represents the composite of a 20 inch-long soil sample and therefore the thin zones with reduced conductivity are not well represented by the grain size data.

There are a number of second order effects which influence hydraulic conductivity, such as porosity, and which are not accounted for by Equations 6-8. Porosity has a significant effect on the hydraulic conductivity, as demonstrated in laboratory testing (Lamb and Whitman, 1969) (Reference 33). An attempt was made to include porosity effects by assuming that, for a given soil type, the tip resistance will increase as soil porosity decreases. Using correlations of the CPT tip resistance to density, back calculated porosities were plotted versus K as determined from the grain size. A crude correlation was observed, but did not significantly improve upon Equations 6-8 and hence was not further pursued.

We concluded that improved predictions of K based on CPT SCN and tip resistance could be made. However, the database would have to be increased to include a significant number of laboratory tests on undisturbed samples from the site. With Equations 6 through 8, the CPT predicted K is within an order of magnitude of the grain size predicted K and less than an order of magnitude for the pumping and slug test data. Including laboratory derived measurements of K in the database could improve the accuracy of the correlation to less than an order of magnitude.

The correlation between CPT SCN and K was used to construct a three-dimensional map for K values using geostatistical methods. The 3-D map is presented in Figure 42 as a block diagram. Shown are the K value as a logarithmic value. The dark shades in the figure represents layers with low K values (10^{-2} feet/day or lower). The light shades represent areas of high K values. The aquitard is clearly visible in the 3-D view as are higher conductivity zones in the aquifer. A low conductivity zone was observed in the upper portion of the aquifer and is thicker at the northern end of the site. This zone becomes thinner and less pronounced toward the southern end of the site.

A lower conductivity zone was observed in the middle and western portion of the site. The CPT tip resistance in this zone was quite high, indicating a consolidated soil. The predicted low K, near the surface zone in Figure 42 may be due to the assumed K for dense soils and may not in fact exist. Additional laboratory testing on soils from this area would assist in improving the prediction of K in the shallow soils.

Filename: log_k2.srf

-1.0
-2.0
-3.0
-4.0
-5.0
-6.0
-7.0

Log(K)

North

Angle Above Horizon: 38 degrees
Viewing Direction: 310 degrees
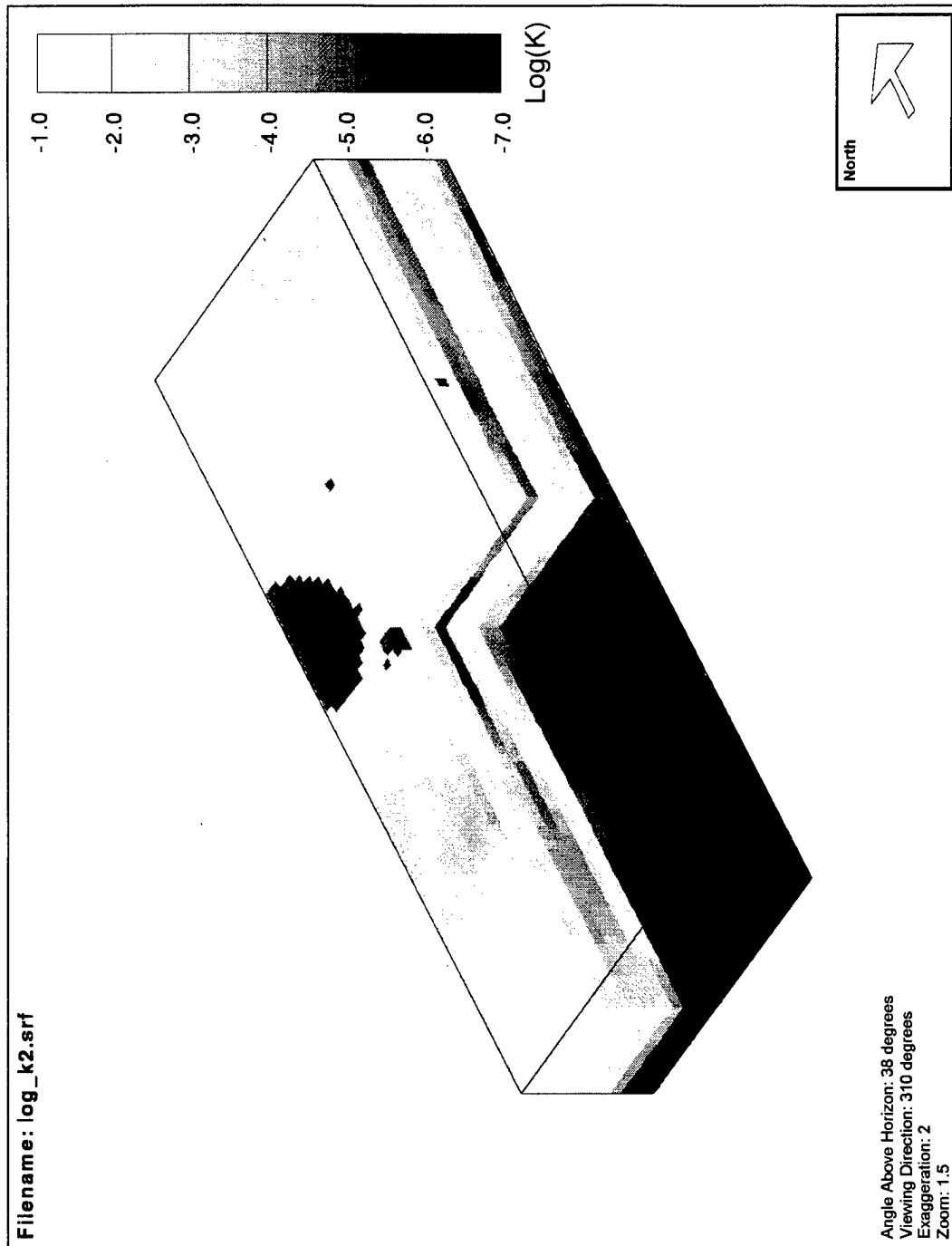Exaggeration: 2
Zoom: 1.5

Figure 42. Three Dimensional Block Model of Log (K) Derived from CPT Soil Class Number Using Equations 6-8. The Dimensions are 198 x 552 50 (X-Y-Z) and the Origin is Located at (-98, -262, -14) in Reference to the GRFL Coordinate System.

B. TRACER TEST

1. Objective

The tracer test objective was to identify variations in hydraulic conductivity over depth, and to determine longitudinal and lateral dispersivity in the various conductivity zones identified. Parameters determined from a tracer test are critical for determining the nature of transport in the subsurface. In a tracer test, a detectable material is released into the subsurface at one location, and its passage at one or more additional locations is then observed. By inverting the observed temporal and spatial distribution of the tracer as it moves through the study area, hydraulic conductivity and dispersion can be quantified. The tracer test supports the dual objective of characterizing both depth-dependent variation in hydraulic conductivity, and longitudinal and transverse dispersion. Tracers are chosen based on the goals of the test, and consist of substances not harmful or toxic. The substance should also be considered conservative, meaning it will not decay or react with the soil or groundwater during the study.

2. Approach

a. Overview

To allow the identification and quantification of variations in hydraulic conductivity over depth, a multilevel, induced-gradient tracer test was conducted. In a multilevel test, the tracer is released uniformly over the depth of the aquifer. Its passage at discrete vertical and horizontal coordinates in the study domain is then observed. The discrete nature of the observations allows the analyst to characterize spatial variability, thus supporting the objective of identifying depth-dependent variations in hydraulic conductivity.

An induced-gradient tracer test was conducted at the GRFL. This type of test involves pumping from an extraction well at a high flow rate to produce a local gradient between the well and the tracer release point. The pumping activity produces a cone of depression around the extraction well; the release well is then located within this zone of influence. The cone of depression captures the tracer in its radial flow field, increasing confidence in the directional predictability of tracer movement. Rows of observation wells, installed between the release well and the extraction well and oriented perpendicular to the flow, provide samples from which the temporal and spatial distribution of the tracer can be observed. Sampling is from discrete depths in the observation wells. The observed concentration distribution over time is used to characterize both the longitudinal and lateral dispersive behavior of aquifer flow.

Two additional benefits of a single extraction well, induced-gradient test are: (1) the greater-than-natural, induced-gradient increases the speed of transport through the aquifer, thus limiting the duration of the test to a manageable time scale; and (2) observations of tracer concentration over time in the extraction well can be used to perform mass balance calculations.

Preceding the tracer test at GRFL, pumping tests were performed in the planned tracer test domain to evaluate transport properties, such as hydraulic conductivity, storage, and specific yield in a vertically averaged context. Estimates of these properties are very helpful in specifying relevant injection and extraction rates, as well as the sampling schedule for a tracer test. The pumping tests were conducted in the same well planned for tracer release and recovery. Results from the first pumping test indicated that the transmissivity at the original tracer test location was too low to support adequate flow for an induced-gradient tracer test. Only one gallon per minute of flow could be sustained in this area. A potentially suitable alternative test location in the vicinity of a previously existing well was identified based on reported yield from earlier pumping tests. Because well yields in excess of three gpm had been reported at an existing well elsewhere on the site, the decision was made to conduct the test at this location if the reported yield could be sustained. A subsequent yield test, conducted at the existing well (Dames and Moore deep well, DM337D (Reference 2), see Figure 9), verified that the three gpm rate was sustainable. Therefore, the tracer test was conducted at this location. After installing monitoring wells in the new test domain, a pumping test was executed, followed by the tracer test.

b. Design Process

The well layout, tracer quantity, and sampling plan were based on analysis of the expected spatial and temporal scales of the test. A widely accepted formulation of dispersive behavior formed the basis of this analysis. It is presented in detail by Freeze and Cherry (1979) (Reference 22). The three-dimensional description of tracer concentration resulting from a point release as a function of time is:

$$C(x,y,z,t) = \frac{M}{8(\pi t)^{3/2}\sqrt{D_x D_y D_z}}\exp(-\frac{X^2}{4D_x t} - \frac{Y^2}{4D_y t} - \frac{Z^2}{4D_z t}) \qquad \textbf{Eq. 9}$$

where

x, y, and z	=	spatial coordinates of the center of gravity of the tracer mass
t	=	time
M	=	the mass of tracer released at the point source
D_x, D_y, D_z	=	the coefficients of dispersion in the x, y, and z directions
X, Y, Z	=	distances in the x, y, and z directions from the racer mass center of gravity.

Ninety-nine point seven percent of the tracer mass occurs in a zone described by an ellipsoid whose dimensions, measured from the center of mass, are $\sqrt{2D_x t}$, $\sqrt{2D_y t}$, and $\sqrt{2D_z t}$ in the x, y, and z directions, respectively. These distances are equivalent to three standard deviations of the spatial concentration distribution with respect to each direction.

To identify appropriate length and time scales for the tracer test, parametric calculations were conducted using Equation 9 and a range of relevant values of dispersion coefficients obtained from the literature. Estimates of the travel speed of the center of gravity (to get migration distance versus time) were made using assumed porosity and hydraulic conductivities determined from either the CPT profiles or pumping test results. The appropriate mass of tracer-to-release was determined in a similar manner by defining the plume boundary as the iso-concentration line within which 99.7% of the tracer mass would occur, and back-calculating a release mass. This would result in a boundary concentration exceeding the minimum detection limit of the analytical technique without exceeding the linear range of the analytical instrument at the release concentration.

The appropriate temporal, spatial, and dilutional scales determined for the test by the described technique are reflected in the details of the well layout, sampling schedule, and quantity of tracer released as described below.

An existing well, 32.8 feet downstream of the release point in the direction of natural groundwater flow, was used to induce the hydraulic gradient through pumping, and to capture the tracer so that mass balance could be checked. Based on a higher transmissivity estimated in this area, the projected travel time for the tracer center of mass was 4 days. The tracer tail was estimated to take up to 8 additional days to pass.

Observations of tracer concentration were made at 6 observation wells, excluding the pumping well. Each observation well is screened throughout the saturated zone. The wells are located along 2 transects orthogonal to the anticipated direction of tracer travel. The well layout is discussed below. Water levels in the release, capture, and observation wells were measured and recorded throughout the duration of the tracer test.

c.   **Assumptions**

The first assumption incorporated into the design of the tracer test was that the three gpm yield of the pumping well was indicative of a higher transmissivity in the area of the Dames and Moore well. This was the primary reason for moving the test location. The vertical hydraulic conductivity in the study area was also assumed as significantly less than the horizontal hydraulic conductivity in the test design. In an aquifer that exhibits significant variation in horizontal hydraulic conductivity with depth, a relatively low vertical hydraulic conductivity suppresses migration of a tracer between adjacent conductivity strata. Variations in the horizontal transport rate cause the tracer in some strata to lead or follow that in another. This assumption is typically used in tracer studies to facilitate tractable analysis of the results.

Additional assumptions incorporated into the tracer test design were that: (1) within the zone of study the aquifer thickness was relatively uniform, (2) the horizontal hydraulic conductivity appeared to have low variability, and (3) the hydraulic conductivity values determined from the pumping test were representative of the aquifer. At the time of

design and execution of the tracer test, all evidence suggested these three assumptions were appropriate and applicable to the study region.

The last assumption, inherent in the analytical formulation described above, is that the mass of tracer released has no volume (i.e. that it is truly a point release). This assumption in any tracer test is a physical impossibility. However, if observation of the tracer's passage is performed at a sufficient distance from the release point, the effect of this unrealistic assumption on the analysis is negligible. Alternatively, if the analysis is based on changes between two separate observations of the tracer distribution, this assumption has no bearing on interpretation of the results.

d. Test Design

Tracers. The tracer released was fluorescein dye. Although fluorescein has a small potential to be retarded in some geologies, earlier analyses of GRFL groundwater indicated insignificant potential for adsorption. Fluorescein is a fluorescent dye with a peak excitation wavelength of 486 nm corresponding to a peak emission wavelength of 514 nm. It was analyzed using a Turner Designs Model 10/AU fluorimeter.

The Model 10/AU can detect fluorescein with adequate precision to as low as 2 parts per billion (ppb) by mass. Given the expected dilution at the plume boundary, defined as the iso-concentration line within which 99.7% of the tracer mass is contained, an initial point release of 3.2 grams of fluorescein was adequate to meet the target detection criteria.

Well Layout. Eight wells were used in this study to provide the means of monitoring the tracer as it moved through the groundwater flow field (see Figure 43). The wells are aligned in the natural direction of groundwater flow, with the most up-gradient well being used for the release of the tracer and the most down-gradient well being used for pumping to induce a higher than natural gradient, increasing the predictability of the flow direction. The natural groundwater gradient in the area is fairly low (0.008). The 7 wells up-gradient of the pumping well are screened from the aquitard, up towards the water table level in the area. The average height of the water above the aquitard in the area is 18 feet. The water table elevation in this area is nearly 26 feet below the ground surface.

The layout supports analysis of tracer transport from the point release to the first transect of observation wells, as well as between the two transects of observation wells. Samples can be collected from the extraction well to verify conservation of mass.
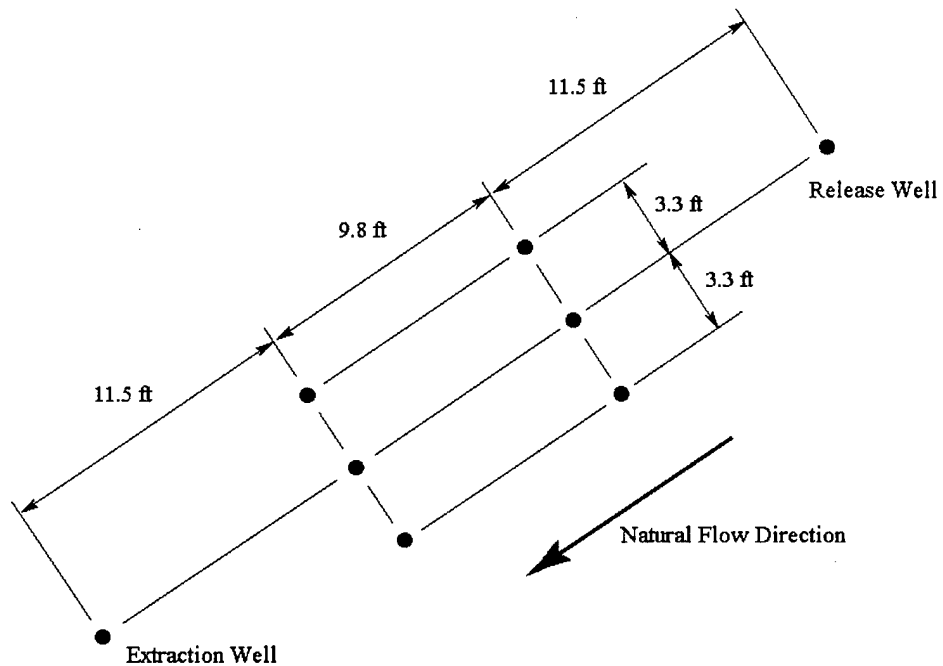
Figure 43. **Tracer Test Well Layout. The Layout Supports Analysis of Tracer Transport From the Point Release to the First Transect of Observation Wells, As Well As Between the Two Transects of Observation Wells. Samples Can Be Collected From the Extraction Well to Verify Conservation of Mass.**

e. **Test Execution**

Tracer Release. A slug of native groundwater tagged with fluorescein dye, a conservative fluorescent tracer, was released at 12:30 PM on April 29, 1996. The tracer was released into the aquifer over the approximate six-meter depth of the screened portion of the release well. The bottom end of the screened section terminates at the aquitard, at an approximate depth of 38 feet.

A hose of smaller diameter than the release well was used to inject the slug of tracer directly throughout the screened depth of the well. This introduction was followed by a slug of untagged water to help push the tracer out of the well and into the aquifer. Some of the tracer remained initially in the well, and slowly flushed out into the aquifer over a period of

several days by mixing with groundwater flowing through the well. The tracer concentration in the release well indicated the logarithmic decay generally associated with diffusive dilution.

Sample Collection. Samples were collected every 6 hours from all wells including well DM337D. Sampling continued until 18:00 on May 20, 1996. At this time, the test was terminated because no tracer concentrations statistically separable from background levels had been detected.

Samples were collected from depths of 41, 39, 35, and 31 feet below the top of the PVC casing at each observation well using a packer. The packer isolates a segment of well screen by inflating two separated diaphragms against the inside the well. A water sample is then allowed to enter a sampling chamber in the packer through a check valve situated between the two diaphragms. The sample is forced to the surface through a tube by the release of compressed air into the sample chamber. Under this internal pressure the check valve closes, preventing the sample from being ejected back out into the medium. The packer was purged of three volume equivalents of the isolated segment by repeated operation before each sample was finally taken for analysis.

f.   Tracer Analysis

Samples from the observation well were analyzed for fluorescein with the fluorimeter equipped with a fluorescein filter kit and set up in cuvette mode. Since the fluorimeter's response to fluorescein dye is linear only in the range from 2 to 400 parts per billion (ppb), the instrument was calibrated in this range. As the concentration of a sample exceeds 400 ppb, the calibration curve becomes nonlinear. Therefore, samples initially reading at or above this limit were diluted to keep the analysis in the linear response range.

g.   Water Level Measurement

Hydraulic head in the release, pumping, and observation wells was measured using a hand-held conductivity water level sensor.

3.   Results

Samples were collected and analyzed from the observation wells, release well, and extraction well over a period of 25 days following release of the tracer. In total, over 1,440 observations were made. No results indicated the presence of tracer which is statistically distinguishable from background noise in the observations.

The upper 99% confidence limit of an assumed normal distribution of background analytical results is generally used as the threshold above which an observed tracer concentrations is considered distinguishable from background noise in a tracer test. A statistical analysis was performed on the analytical results from the first four days of sampling in the observation wells and extraction well, when tracer was expected to have moved far enough to be detected in the observation wells. The upper and lower 99% confidence limits were determined by adding and subtracting three standard deviations from the mean.

Only 10 of 1251 observations made outside the release well exceeded the calculated threshold value of 13.3 ppb. This number of observations is equivalent to 0.8% of the population, and is statistically insignificant since up to 1% of background noise would ordinarily exceed the threshold value. In summary, no tracer was observed outside the release well that was distinguishable from background noise.

4. Discussion

The design of the tracer test, including the observation well layout, sampling plan, and test duration, was based on anticipated temporal and spatial scales of tracer movement, relying on preliminary indications of acceptable hydraulic conductivity and aquifer thickness in the test domain. This analysis indicated that a flow rate of at least 3 gpm was required to conduct the planned induced-gradient tracer test. An existing well, DM337D, was able to provide the required yield of three gpm. Our initial analysis of this well's pumping test data indicated a hydraulic conductivity slightly higher than the average of the other pumping and slug test data. However, the results were within the scatter of slug test data. The higher yield of Well DM337D was taken to indicate that that hydraulic conductivity was great enough in the vicinity of this well to support an induced-gradient test.

Two CPT profiles, CPT-T01 and CPT-T02, were obtained during the installation of the tracer test well array. These CPT profiles showed the soil type distribution over the saturated depth of the aquifer to be characteristic of profiles taken earlier throughout the GRFL site. It was concluded that this location was typical of the GRFL site, with the possible exception of a slight variation at the bottom of the aquifer where pore pressure measurements indicated potentially higher permeability than in other regions.

The planned tracer test was designed to rely on a greater-than-natural hydraulic gradient induced by pumping. This would result in a mean travel time from the point of tracer release to the observation wells on the order of ten days. The fluorescein dye was released as a slug into the aquifer, and sampling and analysis continued for 22 days without detecting tracer in any of the observation wells. The test was then terminated.

After the tracer failed to appear in the monitoring wells and extraction wells as expected, a more detailed analysis of the pumping test, tracer test and CPT data was conducted. A cross-section of the layering derived from this analysis is presented in Figure 44 showing the tracer test wells, drawn curve and layering interpreted from the CPT data. The post tracer test analysis indicates the potential existence of a clean sand overlying the aquitard in a channel on a east-west line from the Dames and Moore well. This conclusion is based on examination of the two CPTs at the tracer location and CPTs 03, 04 and 10. The penetration pore pressure for CPTs 03, 04, 10 and T-02 exhibited hydrostatic pressure immediately above the aquitard, which only occurs in clean sand.

We have attempted to back-calculate a hydraulic conductivity of the lower layer in Figure 44 using the measured drawdown data, water flow rate and hydraulic conductivity measured in the first pumping test. We have assumed that the results of the first pumping test are

representative of the silty-sand overlying the hypothesized clean sand. The flow from the extraction well can be calculated as:

$$Q = \frac{\left(h^2 - H^2\right)\pi K_{x,y}}{\ln\left(\dfrac{r}{R}\right)}$$

Eq. 10

Assuming a $K_{x,y}$ of 3.0×10^{-3} cm/s, we calculate a flow rate of 1.2 gpm, which is less than the measured flow rate by 3.0 gpm. Equation 5.2.2 can be used to calculate flow in layered sites by using an average $K_{x,y}$ determined as (see DeMarsily):

$$K_{AVGx,y} = \frac{\left(K_{1,x,y}\right)\left(t_1\right) + \left(K_{2,x,y}\right)\left(t_2\right)}{t_1 + t_2}$$

Eq. 11

Assuming a two layer condition and that the upper layer $K_{1,x,y}$ is known, the hydraulic conductivity of the lower layer can be estimated by solving Equation 10 for the yield in Layer 1, (1.2 gpm), and then substituting the difference in actual flow rate, (1.8 gpm), in to Equation 10. Equation 10 is then solved for $K_{x,y}$ in Layer 2, given the flow rate needed to meet the actual yield of the well during pumping (3 gpm). The result is a $K_{x,y}$ of 1.2×10^{-2} cm/s for the clean sand layer shown in Figure 44. The estimated $K_{x,y}$ of the clean sand is about a factor of four greater than that of silty sand. This analysis indicates that the 3 gpm yield from Well DM337D is due to additional water supply through the lower clean sands. Consequently, the flow in the upper portion of the saturated aquifer, into which the tracer was released, was much lower than the pre-tracer analyses had anticipated. This resulted in very slow movement of the tracer which was released in the saturated zone above the channel.
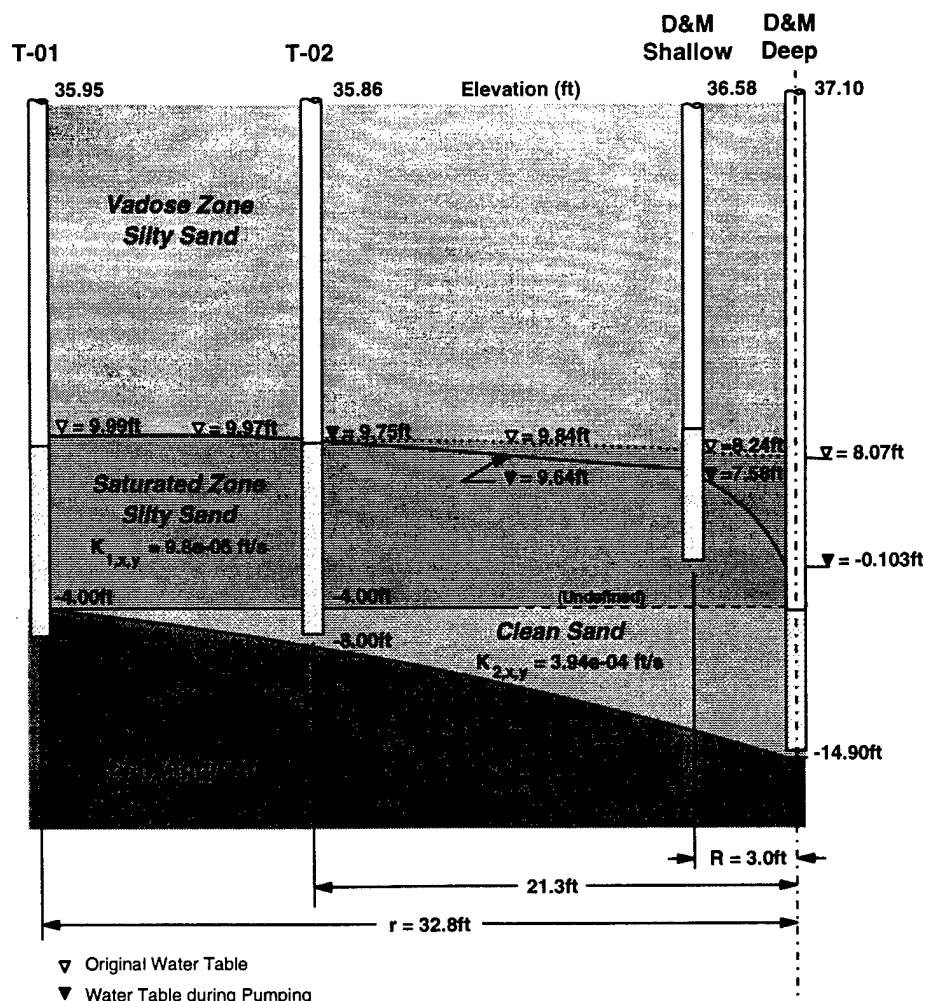
Figure 44. Cross Section in Area of Tracer Test.

Well T-01 is injection well, T-02 one of the monitoring wells, and D&M deep well is extraction well. Evidence of clean sand layer shown from CPT T-02.

Based on the tracer test experience, we are able to make several recommendations for the GRFL site. We first recommend that further investigation be undertaken to characterize the relatively high conductivity channel identified at the north end of the GRFL site. Determining the channel's size and hydraulic properties are important to the understanding of its influences on flow and transport in the area. We have also concluded that a large-scale, induced-gradient tracer test is not feasible at the GRFL site. The combination of low hydraulic heads and moderate hydraulic conductivity in the aquifer will not produce a sufficient cone of depression to support the induced-gradient tracer test. Any future effort to characterize dispersion or depth dependent variability in hydraulic conductivity at the site should employ a natural gradient tracer study. We also recommend that any future tracer test studies include additional laboratory testing of soils to determine hydraulic conductivities (which will also assist in developing correlations to the CPT), and to insure that the tracer selected is conservative.

C. HYDRAULIC CONDUCTIVITY IN THE VADOSE ZONE

1. Objective

The objective of the vadose zone characterization was to provide quantitative data about physical, hydraulic, and pneumatic characteristics that influence the transport and fate of introduced contaminants, along with qualitative information regarding the subsurface geology and lithology. As a part of this effort , ARA and subcontractor Daniel B. Stephens and Associates, Inc. designed and conducted tests to determine the unsaturated hydraulic conductivity of the vadose zone.

2. Approach

It was decided that an in situ measurement would provide the best estimate of the conductivity profile, and as a result, an Instantaneous Profile (IP) or unsteady drainage flux test was initiated. A 3- x 3- meter (9.8- x 9.8-foot) square field site was established at the GRFL site in April of 1996. Time domain reflectometry (TDR) probes, designed by ARA, were installed into 3 inch bore holes at 2-, 4-, 8-, 12-, and 16-foot depths within the 9.8- x 9.8-foot plot. Tensiometers, designed by DBS&A, were also installed into 3-inch bore holes at 2-, 4-, 8-, 16-, and 20-foot depths. Some of the tensiometers were installed in the same bore holes as the TDR probes to reduce disturbance to the plot. The tensiometers incorporated pressure transducers (Omega Scientific Inc.) which allowed data to be recorded with data logging equipment (Campbell Scientific Inc.). After the instrumentation had been installed, a steel border 9.8- x 9.8-foot square) about 8 inches high was driven into the ground and sealed to prevent water from leaking out during saturation of the plot.

3. Results

The initial phase of the test was to saturate the profile to a depth greater than 20 feet below ground surface. This was accomplished by ponding water inside the border to a depth of about 5 inches. The initial saturation phase lasted about 7 days, at which time it was determined, from the TDR and tensiometer data, that the profile was saturated. The water application rate, ponded water head, soil moisture contents, and soil water potentials were recorded at that time. Application of water was stopped and the plot was allowed to drain. The plot was covered with 6 mil plastic and a tarpaulin tent to prevent evaporation from the surface of the plot and to keep precipitation off the plot.

Data collected during the saturation phase were used to estimate saturated hydraulic conductivity at 7 depths (0-, 2-, 4-, 8-, 12-, 16-, and 20-feet) in the profile, corresponding to placement of the tensiometers. The water head data, recorded from the tensiometers, was used to calculate the gradients with depth (dH/dZ) and a water flux was calculated from the water application rate. Knowing the volumetric water flux, the area of infiltration, and the gradient, Darcy's law was used to calculate saturated hydraulic conductivities (Table 15) at each of the seven depths in the profile. The drainage phase of the test began when

TABLE 15. SUMMARY OF UNSATURATED HYDRAULIC PROPERTIES (CALCULATED)

Depth (ft)	α (cm^{-1}) Calculated Value	95% Confidence Limits Lower	Upper	N (dimensionless) Calculated Value	95% Confidence Limits Lower	Upper	θr (%)	θs (%)	Ksat (cm/s)
0	----	----	----	----	----	----	----	----	1.28E-04
2	0.0255	0.0113	0.0737	1.7498	1.0950	2.4447	10.00	29.00	3.39E-04
4	0.0359	0.0307	0.0411	3.2887	2.2958	4.2818	10.00	25.00	2.91E-04
8	0.0321	0.0120	0.0532	2.0529	2.2345	3.0713	10.00	21.00	1.15E-03
12	0.0338	0.0315	0.0361	3.5309	3.0422	4.0197	10.00	32.00	9.78E-03
16	0.0121	0.0063	0.0179	1.7010	1.2973	2.1045	10.00	28.00	4.96E-04
20	----	----	----	----	----	----	----	----	4.96E-04

α -van Genuchten parameter
N -van Genuchten parameter
θr -residual water content
θs -saturated water content
Ksat -saturated hydraulic conductivity

the ponded water head was essentially zero at the soil surface. The time when the water head had drained was recorded and data were collected at 6-hour intervals for 15 days.

4. Discussion

Data collected over the 15-day period were plotted and smoothed, then a closed-form analytical model for the description of the soil moisture content/soil water potential relationship was fitted to the data. (See van Genuchten, 1980.) (Reference 1). The model calculates curve fitting parameters (a and n) that can be used to calculate hydraulic conductivity at designated soil water potentials.

Equation 12 allows calculation of water content from knowledge of water potential and knowledge of the soil moisture characteristic.

$$\Theta = [\frac{1}{1+(\alpha\psi)^n}]^m \qquad \textbf{Eq. 12}$$

where

$$\Theta = \frac{\theta - \theta_r}{\theta_s - \theta_r} \qquad \textbf{Eq. 13}$$

ψ = Water potential (cm water)
α = cm^{-1}
Θ = Reduced water content
θ = water content at a given water potential
θ_r = residual water content
θ_s = saturated water content (total porosity)

θ_r is typically assumed to be the water content at the lowest pressure potential measured, but because the plot did not drain to sufficiently low water potentials, we designated θ_r as 10 percent water content to get a better fit from the model. A second assumption is also typically employed to eliminate one parameter. The value of 'm' is generally set as

$$m = 1-1/n \qquad \textbf{Eq. 14}$$

Unsaturated hydraulic conductivity can be calculated in terms of the pressure head as

$$K(\psi) = \frac{K_s\left[1-(\alpha\psi)^{mn}\left(1+(\alpha\psi)^n\right)^{-m}\right]^2}{\left[1+(\alpha\psi)^n\right]^m} \qquad \textbf{Eq. 15}$$

where K_s = saturated hydraulic conductivity
$K(\psi)$ = unsaturated hydraulic conductivity

Refer to Appendix L for more information on estimated hydraulic conductivity as a function of pressure head and moisture content. The estimates of hydraulic conductivity closely fit the measured soil moisture characteristic functions obtained from the IP test. All of the data can be generated with the knowledge of the parameters listed in Table 15.

D.   AIR CONDUCTIVITY IN THE VADOSE ZONE

1.   Objective

Success of several remediation technologies, such as Soil Vapor Extraction (SVE), bioremediation and air sparging, depends upon the ability of the soil to transport air, as is the case for SVE, or upon the effectiveness of air injection into the soil, as is the case for bioremediation. To date, measurements of air permeability have used injection or extraction wells with monitoring points at several ranges to determine the zone of influence. Once the zone of influence and pumping rates have been determined, a permeability value can be derived and used in the remediation design. Methods typically used for determining air permeability are discussed by Johnson (1990) (Reference 34).

Researchers have recognized that the use of a large-scale monitoring well, while acceptable for use in the design of a remediation system, has limitations with regards to determining of the air permeability of individual layers at a site. The screen interval for air permeability tests may cross several layers and provides little information regarding the properties of the individual layers. Also, analysis of the data from these tests is generally limited to one-dimensional radial flow (see Johnson et al, 1990, 1994) Reference 35) and the influence of layering or impermeable layers is neglected (see Shan et al, 1992) (Reference 36). The effects of layering, anisotropic properties, depth to water table and free surface can have an important influence on the air flow patterns and may severely compromises the assumption of one-dimensional radial flow. The influence of these effects on the air flow patterns for several cases are depicted and described in Figures 45-48.

The objective of this task was to measure the air permeability of the GRFL site using the protocol described in Hinchee, et al, 1992 (Reference 37). However, initial CPT testing at the site indicated that significant variability exists in both the vertical and horizontal direction, and that a single test at one location would not sufficiently characterize the entire site. Therefore, it was decided to conduct a conventional air permeability test to serve as a point of reference. To examine the effects of layering and site variability a special CPT probe was constructed for conducting air permeability testing.

The following sections describe the background and layout of the method and corresponding model of the tests. Also discussed are the results and the limitations of the models used to interpret the data and conclusions.
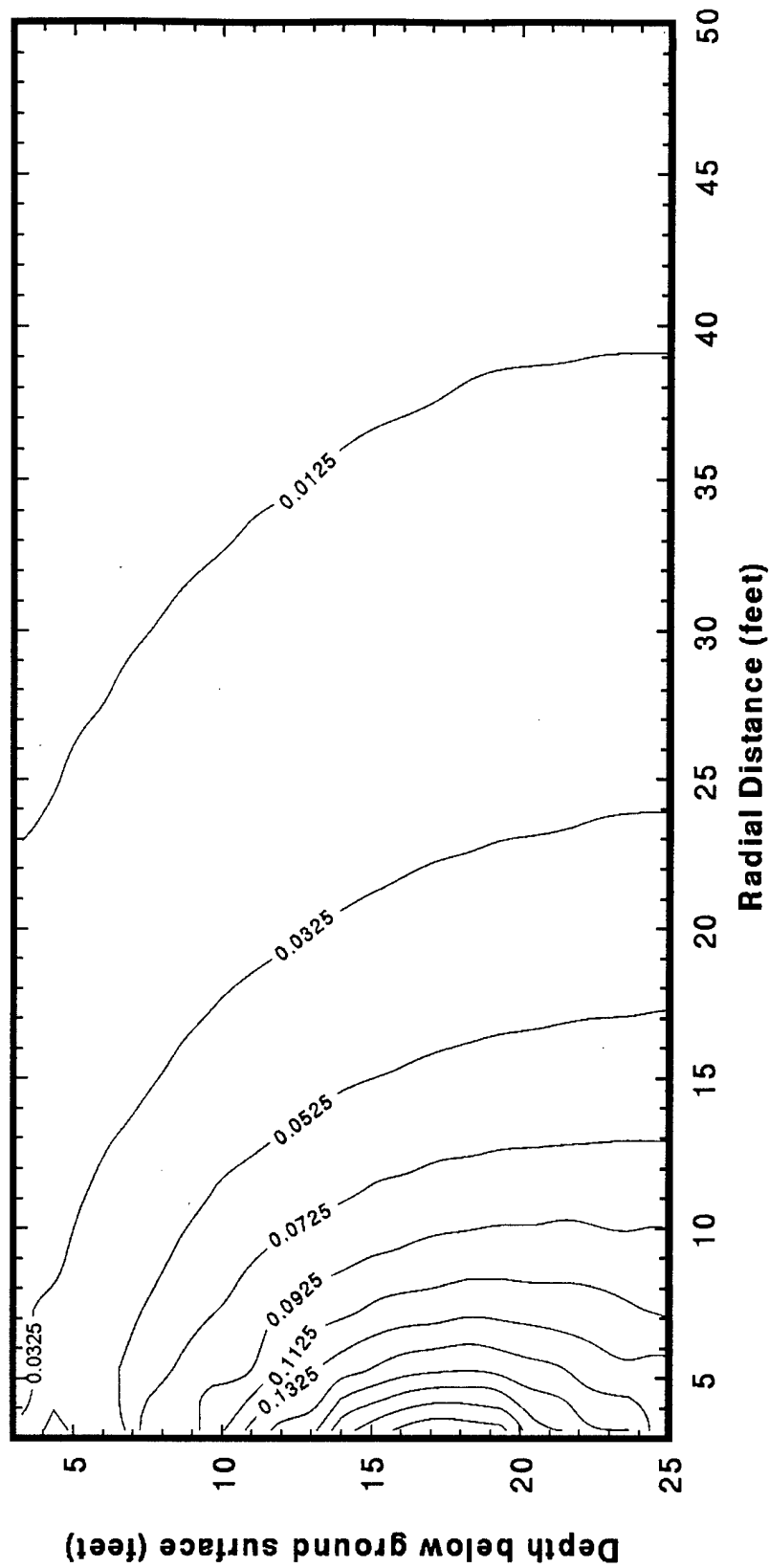
Figure 45. Case 1, Isotropic, Homogeneous, 2 Meter (6.6 feet) Well Screen Placed Between Water Table and Open Surface, No Boundary Effects in Area of Interest, Flow to Well Screen From Horizontal and Vertical Paths.
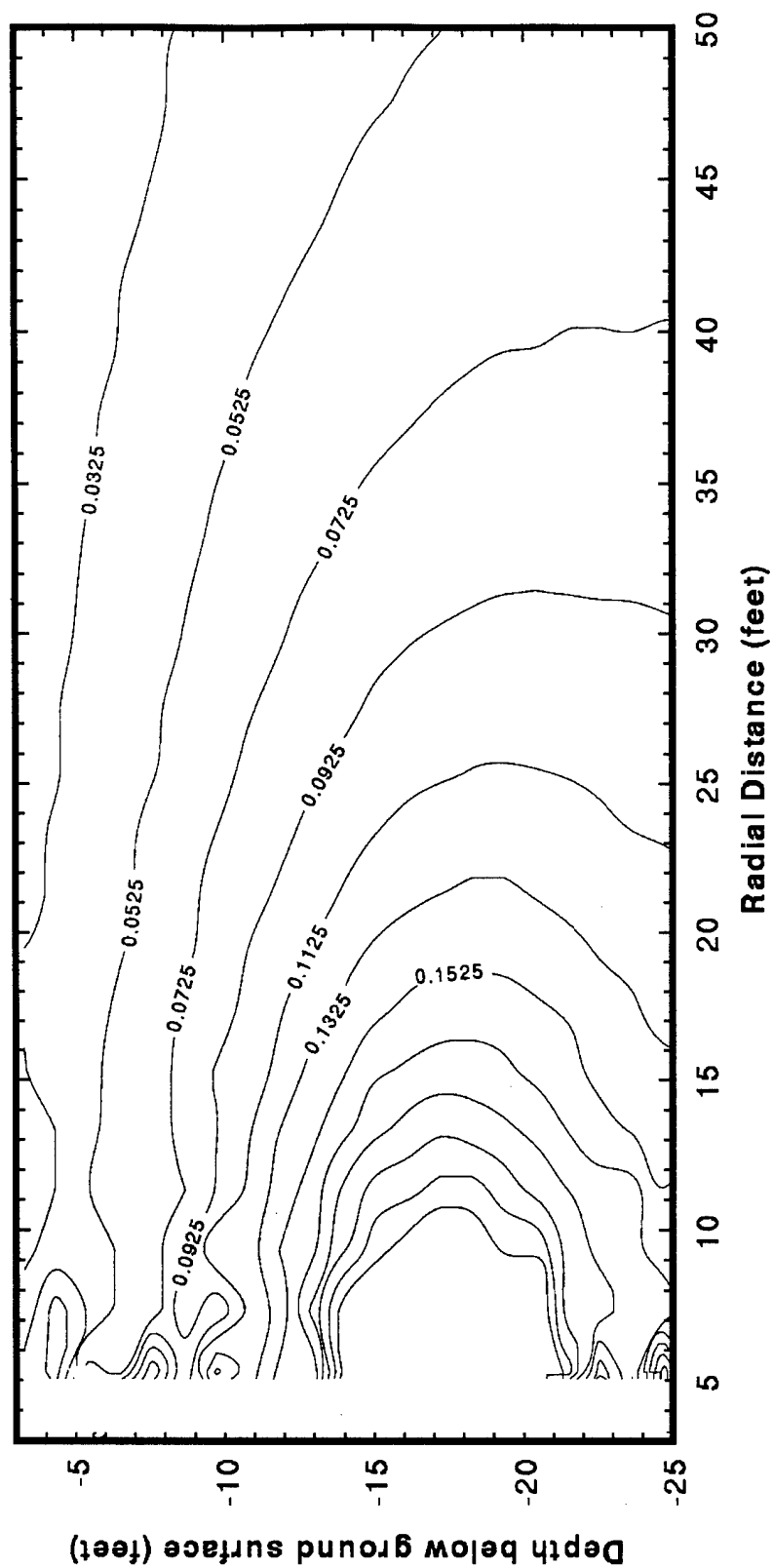
Figure 46. Case 2, Anisotropic, Homogeneous, 2 Meter (6.6 feet) Well Screen Placed Between Water Table and Open Surface, No Boundary Effects in Area of Interest, Flow to the Well Screen From Mainly Horizontal Paths, Influence of Well Extending Beyond 15 Meters (49.2 feet) As Compared to 12 Meters (39.4 feet).

113
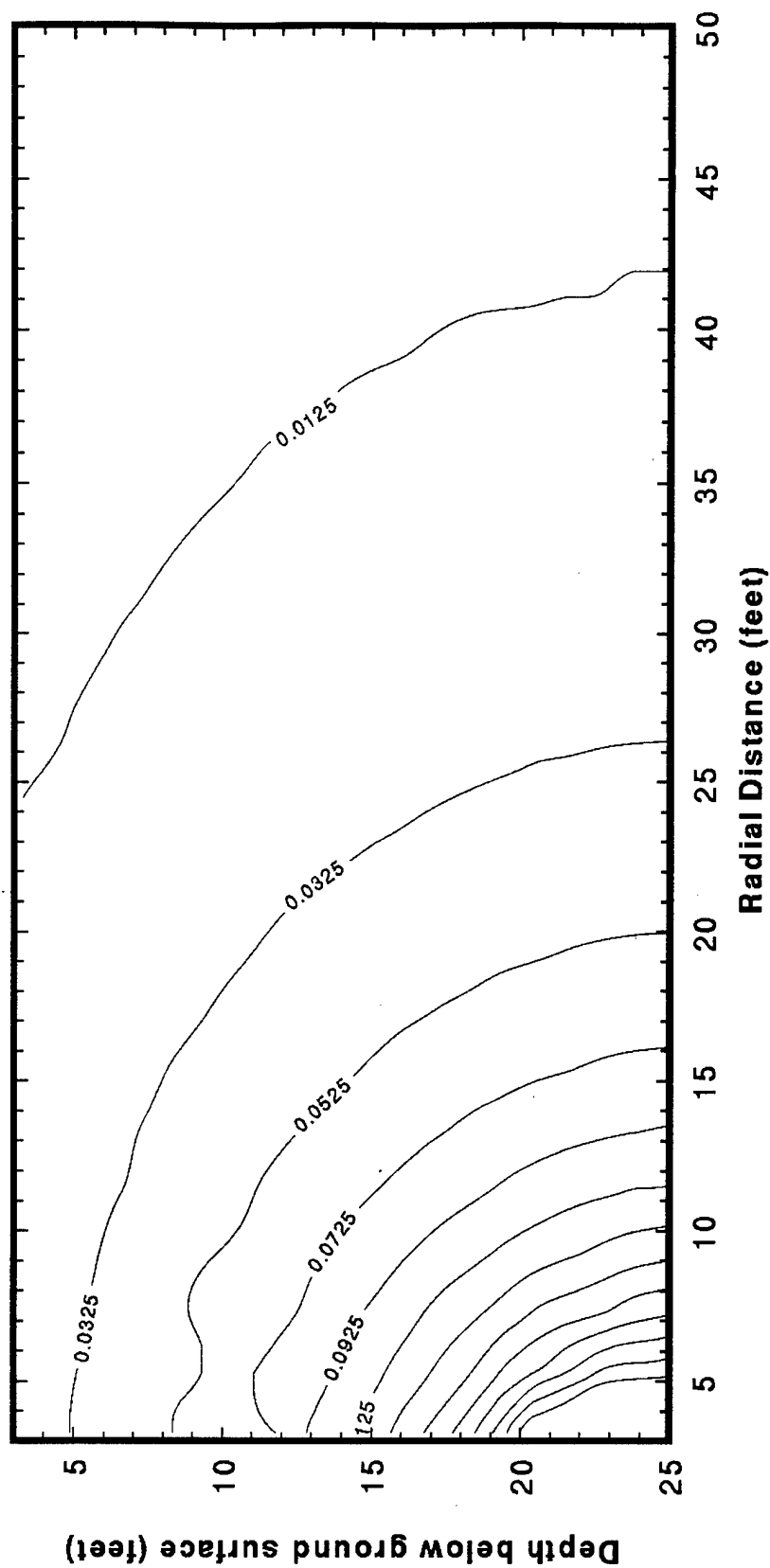
Figure 47. Case 3, Isotropic, Homogeneous, Well Screen Placed Near Water Table Boundary. Nearby Water Table Boundary Reduces Radius of Influence to 11 Meters (36.1 Feet).

Figure 48.   Case 4, Isotropic, Homogenous, 2 Meter (6.6 feet) Well Screen Placed Near Ground Surface, Influence of the Well Is Reduced to 9 Meters (29.5 feet) Compared to 12 Meters (39.4 feet) When Boundaries Are Further Away. Air Flow Supplying the Well Is From Open Air Surface and Horizontal Pathways.
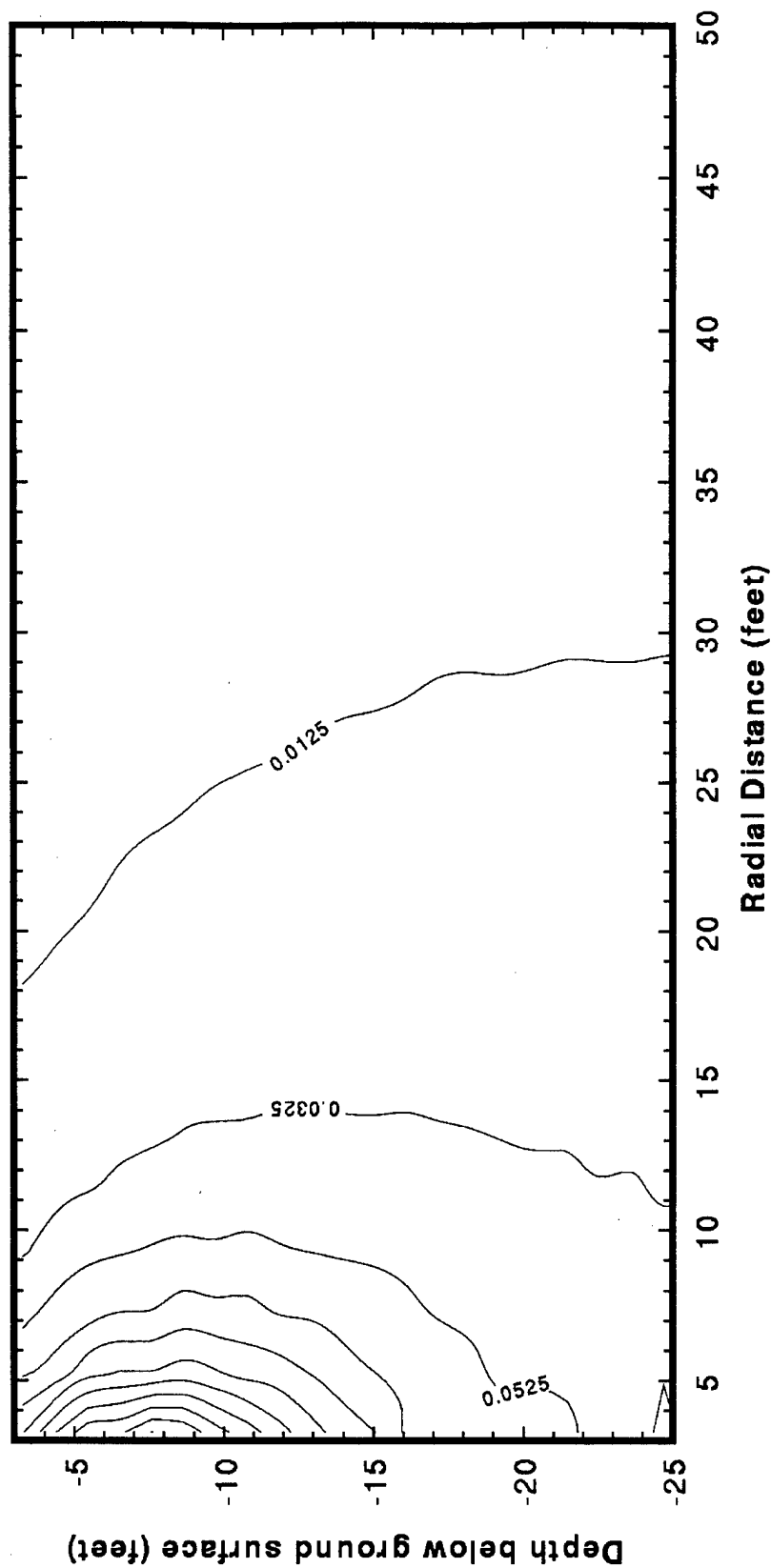
2. Approach

Monitoring Well Tests. The approach used under this effort consisted of conducting a conventional air permeability test using CPT installed injection/extraction wells with monitoring points located near the wells to monitor air pressure. Analysis of the data was conducted to evaluate the effect of large boundaries (the ground surface and water table) and inhomogeneities. A schematic of the test is plotted in Figure 49.

Monitoring points used to measure air pressure changes were distributed over the unsaturated zone at depths from 10.7 to 20.5 feet, and radially from 3.3 to 15.4 feet from the injection/extraction well. The probes are approximately 3.9 inches in length and 0.49 inches in diameter, with a tube extending up to the ground surface where they are attached to a differential pressure gage. (See Figure 49)

A vacuum blower was used to provide the pressure change in the injection/extraction well. The well was installed to a depth of 21 feet (approximately 7 feet above the water table) and screened over the bottom 6.6 feet. The well was installed a sufficient distance from the capillary fringe and the water table to minimize their influence. Differential pressure gages that provided accurate readings for changes as small as a 0.01 psi were selected for the test. Testing was conducted by hooking up the pressure gages to the flexible tubes from one of the depths and recording the air pressure as the test was being performed. Once the pressure reached a steady state, the blower was turned off and the pressure decay was measured to ambient conditions. The pressure gages were then hooked up to the next level and the test repeated. Data was obtained at all four depths for the injection tests with an average injection rate of 28 cfm. In these tests the pressure change was very rapid and only the steady state air pressure distribution was useful for analysis. A typical data set is plotted in Figure 50, with the bulk of the data plotted in Appendix M.

Only two extraction tests were conducted at the 17 feet and 20 feet depths at flows of 4.0 and 15.0 scfm respectively, as high flow rates could not be obtained. The extraction test provided the transient state data, both in the rise and fall-off pressures when the pump was turned on and off.

CPT Permeability Tests. A soil gas sampler developed by ARA and the Westinghouse Savannah River Company was modified to measure air permeabilities. The probe consisted of a conventional CPT probe modified to include the ConeSipper® as well as soil electrical resistivity and moisture content. The modified probe is shown schematically in Figure 51 and consists of three major modules: the CPT probe; the Soil Moisture/Resistivity/ Probe (SMR); and the ConeSipper®. The ConeSipper® was modified to incorporate a large diameter gas sample tube which could be used to either extract or inject air into the soil. The air flow through the gas sampling chamber was monitored as well as the pressure with which the gas was injected into the media. Knowing the gas flow rate and pressure and assuming steady state flow, K can be calculated using methods as described by Johnson in Reference 34.
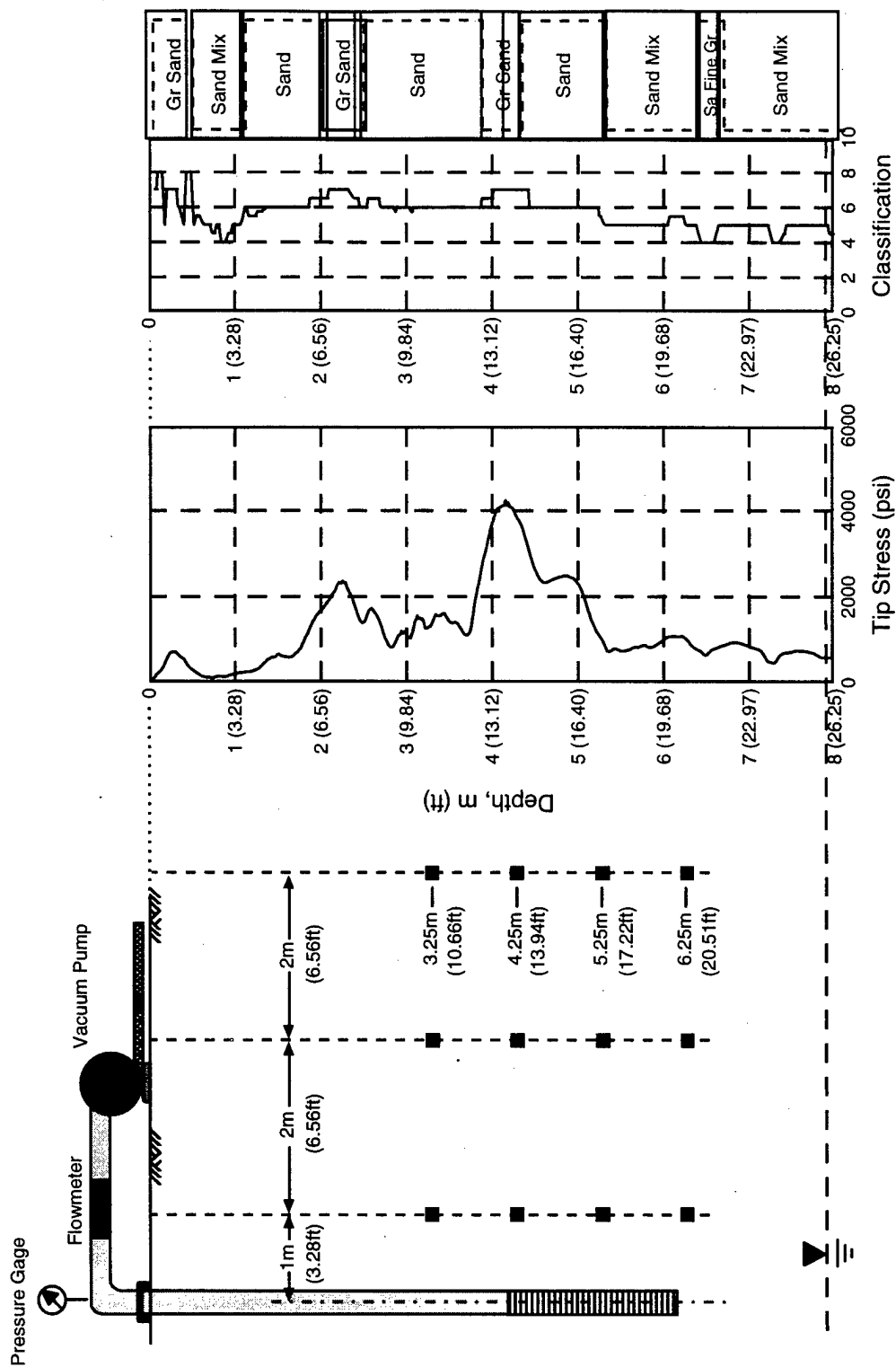
Figure 49. Layout of Vadose Zone Conductivity Test Conducted at GRFL.
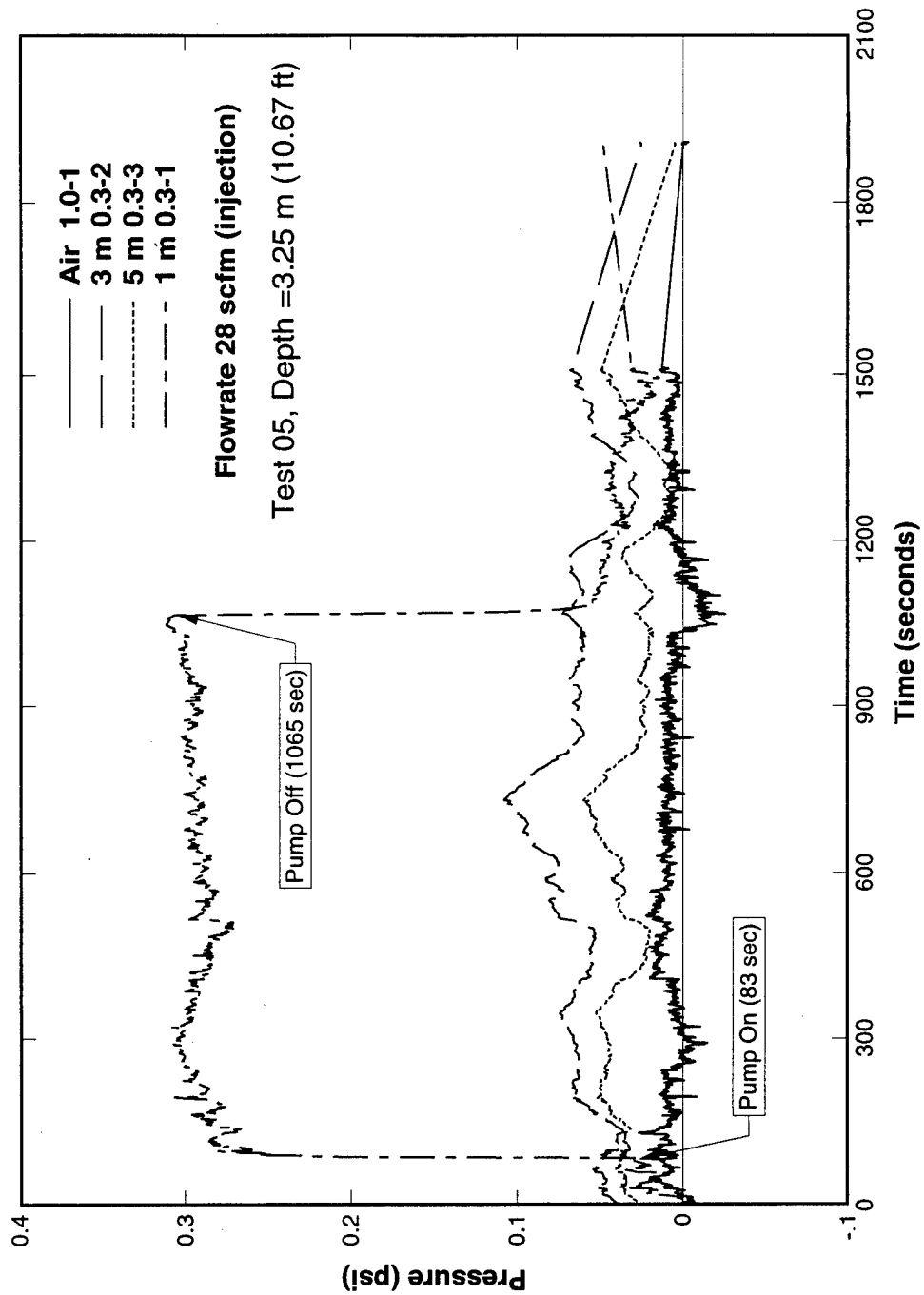
Figure 50. Typical Plot of Data From Injection/Extraction Well Tests.
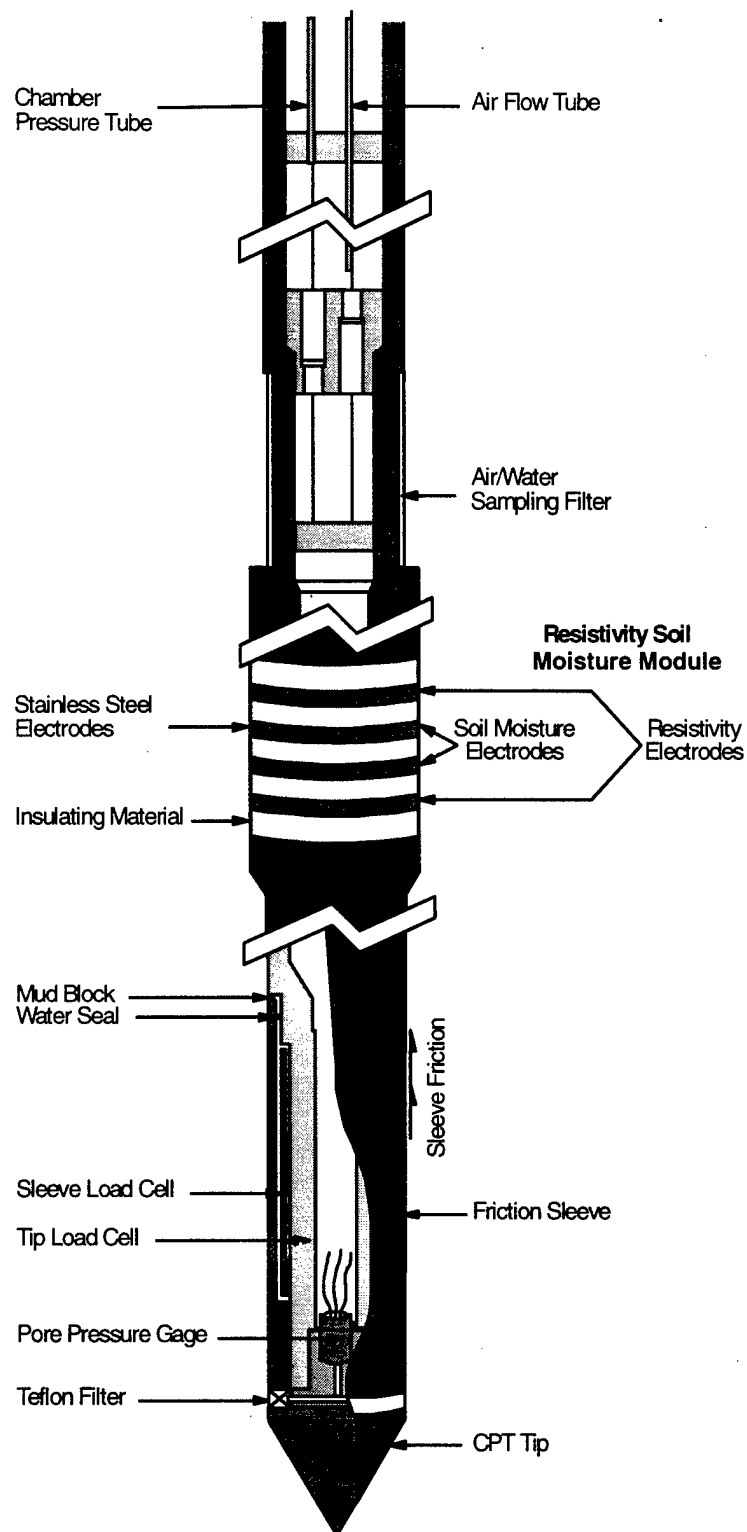
Figure 51. Schematic of CPT Probe Used to Determine Soil Air Permeability, Electrical Resistivity, and Soil Moisture.

Chamber Pressure Tube

Air Flow Tube

Air/Water Sampling Filter

Resistivity Soil Moisture Module

Stainless Steel Electrodes

Soil Moisture Electrodes

Resistivity Electrodes

Insulating Material

Mud Block

Water Seal

Sleeve Load Cell

Tip Load Cell

Pore Pressure Gage

Teflon Filter

Sleeve Friction

Friction Sleeve

CPT Tip

Testing was performed as the probe was being pushed into the ground and during rod changes when the probe was held stationary. The air pressure and flow rate were monitored on a data logger and the data appended to the CPT file once the data was returned to the New England Division of ARA for analysis.

The soil moisture/resistivity probe was also used in conjunction with the CPT probe to provide additional information on the site geology. While measurement of soil electrical resistivity is a common CPT probe function and is fully discussed in Appendix G, the soil moisture probe is a new probe developed under funding by the Ohio University. The principal of the soil moisture probe is that a relationship exists between the apparent dielectric of soils and volumetric soil moisture. Measurement of the apparent dielectric in the soil moisture probe used at the GRFL site is based on measuring the resonant frequency of a 100 MHz oscillator located in the CPT probe and is further discussed by Shinn (1996) (Reference 38).

3. Results

Monitoring Well Air Permeability Test. Two models were used to help define and design these tests. The first model is a steady state air flow model adapted to soil venting (Reference 34). This adaptation has been shown to be useful when the dynamic method is not appropriate (Reference 37). The model was developed by taking the radial solution for air flowing to a fully penetrating extraction well in a homogeneous formation, (Reference 35) as

$$k = \frac{Q\mu \ln\left(\frac{Rw}{R_I}\right)}{H\pi Pw\left[1 - \left(\frac{Patm}{Pw}\right)^2\right]} \qquad \text{Eq. 16}$$

Equation 16 applied only to vent wells operating under a vacuum. If air is being injected into the vent well the equation is modified as shown below:

$$k = \frac{Q\mu \ln\left(\frac{Rw}{R_I}\right)}{H\pi Patm\left[1 - \left(\frac{Pw}{Patm}\right)^2\right]} \qquad \text{Eq. 17}$$

where

Rw	=	radius of the venting well (cm)
k	=	soil gas permeability (cm^2)
μ	=	viscosity of air (1.8 x 10^{-4} g/cm-s at 18°C)
Q	=	volumetric flow rate from the vent well (cm^3/s)
Patm	=	ambient pressure (at sea level 1.013 x 10^6 g/cm-s^2)
H	=	depth of screen (cm)
R$_I$	=	the maximum radius of venting influence at steady

$$\text{state (cm)}$$

$$Pw = \text{the absolute pressure at the venting well (g/cm-s}^2)$$
$$K(ft^2) = K(cm^2) \times 4.48 \times 10^{-2}$$

This model is used for steady-state of the extraction tests. Peak flow rates of 28 cfm were obtained in the injection test, while the extraction test yielded a peak flow rate of 15 cfm. Both tests were run at the maximum blower pressure of 2.9 psi. Analysis of the data indicated that the radius of influence was at least 19 feet. Equations 16 and 17 were used to calculate air permeability and are listed in Table 16. Also listed in Table 16 are results from the 2-D analysis and CPT ConeSipper® test results. A discussion of Table 16 is presented in Section V-D-4.

TABLE 16. SUMMARY OF AIR PERMEABILITY DATA K.

ANALYTICAL METHOD	VALUE (ft²)
1-D Injection Test Analysis	1×10^{-7}
1-D Extraction Test Analysis	2×10^{-7}
2-D Isotropic Analysis	4.5×10^{-9}
2-D Anisotropic Analysis	$K_V = 2.2 \times 10^{-9}$ $K_H = 9 \times 10^{-9}$
CPT Results	9×10^{-9} to 1.3×10^{-6}

A second model, developed by Shan et al (Reference 36) was also used to evaluate the air permeability data. This model uses an analytical solution for steady state gas flow to a single extraction well in the unsaturated zone and applicable to isotropic and anisotropic homogeneous subsurface media in which the ground surface is open to the atmosphere. A significant advantage of this model is that it provides a two dimensional model of the air pressure distribution. The basis of other commonly used models (Johnson, et.al., (Reference 35), and Edwards, 1996) (Reference 39) are 1-D solutions of radial flow to a well adapted to the air phase and which provide no information on the pressure distribution.

The mathematical model used by Shan is the equation for transient gas flow in a homogeneous, anisotropic porous medium, Bear (Reference 31), where neglecting the mass accumulation term results in the steady state equation for gas flow:

$$\nabla \bullet (\bar{k}\nabla P^2) = 0 . \qquad \text{Eq. 18}$$

For the complete analytical pressure solution to this equation, the reader is referred to Shan, Falta and Javandel, (Reference 40) where its computations are presented in full and descriptive detail.

The input parameters to the model that specify the problem are listed in Table 17. The well geometry is that of the actual well used in the test, all parameters were estimated in the original design of the test, and changed to measured values for the analysis of the resulting data

TABLE 17. 2-D AIR FLOW MODEL PARAMETERS.

Parameter	Value
Depth to impermeable boundary (h)	27 feet
Depth to bottom of screen (a)	20 feet
Depth to top screen (b)	14 feet
Radial gas permeability (k_r)	4.5×10^{-13} to 1.3×10^{-8} ft^2
Vertical gas permeability (k_z)	4.5×10^{-3} to 2.2×10^{-13} ft^2 4.5×10^{-9} to 2.2×10^{-9} ft^2
Porosity (F)	0.29
Temperature (T)	50_F
Ambient pressure (p_a)	1 atm = 14.7 psi
Ambient gas density (ρ_a)	7.74×10^{-2} lb/ft^3
Gas viscosity (μ)	2.4×10^{-6} lb-sec/ft

The Shan, Falta, and Javandel (Reference 40) analytical model provided at least two scenarios with which to fit the steady state test data. Calculations were fit to the injection tested data for these two cases and are plotted in Figures 52 and 53. As expected, the anisotropic set of pressure distributions show the flow mainly in the horizontal direction from the well screen. Plotting the test data on both the isotropic and anisotropic models shows a fairly good fit. The radial and vertical permeabilities from the isotropic model show the area to have an average 4.5×10^{-9}ft^2, while the anisotropic model was given a radial permeability (k_r) of 9×10^{-9} feet^2 and a vertical permeability (K_z) of 2.2×10^{-9} feet^2.

The effect of anisotropy on the system is apparent when comparing the two calculations. The flow direction changes when the permeability in that direction changes. If the permeability in the radial direction is higher, the pressure contours extend outwards, primarily influencing the region of higher permeability. Thus, there is less effect in a region the same distance away from the well in a vertical direction than there is in the horizontal direction.

122

Figure 52. Predicted (Contours) and Actual Gage Pressures in Two Dimensions For Monitoring Well Air Permeability Test. Q=28scfm. Conditions Are Steady State. Injection/Extraction Well Screened @ 14 to 20 Feet Below Ground Surface. Isotropic case, $K_h = K_v = 4.5 \times 10^{-9}$ Ft ^{2}.
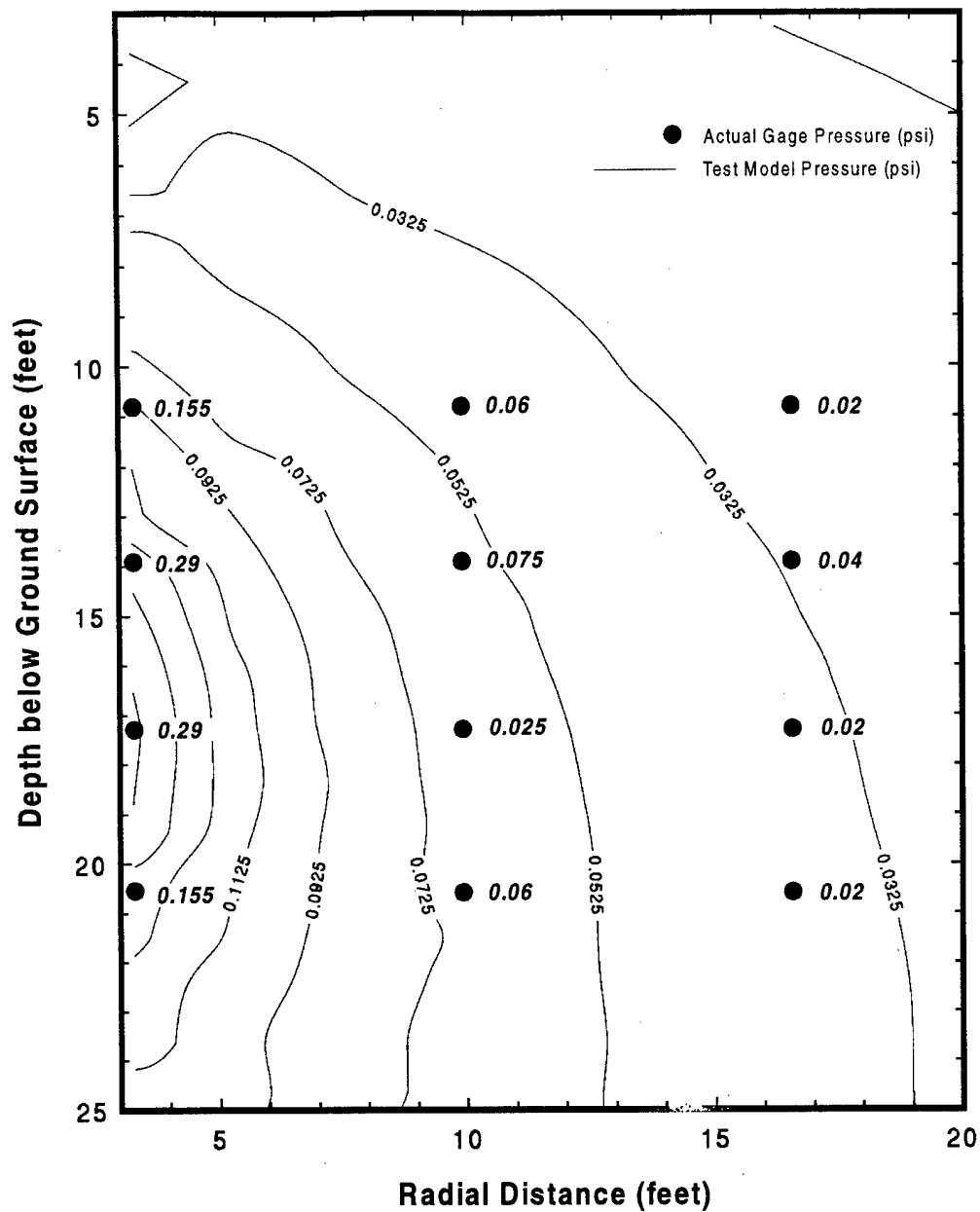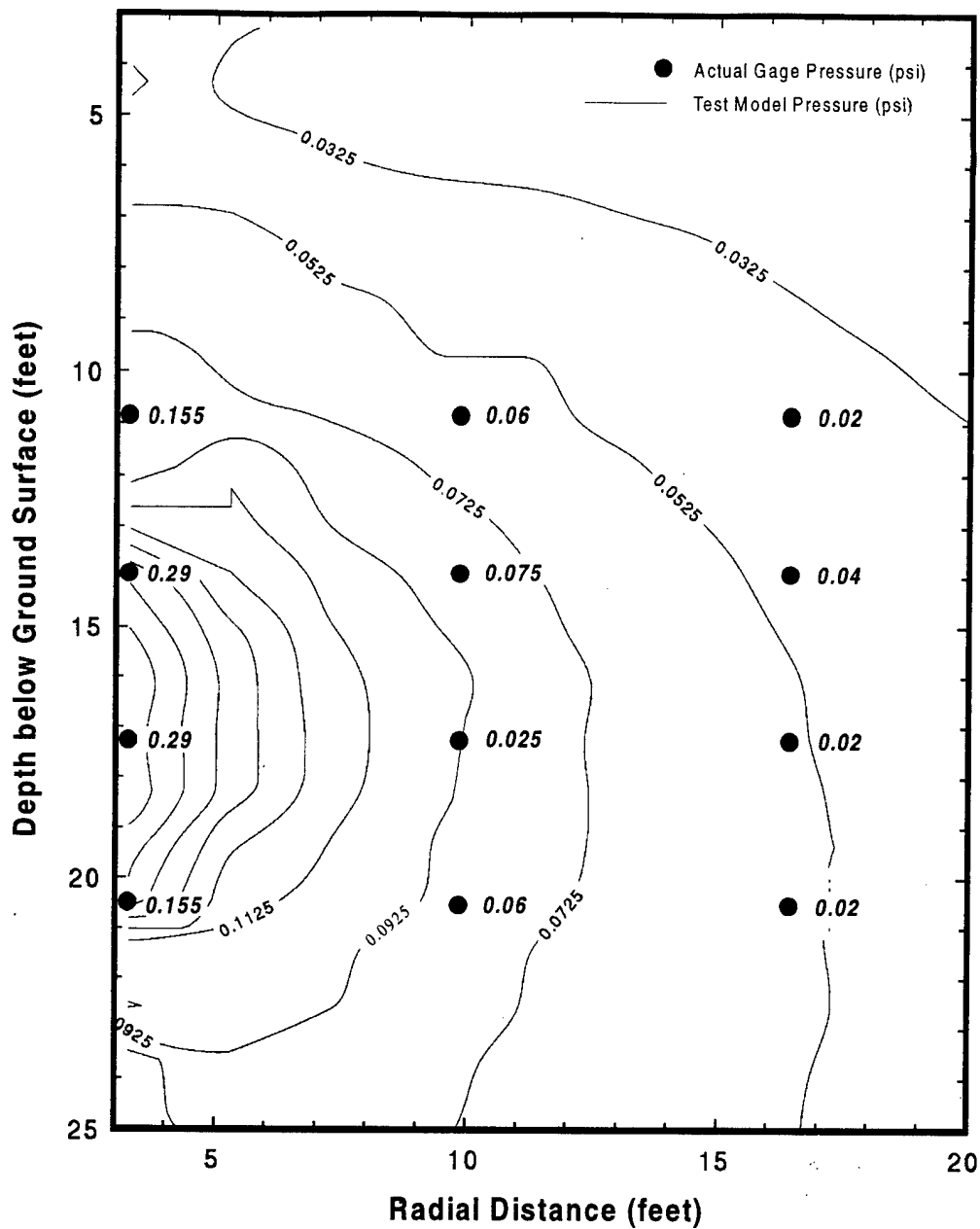
Figure 53. Predicted (Contours) and Actual Gage Pressures in Two Dimensions For Monitoring Well Air Permeability Test. Q=28scfm. Conditions Are Steady-State. Injection/Extraction Well Screened @ 14 to 20 Feet Below Ground Surface. Anisotropic case, $K_h = 9 \times 10^{-9}$ Ft^2, $K_v = 3.6 \times 10^{-9}$ Ft^2.

124

In both figures, there is a discrepancy between the calculation and data at depth 17 feet below the ground surface. Since the Shan et al. (Reference 36), model cannot predict layering in a particular area, this data could have to be treated as if it were the only data available, and another calculation fit to this data to obtain the air permeability of this particular layer. However, the CPT soil classification over the depth of the test reveals a relatively higher permeability sand at the 10.6- and 13.9-foot depths, then moving deeper to the 17.2-foot depth the soil class shows a sand mix, and then at the 20.5-foot depth a sand again. (See Figure 49). The lower pressures recorded in the probes at the 17.2-foot depth are a result of the layering or non-homogeneity of the site, as the CPT soil classification reveals. If the model were able to predict pressures due to layering, model input would consist of a lower permeability at the 17.2-foot depth, and the pressure contours would effectively compress back toward the well screen, and then back out again in the more permeable sand at the 20.5-foot depth.

CPT Air Permeability Test. Results of the CPT air permeability tests are presented in Appendix M for each individual sounding. Typical test results are plotted in Figures 54 -56, for Sounding CPT-A01, which was located near the monitoring well air permeability test. Variations in the CPT data are indicative of changes in the soil type, as can be seen in Figure 55, which shows the soil classification and layering derived from the CPT data. The CPT soil classifications indicate that the site is predominately sands with discontinuous clay lenses. Note that the screened interval in the monitoring wells existed from MSL 22.9 feet to 16.4 feet. The CPT data indicate that the soils over this depth interval are somewhat finer grained than those above and below the zone, and that thin beds of fine grained soils exist within the zone.

The resistivity data shows considerable variation above Elevation 10 feet. This variation is principally due to the variability in the soil moisture content, soil type and density. Below Elevation 10 feet, the resistivity data indicate a nearly constant resistance of about 400 ohms, which coincides with the water table depth. A large decrease occurs at elevation -2.5 feet when the clay aquitard is encountered. The soil moisture profile is similar to the resistivity in that considerable variation exists above Elevation 10 feet. Moisture contents as low as 6% (a very dry soil) to 30% (essentially saturated soil) are observed. The moisture data indicate that the change in soil moisture can be very rapid, as observed at Elevation 27.5 feet. Below the water table elevation at 10 feet, the soil moisture is about 28 percent and increases to about 30% in the clay aquitard.

Data obtained from the CPT air permeability test are plotted in Figure 56 as pressure in the ConeSipper® chamber, air flow rate through the chamber, and calculated air permeability. The instrumentation system was designed to vary the pressure in order to maintain a constant flow rate. Sharp spikes in the data are observed at several locations, which we believe are due to rapid changes in the air flow inducted by changes in soil type. Spikes in the air-flow meter are due to the meter's inability to equilibrate rapidly under changing flow conditions.
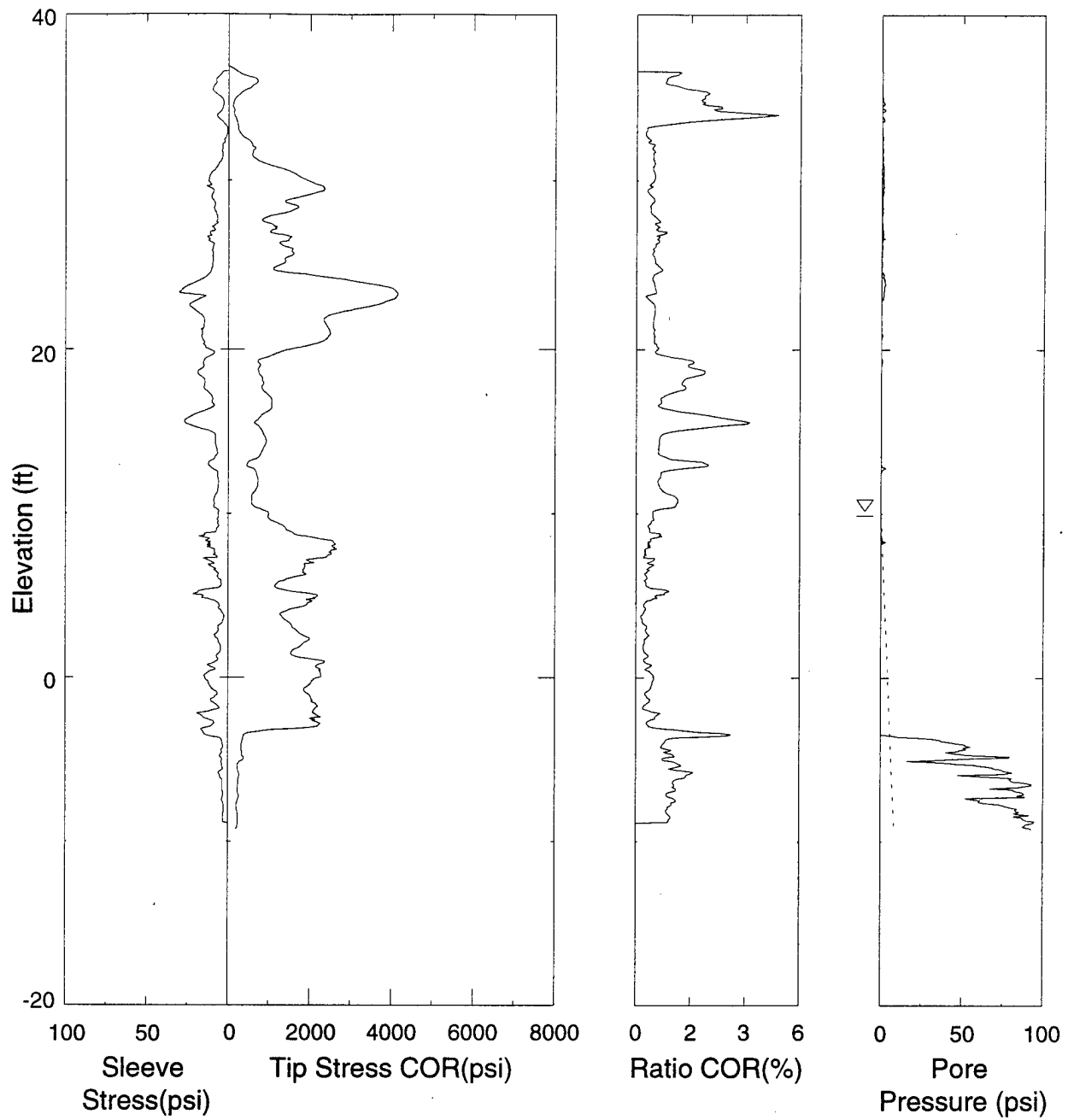
Figure 54.   Typical CPT Profile of CPT Air Permeability Test, Showing Standard CPT Data at the Test Location.
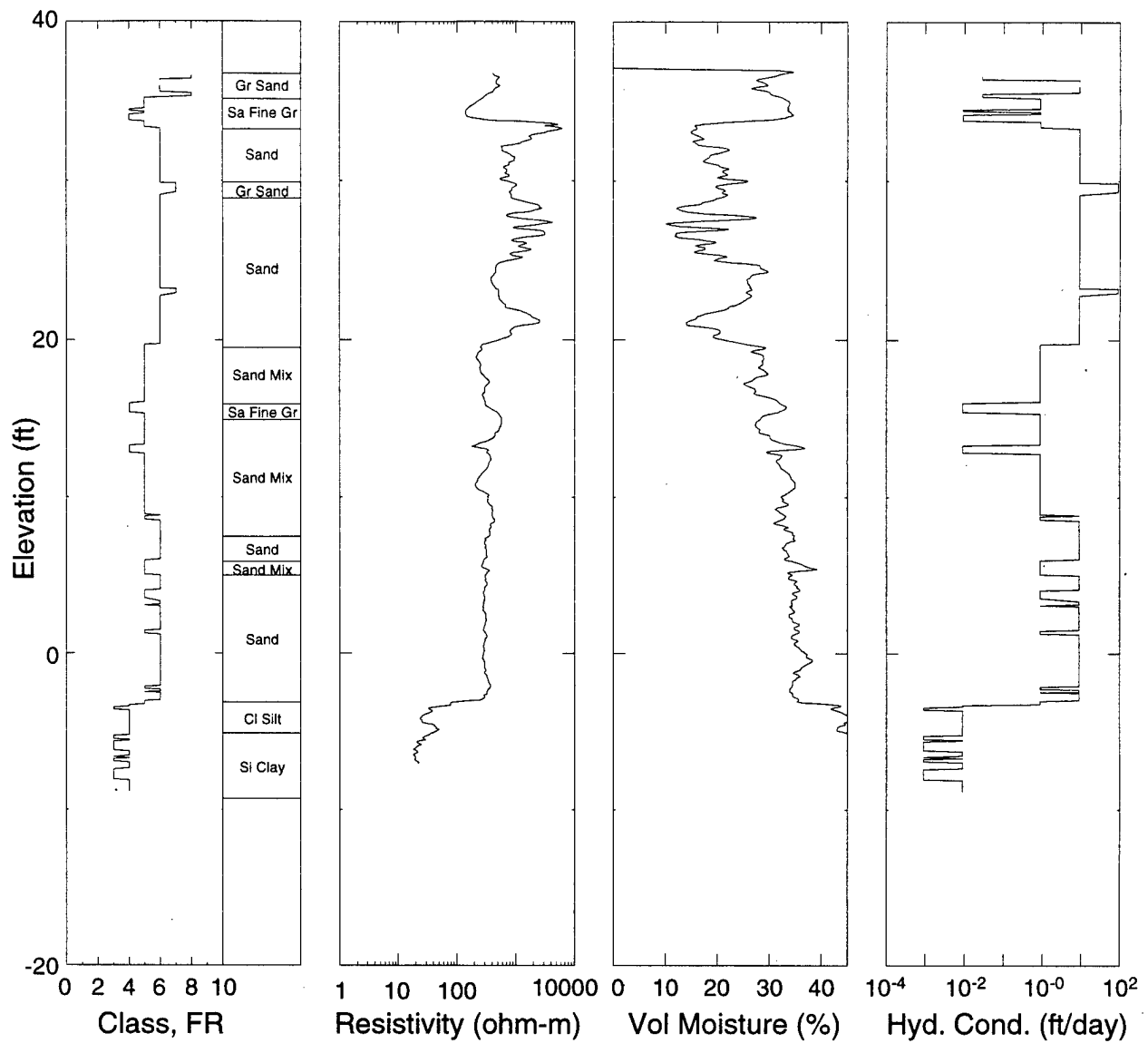
Figure 55. Typical CPT Profile of CPT Air Permeability Test, Showing Soil Type, Resistivity and Soil Moisture at the Test Location.
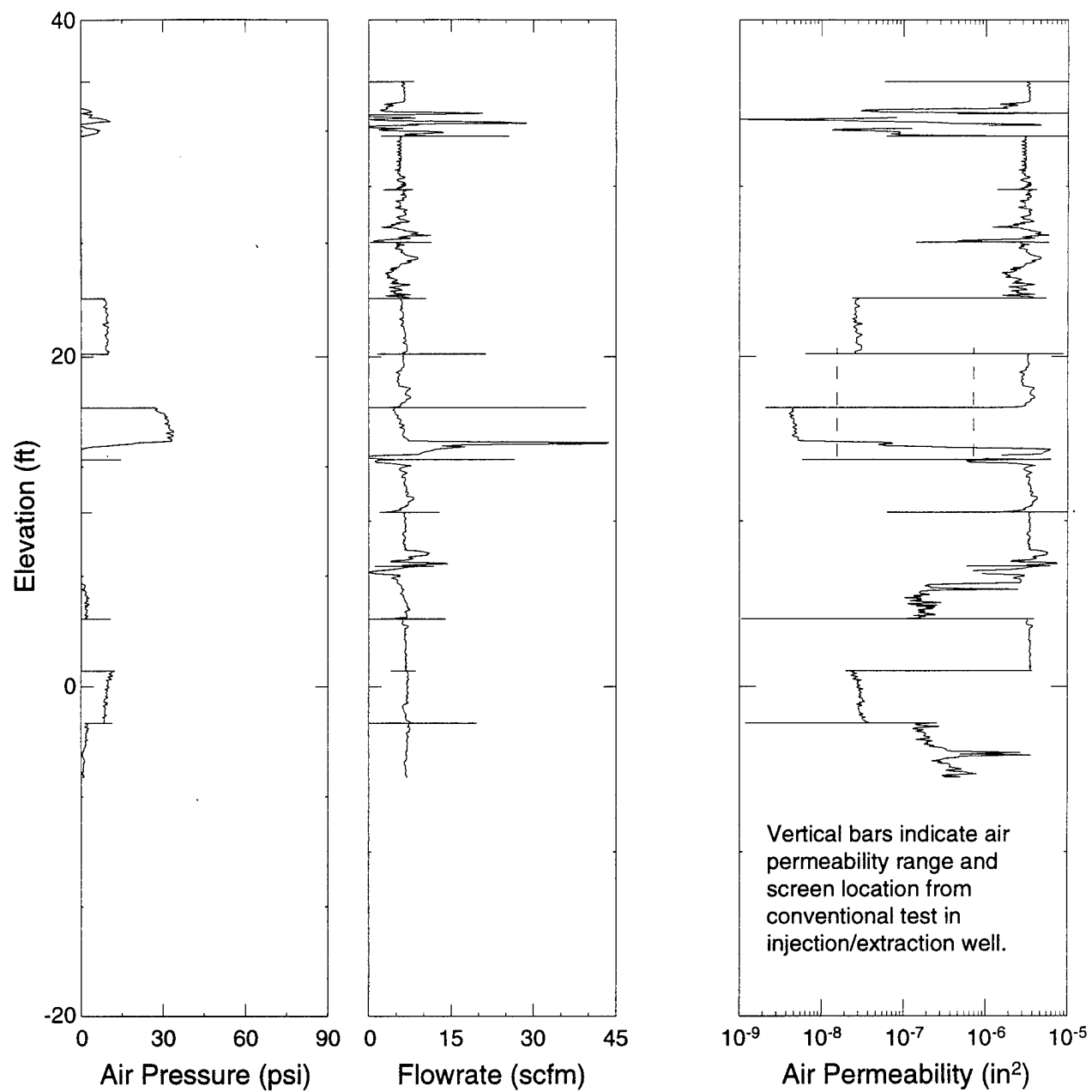
**Figure 56.   Typical Plot of CPT Air Permeability Test Showing Test data and the
Air Permeability Profile.**

These spikes occur at boundaries between soil types and should be ignored. It should also be noted that at many locations the air pressure was quite low, indicating that the soil presented little restriction to the air flow. Also, at many locations the air pressure was below the resolution of the pressure gage and we assumed a cavity pressure of 0.1 psi. The effect of this assumption is to limit the calculated air permeability to a value of about 1.12×10^{-6} feet^2.

The CPT air permeability test was primarily designed for determining the air permeability above the water table. For sounding CPT-A01, the test was continued below the water table, which is at MSL 10 feet. No appreciable change in the back-calculated air permeability was noted above or below the water table (Figure 56).

4. Discussion

Air conductivities were estimated using two field approaches. The first is a conventional monitoring well test in which air is either injected or extracted from the media. A CPT probe was also used to conduct air injection tests through a much smaller screened section, which allowed the air permeability of individual layers to be estimated. Data from both the monitoring well and CPT tests were analyzed using a one-dimensional radial flow model. An analytical model which accounted for boundary effects and site anisotropy was also used to analyzed the results of the monitoring well test.

Monitoring Well Tests. As shown in Table 15, air permeabilities, estimated from the monitoring well data and assuming one-dimensional flow, resulted in higher estimates of the site air permeability than those obtained from the either of the two-dimensional analyses. The difference in the one and two dimensional back calculated air permeability values is due to non-radial air flow. Examination of Figures 45 through 48 shows that air flow from a well can be affected by a variety of two dimensional effects such as the ground surface, impermeable boundaries, and anisotropy. Overall the 2-D model provides a better fit to the GRFL data than does the simplified radial flow model.

However, Shan's model cannot predict the air pressure distribution due to layering effects, while the isotropic model gives the best fit for most of the data, the evidence of layering is clearly seen in the poor fit of data at the 17-foot depth. When reinforced with the CPT soil classification data, the non-homogenous nature of the site is clearly seen. Therefore, Equations 16 and 17, when used in conjunction with the CPT soil classification, can be used to effectively determine representative permeabilities at the site. These equations provide an estimate of the average radial and vertical permeability of the unsaturated zone, and the CPT identifies discrepancies due to layering effects in the data.

CPT Air Permeability Test. Examination of the CPT determined air permeability indicates significant variation in the profile. In layers identified as containing finer grained soils, such as that at Elevations 15 to 17 feet, (see Figure 56), the air permeability was calculated to be as low as 1.6×10^{-9} feet^2. Immediately below this layer the air permeability increases rapidly to 1.1×10^{-6} feet^2, which is an increase of 3 orders of magnitude. These changes reflect the influence of the fine grain content of the soil. The CPT estimated air

129

permeabilities show a much wider variation in air permeability than do the air permeabilities estimated from the monitoring well. This is expected as the air flow from a monitoring well will not be uniform throughout the well but will be influenced by the air permeability in that section. Hence, air permeability testing in conventional monitoring wells analyzed using one-dimensional assumptions will reflect averaged permeability values.

The conclusion drawn from the above analysis is that the CPT-derived air permeabilities provide greater detail than is possible with a conventional monitoring well test. While the CPT test performed under this effort was the first test of the probe, the results of both the CPT and conventional monitoring well were consistent. The CPT air permeability profile shows much greater variation, which is expected, since the CPT probe was designed to measure the permeability of individual layers. While a conventional monitoring well test may be adequate to design a remediation test, the CPT test will provide the detailed data required to analyze experimental remediation programs.

E.   DATA COLLECTION, MANAGEMENT AND ANALYSIS PACKAGE

1.   Objectives

This section describes the computerized data acquisition, data management and data analysis system . The system will acquire the raw data from the field, place the data into a database, provide data security, allow remote data access and experimental control, and provide an analysis and graphics package for the researcher to use in the interpretation and visualization of the data. The computer system design is intended to meet the following objectives:

- Facilitate monitoring and maintaining the site by providing a centralized means to observe data and automate many of the tasks associated with site maintenance, which includes duties such as adding sensors to the system, monitoring out-of-cell contamination levels, enabling or changing pump rates of emergency backup units, etc.

- Provide a basis for experimenters to leverage. Experimenters need only provide the special sensors and equipment that they need to perform the experiment, and simple interface software to control/monitor them. All other functions are provided by this computer system. The experimenters data will be automatically collected and logged, and several tools will be provided to analyze and visualize test data.

- Provide a base set of analytical and visualization tools for use by on-site personnel as well as experimenters. Use of such tools enhance the understanding of phenomena being observed. By providing an integrated package of tools, the experimenter can more readily interact with his data.

- Provide off-site access to data collected, as well as provide off-site means to control sensors. Since experiments require years to complete, it is essential that experimenters be able to remotely interact with the experiment.

- Provide a flexible system for supporting future demonstrations. The computer system should readily accommodate additional sensors, additional test cells, new custom equipment not yet available, etc. with low effort on the part of on-site maintenance personnel.

2.   Approach

This section of the document describes the GRFL computer system architecture. The computer system consists of several PC's performing specific tasks, an Ethernet network connecting the computers, data loggers interfacing with sensors and other controllable equipment, miscellaneous hardware for connecting the data loggers to the computers, color printer for output, and modems for remote connectivity. This computer system also consists of several specialized software components which include an sequential querying language (SQL) database for storing test data, custom software for communicating with data loggers and for

controlling specialized sensors attached to the data loggers, UNCERT software for data extraction, analysis, and visualization, and finally MapInfo/SITEGIS for providing a backbone to host geographical data storage, access, and retrieval using point and click GIS capabilities. More detail is provided below.

The system consist of two primary computers, a portable computer, and a color printer in a local network. One of the primary computers is the Field Monitor and Control Computer, (FMCC). It is used to access the field data loggers which are also special purpose computers used to acquire data from instruments, store the data, and if necessary issue control signals. The second primary computer is the File, Printer, Remote Server (FPRS). This computer is used to perform the analysis and graphic chores, as well as the remote access and printer server needs. The hardware that is available and the detail specifications are presented in Appendix N. The general network schematic is shown in Figure 57. The FMCC connection with the field data loggers is shown in Figure 58. The two primary computers and their associated task will be discussed in the following sections. Also the various software tools available to the researcher are presented.

Field Monitor and Control Computer. The FMCC is hardwired to the CR10 field data loggers from Campbell Scientific which are programmed to acquire and store data independent of the FMCC. The CR10 data acquisition program can be changed at any time by down loading a new program from the FMCC. Generally the FMCC interrogate the CR10s' memory, reformat the data, and place it into the database. This data are then available over the network to the FPRS. If the experimenter needs to change operating parameters of the test, the FMCC would be used to issue commands to the CR10s to set control switches. The FMCC is operating with the MS Windows NT operating system to take advantage of the full 32 bit word configuration.

The FMCC monitors the experimental cell data and the site data, and the safety zone data external to the actual test cell. These data are physically monitored by the site manager to evaluate the risk during the testing.

File, Printer, Remote Server Computer. The FPRS functions as the network monitor and the primary computer for data analysis and display, and provides off site users with access to the system. The FPRS operates with the MS Windows NT system to facilitate full 32 bit computations and displays. Software interfaces reside on the FPRS to expedite importing the field data acquired by the FMCC.

When the researcher is on site the FPRS will be used to inspect the acquired data, perform statistical analysis of it and displays it in 3-D. This display may be overlaid onto a map view of the site and the test cell. Since the FPRS serves the network color plots and Viewgraphs can be prepared on site for data analysis or for presentations.
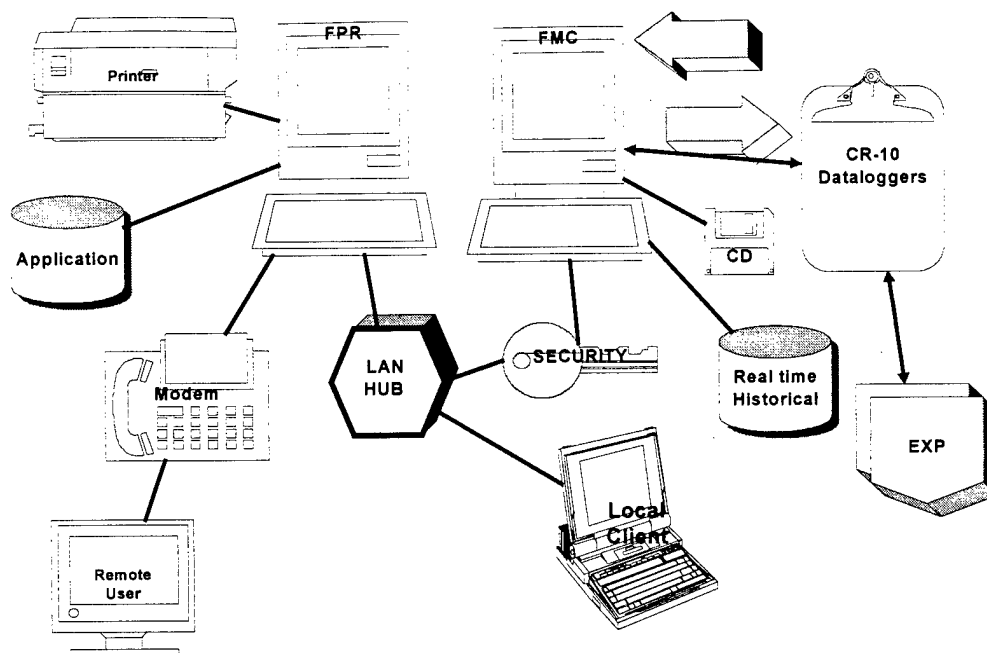
Figure 57. GRFL Data Management.
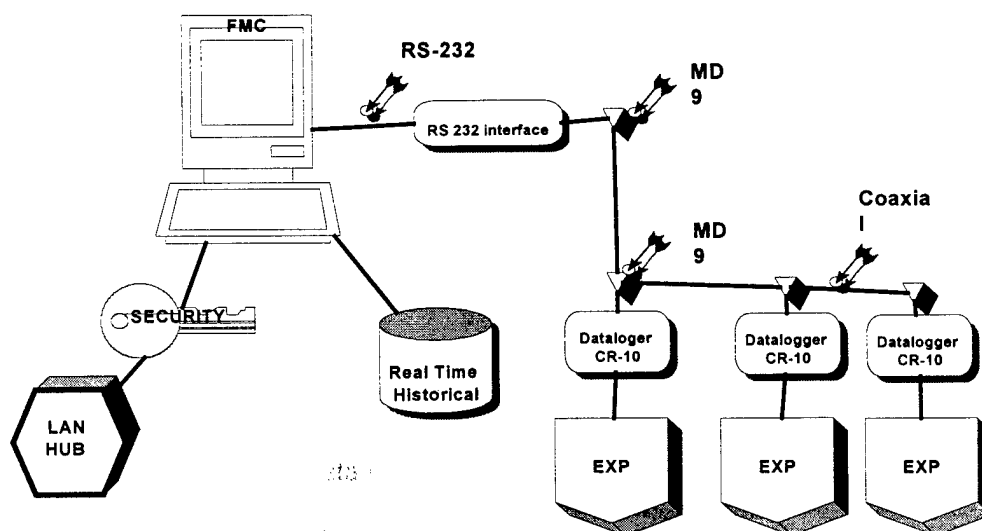
Figure 58. FMC Server System.

Analysis Package. The on site data analysis package is UNCERT which is an uncertainty analysis and geostatistical software package developed at the Colorado School of Mines to operate on workstations. It has been ported to the PC Windows NT system and operates with pull down minus. The package is well suited for evaluating hazardous waste sites and evaluating remediation methods. It has several statistical analysis tool kits such as:

- Basic statistics
- Kriging for variogram analysis
- Semi-variogram fitting and modeling using least squares, latin-hypercube sampling, etc.

There are also several graphic tools available to display and visualize the data. These graphical displays can vary from simple line and histogram presentations to complex 3D surface and contouring. The graphics may be graytone or color.

A 3-D visualization package is also provided by SITEVIEW which uses geostatics and environmental terminology.

MapInfo Implementation. An overlay display onto a map view of the site and the test cell has been developed using MapInfo to provide the users a "point and click" graphical interaction with the database. The researcher will be able to see a 3-D map of the cell with the instrument packages identified. They will be able to "point" to a specific measurement location; "click" the mouse button; and visually interrogate the recorded data, the instrument set up, calibration, etc.

They can retrieve the most current sensor data, details of the sensor, time history sensor data, logger configuration, or graphical and analysis choices. The experimenter is led through the options based on the item of the "point and click". For example, an experimenter may wish to highlight the location of all the sensors in the test cell by a "point and click." Also, the sensors may be sorted by a particular type i.e. oxygen level, and automatically exported to the statistical package UNCERT. A simple three dimensional graphical display is also available which shows the instrument location overlaid on the wells and the cell map. With a "point and click" the selected sensors are exported to the 3D graphics package SITEVIEW.

SQL Data Base Implementation. The SQL data base was chosen to allow researchers general access to the raw database so they can use their own analysis and graphical packages. This can be accomplished locally or remotely via the telephone. SQL also allows careful security control of the access to the data base. The detail database schema is presented in Appendix N along with the necessary technical information to identify and access the data.

3. Security

Security is an important concern. The integrity of on-going experiments and of the GRFL site data must be protected by restricting access to only those need-to-know individuals. Individual experimenters should NOT have access to other experimenter's test cell data. The on-site personnel should be able to access all data. Because the GRFL site will be accessible to the outside world (via modem or INTERNET), anyone securing the modem phone number or GRFL site INTERNET addresses can attempt to hack at the data. Without a formal mechanism in place, eventually someone could gain access and cause harm.

Access to the GRFL site data and all sensors/pumps, etc. is restricted to authenticated users. Every person needing access will need to register an identification name (user ID, name, etc.) and a password only known by the user and the computer database. Prior to accessing any data, the user will be required to clear a login process which matches the identifier with the password. The registration process will time out after some number of mismatches to prevent hackers from feeding identifier/password sequences from automated scripts. Clearly two levels of access are needed, experimenter access which permits read/write access to a single test cell and read-only access to site-wide data, and administrator access which grants access to all data.

Because all changes will be recorded in the database and the original data will still be available, clients can be assured that the integrity of their own data are not compromised by the system administrator.

This security is provided by built-in capability in the SQL database software. Careful organization of the database schema permits us to control read and read/write access to all data. At the application computer level, i.e. the FPR, a single GUI interface may authenticate a user so that their entire working session does not require intermittent password entries. Clients not using the GRFL support software will have to include authentication with their SQL queries.

4.   Results

The software and hardware provide the experimenter with the following capabilities:

- Experimenters can generate color hard copy printouts of results, reports , etc.

- Experimenters can access their data on-site without having to bring special equipment.

- Experimenters can connect their Microsoft based PC to the GRFL network via Ethernet. Customer's PC must have a twisted pair connector (RJ-45) and be configured with TCP/IP software.

- Experimenters have access to their own cell data, as well as some overall site data such as weather information. Experimenters can not access other cell data.

- A mechanism (procedure and/or hardware/software)is available for sensor calibration.

- GRFL personnel have access to all site data, as well as all experimental data.

- Experimenters can control sensor and pump settings within their own test cell only.

- A history log will be kept reflecting the change(s) made to sensor/pump settings, which will minimally retain a time stamp for when the change occurred, the

identification of the experimenters making the change, what·sensor/pump was changed, and it's new parameter(s).

- GRFL personnel have the ability to control all GRFL site sensors/pumps, including peripherals within test cells.

- Experimenters have the ability to perform uncertainty calculations using on-site software.

- Experimenters have the ability to visualize their data and results from their uncertainty calculations.

- The entire site is characterized and the data are accessible to all personnel through the computer system.

- Experimenters have the ability to add sensors to the system (the software can accommodate new sensors without extensive rework).

- Experimenters have the ability to calibrate sensors. Any such calibration is logged for auditing purposes.

- Original data collected by the computer system will remain in storage without modifications, regardless of calibrations, user initiated changes, etc.

- The experimenter has the ability to modify data values, and such modification are tracked in a log.

5.   Discussion

The software and hardware installed at the GRFL site are active and are acquiring data from the weather station and two other CR10's outside of the test cell. As we brought the system on line several became apparent. First, it will be necessary in the future to connect the GRFL system to the INTERNET with a high speed data line. For small data transfers the current telephone modem is adequate but that mode is very slow when a large volume of data must be transferred. Second, the GRFL system has capacity to be the central data handler and retriever for not only the local site experimenters but for remote site experimenters. With only a minimum modification of the acquisition software and some additional hardware, the system can readily query by telephone (line or cell phone) other experiments. A capability also exits, through commercial and federal sources, to use satellite links and acquire data from sites anywhere in the US. In conclusion the GRFL data acquisition and management system is flexible and can be used to the advantage of the experimenter.

F.   GROUNDWATER FLOW MODEL

1.   Objective

The objective of this task was to complete and calibrate a numerical model that would describe the hydraulics of groundwater flow at the GRFL site. The groundwater flow model that we chose for this task is MODFLOW. MODFLOW simulates two-dimensional areal or cross-sectional and quasi or fully three-dimensional transient, anisotropic, heterogeneous, layered aquifer systems using finite-differencing. The groundwater flow model embodies much of the site characterization efforts at the site. It represents the aquifer's behavior, and its accuracy is dependent on its input parameters. The model employs the best estimates of the input parameters. The calibrated model can be used to predict changes in flow patterns in the aquifer at the GRFL when certain conditions, such as pumping tests, changes in rainfall, and installation of drains, are imposed.

2.   Approach

We approached this task by first compiling all the available data which best described the aquifer at the GRFL. This compilation of parameter estimates resulted from tests we conducted at the site, and from prior geologic investigation. Slug tests provided hydraulic conductivity estimates at six areal locations and average conductivity over the screened interval of the well used in the test. Pumping tests provided estimates of the transmissivity, storativity, and specific yield of the area near the test cell. The estimates from the pumping test are representative of the area between the observation wells and the pumping well, and are vertically averaged over the screened intervals of these wells. Ground penetrating radar (GPR) yielded the areal estimates of the depth to the aquitard. CPT pushes at the site gave the most detailed information of the stratigraphy of the aquifer. CPT pushes at many areal locations have resulted in an extensive database of important information, some of which was used in the groundwater flow model. CPT pushes provided information on soil type and layer structure, depth to water table at many areal locations, hydraulic conductivity estimates through empirical correlation, depth to the aquitard at multiple locations, and the conductivity of the aquitard through pore pressure dissipation tests (clay only).

The second step in the development of the model was to set up input data sets. Table 18 is a list of the input parameters used in the model. The parameters designated K_x, K_y, and K_z are hydraulic conductivity in the x, y, and z directions, respectively; x and y defining the horizontal plane, and z being vertical. Hydraulic conductivity is the measure of a porous medium's ability to pass water under as a scalar multiplier of pressure gradient. Darcy's law expresses specific discharge (or flow per area) as the product of pressure gradient, (in units of head per length), times hydraulic conductivity, (in units of length per time). The specific storage, S, of a saturated aquifer is defined as the volume of water that a unit volume of aquifer releases from storage under a unit decline in hydraulic head (Freeze and Cherry, 1979) (Reference 22). Hence, it has the units of inverse head (length^{-1}). Storage is the result of two mechanisms: (1) compression of the pore spaces in an aquifer resulting from an increase in the effective stress on the soil particles which accompanies a decrease in fluid pressure, and (2) expansion of the water

TABLE 18. GROUNDWATER MODEL.

Grid Without Pumping Well			
DIRECTION	LENGTH (feet)	# CELLS	SPACING (feet)
x	4500	45	100
y	2500	25	100
z	37	2	13.5
Grid With Pumping Well			
DIRECTION	LENGTH (feet)	# CELLS	SPACING (feet)
x	4500	49	7 to 100
y	2500	29	7 to 100
z	37	2	13.5

Boundaries			
TYPE	INCLUDED ELEMENTS	COORDINATE RANGE	
Constant Head Boundaries	2 layers, 58 nodes	x 0 y 0 to 2500 z -12 to 15	
No Flow Boundaries	2 layers, 1519 nodes 3 sides	x 0 to 4500 y 2500 z -12 to 15	
		x 0 to 4500 y 0 z -12 to 15	
		x 0 to 4500 y 0 to 2500 z -12 to 15	
Rivers	1 layer	(See MODFLOW files for nodes)	
Streams	1 layer	(see MODFLOW files for nodes)	
Pumping Well	1 extraction	x 2400 y 1700 z -11 to -3.8	
Recharge	All water table blocks	Applied to nodes in layer with highest active head.	

Aquifer Properties				
NAME	MODFLOW Property Number	VALUE	SUB-DOMAIN	
Hydraulic Conductivity	1	K_x = 5.0 feet/day K_y = 5.0 feet/day K_z = 0.5 feet/day	Rows: 1-29 Columns: 1-14 Layers: 1 & 2	
	2	K_x = 10.0 feet/day K_y = 10.0 feet/day K_z = 1.0 feet/day	Rows: 1-29 Columns: 14-35 Layers: 1 & 2	
	3	K_x = 17.0 feet/day K_y = 17.0 feet/day K_z 1.7 feet/day	Rows: 1-29 Columns: 35-49 Layers: 1 & 2	
	4	K_x = 24.0 feet/day K_y = 24.0 feet/day K_z = 2.4 feet/day	Rows: 4-7 Columns: 11-49 Layers: 2	
Storage	N/A	S_s = 1.0 x 10-5 foot^{-1}	All	
Specific Yield	N/A	S_y = 0.27	All	
Porosity	N/A	n = 0.28 (porosity)	All	
Recharge	N/A	R = 4.0 inches/year	All Water Table Blocks	

Solver Settings			
METHOD: PRECONDITIONED CONJUGATE GRADIENT			
Iteration Limits		Convergence Criteria	
Outer	Inner	Head Change	Residual
25	50	0.01 feet	0.01 feet
Switches & Options			
Cell Wetting	Wet/Dry	Initial Head	
Off	0.1 feet	3.24 feet (Everywhere)	

in the pore spaces due to the decrease in fluid pressure. The aquifer property called specific yield, S_y, is closely related to the concept of storativity in that it is the volume of water per unit of area released from an unconfined aquifer per unit decline in the water table. It represents the water released from dewatering of the soil pore space as well as from the same mechanisms that contribute to storativity. Specific yield is unitless. Recharge is simply the volume per time of water that enters the aquifer at the water table by infiltration throughout the unsaturated zone, less the water that leaves the saturated zone at the water table through evaporation, capillary actions, or other mechanisms. Using the best estimates of these parameters that describe the aquifer and the dimensions and location of the aquifer, the input data set was constructed for MODFLOW.

MODFLOW is a widely accepted and extensively verified model developed by the United States Geologic Survey (USGS). It is based on a block-centered finite difference approach using variable grid spacing in the x, y, z directions. Layers may be simulated as semi-confined, unconfined or convertible between the two conditions. The model can also handle layers that pinch out (i.e. do not extend through-out the model domain) -- representing aquifers, aquitards or layers within an aquifer. The model allows for external influences such as constant and time-varying wells, areal recharge, drains, evapotranspiration, and streams. The parameters described above best estimate the aquifer condition at the GRFL and were used as input data to MODFLOW. See Appendix P for the actual input data files in MODFLOW format. To understand MODFLOW and MODFLOW's format for input see the MODFLOW manual which is distributed by the International Groundwater Modeling Center (Boulder, CO).

The third step in this task was to calibrate the model. This step involved changing the conditions of the model and checking the results to ensure it was reacting the way it should. This model was checked by simulating the first pumping test that was conducted at the GRFL.

3.   **Results**

Boundaries. The model boundaries follow the natural boundaries of the aquifer. These natural boundaries consist of a groundwater divide, a river, a stream and the aquitard. The groundwater divide located northeast of the GRFL provides the starting point. It is represented as the left boundary of the model extending from the origin (lower left corner) to 2500 feet northeast (upper left corner). The model domain extends 4500 feet southeast from this boundary to the St. Jones River. The model dimensions are 4500 feet in the x direction, 2500 feet in the y direction, and 27 feet in the z direction. Actual elevations, from 12 feet below sea level to 15 feet above sea level correspond to the 27-foot thickness in the z direction. Two layers represent the range of saturated thickness. Since MODFLOW cannot delineate variable sized layers in the z dimension, the two layers are each 13.5 feet thick. The aquitard is the natural boundary for the bottom of the model and extends in the x and y directions throughout the entire bottom Layer 2. This model is oriented in the direction of natural groundwater flow. The edges of the model domain along the x and z dimensions are considered no-flow boundaries, as they are perpendicular to natural head contours and no flow will cross these boundaries.

Since CPT pore pressure dissipation tests indicate low transmissivity in the aquitard and the flow to be principally horizontal, the aquifer bottom is also a no-flow boundary. The natural groundwater divide is a constant head boundary of 14.8 feet. The river is a constant flux boundary with a transmissivity of 75 square feet per day. This transmissivity is based on estimations of river bottom thickness and soil type. The stream extends upward from the St. Jones river approximately 1500 feet, as the USGS topographic map indicates (Little Creek, Del. 7.5-minute quadrangle, 1993). The stream is also estimated to have a transmissivity equaling that of the river but does not deliver as much volume of water as the river. Two files, *data.bas* and *data.bcf* contain the boundary definitions in MODFLOW format (refer Appendix O for more information on data sets for the model).

Properties. The hydraulic conductivity of the water table aquifer varies spatially and is represented in the model by four distinct values of hydraulic conductivity. Near the groundwater divide, both layers in the model have the hydraulic conductivity of 5.0 feet/day. Approximately 1300 feet southwest of the divide, near the area of the GRFL, both layers have a hydraulic conductivity of 10.0 feet/day, except for the beginning of a higher conductivity channel in the southwestern section of the model in Layer 2. The exact dimensions of the channel are unknown. However, CPT soundings and the results of a pumping test in the vicinity indicate its existence. Layer 2 of the model reflects the higher conductivity of this channel beginning in the area of the GRFL at approximately 2250 feet from the origin along the x axis, and extending to the stream and then to the river. The hydraulic conductivity of the channel is estimated to be 24 feet/day. Between the GRFL area and the St. Jones River, the hydraulic conductivity of the model changes to 17 feet/day. The model properties are isotropic in the x and y direction and anisotropic in the z direction. Vertical hydraulic conductivity is one tenth the horizontal. The specific yield of the model is 0.27 and the storage is 1×10^{-5} feet^{-1}. Recharge to the aquifer is 4.0 inches per year. This value was determined using annual rainfall statistics and estimates of evapotranspiration, interception, and infiltration based on ground cover, soil type, and depth to water table.

Wells. One pumping well was represented in the model. It is the physical well from which the pumping test was completed in the GRFL area. The well extends to the aquitard (lower boundary of Layer 2) and is screened over a 7-foot length beginning at an elevation of 11.10 feet below sea level. In the model the well is turned on for a possible 10 years at a withdrawal rate of 1 gpm to ensure it was at steady state. The actual pumping test was conducted for approximately 14 hours, achieving the delayed yield stage of drawdown.

Grid. The model grid is composed of 49 finite difference blocks in the x direction and 29 blocks in the y direction. Since there are two layers, the total number of finite difference blocks is 2842. The grid cells are all 100 feet in x, 100 feet in y, and 13.5 feet in z, except for near the pumping well where there is a finer mesh. The mesh was refined in the vicinity of the pumping well to better resolve the relatively small areal influence of the one-gpm pumping rate. Since there is a very steep gradient near the well, refining the mesh in this area helps the finite difference solver to better distribute the pressure change through the domain near the well. Because MODFLOW requires a regular grid, the refinement of the mesh extends to the boundaries in the x and y directions. The grid was designed to provide a starting platform for

users and can be solved fairly quickly by the solver. A user can refine the mesh in areas where finer resolution is required; however, the speed of solution will decrease as the number of blocks is increased.

Model Predictions. The model predicts the groundwater table as shown in Figures 59 and 60. The contours show the potential energy along a path through the aquifer in Layers 1 and 2. Sharp bends in the contours of the southwestern section of the model domain show the influence of the stream that is located in this area. These head contours match head contours from prior geologic investigations as well as those derived from CPT pushes and monitoring wells throughout the site. The actual groundwater contours could change depending on the season, amount of recharge received, and induced stresses such as the operation of a water supply well. The contours shown are representative of the groundwater table as it was in October 1995 through May 1996. Natural occurrences, such as changes to the constant head boundaries or recharge rate, can be reflected in the model input so its output would indicate the resulting changes in the water table.

There is not much difference in head from Layer 1 to Layer 2 throughout the aquifer. This result is expected as the material properties are similar. CPT soundings in the area of the GRFL classify the saturated zone as predominantly sand. Figure 63 is a plan view of the potential energy gradients of the aquifer. The arrows are scaled in size and intensity. The length of an arrow's tail reflects the strength of the gradient at that location. Near the stream, the flow changes direction due to the drainage effect of the stream. The average gradient that MODFLOW predicts over the GRFL site is 0.007 feet/foot; 13 percent less than the approximate 0.008 feet/foot gradient calculated from field measurements of the water table elevation. The model would predict higher gradients if lower estimates of hydraulic conductivity were used in the input; but such a change would cause other errors in model output. For example, a severe reduction in head would appear in Layer 2. Since this reduced head was not observed in the field and the head contours and gradient are fairly close, the conductivities as stated above remain in the model.

Calibration with pumping test. Figure 62 and 63 show the model's prediction of the water table in Layers 1 and 2 during the pumping test. For the prediction, the solution was forced to steady state, whereas the actual pumping test was conducted for 14 hours and did not achieve steady state. Analysis of the actual pumping test revealed that 14 hours of pumping at the 1 gpm flow rate put the state of the system into the delayed yield stage of the drawdown curve. Following this stage, a non-equilibrium phase should commence and ultimately higher drawdowns would be experienced. However, given the low transmissivity of the aquifer in this area and the resulting narrow cone of depression, the delayed yield stage produces only slightly less drawdown than a steady state condition would produce. The results of the pumping test are close enough to steady-state for quantitative comparison with the model-predicted condition.

Figure 59.   MODFLOW Prediction of Potential (Feet) in Layer 1. GRFL Site Located Approximately 2200 Feet in X and 1000 Feet in Y.

142

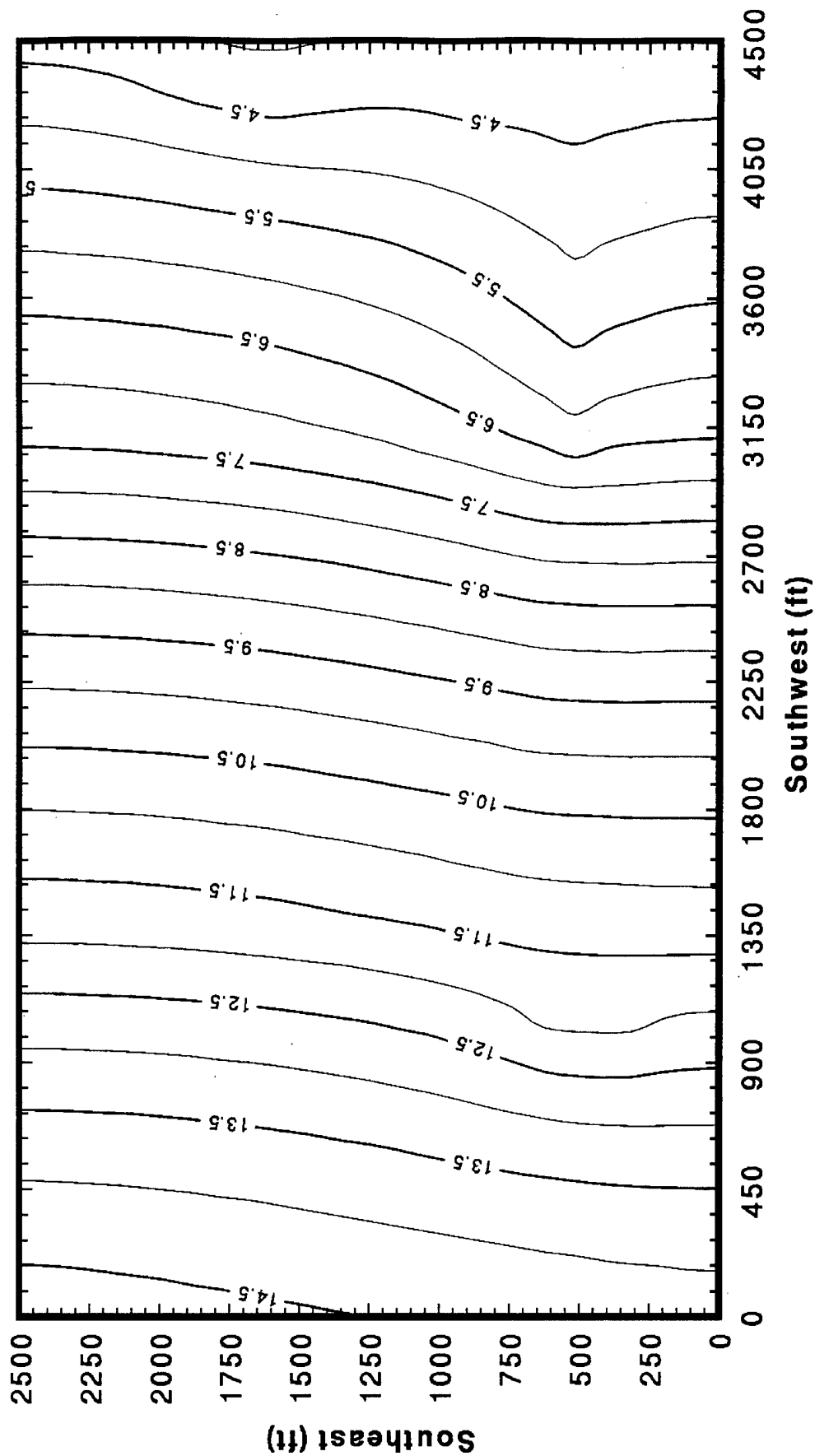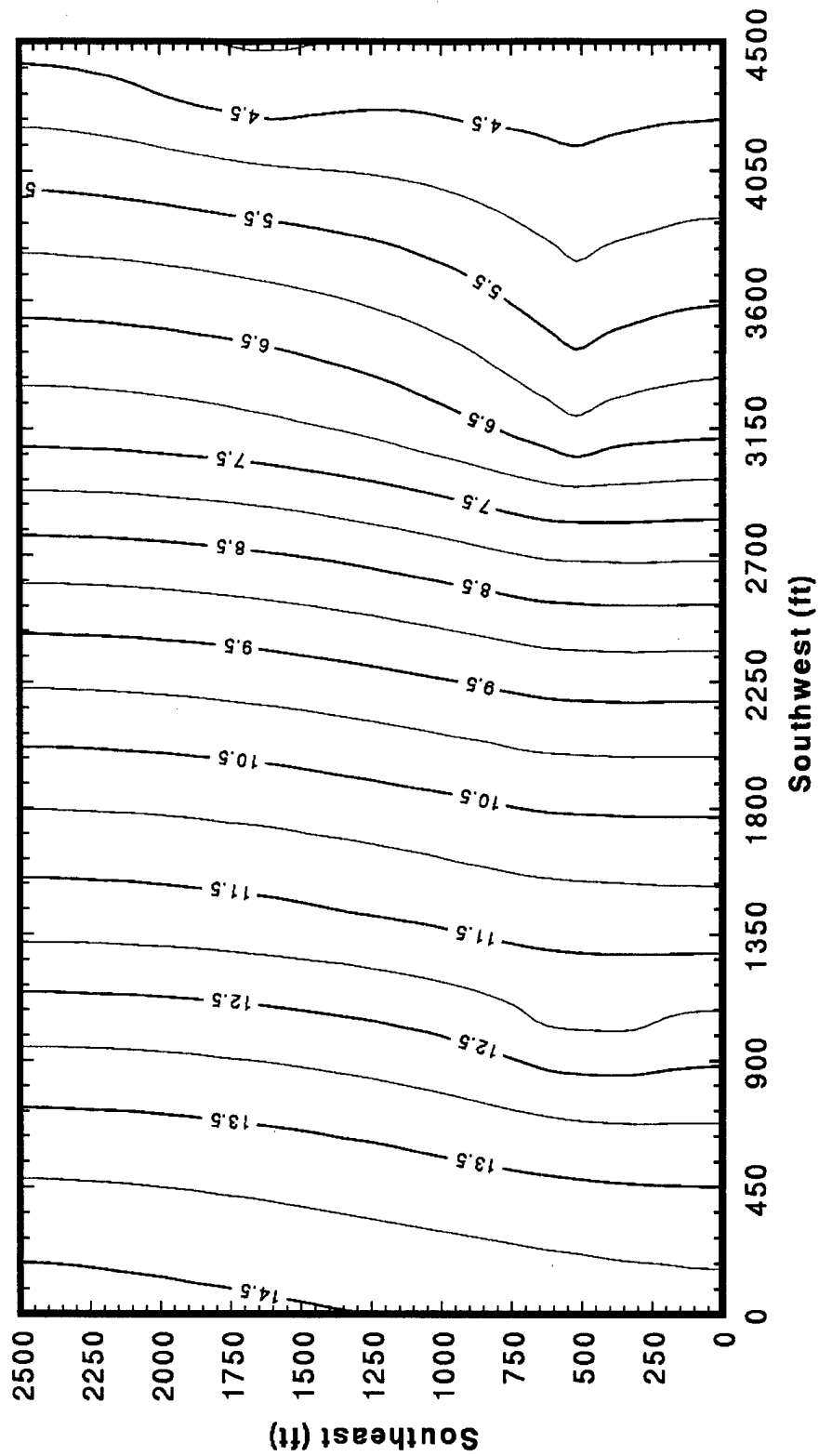**Figure 60.** MODFLOW Prediction of Potential (Feet) in Layer 2. GRFL Site Located Approximately 2200 Feet in X and 1000 in Y.
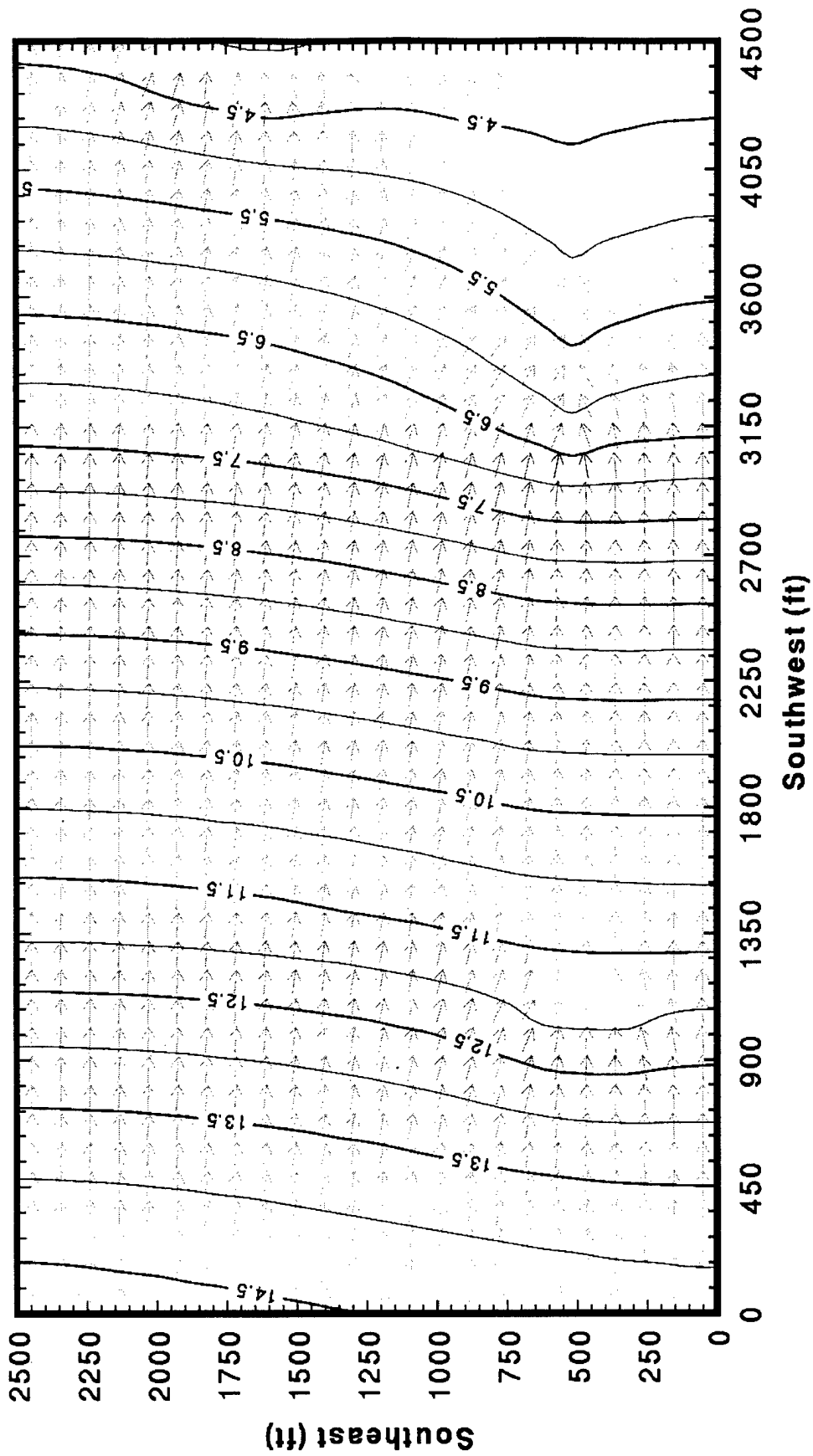
143

Figure 61.   UNCERT Prediction of Gradients for Unconfined Aquifer From MODFLOW
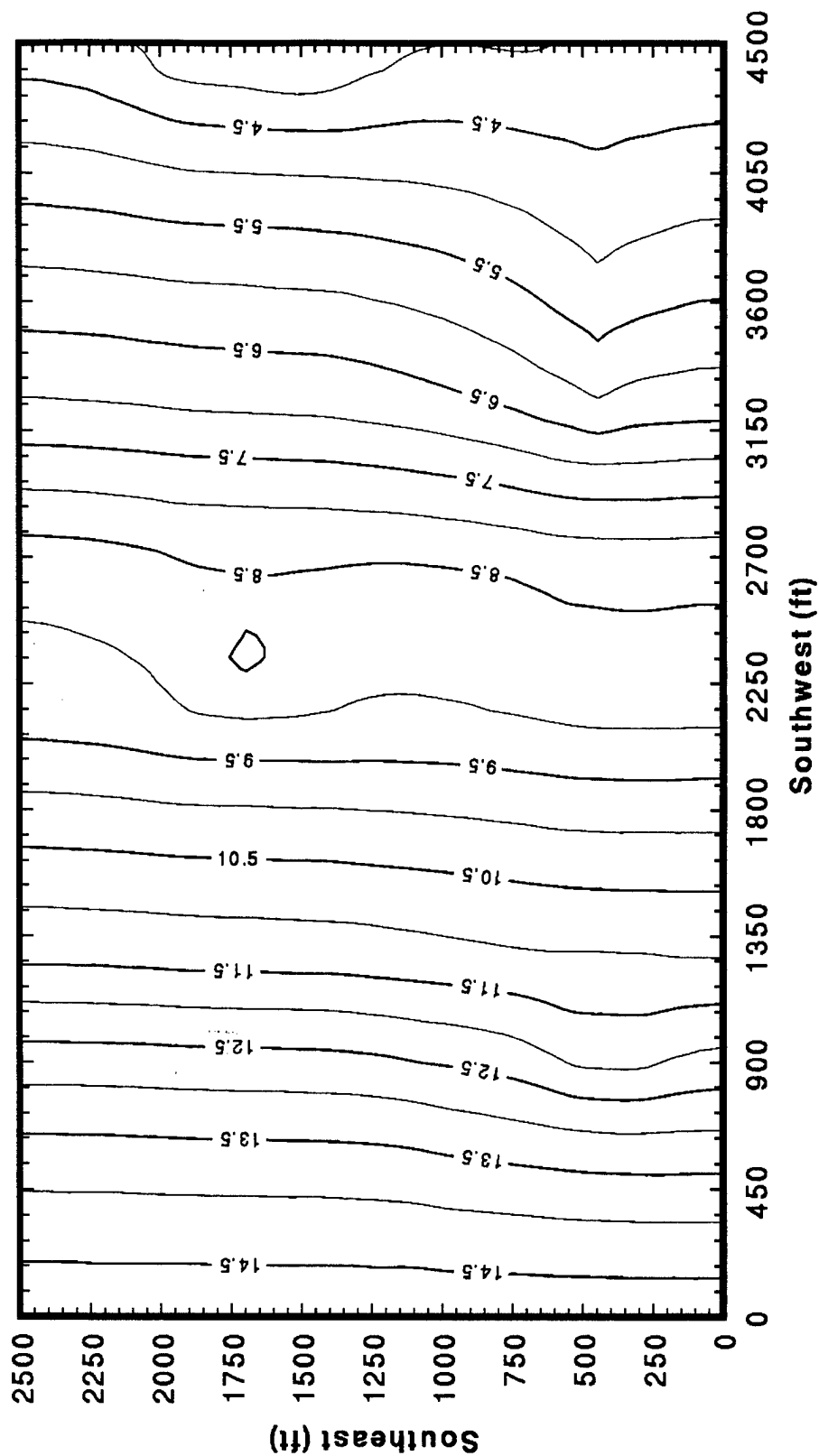Head Estimations Layer 1.

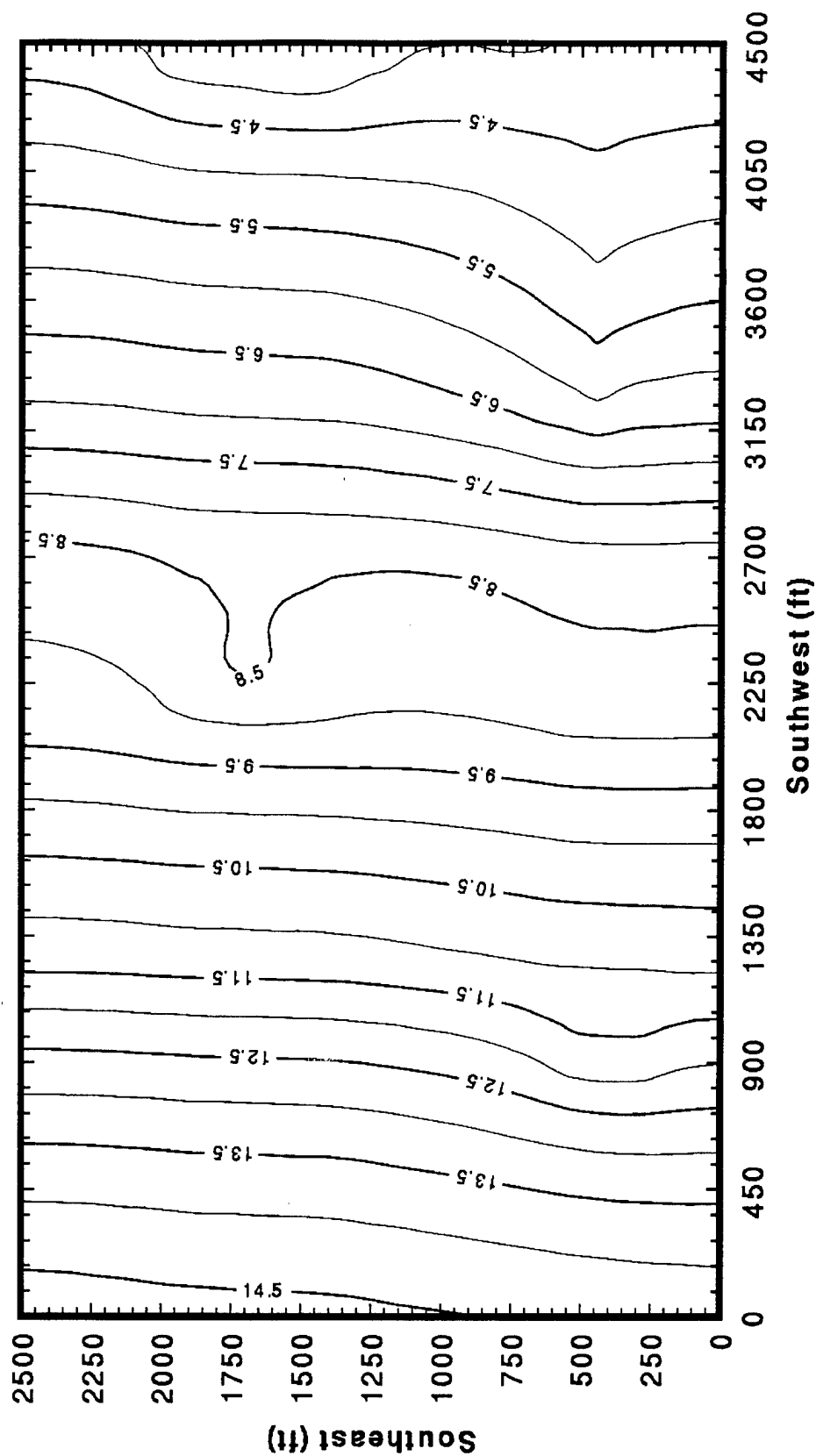Figure 62. MODFLOW Prediction of Potential in Layer 1 During Pumping Test.

Figure 63.   MODFLOW Predicted Potential in Layer 2 During Pumping Test.

The water table elevations in the figures show a simulated tenth of a foot drawdown in the area surrounding the well and approximately a 90 foot radius of influence. This compares favorably to the physical pumping test results. The radius of influence for the physical pumping test shown is approximately 50 feet. (see Figure 64.) Note the greater drawdowns in Layer 1 compared to Layer 2 of the model-predicted potential energy during the pumping test. Because the conductivity of the lower unit in the model is slightly higher than in the upper unit (due to the channel), and the screen in located in this area, lower gradients in this area should be expected. This phenomenon would also contribute to the discrepancy between the simulated and actual radii of influence. Also, the bottom of the aquifer in the model is simulated as a no-flow boundary. Therefore, all flow supplying the well in the prediction is from Layers 1 and 2. It is possible that some water was supplied to the pumping well through the aquitard during the physical pumping test. Figures 65 and 66 show expanded views of the contours and gradients of the water table in Layers 1 and 2 and in the area of the GRFL. Overall, the model does well in predicting the water table when a stress such as pumping is exerted on the aquifer. See Appendix O for the input data fields and corresponding model output in MODFLOW format.
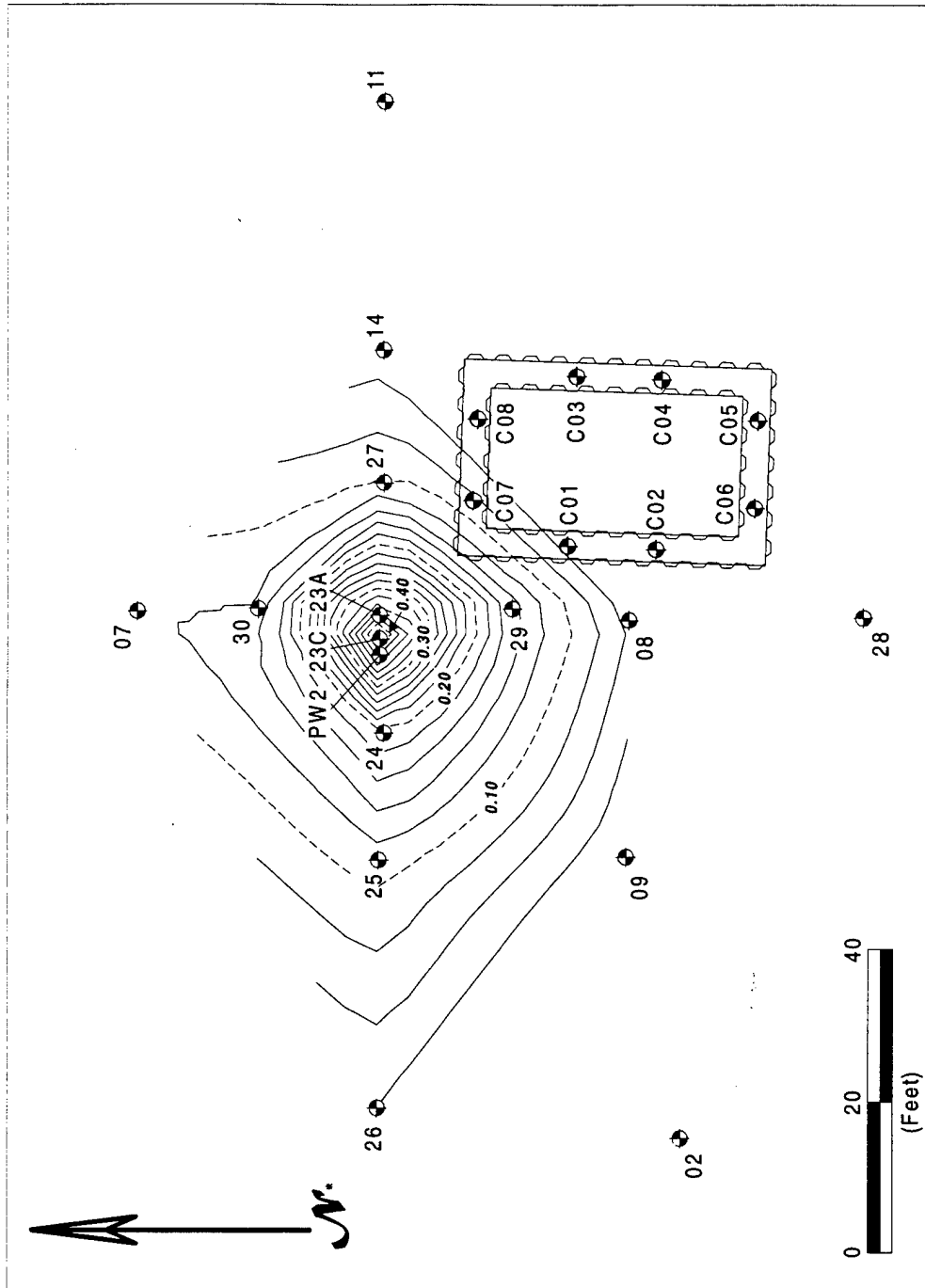
Figure 64. Drawdown Contours During GRFL Pumping Test Before Cell Construction, Showing Radius of Influence of Pumping Well. Test Cell Shown for Reference Only.

* North based on GRFL coordinate system

148
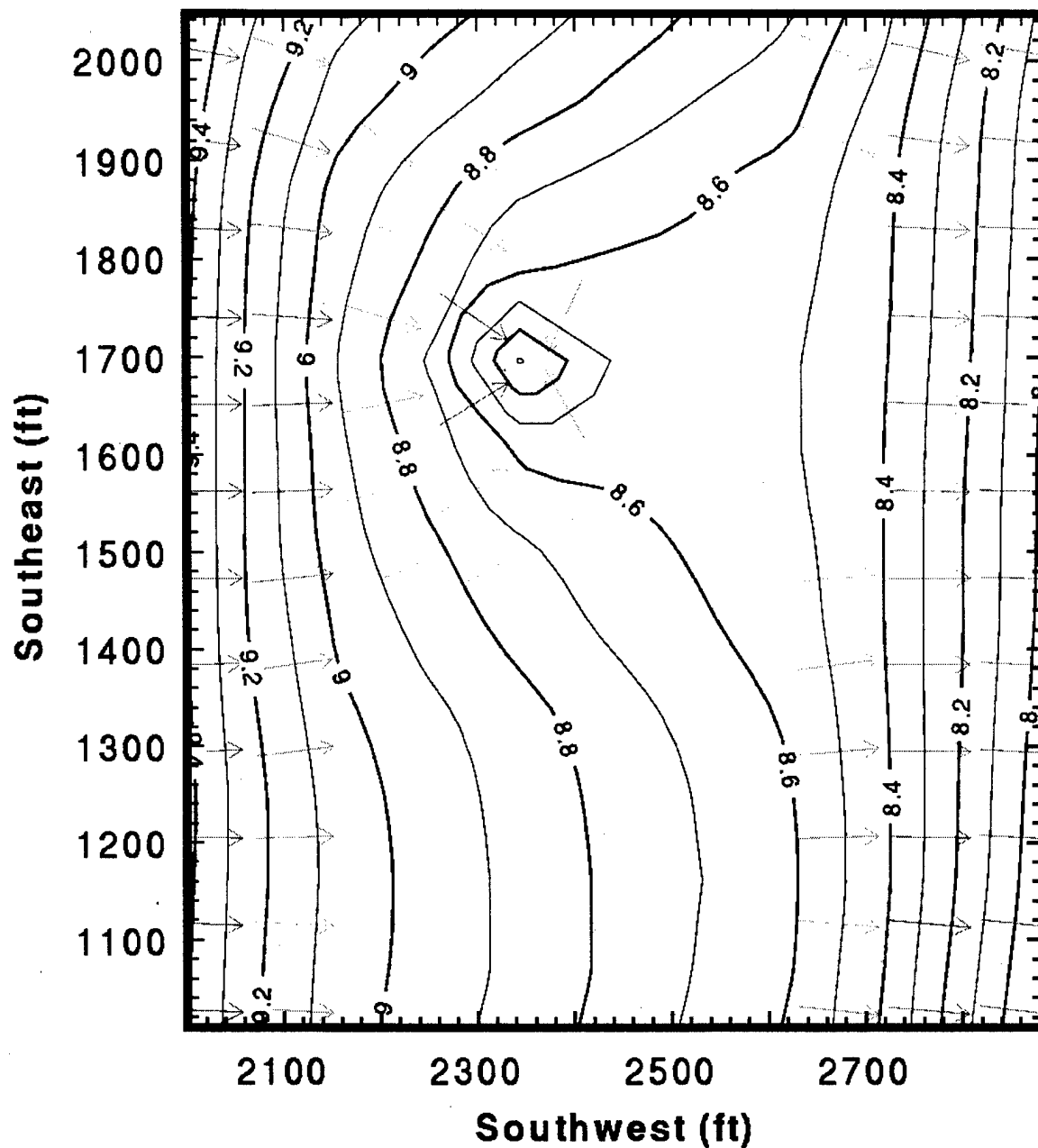
Figure 65. Expanded View of Layer 1 Contours and Gradients in GRFL Area During Pumping Test.
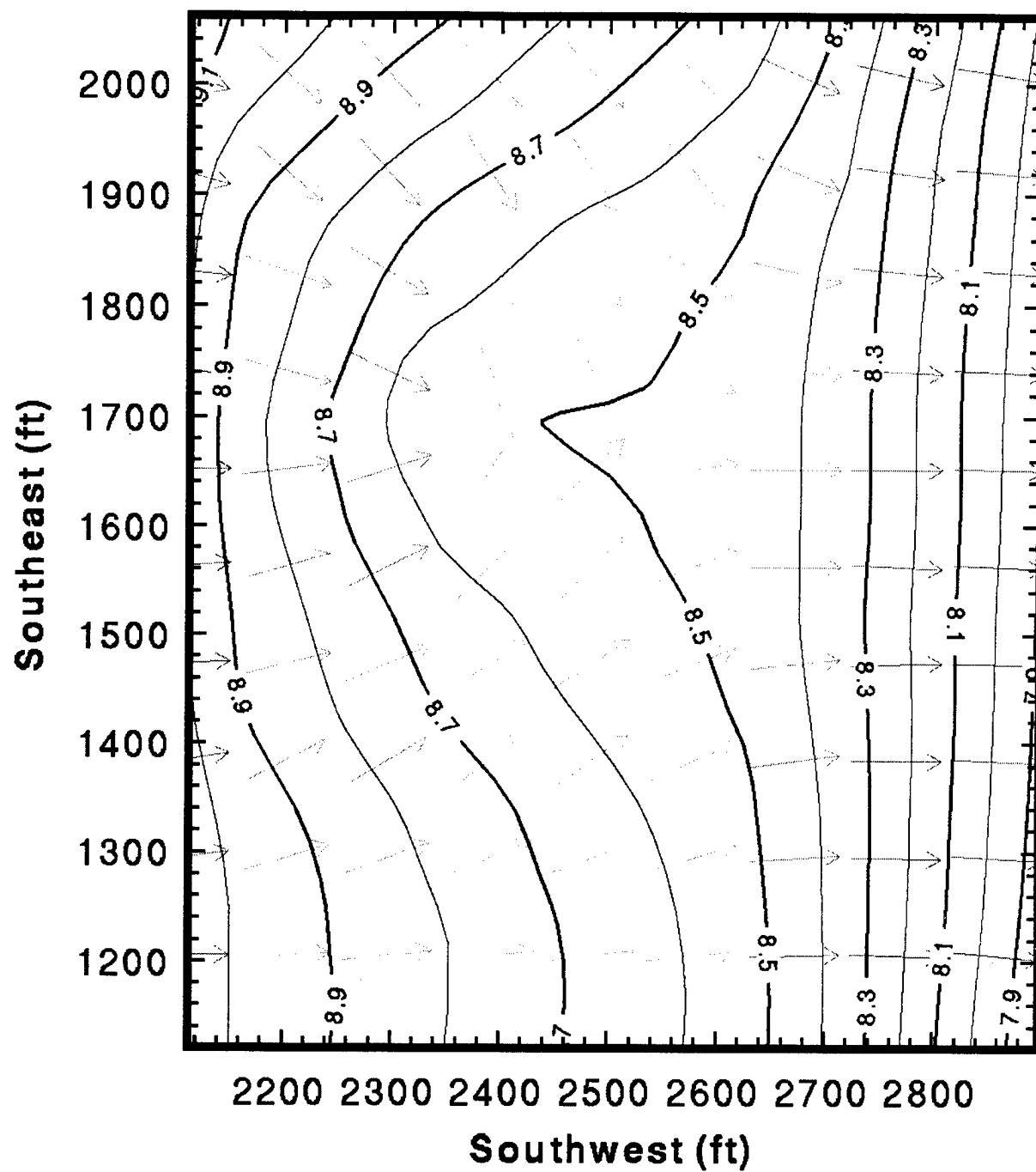
Figure 66. Expanded View of Layer 2 Contours and Gradients of GRFL Area During Pumping Test.

150

SECTION VI

EMERGENCY GROUNDWATER PUMP AND TREATMENT SYSTEM

A.   OBJECTIVE

The objective of this task was to design and install an emergency groundwater pump and treatment system to contain and treat any unexpected leakage of contaminants from the test cells during demonstrations of treatment technologies. Figure 67 is a drawing of the test cell showing dimensions and locations of the extraction/injection wells for the treatment system. This system provides protection against contamination of groundwater and soil outside the test cell in the unlikely event of contaminants leakage during the future technology demonstrations.
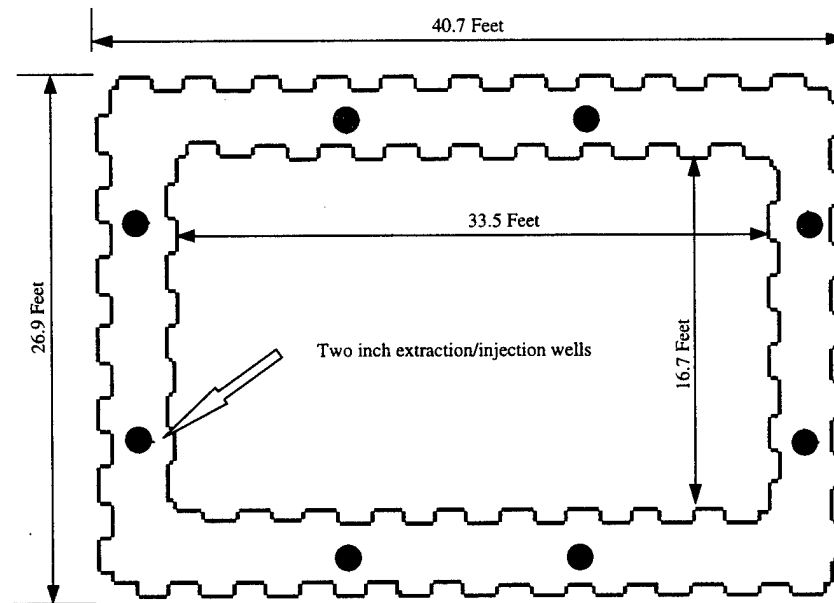
Figure 67. Drawing of Test Cell and Locations of Extraction/Injection Wells.

B.   APPROACH

Extensive measures were taken to minimize any potential impacts to the GRFL environment. Protective measures include two engineered barriers, maintaining an inward hydraulic gradient between the outer and inner barrier, and monitoring wells which can be converted to contain and pump and treat in the unlikely event of a release. Demonstrations at the GRFL will involve controlled releases of DNAPLs which are major environmental contaminants for the DOD.

The most common DNAPLs encountered throughout the DOD are tetrachloroethylene (PCE), and trichloroethylene (TCE). Therefore the emergency treatment system was designed to treat these compounds and other chlorinated compounds. The compound of most concern, due to its pervasiveness and high toxicity, is TCE. For this reason, the system was designed using TCE as the DNAPL to treat as a worst case scenario.

However, the system was designed to be flexible enough to provide treatment of a wide range of contaminants including the following: TCE, PCE, benzene, toluene, ethylbenzene, xylenes, (BTEX), and other volatile contaminants.

The remediation of water contaminated with volatile organic compounds generally can be accomplished with air stripping techniques. Stripping is commonly defined as a process to remove dissolved, volatile compounds from water. A carrier gas, such as air or steam, is purged through the contaminated water, with the volatile components being transferred from the water into the gas phase. Given the vapor pressure and aqueous solubility of a volatile chemical, its propensity to be volatilized can be estimated by its Henry's Law constant. This constant is the ratio of the vapor pressure to the aqueous solubility. The general principles of air stripping are quite simple. Within the air stripper the surface area of contaminated water is maximized, while air is directed across it. Contaminants at the air-water interface volatilize and are discharged to the atmosphere or to an off-gas treatment system.

During recent years, compact, low-profile air strippers have gained increasing acceptance over the packed tower air-stripping systems, and now represent more than half of the air strippers used at new remediation sites. The GRFL system was designed using the most common style of low profile air stripper shown in Figure 68. It is the tray-type unit in which a shallow layer of water is allowed to flow along one or more trays (the GRFL unit has six trays). Air is blown through hundreds of holes in the bottom of the trays to generate a froth of bubbles which provides a large mass transfer surface area where the contaminants are volatilized. With the tray-type, low-profile system, the air does two jobs simultaneously, creating the surface area and volatilizing the chemical compound.

The amount of contamination that can be removed from water during a single pass through an air stripper depends on a wide range of factors, including:

- The strippability of the compounds;
- Flow rate of the water;
- Surface area of the water;
- Air flow;
- Water temperature;
- Air temperature;
- The effect of minerals and other chemicals in the water; and
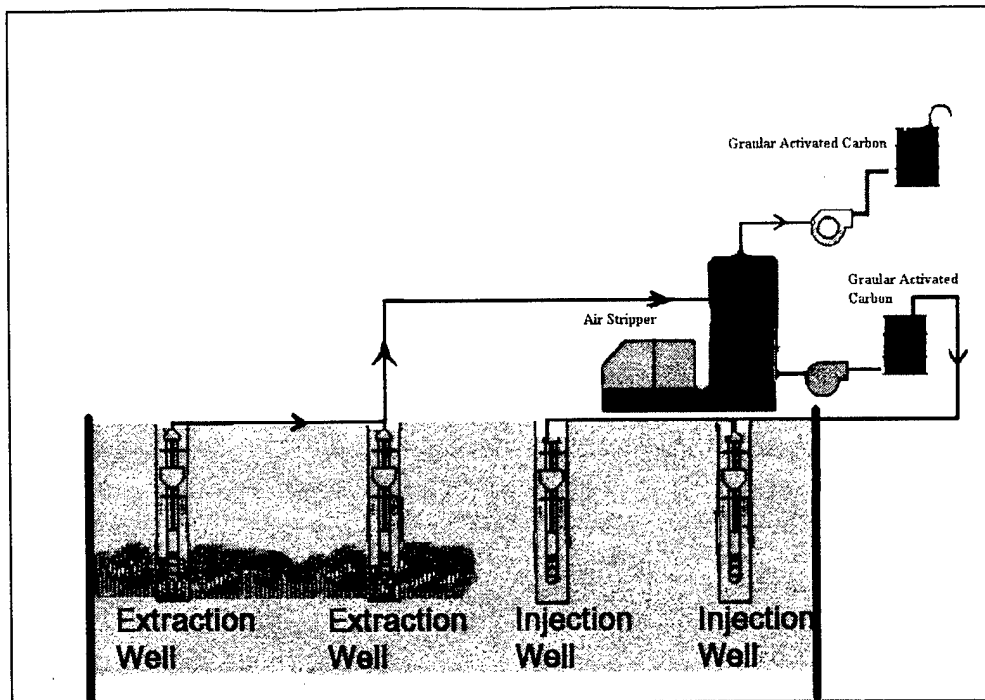- Residence time of water in the system.

152

Figure 68. Schematic of Treatment System and Extraction/Injection Wells

The air stripper is a powerful treatment system because most of these variables can be controlled to obtain an optimal, site-specific solution for contaminant removal. The higher the concentration of contamination in the water, the more air will be needed to volatilize and carry it away. It is therefore necessary to increase the air-water ratio to improve treatment efficiency. Tray-type, low profile strippers have inherently high air-water ratios because relatively large volumes of air are required to transform water in the tray into a froth. Without oversizing the blowers, such units are capable of removing such highly soluble contaminants as methyl(tert)butyl ether (MTBE), methylene chloride, and acetone. The higher the volatility and the lower the solubility, the easier it is to strip a contaminant from water. Conversely, it is impractical to attempt removing marginally volatile but highly soluble chemicals with an air stripper. If additional treatment efficiency is required, it is possible to further increase the air-water ratio by reducing the flow rate of water through the system. Tray type units may be operated anywhere within their rated water flow range. A small system may have a flow rating of 1 to 15 gallons per minute (gpm), while a large unit may have a range of 16 to 360 gpm. Either system may be operated at the lower limit to obtain a high contaminant removal efficiency. Based on pumping test at GRFL, each extraction well will likely produce less than one gpm. Therefore the GRFL treatment is a small system with the capability to treat flow rates from 1-20 gpm. Based on hydraulic conductivities determined in this study, the emergency treatment system has adequate capacity to treat any leakage that might occur during demonstrations at up to three other test cells constructed at the GRFL.

Residence time can also be a factor for improving treatment efficiency. Residence time in the GRFL stripper can be improved by adding more trays. In the GRFL multi-tray system, when water has reached the end of one tray, it falls into the next for additional treatment. Adding trays also makes it possible to operate at higher water flow rates with out sacrificing air stripping efficiency. The ability to remove or add trays in the system makes it possible to tune the system for improved performance or reduced operating costs.

C.   RESULTS

Manufacturers of air stripping systems can accurately predict the performance of their systems based on extensive laboratory studies. The data have been incorporated into computer models that are used to select air stripping equipment according to the environmental requirements. The air-stripper designed for the GRFL is based on calculations provided by ORS Environmental Systems. The ORS LO-PRO II air stripping system was selected for treating any contamination that might escape from the GRFL tests. The LO-PRO II is a modular, counter-current, cascade, multi-stage air stripper. The results of model calculations for design of the air stripping system are as shown in Table 19. Specifications and operators manual are provided in Appendix Q.

TABLE 19. RESULTS OF CALCULATIONS FOR DESIGN OF THE AIR STRIPPING SYSTEM.

Contaminant	Influent (ppb)	Required Effluent (ppb)	Calculated Effluent	Excess Level	Removal Efficiency
Trichloroethylene	2000	5	0.83	0.0	0.9996
Trichloroethylene	1000	5	0.42	0.0	0.9996
Tetrachloroethylene	2000	5	0.16	0.0	0.9999
Tetrachloroethylene	1000	5	0.08	0.0	0.9999
Ethylbenzene	2000	5	3.11	0.0	0.9984
Ethylbenzene	1000	5	1.56	0.0	0.9984
Xylene	2000	5	2.37	0.0	0.9988
Xylene	1000	5	1.18	0.0	0.9988
Toluene	2000	5	2.69	0.0	0.9987
Toluene	1000	5	1.35	0.0	0.9987

*These removal efficiencies do not include the effects of the secondary treatment with GAC.

Start at:	179 cubic feet/minute
Clean trays at:	169 cubic feet/minute
Number of trays:	6
Tray height:	10 inches

Flow rate: 8 gpm
Temperature   55.00 degrees F
Air/Water ratio: 158

For contaminants such as trichloroethylene, tetrachloroethylene, benzene, toluene, ethylbenzene, and xylenes (BTEX) in groundwater, air stripping performance is well understood and no pilot study is required. There are other compounds that may be released in the GRFL test beds where air stripping is certainly applicable, but the exact performance of the system is not as predictable because of less documented experience. These compounds include (e.g., acetone and methylene chloride), chlorinated hydrocarbons (e.g., dichloroethane), extractables (e.g., diesel fuels), soluble gases (e.g., ammonia), and complex industrial waste streams. In these instances, the operation of the GRFL emergency treatment system must be based on the results obtained from bench level testing of the compounds to be released in the test cells.

In the unlikely event that the contaminant is able to penetrate both the interior and exterior cell walls, there are 2-inch wells capable of containing and removing the aqueous phase contaminant plume. Figure 69 shows the radius of influence from one well pumping at 1 gpm to be on the order of 32.8 feet. If all five wells, (wells 28, 08, 29, 23, and 27), designated for use in the emergency pump and treatment system, are pumping at comparable rates, the groundwater around the cell should be completely captured. The data contained in this report should be used to develop a contingency plan for plume capture at the GRFL test cells.

D.   DISCUSSION

The air stripper designed for the GRFL is capable of greater than 99% removal efficiency of the listed compounds. As an additional treatment, granular activated carbon (GAC) units are provided to treat the liquid and gas phase effluents from the air stripper. Although air stripping removes organics from the groundwater, it causes a phase transfer of the contaminant from water to the atmosphere; air pollution control equipment must be used if VOCs are discharged at a rate greater than 0.453 kg/d. There the system was designed as a dual system with aqueous- and vapor-phase GAC adsorption. Since the system operates as a closed loop system for treating any contaminants that might escape through the test cell barrier, it is not technically necessary to treat the liquid-phase effluent. However, as an extra measure of safety, the system is also designed with aqueous-phase GAC adsorption. In addition to treating any remaining VOCs from the air stripper, the aqueous-phase GAC adsorption provides additional treatment for a wider range of contaminants that may be harder to remove by the air stripping process.
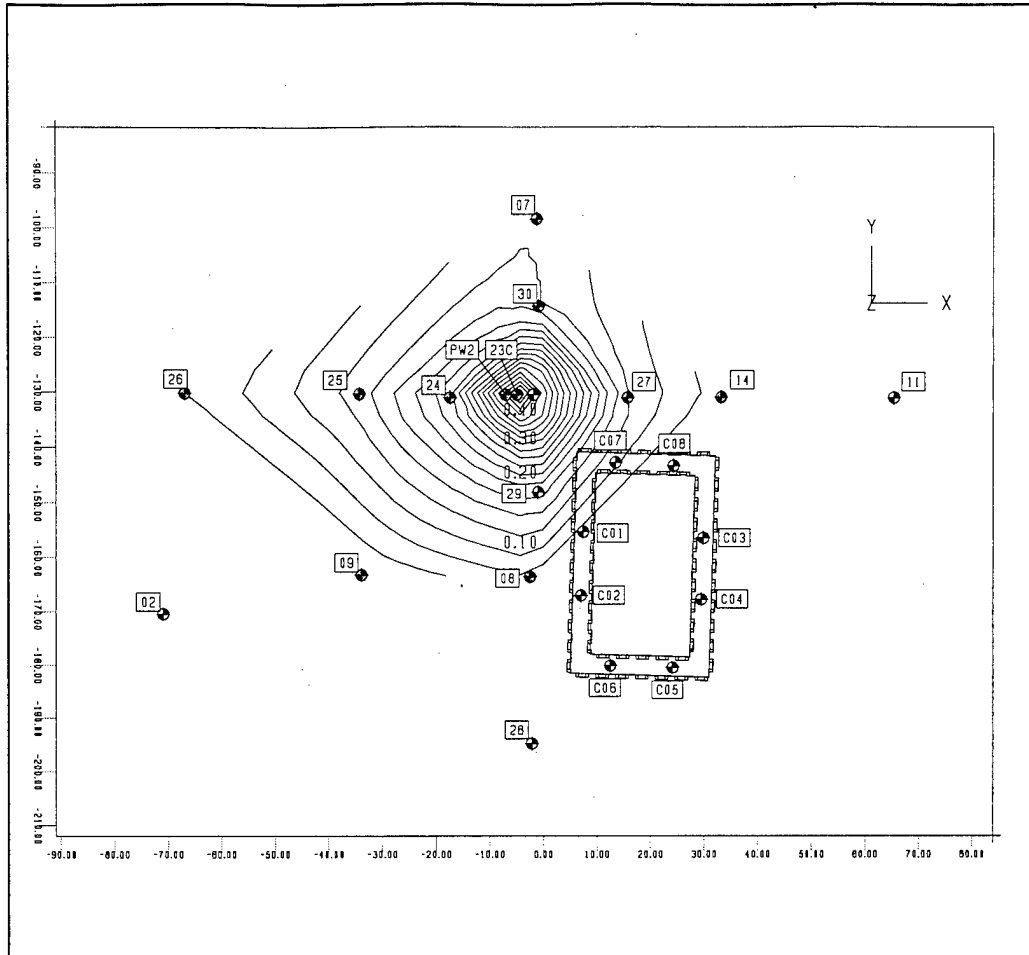
Figure 69   Drawdown Contours from Pumping Test Near Test Cell Location

The GRFL treatment system is portable and reusable. It can be easily packed on a truck and moved around the GRFL site or to other locations at the Dover National Test Site. The unit can be used for long periods with essentially no deterioration in performance. Figure 70 shows a photograph of the treatment system, being set up on the concrete pad adjacent to the test cell. Also, the bioventing demonstration equipment is shown in the center of this photograph.

The air stripper system's stainless steel plates, large diameter aeration holes, and high air and water turbulence reduce fouling. If cleaning is necessary to remove iron, calcium, and biological fouling, the polyethylene trays can be opened and closed easily by hand. This makes the system easy to disassemble and clean, without special tools or equipment. The GAC units are simply replaced when their efficiency drops below acceptable limits. Since this system is for emergency use in the unlikely event of leakage from the test cell, use of the system is not expected to be extensive. Therefore maintenance should not be a major activity of the GRFL staff.

156
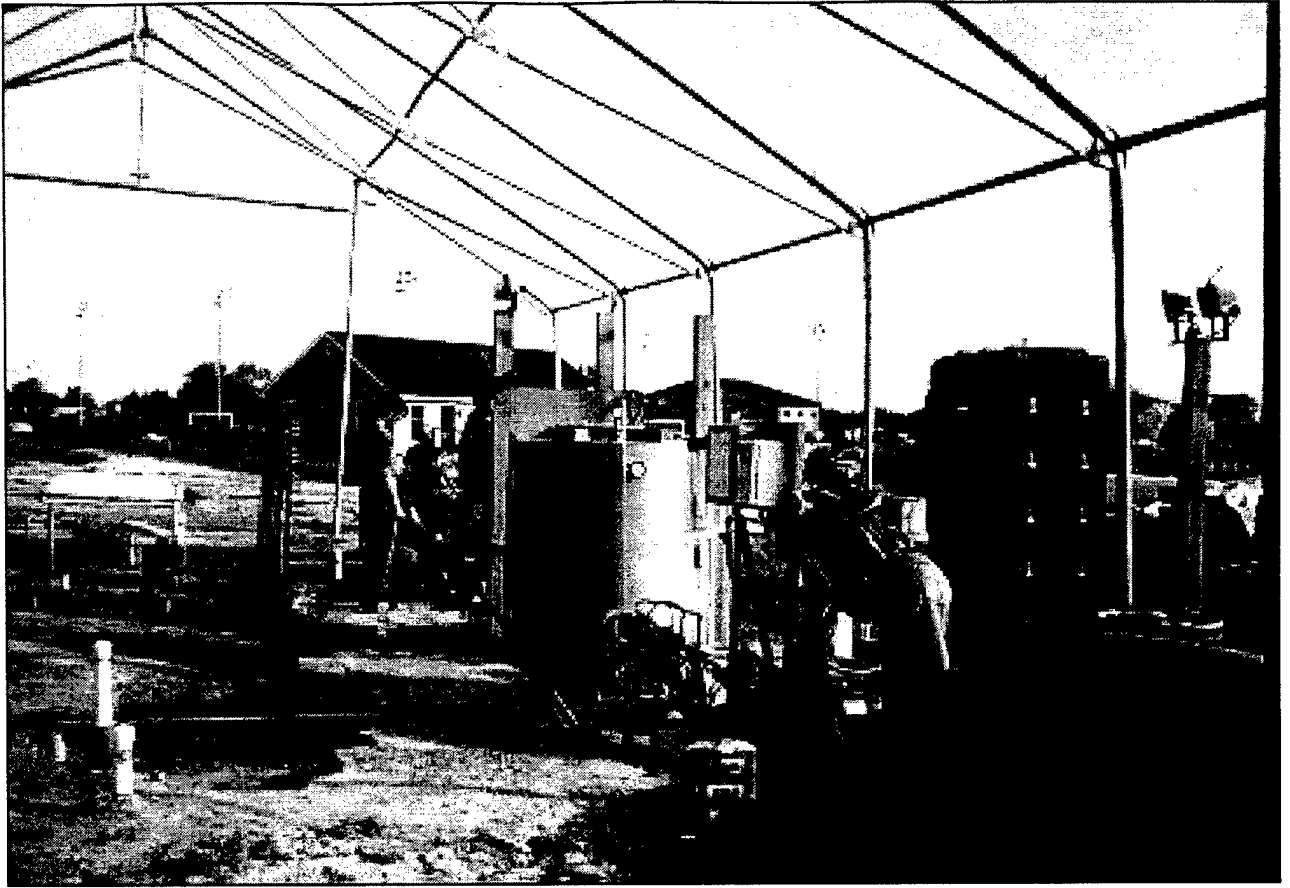
Figure 70. Photograph of Emergency Treatment System During Placement.

SECTION VII

PREPARATION OF SITE FOR GRFL

A.   OBJECTIVE

The objective of this task was to prepare the GRFL site for the performance of controlled field tests under carefully monitored pilot demonstrations. The GRFL, which is modeled after the facility at the Canadian Forces Base Borden in Ontario, was developed to permit very accurate, quantitative performance indicators of cleanup technologies emerging from the SERDP and other DOD research programs. Figure 71 is an aerial photograph showing the site location.

Figure 71. Aerial Photograph of GRFL Site.

Sub-objectives of this task included:

- designing, laying out, and surveying the site;
- designing the utility services (water, sewer, electrical and communications);
- drafting the plans;
- coordinating the plans with all concerned functional agencies on Dover AFB;
- installing the utility services;
- constructing the sidewalk;

- selecting, purchasing, and erecting the test cell cover;
- planting the tree screen for the site and landscaping around the lab;
- cleaning up the site; and
- preparing the as-built drawings.

B.   APPROACH

McCrone Inc. of Odessa, DE was contracted to survey the site, design the utility lines and prepare the construction drawings according to the concept plan included in the proposal. The plans were then coordinated with all required functional agencies at Dover AFB and all requested changes were made to the drawings.

George and Lynch, Inc. of New Castle, DE was contracted to install the utility lines, construct the sidewalk, and clean up the site. Tele-communications requirements were coordinated with the Dover AFB Communications Squadron. Their operating contractor, Tennmark, was contracted to provide the telephone wiring and connect the facility to the base tele-communications system.

All Seasons Landscaping Dover, DE was contracted to furnish and plant the tree screen around the periphery of the test site. They were also contracted to provide extra landscaping around the modular facility to satisfy the special needs of Earth Day.

The test cell cover was purchased from Rubb Inc. of Sanford ME. The contract required immediate delivery to the site and erection upon notice.

C.   RESULTS

The only change to the site concept from the proposal was to locate the first test cell near the south edge of the site and orient it parallel to the site fence. The test cell location and orientation are shown in Section II as Figure 1.

The utilities were designed to provide normal services to the site. The base engineers did not want us to cross Arnold Drive Extension with any of the service lines, so the water line had to be brought in from much further away than anticipated in the proposal. They directed us to connect the water into a 3/4 inch plastic water line serving a water fountain at the south end of the running track. There are two problems with this service. First, this line starts in a locker room in the south end of building 913 and exits the building above ground. The water plant routinely shuts this line off each fall to keep it from freezing. They agreed to fix it before the first freeze this fall, but if they don't, the site will be out of water. Second, the total length of 3/4 inch line serving the GRFL facility is 670 feet which results in a 20 psi pressure drop at a flow rate of 5 gpm. There should be adequate water pressure in the laboratory for the anticipated usage, but it will be lower than normal.

The design for the electrical service for the site was changed twice -- from single phase to three phase and then back to single phase. We proposed bringing electrical power from an existing pad mounted single phase 100 kva transformer adjacent to the site. This transformer serves the running track lighting and has some excess capacity. However, the equipment initially selected for the emergency pump and treat system and bioventing experiment required three phase power so we changed the subcontract with McCrone to design three phase power for the site.

The primary cables to the existing 100 kva transformer adjacent to the site will not support three phase power. The closest available power pole with three phase power is 200 feet from the site and has an existing transformer installed. Consequently, the three phase design required moving the existing pole mounted transformer and installing 360 feet of 4 wire underground primary electrical service line. The estimated construction cost for this was excessive, so the emergency pump and treatment system and electrical service for the site were redesigned for single phase power.

The modular facility electrical power is serviced by the existing 100 kva single phase transformer that powers the lights on the adjacent running track. The test cell electrical power is provided by a new 100 kva single phase transformer that was installed adjacent to the existing transformer and connected with feed-through inserts. A power panel was constructed at the test cell to provide 110-220 volt single phase power for the emergency pump and treatment system and the equipment to be used by the various test activities. The electrical power to the site is shown in Figure 1.

A 2 inch conduit was buried between the test cell and the laboratory to accommodate multiple instrumentation cables. This line follows the line of the electrical service lines to the first test cell.

Two 8- x 16- x 4-foot concrete pads reinforced with 6-inch welded wire fabric were constructed adjacent to the exterior wall of the test cell to provide a solid foundation for test equipment. The sidewalk to the modular facility was sloped from the existing parking lot to the base of the handicap ramp to provide handicap access to the GRFL operations facility. Steps were provided at each of the rear doors.

An effective visual screen to the site was provided by planting 275 four to six feet tall White Pine trees in multiple rows on three sides of the site (Figure 1). The trees were staggered in a random pattern to enhance their visual appeal and help them blend the site into the base landscape. In addition, a landscaping scheme around the modular facility was developed by the base landscape architect to blend it into its surroundings and provide a more visually appealing facility for the base (Figure 72).

A 39.4- x 60-foot THA Rubb shelter with 11-foot side walls was erected over the completed test cell. It has a galvanized steel structure covered with high strength, PVC coated polyester flame retardant fabric. The wall coloring conforms to the base paint scheme and the roof is white translucent. It was erected off-center to cover the entire

equipment pad and provide 15-foot of clear covered area on the north end of the test cell nearest the laboratory. It has an 11-foot wide by 14-foot high door equipment access door in each end.

Telephone connections to the facility were provided by the base communications contractor. The timing was coordinated so that the communications cable could be placed in the electrical service trench to save construction costs.

Finally, the entire construction site was cleaned up and all disturbed areas were seeded.

Figure 72. Photograph Showing Rubb Building Covering Test Cell and Landscaping.

D.   DISCUSSION

All tasks were accomplished as intended and a properly prepared site is available for the GRFL. The base engineers need to reroute the water line where it exits building 913 to prevent it from freezing this winter. The trees and shrubs that were planted may need to be watered this summer unless there is at least average rainfall. The water service

to the facility was super-chlorinated under the guidance of the Base Environmental Engineer before it was connected to the base water system. The electrical connections to the existing transformer were conducted under the supervision of the Base Engineer Electrical Shop.

A 19.6- x 40-foot Rubb building was proposed, but when the shop drawings were received for the Waterloo Barrier ™ Test Cell the outer cell had dimensions of 26- x 40.8-feet. The proposed cover was not large enough. Several different size covers were then evaluated. The 39.4- x 60-foot cover was selected because it provides sufficient covered space around the test cell to accommodate future test equipment and instrumentation (Figure 73). A personnel door and vent fan would enhance the cover's functionality and should be added at the earliest opportunity.
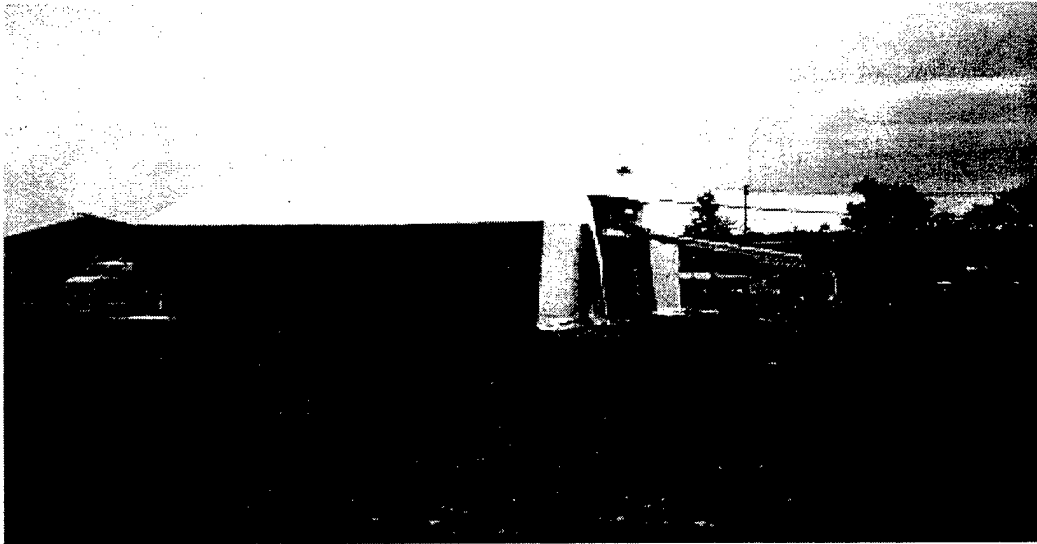

Figure 73. Rubb Building Covering the Test Cell.

SECTION VIII

GRFL OPERATIONS FACILITY

A. OBJECTIVE

The objective of this task was to prepare a laboratory capability infrastructure for the GRFL. Subobjectives were to purchase a field laboratory shell, transport it to the site, erect it, equip it to perform, and develop a business relationship with a local calibrated analytical laboratory. Additionally, we were to provide appropriate drilling equipment, scaffolding, and sampling manifolds.

B. APPROACH

GRFL Operations Facility. A 30- x 50-foot single story modular building was purchased from Nanticoke Homes in Greenwood, DE to serve as the combination field office and laboratory. The facility was fabricated at the plant in Greenwood and shipped to the site in two 15- x 50-foot modules. While the facility was being fabricated, the footings were excavated and poured and five courses of 8- x 8- x 16-inch concrete block were laid for the foundation. Upon arrival at the site, the sections were set onto the foundation, connected, and weathered in one day. During the next four weeks the utilities were connected, cabinet tops installed, finish floors laid, exterior accesses constructed, and interior finishes completed. The furnishings were then moved in and the phones and computers installed. Lastly, a chemical vent hood and deionized water supply were installed in the laboratory.

Laboratory Instrumentation. The field operations facility was equipped with the capability to perform analyses in support of the GRFL demonstrations. The major analytical capability is provided by the laboratory quality Gas Chromatograph (GC). The advantages of using a GC in the field are the ability to obtain quantitatively reliable data and to do so rapidly. There are different approaches possible for applications of a GC in the field. These range from portable GCs operated under ambient conditions to laboratory quality GCs operated either under ambient conditions or in climate controlled mobile laboratories. Although field operation of a GC under ambient conditions may not ultimately provide data as accurate and reliable as that produced by a laboratory, the field GC can provide data of adequate quality to delineate an area for remediation. The GRFL test bed where emerging technologies will be proven and validated, requires greater degree of accuracy and reliability for GC analyses.

The GRFL operations facility was equipped with an HP 6890 Series GC that will be operated under climate controlled conditions in the field laboratory. Other laboratory instrumentation includes an pH/ION Meter, Dissolved Oxygen Probe, portable monitoring/sampling pumps, and other miscellaneous laboratory equipment and supplies.

CPT System. The field operations facility was equipped with a trailer mounted CPT system. A users guide for the system is provided in Appendix P. The Cone Penetrometer Test (CPT) was originally developed in the Netherlands in about 1934 for geotechnical site investigations. The original cones involved mechanical measurements of the penetration resistance on a conical tip. A friction sleeve was added in 1965. Electronic measurements were added in 1948 and improved in 1971. Pore pressure probes were introduced in 1975, originally as independent probes but were soon added to the cone penetrometer instrumentation. The CPT probe contains the primary geotechnical sensors for tip stress, sleeve friction, pore pressure along with an inclinometer to measure the tilt of the probe, and resistivity as discussed later. This type of cone is used widely in Europe for geotechnical investigations due to the soft nature of many of the European soils. Its acceptance in the United States has been rather limited due to the stiffer nature of many U.S. soils, (especially those in the western regions of the U.S.), when compared to European soils. However, the significant advantages provided by cone penetrometer are leading to much wider acceptance by the environmental site characterization community. This acceptance is due largely to the development of new sensors which allow in situ detection of chemical pollutants.

Major components of the modern cone penetrometer system are the instrumented probe, the instrumentation conditioning and recording system, the hydraulic push system, and the vehicle on which the system is mounted. The common configuration provides the reaction mass for a hydraulic push force of about 20 tons (18,000 Kg). Standardization for the geotechnical applications of the cone penetration test was established by the American Society of Testing and Materials in 1986. This standard allows for a probe diameter of 1.44 or 1.75 inches (3.658 cm or 4.445 cm).

Using the cone penetrometer for environmental site characterization represents a relatively recent application of the technology. Significant advantages of the CPT include: eliminating drilling wastes and the need for treatment and disposal of drill spoils as hazardous material; providing continuous data on the subsurface stratigraphy in real time; identifying thin layers of significantly different hydraulic conductivity; eliminating the possibility of the crew being exposed to the potentially hazardous material; reducing the possibility of cross contamination (by pressure grouting the hole as the probe is withdrawn); and speed, when compared to conventional drilling and sampling. CPT is an excellent platform for making continuous measurements of contaminant information with depth, is useful for pushing monitoring sensors into the subsurface and for taking gas, water, or soil samples for environmental testing. A detailed description of the CPT test methodology is presented in Appendix G.

C. RESULTS

A functional and attractive laboratory/office that meets all the requirements for the GRFL operation was provided. A floor plan for the GRFL operations facility is

shown in Figure 74. The facility complies with the Dover AFB comprehensive plan and fits into the base architectural theme. The roof has a 7/12 pitch and is covered with IKO "Dual Brown" colored, 25 year life, asphalt shingles. The exterior walls are covered with vinyl siding having a field color of Glidden 78-77 "Eagle Feather Tan" and a trim color of Glidden 69-46 "Bald Eagle Brown". Photographs of the finished facility are included as Figure 75 and 76. A copy of the as-built drawings of the facility was provided to the base engineers.

One end of the facility was designed and equipped as a laboratory, one end was designed and equipped as an office, and the center portion houses a bathroom and kitchenette that can be used as a break area.

The laboratory has standard bench height counters on three sides. Cabinets were provided below the counters. A laboratory quality sink complete with deionized water, standard hot and cold water, and vent hood was also provided. Electrical power (110/220V) power outlets were provided at regular spacing above the counter. An eye wash and emergency shower were also provided in the laboratory.
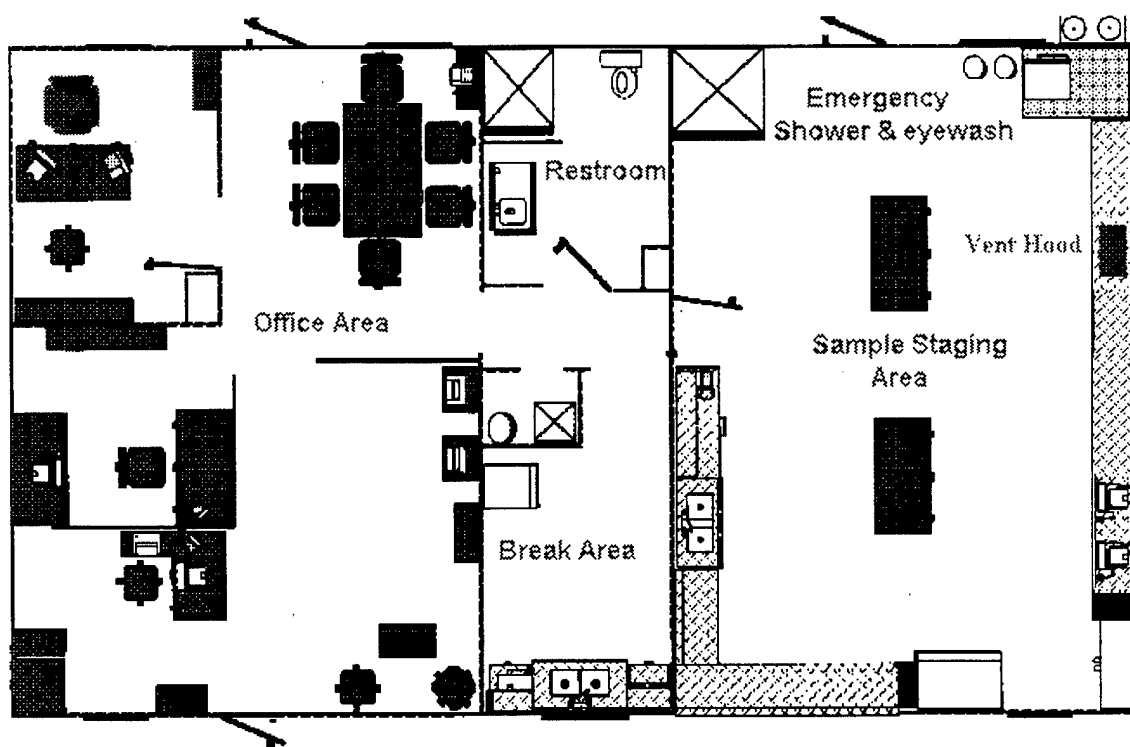
Figure 74. Floor Plan of GRFL Operations Facility.

The office is equipped with four desks, tables and chairs. Voice, data, and facsimile phone lines were installed to accommodate all tele-communication needs. A

plain paper facsimile and light duty copier were provided. The office was carpeted as indicated in the attached specifications. Detailed specifications for the facility are provided in Appendix R.

D. DISCUSSION

The Nanticoke Facility purchased and installed for the laboratory/office is an attractive and functional facility that meets all stated GRFL requirements. It is solidly constructed and although it is classed as a temporary facility on Dover AFB, it could well be entered into the real property records as a permanent facility if the GRFL mission ends prematurely.

Figure 75. Photograph of GRFL Operations Facility.

76. Photograph of GRFL Operations Facility and Aquifer Testing Equipment.

SECTION IX

CONTROLLED-RELEASE CELL

A.   OBJECTIVE

The objective of this task is to construct a test cell that can accommodate field verification of treatment technologies under experimental contro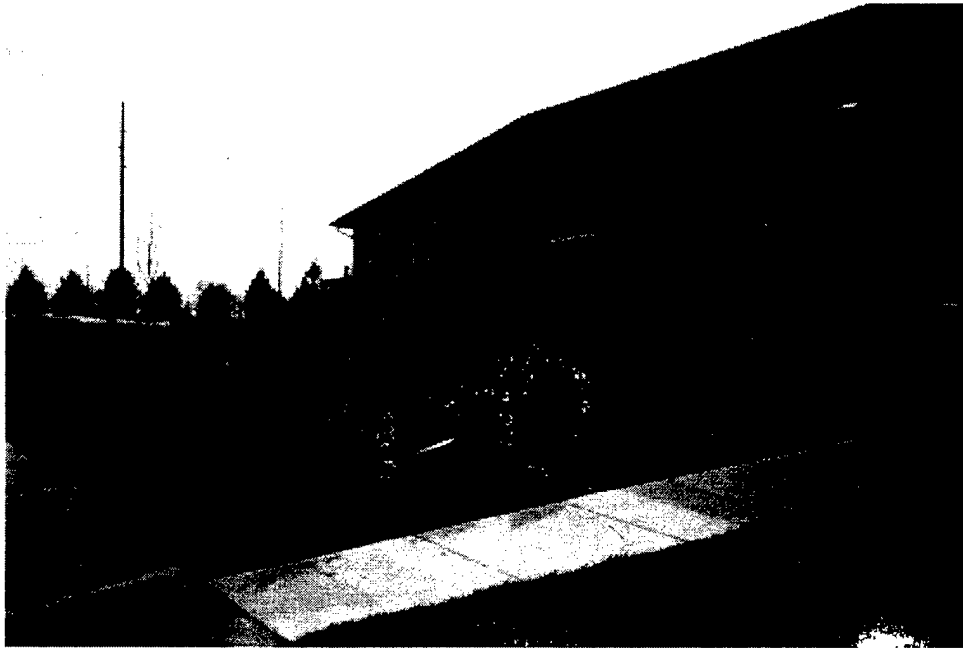lled releases of DNAPLs. The scope of work for this task consisted of constructing a 16.7- x 32.5-foot controlled/contained release test cell by:

- selecting the location for the test cell on the site;
- purchasing the Waterloo Barrier ™ WZ-75 Sheet Piling:
- installing the sheet piling;
- grouting the sheet pile joints;
- installing injection and extraction wells;
- installing monitoring points; and
- installing sampling points.

B.   APPROACH

One test cell was constructed at the appropriate location based on results from the site characterization tasks. The test cell was constructed using the sealable steel sheet piling developed by the University of Waterloo's Institute for Groundwater Research. Construction techniques were carried out according to the construction practices developed by the developer. The sealable steel sheet piling have a number of advantages over conventional sheet piling for containing polluted ground water. The materials and construction techniques make the Waterloo sheet piling less prone to leaking than other types of containment walls, thus providing a greater degree of confidence in its performance.

1.   Cell Construction

This task was accomplished by contracting with George and Lynch of New Castle, DE to purchase and install a double walled cell of WZ-75 Waterloo Barrier ™ Sheet Piling as specified in the SOW. Waterloo Barrier ™ Sheet Piling is a low permeability cutoff wall developed for groundwater containment by researchers at the University of Waterloo. It is patented in both Canada and the United States. As shown in Figure 77, these special sheet piles have an enlarged groove that can be fully grouted to provide an impervious boundary for the cells. The sheets were supplied by Canadian Metal Rolling Mills Cambridge, Ontario. C3 Environmental, a division of Canadian Construction Controls Limited, provided the Quality Assurance/Quality Control (QA/QC) inspection of the installation, flushed the joints, and grouted them with a specially designed grout.
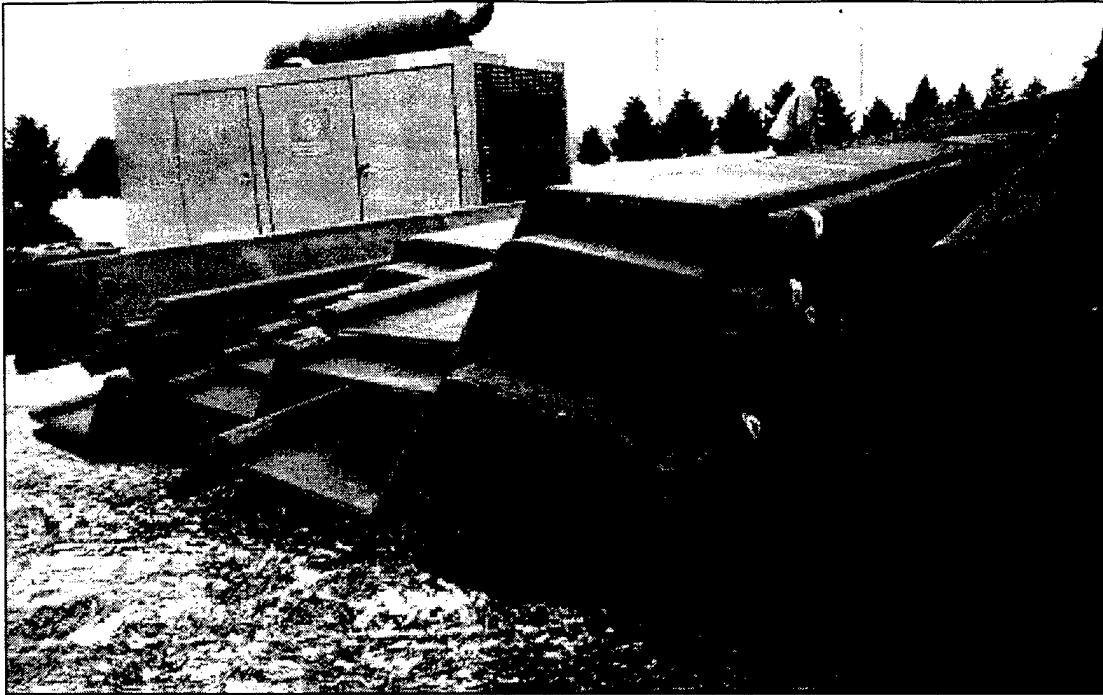
Figure 77. Photograph of Waterloo Barrier Sheet Pile.

The Waterloo Barrier ™ WZ-75 sheet pile is a patented section with an enlarged female joint which allows for the installation of a site specific sealant material to reduce the permeability of the barrier cell. A key procedure in ensuring proper installation of the WZ-75 pile is the attachment of a driving shoe (foot plate) at the base of every female joint. This shoe minimizes the entry of debris into the joint during driving which aids in a proper joint flushing prior to grouting the joint full.

The piles were driven with an ICE (International Construction Equipment) 416 hammer. A 500 HP hydraulic power unit provided the power for the hammer. A 100 ton Link Bell truck mounted crane was used to position the sheets and hold the hammer. A Condor Snorkel Lift was used as a platform to aid in positioning the sheets. Figure 78 illustrates the pile driving.
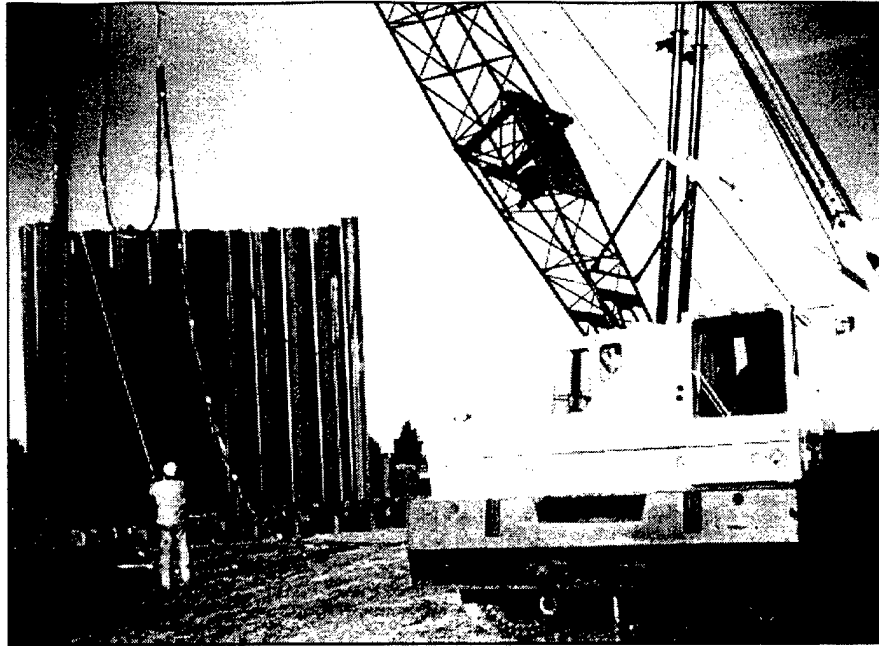
Figure 78. Pile Driving Operation

After the piles were driven, C^3 Environmental flushed the joints using a high pressure water pump and rigid hose to remove any loose material in the sealable cavities. Flushing was conducted until the return water was free of debris. Whenever stubborn deposits were encountered in a cavity, the driving hammer was hooked onto the top of the adjacent pile and vibrated during the flushing operation.

A prepackaged attapulgite clay based grout (Impermix™), modified for use with the Waterloo Barrier™ system, was used to seal the sheet pile joints of the containment cell. The sealant consists of a blend of attapulgite clay and mineral powders that form a stable self-hardening grout. It was chosen because it exhibits very low permeability and chemical resistance properties. Figure 79 shows the sealing of sheet pile joints.

Figure 79. Photograph Showing Sealing of Sheet Pile Joints.

2.   **Injection / extraction wells, monitoring / sampling points**

        Eight 2-inch extraction/injection wells were installed in the outer ring of the test cell as part of the emergency treatment system discussed in Section VI. The layout of the wells is shown in Figure 67. In addition four piezometers were located outside the test cell to monitor ground water quality during demonstrations. This system of wells and monitoring points are part of the three tiered safety plan to protect against any unlikely leakage and contamination of the surrounding area during controlled release demonstrations.

C.   **RESULTS**

        Cell Construction. A double-walled test cell was constructed with 45' long sheets of W275 Waterloo Barrier Sheet Piles. The joints were flushed clean and tremie grouted with a specially designed attapulgite grout. Figure 72 shows the location of the test cell at the site.

        The C^3 Environmental Report (Appendix S) includes the driving logs, flushing summary and QA observations. The driving logs list the depth of each sheet and the

171

verticality of the top of the sheets. The flushing logs list the depth that each joint was flushed clean in preparation for grouting.

　　　Injection/extraction wells and monitoring/sampling points. The injection/extraction wells will be pumped during the unlikely event of leakage from the inner test cell and the contamination will be removed by air stripping and carbon adsorption treatment. The treated water will be injected back into the outer ring of the test cell. The GRFL pumping tests indicate that the wells can be pumped at a rate of about one gallon per minute.

D.　　DISCUSSION

　　　Cell Construction. George and Lynch started driving the sheet piles on the northwest corner of the exterior cell using the standard technique of driving each sheet all the way in. The tops started drifting to the south by 2-3 degrees which caused so much friction to develop that pile 14 burned through and had to be pulled and discarded. C3 Environmental suggested that prior experience indicated the best way to drive WB sheet piles is to drive each of them no more than 10-15 feet, "key" the last sheet in, then "stage" them in by driving each pile no more than 10-15 feet at a time. The WB sheet piles have a smaller joint tolerance along the sheet than standard sheet piles (.25 inches).

　　　After a 2-day weather hold (winds > 15 mph), they pulled the remaining sheets and started driving the interior cell using the procedure C3 had suggested. It took 12 hours to stab in the sheets and key in the interior cell. It took another 12 hours to stage the sheets down to 1-2 feet above grade. The sheets were driven into the aquitard an average of 4 feet. C3 then flushed the joints with a high pressure water stream (110 psi) from a 1/2 inch rigid plastic hose that was forced down each joint (Figure 78). Logs were created recording the depth to which the joints were flushed clean.

　　　The exterior cell was constructed with the same technique as the inner cell. Construction was slowed by the extremely cold weather and high winds. The joints were flushed by C3 Environmental after the outer cell was driven to the required depth. Temporary sheet piles were then driven across each end of the inner cell approximately 2 ft from the ends. The soil inside these enclosed areas was then excavated to a depth of 15 feet, a geotextile membrane installed on all sides, and the trenches back filled with 1/2 inch pea gravel. Three 4 inch steel pipes were installed in each trench to allow the injection / extraction wells to be installed at a later time. Three 1.5 inch PVC wells were also installed in each trench for the air sparging.

　　　The tops of the sheet piles were cut off approximately one foot above grade and the ground sloped up to their tops.

SECTION X

WASTE MANAGEMENT

A.   OBJECTIVE

The objective of this task is to insure that proper waste management guidance is provided for the GRFL users. Waste generated at the GRFL site must be managed in accordance with Dover AFB requirements as well as municipal, state and Federal regulations. The Dover National Test Site Manager will be responsible for insuring that the GRFL Staff and GRFL users comply with all appropriate regulations and requirements.

B.   APPROACH

Investigations were conducted to evaluate potential waste handling and treatment options. These investigations indicated that the GRFL would have to develop and implement a waste management plan for the waste generated during operation of the GRFL.   It was anticipated that GRFL waste could be stored in existing on base hazardous waste storage facilities and disposed of along with other regulated waste from the installation.

C.   RESULTS

The GRFL facility will be expected to manage waste to minimize any generation of hazardous waste material and dispose of any waste generated during demonstrations in an appropriate manner. The GRFL users will be required to prepare a waste management plan along with their demonstration project plan. The users will be expected to bear the cost of treating and disposing of any waste generated during demonstrations. The GRFL manager will be responsible for approving waste management plans prior to demonstrations.

D.   DISCUSSION

All users of the GRFL, including staff, contractors, and tenants will comply unequivocally with environmental regulations. Everyone associated with the GRFL must be cognizant of their responsibilities regarding waste management. If anyone encounters difficulty in meeting this commitment, they should immediately contact the GRFL manager. Any environmental compliance issues that cannot be resolved promptly by the GRFL manager should be elevated, through the proper chain of command.

The GRFL manager should weekly survey all work areas to ensure that waste is being managed properly. Particular attention should be given to any waste chemicals or liquids. A general waste management plan is provided in Appendix T. This plan was

173

adapted from a plan developed by the Armstrong Laboratory for the Dover National Test Site (DNTS).

SECTION XI

SITE SAFETY PLAN

All aspects of the work will be conducted in accordance with the Site Safety Plan (SSP) presented in Appendix U to ensure that the GRFL demonstrations and operations are carried out in a safe manner. The SSP is intended to act as a supplement and appendix to the existing Dover Air Force Base Health and Safety Plan (HASP). The SSP will be obtained from the on-site GRFL manager, read thoroughly prior to start of work by all personnel involved in field activities, and retained for reference on site.

A.   OBJECTIVE

The objective of this plan is to provide specific health and safety requirements for the planned demonstrations at the GRFL.

B.   APPROACH

This plan contains guidelines and directives which establish minimum standards for chemical monitoring and exposure control, safety criteria, and emergency response procedures. It is written to enable the Site Safety Officer (SSO) to respond to changing conditions and make professional judgments regarding the interpretation of monitoring data and related control measures. This plan applies to all personnel involved in GRFL activities.

C.   RESULTS

A health and safety plan was developed specifically for demonstrators using the GRFL test site. Tasks involved in the operation of the GRFL where the potential for exposure or skin contact with hazardous chemicals exists include:

- Application of chemicals to the soil for test purposes;
- Collection of ground water, soil and soil gas samples; and
- Chemical testing of soil, soil gas, and ground water in the on-site laboratory.

This SSP addresses the work tasks to be performed at the GRFL at Dover Air Force Base, Dover, Delaware. Use of this SSP is intended to:

- Assess potential site hazards prior to work;
- Ensure the awareness of all personnel to potential hazards;
- Minimize or mitigate potential hazards;
- Provide a means of personnel protection and incident reporting; and
- Complete the project with zero lost-time injury or illness and zero reportable incidents.

D.   DISCUSSION

The safety plan presented in Appendix U is a guidance document for the GRFL manager and engineers and scientists responsible for personnel health and safety at the GRFL test site. It assumes a basic knowledge of science and experience in occupational safety and health. The plan is not a detailed industrial hygiene document or a comprehensive guidance document on occupational safety and health. It provides specific guidance for GRFL staff and users of the test site. However, each demonstration project must prepare a health and safety plan specifically for the planned demonstration. The plan presented in Appendix U should be used as a basis for developing a specific project health and safety plan. The development of a written project safety plan helps ensure that all safety aspects of site operations are thoroughly examined prior to commencing field work. The project site safety plan should be modified as needed for every stage of the demonstration project.

SECTION XII

CONCLUSIONS AND RECOMMENDATIONS

This study has shown that Dover AFB was an excellent choice for locating the GRFL which is a national test site funded by the SERDP as part of the NETTS Program. The site designated for the GRFL was successfully characterized and the data was used to locate and construct the first GRFL test facility. Through this work an excellent and unique test facility has been established for use in demonstrating new technologies for cleaning up contaminated soil and groundwater. The impact of technologies verified at the GRFL is expected to benefit all areas of environmental restoration within the Air Force, DOD, and private industry, as well as international environmental restoration efforts.

The following conclusions and recommendations are made to help in the operations and management of the GRFL facility, provide information for development of future test cells at the site, and to assist future users of the GRFL facilities.

A.   CONCLUSIONS

General conclusions from site characterization investigations include the following:

- The vadose zone extends to a depth of about 26 feet below the ground surface and consists of sands with clay seams. Silty sands are the dominant soil type in the vadose zone, with a clay layer observed in the northern end of the site which becomes less distinct in the southern part of the site. A very stiff layer occurs at a depth of about 13 feet below ground surface and is 2 to 4 feet thick.

- The aquifer extends from about 26 feet to 40 feet below the ground surface and also consists of silty sands with thin clay seams. The aquifer becomes thicker toward the northern end of the site. A suspected clean sand channel appears to traverse the site in an east-west direction. The hydraulic conductivity of the sand channel is higher than that of the bulk of the aquifer.

- The aquitard occurs at a depth of 40 to 50 feet below the ground surface and consists of a clayey silt with an average hydraulic conductivity of about 2.07×10^{-2} feet/day (7.32×10^{-6} cm/sec). Geophysical testing and cone penetration testing indicated that the aquitard was continuous. The hydraulic head in the first confined unit beneath the aquitard was monitored during pumping in the unconfined unit and indicated no connections between the two aquifers.

Conclusions from the individual tasks include the following:

Geophysics Survey

- The surface geophysics surveys were used to determine a three-dimensional map of the surface of the aquitard elevation. In addition a near-surface clay layer was identified in the northern half of the site. The GPR and CPT surveys indicated that the aquitard was continuous throughout the site.

CPT Site Survey

- A geostatistical model of the CPT soil classification was used to develop a detailed three-dimensional map of the site stratigraphy. An uncertainty analysis of the model showed a higher degree of certainty in the area of the installed test cell. This result was expected, as more CPTs were conducted in the area of the first test cell. The geology of the northern portion of the site is more uncertain due to the greater spacing between CPT locations and more complicated geology.

- The CPT soil classification was correlated to hydraulic conductivity and is accurate within an order of magnitude. The correlation shows that the hydraulic conductivity vary by three orders of magnitude over short vertical distances. The correlation between CPT and hydraulic conductivity was based on a limited field-test data set and laboratory tests. Improvements could be made to its accuracy by developing a larger data set using laboratory tests.

- The CPT was successful in installing 2-inch monitoring and pumping wells to the aquitard and in installing instrumentation packages such as soil moisture, air pressure and temperature probes. Due to the silt content at the site, advanced well development techniques, such as the Aardvark system, needed to be used.

Chemical Properties

- The basic physicochemical properties of the soil are typical of sandy, moderately acidic Atlantic Coastal Plain soils. The soils have low contents of clay and organic matter and thus low CECs. Consequently, leaching of metals and organic chemicals could be a problem. However, the small contents of clay and organic matter could still play an important role in contaminant retention.

Microbiological Properties

- The enumeration results indicated that, both heterotrophic and denitrifying bacteria were present at detectable levels in all samples. Bacterial numbers generally decreased with depth, although in some cases counts remained elevated at considerable depths. The autotrophic nitrifying bacteria were only detected in the more shallow samples. The eukaryotic fungi and protozoa were also found to be more prevalent at shallow depths, although significant populations were detected as deep as 37 feet in some instances.

- Based on several of the analyses, it appears that microbial populations present in the more shallow samples tended to be larger and more active than those examined from the deeper soil-sediment layers.

Mineralogical Properties

- Analyses performed on the GRFL soil samples revealed a wide range of mineralogical properties. The highest total sand content (93%) was found between elevations 23 and 29 feet. msl at CPT 12 with a preponderance of sand in the medium (42%) and fine (28%) fractions. A high total sand fraction (84%) also occurred between elevations 4 and 10 ft. msl at CPT 22. Total clay dominated (47%) the soil between elevations -10 and -12 feet msl at CPT 12 and was a significant component (36%) between elevations 20 and 22 feet msl at this location. Significant silt (40 to 49%) occurred between elevations -10 and -12 ft msl, and between 20 and 22 ft. msl at CPT 12. The soil contained 35% silt at between elevations -7 and -9 feet. msl at CPT 10.

Aquifer Tests

- The aquifer at the GRFL site is predominantly made up of fine sands with an average hydraulic conductivity of 8.50 feet/day (3 x10^{-3} cm/s). There are silts and clays present in the sands which lower the hydraulic conductivity of the clay rich layers. The combination of low hydraulic conductivity and a very low groundwater gradient in the area result in low groundwater flows. There is evidence of a clean sand channel in the vicinity of the tracer test, which was identified in the CPT profiles. This hydraulic conductivity of the sand channel is estimated to be a factor of four greater than the average hydraulic conductivity of the GRFL site. Wells in the aquifer will have a maximum flow rate of about one gpm due to the relatively thin saturated aquifer thickness and moderate hydraulic conductivity (average of about 8.50 feet/day (3 x 10^{-3} cm/sec)). Wells in the sand channel will sustain flow rates as high a 3 gpm due to an increased thickness of the aquifer and the higher hydraulic conductivity of the clean sand.

179

Tracer Tests

- From analysis of the tracer test effort and CPT logs discussed above, we have concluded that a channel of clean sand overlying the aquitard may exist at the north end of the GRFL site. CPT pore pressure measurements indicate that the hydraulic conductivity in this channel is uncharacteristically high compared to the rest of the site. Because this channel was penetrated by the pumping well used for the induced-gradient tracer test, the flow field required for the test was short-circuited. The elevated yield from the pumping well, originally thought to be attributable to the deeper drawdown afforded by a thicker saturated zone in this area, was actually made up of water flowing to the well through the higher conductivity channel. Consequently, pumping from the well did not produce a sufficient increase in hydraulic gradient over the entire saturated depth to support the test.

- A second conclusion derived from the tracer test is that a natural-gradient test has a higher probability of success at this site than does an induced-gradient test. The hydraulic conductivity typical of the site and limited aquifer thickness are insufficient to create the large cone of depression necessary for an induced-gradient tracer test.

Hydraulic Conductivity in the Vadose Zone

- Cone penetration and laboratory tests indicate that the GRFL vadose zone soil moisture varies from less than 10% volumetric soil moisture in silty sands, (which is very dry), to 30% or greater in the clays, (which is essentially saturation). This variability in soil moisture content results in widely varying unsaturated hydraulic conductivity in the vadose zone. Infiltration testing indicated unsaturated hydraulic conductivity as low as 8.6×10^{-1} feet/day for dry silty sands to a high of 8.6 feet/day for saturated clean sands. As demonstrated by the infiltration test, the unsaturated hydraulic conductivity is highly dependent upon the soil type and moisture content, and it was not possible to correlate the CPT to the current database. Hence, estimates of the vadose zone hydraulic conductivity at other locations on the GRFL site will be highly uncertain.

Air Permeability in the Vadose Zone

- Two types of tests were conducted to determine air conductivities of the vadose zone. The first was a conventional monitoring well air pumping test which indicated an air conductivity of about 1.3×10^{-7} feet^2. This value was calculated using a widely accepted model in which the air flow is assumed to be radial. Further analysis of the monitoring well data was conducted to evaluate the radial flow assumption using a two dimensional analytical solution. The two dimensional solution modeled the effects of boundaries

(i.e. distance to the free surface or watertable) and anisotropy. This analysis indicated that (1) these effects can have a significant influence on air permeability estimates back-calculated from field tests; (2) air permeabilities calculated using the common assumption of radial air flow should be viewed as an approximation of the actual flow conditions; and (3) for tests located in layered media or near boundaries, significant non-radial flow can occur.

- A second type of test was conducted using a modified CPT probe. The CPT air conductivity test consisted of a conventional CPT probe with a ConeSipper® installed above the CPT probe. As expected, the CPT provided air permeability estimates of individual layers and demonstrated that three orders of magnitude variations can occur between adjacent soil layers.

- The conclusion drawn from this task are: (1) large scale air permeability tests provide only average site values with little detail on individual layers; (2) the CPT-derived air permeabilities provide greater detail than the level of detail possible with a conventional monitoring well test; (3) the CPT air permeability test can be used to evaluate air permeabilities at other locations on the GRFL site; and (4) non-radial flow occurred on the large scale test and this must be included in analysis of the test data.

B. RECOMMENDATIONS

The site characterization program conducted under this effort determined the general characteristics of the vadose zone, aquifer and aquitard and can be used to determine the stratigraphy of the site. However, there are areas where the understanding of the site geology and properties could be improved:

- The geology of the southern end of the site is well documented. The northern end of the site is more geologically complex and additional CPTs should be conducted at the northern end of the site to better characterize the near surface clay layer. Further CPT and hydraulic conductivity investigation should be undertaken to characterize the relatively high conductivity sand channel identified at the north end of the GRFL site. The channel lies just above the aquitard and will influence flow and transport in the area.

- An additional effort to characterize site dispersion and depth dependent variability in hydraulic conductivity should be conducted. This effort should use either a natural-gradient tracer study or a test of smaller scale because of the inability to dramatically change the groundwater flow field over a large area.

- Current correlation of hydraulic conductivity to the CPT relied upon a limited number of field slug and pumping tests and laboratory grain size test. The

181

correlation has a high degree of uncertainty (about an order of magnitude) which could be reduced by increasing the database upon which the correlation is based. Additional laboratory hydraulic conductivity tests on undisturbed samples should be conducted. Samples should be obtained from CPT test locations and used to improve the correlation.

- As with the saturated hydraulic conductivity, the unsaturated hydraulic conductivity database is quite limited. A correlation between the CPT and unsaturated hydraulic conductivity could be developed, given a sufficient database. Laboratory tests such as the Unsaturated Flow Apparatus could provide the required information in an economical and timely manner.

- It is recommended that geophysical measurements be made within the cells before and after a release. The Borden (Canada) Experiment included surface GPR surveys as the injected fluid migrated down through the soil in the cell and successful mapping of the fluid migration. Geophysical methods can also be used to monitor remediation in the cell. There is evidence that GPR, both surface and borehole, and Electrical Resistivity Tomography (ERT) can map the migration of DNAPLs.

- In the future, when new test cells are installed, we recommend that the GRFL CPT system be utilized to conduct additional CPT soundings near the proposed location. Additional CPT soundings will increase the level of detail and can be added to the three-dimensional model of the site stratigraphy to increase the level of certainty of the estimated values in proposed test cell area.

- Results from the CPT ConeSipper® air permeability test developed as a part of this effort were quite encouraging. Improvements to the test, such as refining the analytical model and instrumentation system, should be made. The test should also be extended to conduct hydraulic conductivities in the saturated zone.

- The GRFL is a unique resource for the Air Force and DoD in providing opportunities to verify treatment technologies for wide technology transfer applications to the user community. An aggressive plan should be developed to market the full capabilities of the GRFL to potential users.

SECTION XIII

REFERENCES

1. Th. van Genuchten, "A closed-form equation for predicting the hydraulic conductivity of unsaturated soils." Soil Sci. Soc The full reference is:. Am. J. 44:892-898, 1980.

2. USACE, Dames and Moore, "Draft West Management Unit Remedial Investigation Dover Air Force Base, Dover, DE", AMC Project # FJTX927000, Contract # DACW-45-93-D-0021, April 1995

3. Zuberer, D. A. 1994. Recovery and enumeration of viable bacteria. p. 119-144. *In*: R. W. Weaver, et al. (ed.) Methods of soil analysis. Part 2. Microbiological and biochemical properties. Soil Science Society of America, Madison

4. Brockman, F. J., T. L. Kieft, J. K. Fredrickson, B. N. Bjornstad, S-m. W. Li, W. Spangenberg, and P. E. Long. 1992. Microbiology of vadose zone paleosols in south-central Washington state. Microb. Ecol. 23:279-301.

5. Wollum, A. G. 1982. Cultural methods for soil microorganisms. p. 781-802. *In:* A. L. age et al. (ed.) Methods of soil analysis. Part 2. American Society of Agronomy, Madison, Wis.

6. Woomer, P. L. 1994. Most probable number counts. p. 59-79. *In*: R. W. Weaver, et al. (ed.) Methods of soil analysis. Part 2. microbiological and biochemical properties. Soil Science Society of America, Madison, Wis.

7. Ingham, E. R. 1994. Protozoa. p. 491-515. *In*: R. W. Weaver, et al. (ed.) Methods of soil analysis. Part 2. Microbiological and biochemical properties. Soil Science Society of America, Madison, Wis.

8. Schmidt, E. L., and L. W. Belser. 1994. Autotrophic nitrifying bacteria. p. 159-177. *In*: R. W. Weaver, et al. (ed.) Methods of soil analysis. Part 2. Microbiological and biochemical properties. Soil Science Society of America, Madison, Wis.

9. Tiedje, J. M. 1994. Denitrifiers. p. 245-267. *In*: R. W. Weaver, et al. (ed.) Methods of soil analysis. Part 2. Microbiological and biochemical properties. Soil Science Society of America, Madison, Wis.

10. Horwath, W. R., and E. A. Paul. 1994. Microbial biomass. p. 753-773. *In*: R. W. Weaver, et al. (ed.) Methods of soil analysis. Part 2. Microbiological and biochemical properties. Soil Science Society of America, Madison, Wis.

11. Amato, M. and J. N. Ladd. 1988. Assay for microbial biomass based on ninhydrin-reactive nitrogen in extracts of fumigated soils. Soil Biol. Biochem. 20:107-114.

12. Joergensen, R. G., and P. C. Brookes. 1990. Ninhydrin-reactive nitrogen measurements of microbial biomass in 0.5 M K_2SO_4 soil extracts. Soil Biol. Biochem. 22:1129-1136.

13. Tiedje, J. M. 1982. Denitrification. p. 1011-1026. *In:* A. L. age et al. (ed.) Methods of soil analysis. Part 2. American Society of Agronomy, Madison, Wis.

14. Tabatabai, M. A. 1994. Soil enzymes. p. 775-833. *In*: R. W. Weaver, et al. (ed.) Methods of soil analysis. Part 2. Microbiological and biochemical properties. Soil Science Society of America, Madison, Wis.

15. Zak, J. C., M. R. Willig, D. L. Moorhead, and H. G. Wildman. 1994. Functional

diversity of microbial communities: a quantitative approach. Soil Biol. Biochem. 26:1101-1108.

16. Cavigelli, M. A., G. P. Robertson, and M. J. Klug. 1995. Fatty acid methyl ester (FAME) profiles as measures of soil microbial community structure. Plant Soil 170:99-113.

17. Wingle, William L., Eileen P. Poeter, and Sean A. McKenna, UNCERT User's Guide, Colorado School of Mines, Department of Geology and Geological Engineering, 1995.

18. Robertson, P.K., "Soil Classification Using the Cone Penetrometer Test," Canadian Geotechnical Journal, Vol. 27, No. 1, February 1990.

19. Isaaks, Edward, H. and R.M. Srivastava, Applied Geostatistics, Oxford University Press, New York, NY., 1989.

20. McElwee (1995)

21. Butler, J., Jr. And Z. Hyder, "An Assessment of the Nguyen and Pinder Method for Slug Test Analysis", Gound Water Monitroing and Remediation, Vol. 14. No. 4, pp 124-131, 1994.

22. Freeze, R.A., and Cherry, J.A., "Groundwater", Prentice-Hall, Inc. Englewood Cliffs, N.J., 1979.

23. Boulton, N.S., "Analysis of data form non-equilibrium pumping tests allowing for delayed yield from storage", Proc. Inst. Civil. Eng. Vol. 26, No. 6693, pp. 469-482, 1963.

24. de Marsily, G., Quantitative Hydrogeology. Academic Press, Inc., Harcourt Brace Jovanovich, pub. San Diego, CA, 1986.

25. Jacob, C.E., "Notes on Determining Permeability by Pumping Tests Under Water-Table Conditions", U.S. Geological Survey, Open File (Mimeo) Report, 1952.

26. Domenico, P.A. and F. W. Schwartz, Physical and Chemical Hydrogeology, John Wily & Sons, Inc., New York, 1990.

27. Baligh, Mohsen M. and Jacques-Noël Levadoux, "Pore Pressure Dissipation After Cone Penetration", Report No. MITSG 80-13, Index No. 80-313-Cim, MIT, Cambridge, April,1980.

28. Taylor, D.W., Fundamentals of Soil Mechanics, John Wiley and Sons, New York, 1948.

29. Lane, K.S. and D.E. Washburn, "Capillarity Tests by Capillarimenter and Soil Filled Tubes," Proc. Highway Research Board, 1946.

30. Masch, F.D. and K.J. Denny, "Grain-size distribution and its effect on the permeability of unconsolidated sands", Water Resources Res., Vol. 2, pp. 665-677, 1966.

31. Bear 1972Baehr, A.L., and Hult, M.F. "Evaluation of Unsaturated Zone Air Permeability Through Pneumatic Tests", Water Resources Research, Vol. 27, No. 10, pp. 2605-2617, 1991.

32. Todd, D.K., Groundwater Hydrology, Wiley, New York, 1959.

33. Lamb and Whitman, 1969 Lambe, T. William and Robert V. Whitman, Soil Mechanics, John Wiley and Sons Inc, New York, 1969

34. Johnson (1990). (see reference 55)

35. Johnson, P.C., C.C. Stanley, M.W. Kemblowski, D.L. Byers, and J.D. Colthart, "A Practical Approach to the Design. Operation, and Monitoring of In Situ Soil-Venting Systems", *Ground Water Monitoring Review*, Spring 1990.
36. Shan, C., R.W. Falta, and I. Javandel, "Analytical Solutions For Steady State Gas Flow To A Soil Vapor Extraction Well", <u>Water Resources Research</u>, Vol. 28 No. 4, pgs. 1105-1120, 1992.
37. Hinchee, R.E., S.K. Ong, et al. , "Test plan and technical protocol for a field treatability test for bioventing", Prepared for the U.S. Air Force Center of Excellence, Brooks Air Force Base, Texas, 1992.
38. Shinn, James D., "Calibration and Field Evaluation of ARA Soil Moisture Probe", White Paper, Applied Research Associates, Inc. 1996
39. Edwards, Kenneth, B. *Journal of Environmental Engineering*, Vol. 122, No. 3, March, 1996, pg. 232-234.
40. Shan, C., Falta, R.W., and Javandel, I., "Analytical Solutions For Steady State Gas Flow To A Soil Vapor Extraction Well.", *Water Resources Research*, 28(4), 1105-1120, 1992.